Universitat de Girona

MOLECULAR INSIGHTS ON ARRHYTHMOGENIC CARDIOMYOPATHY: ASSESSMENT OF PREMATURE TERMINATION CODONS IN DESMOSOMAL GENES AND VARIANTS RECLASSIFICATION

Marta Vallverdú Prats

DOCTORAL THESIS

MOLECULAR INSIGHTS ON ARRHYTHMOGENIC CARDIOMYOPATHY: ASSESSMENT OF PREMATURE TERMINATION CODONS IN DESMOSOMAL GENES AND VARIANTS RECLASSIFICATION

Marta Vallverdú Prats

2022

DOCTORAL THESIS

MOLECULAR INSIGHTS ON ARRHYTHMOGENIC CARDIOMYOPATHY: ASSESSMENT OF PREMATURE TERMINATION CODONS IN DESMOSOMAL GENES AND VARIANTS RECLASSIFICATION

Marta Vallverdú Prats

2022

Doctoral Programme in Molecular Biology, Biomedicine and Health

Supervised by:
Mireia Alcalde Masegu, Ph.D.
Ramon Brugada Terradellas, Ph.D., M.D.
Oscar Campuzano Larrea, Ph.D.

Tutorized by:
Ramon Brugada Terradellas Ph.D., M.D.

Presented to obtain the degree of Ph.D. at the University of Girona

La Dra. Mireia Alcalde Masegu, investigadora de l'Institut d'Investigació Biomèdica de Girona i professora associada de la Facultat de Ciències de la Universitat de Girona.

El Dr. Ramon Brugada Terradellas, catedràtic de la Facultat de Medicina de la Universitat de Girona, director del Centre de Genètica Cardiovascular de l'Institut d'Investigació Biomèdica de Girona i cap de Cardiologia de l'Hospital Trueta i l'Hospital Santa Caterina de Girona.

El Dr Oscar Campuzano Larrea, professor Agregat de la Facultat de Medicina de la Universitat de Girona i investigador de l'Institut d'Investigació Biomèdica de Girona.

DECLAREM: Que el treball titulat "**Molecular insights on arrhythmogenic cardiomyopathy: assessment of premature termination codons in desmosomal genes and variants reclassification**" que presenta la **Marta Vallverdú Prats** per a l'obtenció del títol de doctor, ha estat realitzat sota la nostra direcció. I, perquè així consti i tingui els efectes oportuns, signem aquest document.

Girona, 2022

Acknowledgements

Primer de tot, vull agrair al Ramon que em donés l'oportunitat de formar part de Gencardio, ha sigut una gran experiència que m'ha permès desenvolupar-me com a científica i créixer en molts sentits. També a la Mireia, moltes gràcies per fer-me de guia, sento que al teu costat he après moltíssim durant tots aquests anys, tant a nivell tècnic per fer els experiments, com a nivell d'expressió escrita amb les teves correccions dels articles i de la tesi. Admiro la teva creativitat científica per pensar nous projectes i experiments alternatius quan les coses no surten i estan encallades. Realment t'estic molt agraïda per haver ideat i confiat en tot el projecte de les HL1, va ser una bona pensada i aquesta tesi n'és la prova. I finalment a l'Oscar per l'oportunitat que em va donar per poder escriure el meu primer article científic i per les teves ràpides respostes.

Evidentment, aquesta tesi no hagués estat possible sense l'ajuda i el suport de tot el grup de Gencardio. Gràcies als ex-predocs Èric i Rebecca, i també als que ben aviat ho seran David, Adrià i Yajaira, per tots els moments compartits intentant ofegar les penes. Especialment al David, per estar tant disposat a col·laborar, quina sort haver pogut comptar amb tu pels registres de calci, junts hem tret un dels resultats més interessants d'aquesta tesi. També al Saul, gracias por tu actitud positiva, trabajadora y paciente. A la Marta, Laura, Mònica, Núria, Alexandra, Ferran, Anna I, Marcel, Marina, per totes les consultes sobre genètica i l'ajuda amb la seqüenciació. A la

Mel·lina, Bernat, Anna F. i Adrià S. per tots sopars que hi van haver en l'època pre-covid. A l'Eli S., el Marcel, la Sara, la Fabi i el Guille per la vostra experiència i ajuda en moments de dubtes. A l'Eli C. per tot el suport a l'hora de fer comandes, enviar paquets o liquidar despeses. I també a tots els estudiants de màster que han col·laborat en projectes associats a aquesta tesi, Marcel, Cristina, Dídac i Natàlia.

To all the people that have helped me in Copenhagen. To Alicia Lundby that gave me the opportunity to be part of Cardiac Proteomic Group for some months. I también a Eduardo, muchas gracias por tu ayuda incondicional con los experimentos y por tener tantas ganas de colaborar siempre. And also, to Mari, our friendship started in Copenhagen, but it has no end, thank you for teaching me a lot about being positive and grateful every day for all the things that I have. I am sure that you will achieve all your goals in your life.

També voldria afegir un agraïment a la gran contribució que fa l'Aleksandra Elbakian obrint l'accés del coneixement a tota la comunitat científica. La recerca biomèdica no avançaria igual sense la seva tasca.

A les genetistes Elena, Laura, Ana, Sara, Mireia i Núria per totes les quedades, els scape rooms, les escapadetes i les converses sobre ciència i no ciència. I també a la Miruna, la genetista més internacional del grup, per les videotrucades i totes les visites.

També a la Yajaira i l'Adrià, per totes les "girl's nights" que mai oblidarem. Al Pau per totes les excursions i propagandes de rellotges

intel·ligents, sacs de dormir i frontals. A la família més bonica de Platja d'Aro, Hugo, Judit i Aran, per tots els dinars, sopars i aniversaris temàtics. I a l'Ivan per tot el suport informàtic i pels trasllats de potes de llits pels carrers de Girona.

A les espluguines Rali, Raquel, Odin i Mercè per ajudar-me a desconnectar de la tesi amb els bons plans que sempre acaben al bar. També pel vostre suport i les vostres preguntes sobre zombis o coses curioses sobre el cos humà que encara no he pogut respondre.

A l'Anna, la meva sardanista preferida, per totes les curses que hem corregut juntes, el recolzament en moments baixos i per compartir la passió per la ciència i també les penes associades a aquesta. Em fa moltíssima il·lusió que siguis la il·lustradora de la portada d'aquesta tesi, gràcies per aquest regal!

A la Txell, la millor pianista de Catalunya, per tots els dinars al costat de l'Hospital que ens han animat la setmana i per totes les trobades a concerts, a casa teva o a casa meva que hi ha hagut i que vindran. I també per la companyia del Jan, per la tranquil·litat que em transmeteu i pels bons consells.

A la família Carrión per tot el suport en la 1a etapa de la tesi, al Gerard per donar-me ànims sempre i creure tant en mi, al Toni per totes les converses interessants sobre feina i no feina i per creure que la recerca biomèdica és important (encara guardo els teus retalls de diari!). I a tots ells i a la Margi per tot el suport logístic en els dies d'estabulari, realment vau ser un gran suport per mi!

Vull agrair també a la Maribel, l'Alfredo, la Candela i la Petrina la bona acollida que sempre he tingut a casa seva i per tots els dinars espectaculars. I a la Isabel i al Carlos per sempre desitjar-me el millor i per totes les xocolates suïsses, realment també han contribuït positivament en aquesta tesi! I evidentment, a l'Àngel, em sento molt afortunada d'haver-te tingut al meu costat durant l'etapa més dura de la tesi. Has estat el meu confident de dubtes, entrebancs, resultats prometedors, disgustos, contratemps, decisions importants, estratègies vitals i de tot el que vingués. Gràcies per totes les abraçades reparadores, els bons consells i per tractar-me amb tanta tendresa i estima sempre.

Als meus quatre padrins, per estimar-me i cuidar-me tant bé, però especialment a la padrina Ernestina, l'única que ha pogut veure l'inici i la culminació d'aquesta tesi. Per tots els ànims que m'has donat i per la certesa i tranquil·litat que m'has transmès de que jo podia amb això i més. Si haguessis viscut a la meva època estic convençuda de que almenys tindries tres tesis. Per totes aquelles dones intel·ligents i treballadores que mai van tenir l'oportunitat ni la llibertat d'escollir el seu camí a la vida ni d'explotar el seu potencial intel·lectual.

A la meva mare, tinc molt clar que sense tu res seria igual, has estat clau en totes les etapes de la meva vida, des de l'inici fins a l'actualitat. T'agraeixo molt especialment tot l'esforç que vas fer per tal que pogués estudiar el que realment m'agradava, Genètica. La situació en aquell moment no era fàcil; gràcies per entendre que

això era important per mi, gràcies per valorar tant els estudis i gràcies per donar-me la llibertat d'escollir. Aquest va ser el punt de partida que ha fet possible que avui existeixi aquesta tesi. Em fa molt feliç que part d'aquesta tesi també hagi estat engendrada a Cal Peret de Senan, a casa nostra i de tants altres Vallverdú. T'agraeixo tot el teu suport, sempre t'he tingut al meu costat quan ho he necessitat i, el més important, tinc la certesa que sempre hi podré comptar.

Pere, estic molt contenta que existeixis a la meva vida, has estat i ets un company crucial en molts moments. En qüestions familiars, sento que ets l'única persona que em pots entendre i que podem compartir dubtes, inquietuds o decisions. M'agrada molt el teu tarannà tranquil, d'anar avançant, però sense estressar-se, pas a pas; em transmets molta calma. Et desitjo molta sort i molts èxits en el teu camí.

I al meu pare, per tots els sopars a Girona, per totes les converses sobre la història de Catalunya i la vida en general, per les ajudes amb tants trasllats de pis i per oferir-me el teu durant unes setmanes. Quina convivència més intensa! En guardo molt bon record, gràcies per oferir-me un punt de vista de les coses diferent al que estic acostumada. M'agrada tenir-te a la meva vida.

Moltes gràcies a tots!

"... i tenia els ulls cansats
de mirar en tots els racons
però, en mirar-lo, el camí
no diu si vas
a la glòria o al fracàs."

Cançó del dubte - Manel

List of original scientific publications

The present thesis is a compendium of research articles based on the following three publications:

Vallverdú-Prats M, Brugada R, Alcalde M. Premature Termination Codon in 5' Region of Desmoplakin and Plakoglobin Genes May Escape Nonsense-Mediated Decay through the Reinitiation of Translation. Int J Mol Sci. 2022 Jan 7;23(2):656.

Impact Factor: 6.208, Q1 (Biochemistry & Molecular Biology)

Vallverdú-Prats M, Carreras D, Pérez G, Campuzano O, Brugada R, Alcalde M. Alterations in calcium handling are a common feature in Arrhythmogenic Cardiomyopathy cell models triggered by desmosome genes loss

Under Review

Vallverdú-Prats M, Alcalde M, Sarquella-Brugada G, Cesar S, Arbelo E, Fernandez-Falgueras A, et al. Rare Variants Associated with Arrhythmogenic Cardiomyopathy: Reclassification Five Years Later. J Pers Med. 2021 Feb 26;11(3):162.

Impact factor: 3.508, Q2 (Health Care Sciences & Services)

Other scientific publications derived from this Thesis:

Sarquella-Brugada G, Fernandez-Falgueras A, Cesar S, Arbelo E, Coll M, Perez-Serra A, et al. Clinical impact of rare variants associated with inherited channelopathies: a 5-year update. Hum Genet [Internet]. 2021 Sep 21 [cited 2021 Nov 3]; Available from: https://link.springer.com/10.1007/s00439-021-02370-4

Martínez-Barrios E, Sarquella-Brugada G, Pérez-Serra A, Fernández-Falgueras A, Cesar S, Coll M, et al. Discerning the Ambiguous Role of Missense TTN Variants in Inherited Arrhythmogenic Syndromes. J Pers Med. 2022 Feb 8;12(2):241.

Oliva A, Grassi S, Pinchi V, Cazzato F, Coll M, Alcalde M, et al. Structural Heart Alterations in Brugada Syndrome: Is it Really a Channelopathy? A Systematic Review. J Clin Med. 2022 Jul 28;11(15):4406.

Coll M, Fernandez-Falgueras A, Iglesias A, del Olmo B, Nogue-Navarro L, Simon A, et al. Unpredicted Aberrant Splicing Products Identified in Postmortem Sudden Cardiac Death Samples. Int J Mol Sci. 2022 Oct 20;23(20):12640.

Abbreviations

ACE-I	Angiotensin-Converting-Enzyme Inhibitors
ACM	Arrhythmogenic Cardiomyopathy
AJ	Adherens Junction
ALVC	Arrhythmogenic Left Ventricular Cardiomyopathy
ARB	Angiotensin II Receptor Blockers
ARVC	Arrhythmogenic Right Ventricular Cardiomyopathy
ATP2A2	Calcium ATPase 2
AV	AtrioVentricular
B	Benign
BA1	Benign Stand-Alone
BiVACM	BiVentricular Arrhythmogenic Cardiomyopathy
bp	base pairs
BP1-6	Benign Supporting
BrS	Brugada Syndrome
BS1-4	Benign Strong
CAP	Cardiac Action Potential
Cas	CRISPR-associated
CDH2	Cadherin2
C/EBPα	CCAAT enhancer-binding protein-α
CPVT	Catecholaminergic Polymorphic Ventricular Tachycardia
CRISPR	Clustered Regularly Interspaced Short Palindromic Repeats
crRNA	CRISPR RNA
CTNNA3	Catenin-α3
Cx43	Connexin43
DCM	Dilated Cardiomyopathy
DES	Desmin
Dvl	Dishevelled
DSB	Double-Strand Break
DSC2	Desmocollin2
DSG2	Desmoglein2
DSP	Desmoplakin
ECG	Electrocardiogram
EJC	Exon Junction Complex

FLNC	Filamin C
fQRS	Filtered QRS
GJ	Gap Junction
GSK-3β	Glycogen Synthase Kinase 3β
HCM	Hypertrophic Cardiomyopathy
HDR	Homology-Directed Repair
HF	Heart Failure
hiPSCs	human induced Pluripotent Stem Cells
ICD	Implanted Cardioverter Defibrillator
IDs	Intercalated Disks
IF	Intermediate Filaments
IHD	Ischaemic Heart Disease
ITFC	International Task Force Criteria
JUP	Junction Plakoglobin
KO	KnockOut
LA	Left Atrium
LB	Likely Benign
LBBB	Left Bundle-Branch Block
LMNA	Lamin A
LP	Likely Pathogenic
LQTS	Long QT Syndrome
LV	Left Ventricle
LVNC	Left Ventricular Non-Compaction Cardiomyopathy
MAGUK	Membrane-Associated Guanylate Kinase
MAPK	Mitogen-Activated Protein Kinase
miRNA	microRNA
NCX	Sodium-Calcium Exchanger
NHEJ	Non-Homologous End Joining
NMD	Nonsense Mediated mRNA Decay
P	Pathogenic
PAM	Protospacer Adjacent Motif
PG	Plakoglobin
PKP2	Plakophilin2
PLN	Phospholamban
PM1-6	Pathogenic Moderate
PP1-5	Pathogenic supporting

PPARɣ	Peroxisome Proliferator-Activated Receptor-Ɣ
PS1-4	Pathogenic Strong
PTC	Premature Termination Codon
PVS1	Pathogenic Very Strong
RA	Right Atrium
RCM	Restrictive Cardiomyopathy
ROS	Reactive Oxygen Species
RV	Right Ventricle
RVOT	RV Outflow Tract
RyR2	Ryanodine Receptor 2
SA	SinoAtrial
SAECG	Signal-Averaged ECG
SCD	Sudden Cardiac Death
SCN5A	Sodium Channel $Na_v1.5$
SERCA	Sarcoplasmic Reticulum Ca-ATPase
sgRNA	single guide RNA
SQTS	Short QT Syndrome
SR	Sarcoplasmic Reticulum
TALEN	Transcription and Activator-Like Effector Nuclease
TAZ	Transcriptional co-Activator with PDZ-binding motif
TEAD	TEA Domain family member
TGFβ3	Transforming Growth Factorβ3
TMEM43	Transmembrane protein 43
TNF	Tumour Necrosis Factor
TrJ	Transitional Junction
TTN	Titin
T tubules	Transverse tubules
VGSC	Voltage-Gated Sodium Channels
VT	Ventricular Tachycardia
VUS	Variant Uncertain Significance
WT	Wild Type
YAP	Yes Associated Protein
ZFN	Zinc-Finger Nuclease
ZO-1	Zona Occulens-1

Index of figures

Index of tables

Index of contents

Resum

La cardiomiopatia arritmogènica (CA) és una entitat que agrupa diverses formes clíniques de malalties cardíaques hereditàries associades a arrítmies ventriculars i mort sobtada cardíaca. La majoria de casos estan caracteritzats per la substitució dels cardiomiòcits per teixit fibro-adipós. Les variants genètiques rares en gens desmosomals són la principal causa genètica, tot i que altres gens no-desmosomals també estan associats a la CA. El diagnòstic de la malaltia es basa en els "International Task Force Criteria" que inclouen diversos paràmetres per complir els criteris majors i/o menors per tal d'obtenir un diagnòstic definitiu, "borderline" o possible. La història familiar i el diagnòstic genètic és un d'aquests paràmetres, per la qual cosa hi ha cada vegada més estudis centrats en descriure el paper de les variants genètiques i les alteracions moleculars associades a aquestes. Tot i això, encara queden incerteses per resoldre en aquesta direcció.

La present tesi té l'objectiu de descriure els mecanismes moleculars i les conseqüències funcionals desencadenades pels codons stop prematurs (CSP) en gens desmosomals utilitzant una línia cel·lular editada per CRISPR com a model de la CA. A més a més, també té com a objectiu determinar quin impacte tenen les dades actualitzades sobre les variants genètiques associades a la CA en la seva classificació.

Els nostres resultats en el model cel·lular mostren que els CSP a la regió 5' de *DSP* i *JUP* desencadenen el reinici de la traducció gràcies al context genòmic d'ATGs alternatius dins del marc de lectura mentre que els CSP situats a la regió 5' de *PKP2, DSG2* i *DSC2* activen el "nonsense-mediated decay" causant l'absència de l'expressió proteica associada a un efecte més patogènic. Funcionalment, l'absència dels gens desmosomals estudiats desencadena alteracions en el cicle de calci. Específicament, la pèrdua de *PKP2, DSG2* i *DSC2* causa una major amplitud del pic de calci mentre que la pèrdua de *DSP* desencadena una recaptació del calci més ràpida amb una menor amplitud del pic. Finalment, aquesta tesi també descriu com les noves dades generades sobre les variants genètiques associades a CA, com ara les freqüències globals actualitzades, contribueixen a reduir la incertesa en termes de classificació de variants.

En resum, tot i que la fisiopatologia de la CA sigui complexa i hi hagi encara forces qüestions per resoldre, la present tesi desemmascara alguns mecanismes moleculars patofisiològics claus de la malaltia assenyalant noves direccions que valen la pena ser explorades en futurs estudis de CA.

Resumen

La cardiomiopatía arritmogénica (CA) es una entidad que agrupa diversas formas clínicas de enfermedades cardíacas hereditarias asociadas a arritmias ventriculares y muerte súbita cardíaca. La mayoría de casos están caracterizados por la sustitución de los cardiomiocitos por tejido fibro-adiposo. Las variantes genéticas raras en genes desmosomales son la principal causa genética, aunque otros genes no-desmosomales también están asociados con la CA. El diagnóstico de la enfermedad se basa en los "International Task Force Criteria" que incluyen varios parámetros para cumplir los criterios mayores y/o menores a fin de obtener un diagnóstico definitivo, "borderline" o posible. La historia familiar y el diagnóstico genético es uno de estos parámetros, por eso cada vez hay más estudios centrados en describir el papel de las variantes genéticas y las alteraciones moleculares asociadas a estas. Si embargo, aún quedan incertidumbres para resolver en esta dirección.

La presente tesis tiene como objetivo describir los mecanismos moleculares y las consecuencias funcionales desencadenadas por los codones stop prematuros (CSP) en genes desmosomales utilizando una línea celular editada por CRISPR como modelo de la CA. Además, también tiene como objetivo determinar cual es el impacto de los datos actualizados sobre las variantes genéticas asociadas a la CA en su clasificación.

Nuestros resultados en el modelo celular muestran que los CSP en la región 5' de *DSP* y *JUP* desencadenan el reinicio de la traducción gracias al contexto genómico de ATGs alternativos dentro del marco de lectura mientras que los CSP situados en la región 5' de *PKP2, DSG2* y *DSC2* activan el "nonsense-mediated decay" causando la ausencia de la expresión proteica asociada a un efecto más patogénico. Funcionalmente, la ausencia de los genes desmosomales estudiados desencadena alteraciones en el ciclo de calcio. Específicamente, la pérdida de *PKP2, DSG2* y *DSC2* causa una mayor amplitud del pico de calcio mientras que la perdida de *DSP* desencadena una recaptación del calcio más rápida con una menor amplitud del pico. Finalmente, esta tesis también describe como los nuevos datos generados sobre las variantes genéticas asociadas a CA, como por ejemplo las frecuencias globales actualizadas, contribuyen a reducir la incertidumbre en términos de clasificación de variantes.

En resumen, aunque la fisiopatología de la CA sea compleja y haya aun varias cuestiones por resolver, la presente tesis desenmascara algunos mecanismos moleculares patofisiologicos claves de la enfermedad señalando nuevas direcciones que valen la pena ser exploradas en futuros estudios de CA.

Summary

Arrhythmogenic cardiomyopathy (ACM) is an entity that groups different clinical forms of hereditable cardiac diseases that are associated to ventricular arrhythmia and sudden cardiac death. The main cases are characterized by the substitution of cardiomyocytes with fibro-fatty tissue. Rare genetic variants in desmosomal genes are the principal genetic cause, but some non-desmosomal genes are also associated with ACM. Its diagnosis is based on "International Task Force Criteria" that include several parameters to fulfil major and minor criteria to obtain definitive, borderline or possible diagnosis. The family history and genetic diagnosis is one of these parameters, so many studies are increasingly focused on describing the role of genetic variants and its associated molecular alterations. However, there are still uncertainties to be answered on that direction.

The present thesis has the aim to describe the molecular mechanisms and functional consequences triggered by premature termination codons (PTC) in desmosomal genes using a CRISPR edited cellular line as an ACM model. Moreover, it also aims to determine how updated data of genetic ACM-associated variants impacts its classification.

Our results on the cellular model showed that a PTC in 5' region of *DSP* and *JUP* triggers reinitiation of translation due to an optimal genomic context of alternative ATG in-frame while PTC in 5' located

in *PKP2, DSG2* and *DSC2* activates nonsense-mediated decay causing the absence of the protein expression associated to a more deleterious effect. Functionally, the absence of the studied desmosomal genes triggered alterations in calcium handling. Specifically, the loss of *PKP2, DSG2* or *DSC2* causes a higher amplitude of the calcium peak while *DSP* loss triggers a quicker calcium uptake with a shorter amplitude of the peak. Finally, this thesis also described that new data of genetic variants associated to ACM, such as updated global frequencies, contribute to reduce the uncertainty in terms of variant classification.

 In summary, although ACM physiopathology is complex and there are still lots of questions to be solved, the present thesis elucidated some of the key molecular pathophysiological mechanisms underlying the disease pointing into some directions worth to be explored in future ACM studies.

I. INTRODUCTION

1. The heart

1.1. Structure and function of the heart

The heart is a vital organ that pumps blood through the whole body to maintain the oxygen and nutrients homeostasis in all tissues. It is covered by the pericardium, a protective sac composed of an outer layer, the fibrous pericardium made by connective tissue, and an inner layer, the serous pericardium that is divided into an outer or parietal layer and an inner or visceral layer which is also known as epicardium. Between the parietal layer and epicardium, there is the pericardial cavity which contains a small amount of serous pericardial fluid (1) (Figure 1).

Moreover, the heart is composed of three layers (from outside to inside): epicardium, myocardium and endocardium. Epicardium contains basically fat tissue and the main coronary blood vessels that supply and drain blood to and from the heart. The myocardium is the thicker layer of the heart and it is composed of cardiac muscle that has the specific ability to contract and pump blood outside the organ. Finally, the endocardium covers the inside cavities of the heart and all the associated valves and it is composed of simple squamous epithelial tissue and connective tissue (1) (Figure 1).

The heart contains 4 chambers: Right atrium (RA), right ventricle (RV), left atrium (LA) and left ventricle (LV) (Figure 1). The right and left parts are separated by a muscle wall called the septum. The atrium is the top part and ventricles are located below the atrium.

In a normal heart, blood flows from the atria to the ventricles, never the other way thanks to atrioventricular valves: tricuspid and bicuspid/mitral valve. The tricuspid valve is located between the atrium and the ventricle of the right part of the heart and it has three cusps whereas the bicuspid or mitral has two cusps and it is located on the left part. Finally, semilunar valves allow blood to flow from RV to the pulmonary artery and from the LV to the aorta, each of them has three cusps (Figure 1). Valves are made of the endocardium layer reinforced by dense connective tissue (1).
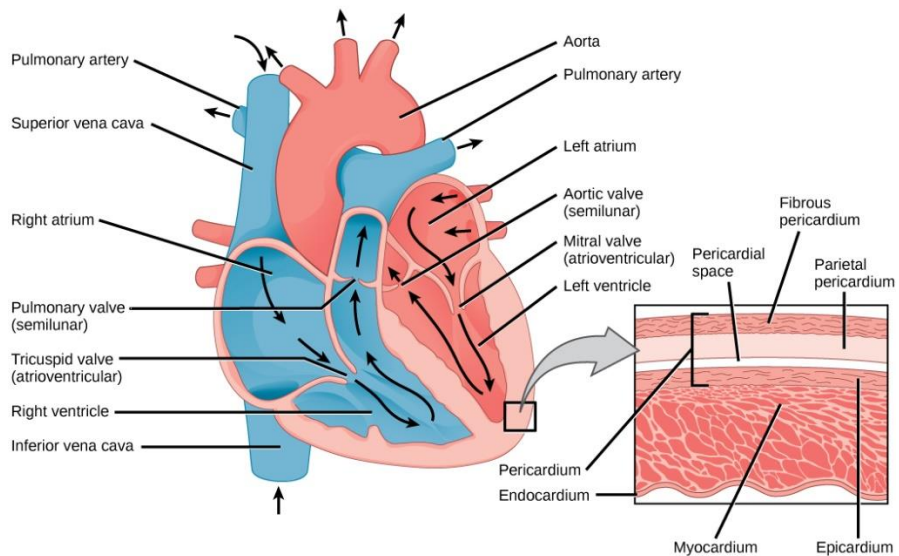
Figure 1. Anatomical heart structure and the blood flow. Image from Lumen Learning (2).

Blood circulates in a closed system of vessels, pumped from the heart out to elastic arteries that will lead to tiny capillaries and

through veins back again to the heart. The path of blood inside the heart can be divided into 4 steps (Figure 1):

1. Blood enters the atria.

Oxygen-poor blood from the body flows into the RA through superior and inferior vena cava and newly oxygenated blood from the lungs flows into the LA through pulmonary veins. Approximately 75% of this blood in the atria passes into the ventricle before atrial contraction.

2. Blood is pumped into the ventricles

Atria contracts and blood remaining in the atria is forced through the atrioventricular valves into the relaxed ventricles.

3. Atria relaxes and ventricles are still relaxed filled with blood.
4. Ventricles contract sending blood to the body (systemic circulation) and lungs (pulmonary circulation).

The ventricular contraction generates pressure that closes the atrioventricular valves while opening the semilunar valves leading out of the ventricles. The RV forces blood low in oxygen out through pulmonary arteries to the lungs and the LV pumps the newly oxygenated blood through the aorta to the body. RV and LV pump simultaneously and force equal volumes of blood to leave the heart. However, the wall of LV is thicker than RV because it has to be strong enough to supply blood to all parts of the body, whereas RV supplies blood only to the lungs (1). Contraction is also known as systole, while diastole regards muscle relaxation.

1.2. Electrical properties of cardiomyocytes

Cell membranes have an electrochemical gradient across the phospholipid bilayer that is maintained by protein channels. These channels allow selective movement of sodium, potassium and calcium ions between the inner and outer space of the cardiomyocytes that generate the cardiac action potential (CAP). CAP travels through the heart, each cardiac muscle cell produces and conducts its CAP and it can be divided into five phases (Figure 2):

    0- Depolarization phase

There is an inward movement of sodium ions through fast voltage-gated sodium channels (VGSC) which causes the membrane potential to reverse from a resting of -90mV to a potential of about +30mV.

    1- Early repolarization phase

Partial repolarization occurs due to a rapid decrease in sodium-ion entrance as the fast sodium channels close.

    2- Plateau phase

Positively charged calcium ions enter the cell through an L-type calcium channel, a slow voltage-gated calcium channel. This entrance of Ca^{2+} activates Ca^{2+} release from the sarcoplasmic reticulum (SR) causing a large increase in cytosolic Ca^{2+} that will trigger muscle contraction. Moreover, this high concentration of

cytosolic Ca^{2+} prevents the membrane from returning to its normal electrical potential. Moreover, membrane permeability to potassium decreases as the slow potassium channels close, so less potassium will leave the cell, contributing also to the plateau phase.

3- Repolarization phase

Calcium ion channels close (calcium ion stop entering into the cell) and potassium ion channels reopen (potassium ion move out). This increasing negativity will lead the membrane to its normal resting potential.

4- Resting potential phase

The cell membrane returns to its normal resting potential of -90mV.
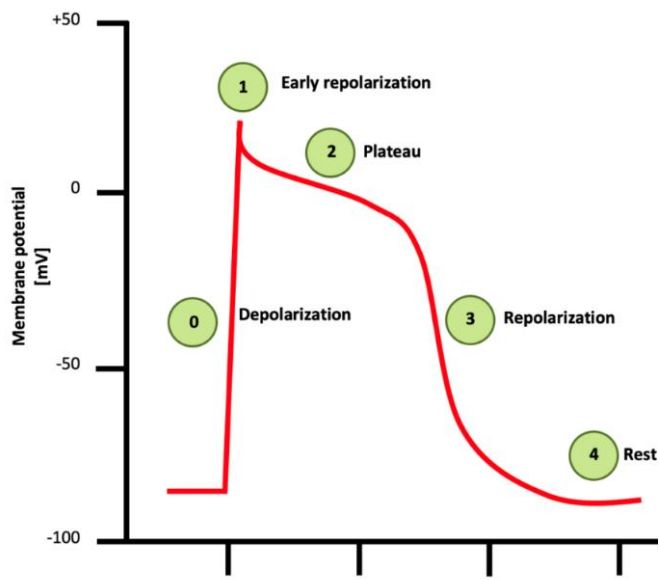
Figure 2. Phases of the cardiac action potential. Adapted from 2007 Pearson Education, Inc publishing as Benjamin Cummings (3).

1.3. Heart conduction system

All cardiomyocytes transmit CAP, but specific cells are required to initiate it, and these are the autorhythmic pacemaker cells. Pacemaker cells initiate and establish the rhythm for the heartbeat independently of the central nervous system. The electrical stimulation starts in the sinoatrial (SA) node, a specialized heart muscle tissue mass located in the superior wall of RA that controls its rhythm (Figure 3). SA node is the normal pacemaker of the heart because its inherent rhythmicity is faster than any other area of the heart. SA node shows spontaneous depolarization at regular intervals, 70 to 80 times a minute.
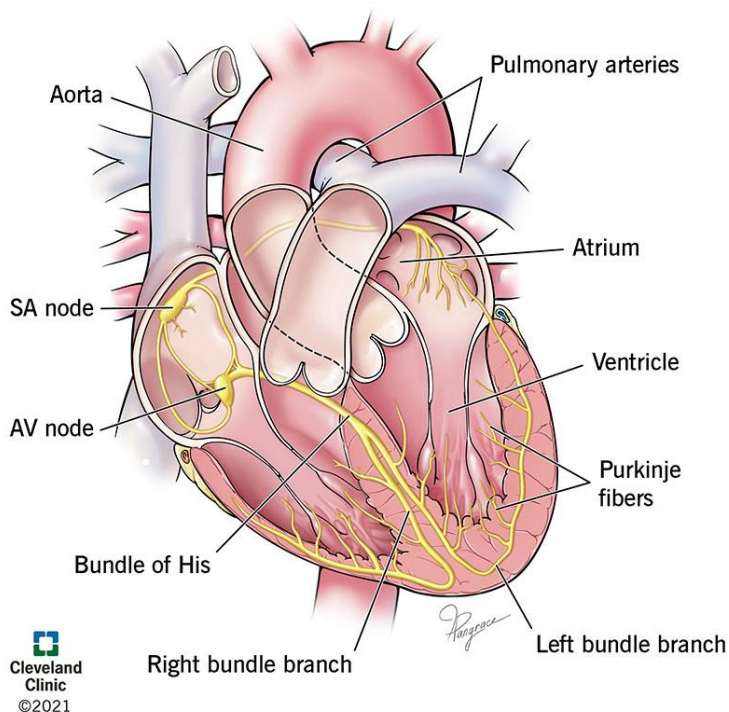
Figure 3. Electrical conducting system of the heart. Image from Cleveland clinic (4)

This depolarization is transmitted through the right and then left atrium thanks to specialized cell unions in cardiomyocytes: the intercalated disks (IDs). Atrium contracts due to this electrical stimulation that continues and reaches the atrioventricular (AV) node (Figure 3). AV node lies at the base of RA, between the atrium and ventricle and delays the conduction of electrical activity of about a second before allowing it to pass into the ventricles. If the SA node is damaged, the AV node may become the pacemaker, beating between 40-50 beats per minute.

Electrical conduction continues from the AV node to the atrioventricular bundle, also known as the bundle of His that runs for a short distance and then divides into two branches, right and left, which spread along the septum, one branch for each ventricle (Figure 3). When the branches reach the apex of ventricles, they divide into hundreds of specialized cardiac muscle fibres called cardiac conducting myofibers or Purkinje fibres that follow along the muscular walls of ventricles (Figure 3). These fibres rapidly direct the electrical impulse in a definite pathway making possible a coordinated contraction. These conducting myofibers are modified cardiac muscle cells that conduct CAP at a higher velocity than normal ones and have feeble contractile properties. If the SA and AV nodes are ineffective, the AV bundle, bundle branches or cardiac conducting myofibers may take over pacing the heart, but their inherent rhythmicity is very slow -20 to 40 beats per minute. If this condition occurs, an artificial pacemaker may be required (1).

1.4. Electrocardiogram

The rhythm and the CAP that circulates through the heart can be measured by electrocardiogram (ECG). Thanks to electrical current, CAP spreads from the heart into adjacent tissues and also reaches the surface of the body, it is possible to perform an ECG by placing electrodes on the skin of the left anterosuperior part of the chest. ECG produces a recording of the electrical waves of the heart (Figure 4):

- P wave: represents the electrical potentials generated by atrium depolarization before the atrial contraction begins.
- QRS complex: it contains three different waves (Q, R and S waves) and is caused by potentials generated when the ventricles depolarize before contraction.
- T wave: represents the potentials generated during the repolarization of ventricles (3).
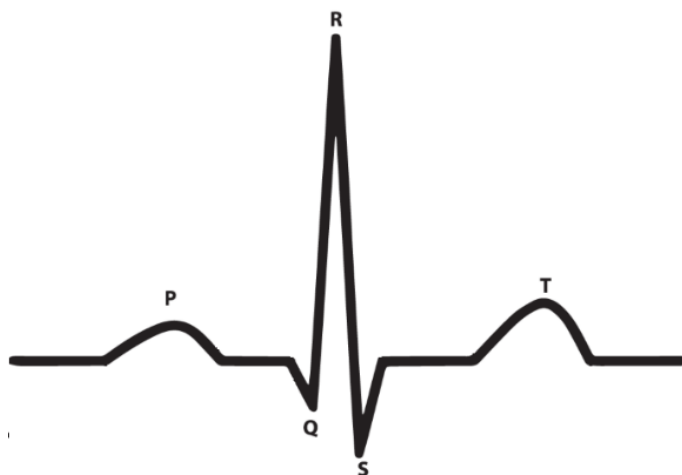
Figure 4. Waves of a normal ECG. Adapted from Zheng et al., 2020 (6).

2. Structure and functionality of cardiomyocytes

2.1. The sarcomere and cell contraction

Cardiomyocytes are single striated cells that contract rhythmically and involuntary. They present a centrally located nucleus and a large number of mitochondria, which provide a constant source of ATP. When viewed with a light microscope, cardiomyocytes show a pattern of alternating light and dark bands corresponding to the I band (actin filaments) and the A band (actin and myosin filaments overlapped) (Figure 5). Cutting across each I band there is a dark Z line that marks the beginning and the end of the fundamental unit of muscle contraction: the sarcomere (1). Muscle contraction occurs when sarcomere shortens due to myosin heads binding to actin filaments and pulling them inwards (2). This action requires ATP and it is triggered by the binding of Ca^{2+} to troponin C. Therefore, the major factor that regulates contraction is the amount of intracellular Ca^{2+} that binds troponin C (4). This intracellular Ca^{2+} comes from the opening of the L-type calcium channel in the cell membrane and the Ca^{2+} release from SR in phase 2 of CAP.
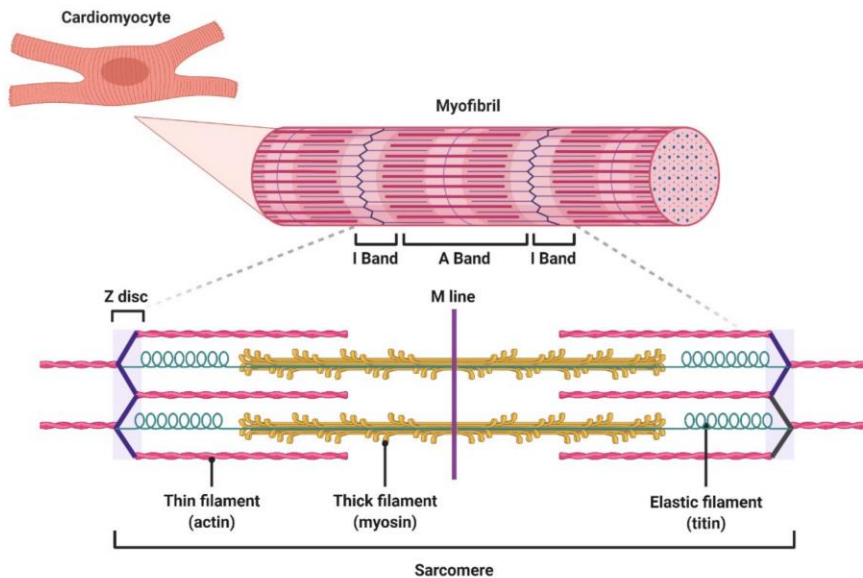
Figure 5. Sarcomere structure of cardiomyocytes. Image from Santiago et al., 2021 (8).

2.2. Excitation-contraction coupling and calcium cycle

Excitation-contraction coupling links the electrical excitation of CAP to muscle contraction. Transverse tubules (T tubules) and dyads are crucial structures that make possible this coupling. T tubules are invaginations of cell membrane rich in several ion channels and they are paired with a terminal cisterna of the SR to form the dyad. When depolarization of cell membrane occurs, L-type Ca channels that are located in T tubules open and a small amount of Ca^{2+} enters the cell. Because of the dyad structure, this Ca^{2+} enters close to SR and binds ryanodine receptors (RyR). This binding will cause RyR opening and a great amount of Ca^{2+} releasing from SR to the cytosol (Figure 6). This process is known as calcium-induced calcium release (4).

Intracellular Ca^{2+} will bind troponin C and muscle contraction will be triggered.

The proper cardiac function requires adequate regulation of intracellular Ca^{2+} concentration. Achieving high levels of intracellular Ca^{2+} during systole is as important as managing a quick intracellular Ca^{2+} decrease during diastole for an adequate muscle relaxation that will allow the heart to be refilled again with blood. For that reason, after contraction, Ca^{2+} must be removed from the cytoplasm. Therefore, RyRs closes and Ca^{2+} are pumped back into SR by SR Ca-ATPase (SERCA) and out of the cell largely by the sodium-calcium exchanger (NCX) (4). The activity of SERCA is controlled by Ca^{2+} and phospholamban (PLN), an inhibitor of SERCA in its unphosphorylated state (5). Moreover, NCX pumps Ca^{2+} out of the cell by exchanging it by three Na^+ ions generating an electric current. These processes regarding the release and reuptake of Ca^{2+} is known as calcium cycling (Figure 6).

To maintain the Ca^{2+} flux balance of the cycle, the amount of Ca^{2+} entering the cell must be equal that pumped out, and the amount released from SR must be equal that taken back to SR (5). A disequilibrium of these fluxes may cause changes in the Ca^{2+} content of the SR and this would lead to variability in the amplitude of cytoplasmic Ca^{2+} concentration that mainly controls the contractibility of the heart. If the Ca^{2+} content of the SR exceeds a threshold level, Ca^{2+} released diffuses to the next region of the SR propagating wave of Ca^{2+}induced - Ca^{2+} release contributing to

arrhythmias. So, a proper regulation of the Ca^{2+} flux balance is important for the correct heart beating (5).
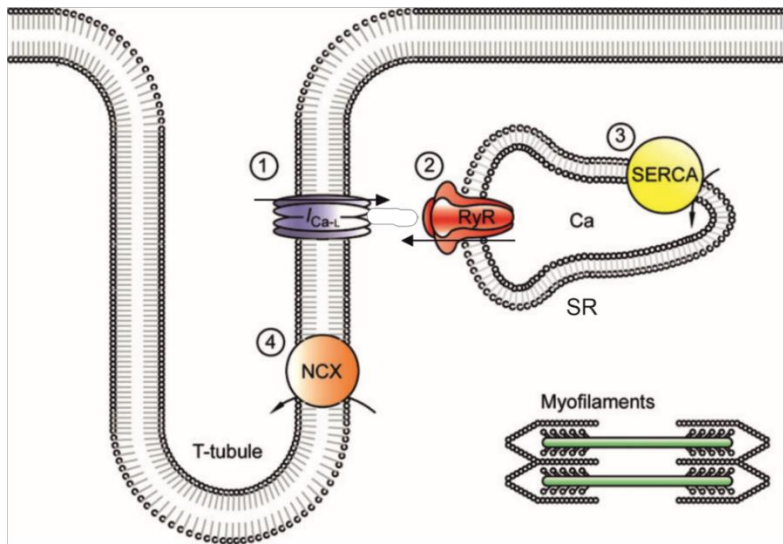
Figure 6. Calcium cycling and regulation of intracellular calcium concentration. Adapted from Eisner 2014 (9).

2.3. Cell unions: Intercalated disks

Cardiac muscle functions as a coordinated unit in response to physiological stimulation due to a complex structure that connects and joins together adjacent cardiomyocytes: the cardiac ID. Cardiomyocytes act as a functional syncytium, both electrically and mechanically thanks to ID which also play a role in signalling cascades due to their close connection with the cytoskeleton. IDs are composed of three main structures: Gap junctions (GJs), Adherens junctions (AJs) and Desmosomes. Moreover, several proteins such as ion channels that are not related to cell unions

reside in IDs, specifically K_v channels, Kir channels and Na_v channels (6) (Figure 7).
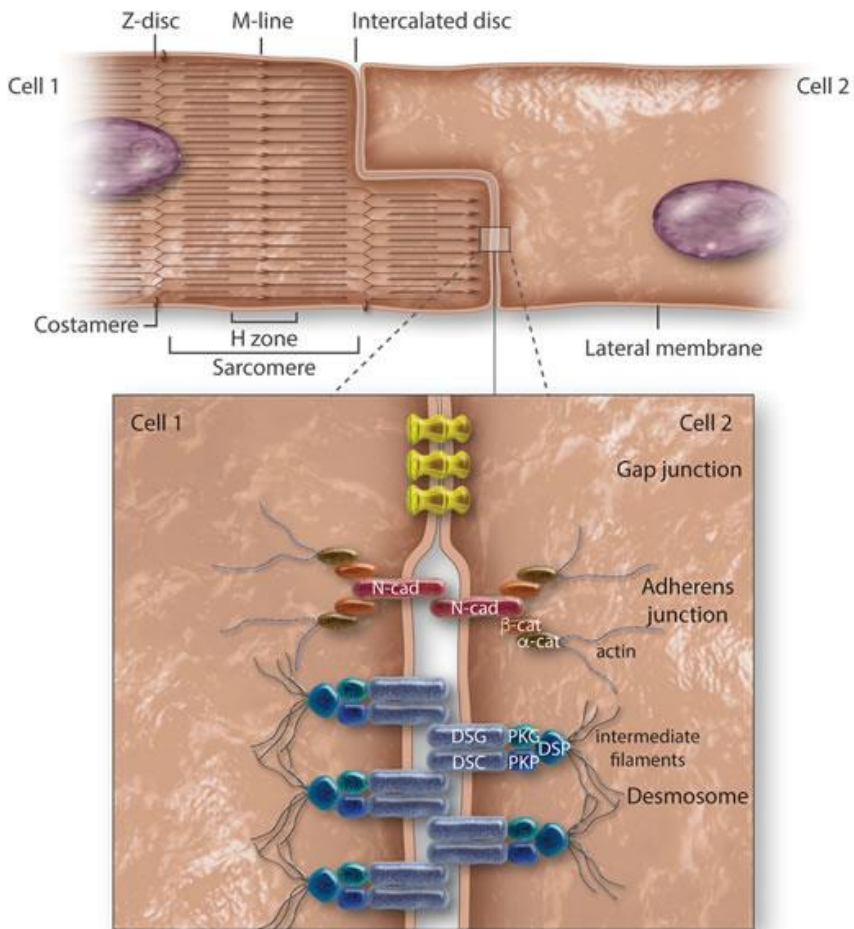
Figure 7. Representation of IDs in cardiomyocytes. They are composed of GJ, AJ and desmosomes. Image from Vermij et al., 2017 (10)

2.3.1. Gap junction

GJ couple cells electrically enabling conduction of the action potential with low resistance between adjacent cells (6,7). Moreover, GJ also connects cells metabolically allowing small solutes to pass between them. Commonly, GJ is constituted by 12 connexins, 6 molecules from a connexon per cell. The most frequent connexin in ventricular cardiomyocytes is connexin43 (Cx43) which is also crucial for the correct function of the sodium channel and can be found in mitochondria too (6).

Recently, it has been identified the Perinexus, an area around GJs where free connexons interact with zona occulens-1 (ZO-1), a member of the membrane-associated guanylate kinase (MAGUK) family that have roles in channel clustering, trafficking, signalling, and cell polarity (6,8). It is accepted that GJ is surrounded by a perinexal scaffold containing ZO-1 that controls Cx43 GJ size and, indirectly, its function (8).

2.3.2. Adherens junction

AJ transmit mechanical forces from cell to cell by connecting the actin cytoskeleton allowing the cell to retain shape upon mechanical stress. Its main constituent is N-cadherin that interacts with the same cadherins from adjacent cells to form homodimers in the extracellular space. This binding between the same cadherins provides tissue specificity during development. Moreover, N-

cadherin can interact with β-catenin, APC/Axin/GST complex and p120-catenin and it can be associated with vinculin and hXinα and hXinβ having also regulatory functions (6).

2.3.3. Desmosomes

Desmosomes hold the cells together functioning as cell anchors through a robust connection with intermediate filaments (IF). They are mainly located in tissues that suffer high mechanical stress such as the epidermis or myocardium and they are constituted by five proteins belonging to three different families: cadherins, armadillo proteins and plakins.

2.3.3.1.   Cadherins: Desmoglein (DSG) and desmocollin (DSC)

DSGs and DSCs are single-pass transmembrane cadherins that bind in a heterologous way. They present high homology to E-cadherin, the ancestor of cadherins. Their processed extracellular domain is composed of five extracellular cadherin repeat domains with three calcium-binding sites. Then, a single transmembrane domain links the extracellular part with a cytoplasmic tail. This cytoplasmic domain is where the principal differences between DSGs and DSCs reside. The intracellular membrane-proximal part is common for both proteins (except for short DSCb splice variants), and it consists of an anchor domain and intracellular cadherin segment domain. Then, only DSGs present an intracellular proline-rich linker region, a

repeated unit domain containing different numbers of 29±1 amino acid repeats, and a glycine-rich DSG-terminal domain at the C terminus (9) (Figure 8). The cardiac cadherins are DSG2 (122,3KDa) and DSC2 (99,9KDa).

2.3.3.2. Armadillo proteins: Plakoglobin (PG) and plakophilin (PKP)

Armadillo proteins mediate the desmosomal attachment by binding cadherins with desmoplakin (6). They are composed of a basic N-terminal head domain followed by armadillo repeats, that consist of a 42 amino-acid repeat motif, and a short C-terminal tail (Figure 8). Moreover, they have also been localized in the nucleus which may indicate a regulatory role in specific signalling pathways. On the one hand, PG (81,7KDa) binds desmosomal cadherins at the intracellular cadherin segment and it also acts as an adaptor to assemble further plaque proteins. Additionally, PG can also be found in adherens junctions linking E-cadherin to actin. Furthermore, as its structure is similar to β-catenin, it has been suggested that activates transcription in association with LEF-1/TCF (9). On the other hand, PKPs interact with desmoplakin and desmosomal cadherins. PKPs have also been detected in the nucleus and they may have a regulatory role apart from their structural role in desmosomes (10). PKP2 (97,4KDa) is the only isoform expressed in the myocardium.

2.3.3.3.   Plakins: Desmoplakin (DSP)

DSP connects the desmosome to desmin. Its N-terminus is a globular domain that binds to desmosomal cadherins through PG and PKPs. On the other side, globular C-terminus binds to intermediate filament desmin (9). In the middle, there is the Rod domain which is a coiled-coil domain involved in homodimerization (Figure 8). There are two isoforms of DSP protein, DSP1 (331,7KDa) and DSP2 (260KDa) generated by alternative splicing. DSP2 lacks parts of the Rod domain and it is thought to form monomers. In the myocardium, DSP1 is abundant, while DSP2 has minimal expression in that tissue (11).
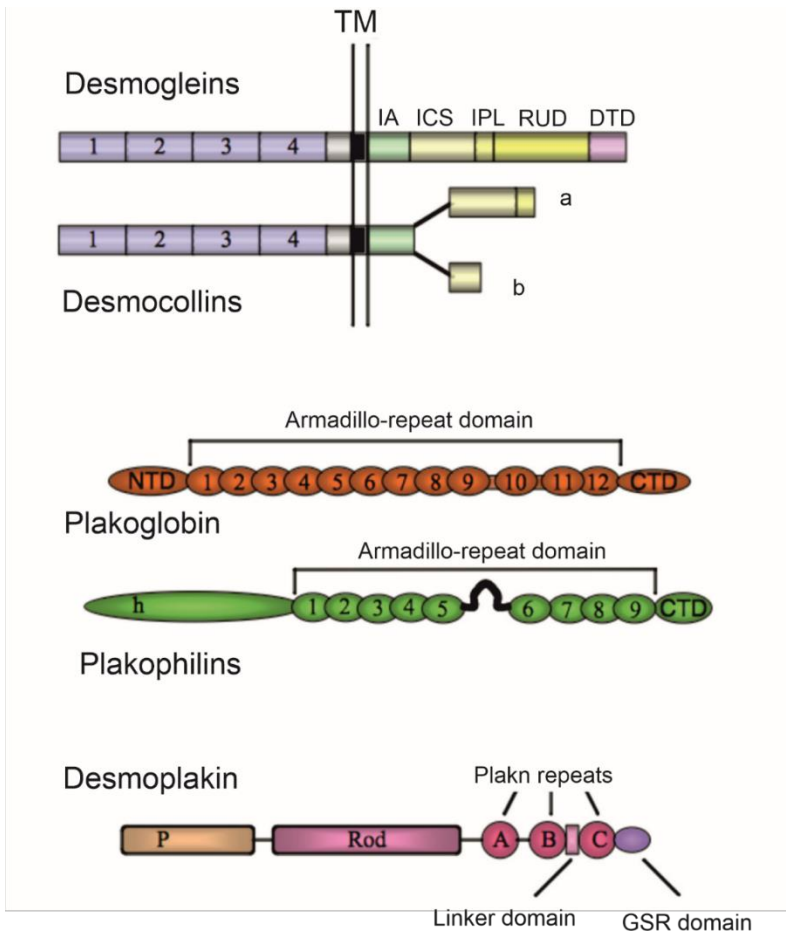
Figure 8. Structure of desmosome proteins. Adapted from Cirillo, 2016 (13).

*Abbreviations: **IA**, intracellular anchor; **ICS**, intracellular cadherin segment; **IPL**, intracellular proline-rich linker; **RUD**, repeated unit domain; **DTD**, desmoglein-terminal domain; **TM**, trans-membrane motif; **GSR**, glycine-serine-arginine rich.*

2.3.3.4.   Desmosome assembly and disassembly

Apart from structural components of desmosomes, there are accessory proteins including kinases, phosphatases, and caspases that play an important role in the assembly and disassembly of desmosomes (9). Disruption of desmosomes is an organized process that can occur in the early stages. However, after maturation, this process becomes more difficult to occur due to the "hyperadhesion" state of mature desmosomes. There is a regulatory subnet that regulates these dynamic processes and modulates activation and inhibition of desmosome formation by multiple signalling interactions (9).

In desmosome formation, membrane assembly occurs first and it is followed by the cytoplasmic plaque assembly. DSC2 may initiate desmosome assembly by being transported in vesicles to the plasma membrane. This transportation requires PKP2 for kinesin-2, a motor protein that controls vesicle trafficking of DSC2. Then, vesicles rich in DSG2 traffic to the membrane by kinesin-1 (9,12). DSC2 and DSG2 transportation to the membrane depends on microtubules and they localize into cholesterol-rich raft domains. Once at the membrane, the DSG2 C-terminus stabilize cadherin tail-tail interactions that mediate its dimerization with DSC2 (12,13). It is known that extracellular calcium is needed for desmosomal cadherins to be clustered and become more stabilized. Cytoplasmic plaque assembly is initiated by cell-cell contact and starts with DSP accumulation near the newly forming contact at the same time

DSG2 appears. Then, DSP associates with desmin and finally this complex is translocated to cell-cell contacts (9,12).

2.3.4. Collaboration in IDs: new functional unit terms

Some new terms have been created to name collaborations in ID involving great diversity of proteins. On one side, connexome and area composita regard functional units of ID components that are connected working together and sharing accessory proteins. On the other side, transitional junctions point out a collaboration between different structures in cardiomyocytes: IDs and sarcomeres.

- Connexome

Connexome is constituted by the VGSC complex, Cx43 and desmosomes. All these structures constitute a functional unit that regulates excitability, cell-cell adhesion and intercellular contact (6,14).

- Area composita

Area composita classically was constituted by AJ and desmosomes, which were detected as one structure with electron microscopy. However, nowadays, it also includes GJ and ion channels. ID is one functional unit in which all structures interact with each other to make cardiac tissue become an operative syncytium (6).

- Transitional junction

Transitional junction (TrJ) is a region of IDs that is junction-free, where there are no transmembrane proteins and sarcomeres are connected to the membrane. The TrJ is the proposed site for sarcomerogenesis, where myofibrils are elongated and the cardiomyocyte grows longitudinally. This region is an anchor for new filaments, incorporating titin and subsequently maturing into a Z-disc (6,15).

3. Sudden Cardiac Death

3.1. General characteristics of Sudden Cardiac Death

Sudden Cardiac Death (SCD) is defined as decease within 1 hour after the first symptoms of cardiac disease or, if the demise is unwitnessed, within 24 hours of last being seen alive and without any health problem (16–20). Affecting more than 5 million people per year, SCD is the most common cause of death worldwide and, therefore, one of the most important public health issues (17,18,21). The incidence of SCD increases with age being adults the most affected. In Western countries, the annual incidence is between 50-100 cases per 100.000 persons (17).

SCD risks factors include increased age, male gender, cigarette exposure, hypertension, obesity, hypercholesterolemia, diabetes mellitus and family history (21,22). Furthermore, some studies support the hypothesis that having African origin could also be a risk for SCD (22,23). SCD is associated with LV dysfunction, history of Heart Failure (HF), LV hypertrophy, poor heart functional status, elevated heart rate and abnormal ECG (21).

What leads to SCD is an irregular cardiac activity that causes a restriction in blood supply to the brain, triggering the death of brain cells (21). This irregular cardiac activity could be explained by different cardiac and cardiovascular diseases. The main cause of SCD

is Ischaemic Heart Disease (IHD) being responsible for 50-80% of SCD cases (20). Secondary, around 15-30% of SCD is due to structural heart diseases, including non-ischaemic cardiomyopathies, valvular heart disease and others such as myocarditis or congenital heart diseases. The remaining 5-10% of SCD is explained by channelopathies, such as Long QT Syndrome (LQTS), Brugada Syndrome (BrS), Catecholaminergic Polymorphic Ventricular Tachycardia (CPVT) and Short QT Syndrome (SQTS) (17).

It is important to develop techniques for risk stratification, prediction and prevention for each of the diseases that lead to SCD. This would facilitate the decrease of the number of deaths and the anxiety of the relatives for having the possibility of being affected. The incidence of SCD has experimented a significant decline over the last ~60 years thanks to the advances in diagnosis, management and prevention of IHD. However, a minor reduction has been observed in SCD affecting young people (17,20). For this reason, it is completely necessary to increase the knowledge of those diseases associated with SCD in the young.

The incidence of SCD in young people (1-35 years old) rates between 1.3 and 2.8 per 100,000 persons being those aged 31-35 years to have a higher risk for suffering SCD (16). It has been described that the main diseases that lead to SCD in the young are hypertrophic cardiomyopathy (HCM), dilated cardiomyopathy (DCM), arrhythmogenic cardiomyopathy (ACM), myocarditis and

channelopathies (16). So, it is evident that SCD in the young population is induced mostly by diseases with genetic causes.

3.2. Cardiomyopathies

Cardiomyopathies are myocardium pathologies characterized by structural and functional alterations of the heart (24,25). They can be classified into primary and secondary. Primary cardiomyopathies include those pathologies that alterations are localized only in the heart, and secondary cardiomyopathies describe those diseases in which cardiac involvement is just a part of several systemic conditions (26,27). Secondary cardiomyopathies could be caused by autoimmune, endocrine, infectious, infiltrative, neuromuscular or storage disorders. Moreover, toxic consumption and nutritional deficiencies could also deriver to secondary cardiomyopathy (26,27).

The aetiology of primary cardiomyopathies can be genetic, acquired or mixed. Examples of acquired cardiomyopathies could be Myocarditis (induced by inflammation), Peripartum (induced by pregnancy) or Takotsubo (induced by stress) (27). Five of the most common primary cardiomyopathies with genetic or mixed causes are DCM and Restrictive cardiomyopathies (RCM) -mixed causes- and HCM, ACM and LV non-compaction cardiomyopathy (LVNC) -genetic causes- (26,27). Figure 9 shows the structural abnormalities of the heart of these 5 cardiomyopathies.

3.2.1. Dilated Cardiomyopathy

DCM is defined as an enlargement of ventricles and systolic dysfunction with normal LV wall thickness (26,27). It is the third cause of HF and the most common cause of heart transplantation with an estimated prevalence of 1:2500. The main cases of DCM have acquired causes such as infections, toxins, chronic excessive consumption of alcohol, chemotherapeutic agents, metals or other disorders. However, around 20-35% of DCM are explained by genetic causes, mainly by rare deleterious variants located in genes encoding sarcomeric proteins, but also cytoskeletal or nuclear envelope proteins (26,27).

3.2.2. Restrictive Cardiomyopathy

RCM is characterized by an impaired ventricular filling with normal systolic function due to an increased myocardial stiffness (24,27). This myocardial stiffness is mostly caused by the infiltration of proteins between the muscle fibres (28). Although genes coding for sarcomeric proteins, sarcomere associated proteins or binding partners are associated with RCM, few cases have genetic causes (28). The prevalence of RCM is difficult to estimate, it has high variability depending on the region, mainly because the majority of RCM is acquired and its prevalence is directly dependent on the prevalence of the diseases that trigger RCM such as cardiac

amyloidosis. However, it is known that it is the least common of cardiomyopathies (29,30).

3.2.3. Hypertrophic Cardiomyopathy

HCM is the most common primary cardiomyopathy with a prevalence of 1:500 (26,27). Principally, it is caused by deleterious rare variants located in genes encoding contractile proteins of the cardiac sarcomere such as myosin, troponin or titin and it follows an autosomal dominant inheritance pattern (26). HCM is characterized by a hypertrophied non-dilated LV with septal thickening. The most common symptoms are atypical chest pain and SCD. Variability in phenotype expression is frequent and many patients affected by HCM have a normal life expectancy or are asymptomatic (27).

3.2.4. Left Ventricular Non-Compaction Cardiomyopathy

LVNC is a congenital cardiomyopathy, due to an impaired embryonic development, characterized by sponge-like ventricle and dilation as a result of abnormal trabeculations (26,28). LVNC often coexists with other cardiomyopathies and sometimes is difficult to classify (28,31). Its prevalence rounds from 1:1000 to 1:2000 (31). Genetic causes are rare variants in genes encoding dystrophin–related protein family, tafazzin, dystrobrevin, lamin or sarcomeric proteins. The most common symptoms of LVNC are left ventricular

dysfunction and severe arrhythmia, SCD, HF and embolic stroke due to an enhanced risk of thrombus formation within the trabeculaes (28).

3.2.5. Arrhythmogenic Cardiomyopathy

ACM groups different clinical forms of heritable myocardial diseases with an intrinsic tendency to cause ventricular arrhythmia (32). The classical arrhythmogenic right ventricular cardiomyopathy (ARVC) is its main form, characterized by the replacement of cardiomyocytes by fibro-fatty tissue in the RV (28). Apart from ARVC, ACM also includes biventricular (BiVACM) and left-dominant (ALVC) forms (33). Its principal manifestations are cardiac arrhythmias, syncope, SCD, and HF in the advanced stages (34). The present thesis is focused on that pathology, so the following sections will present more information and data about ACM.
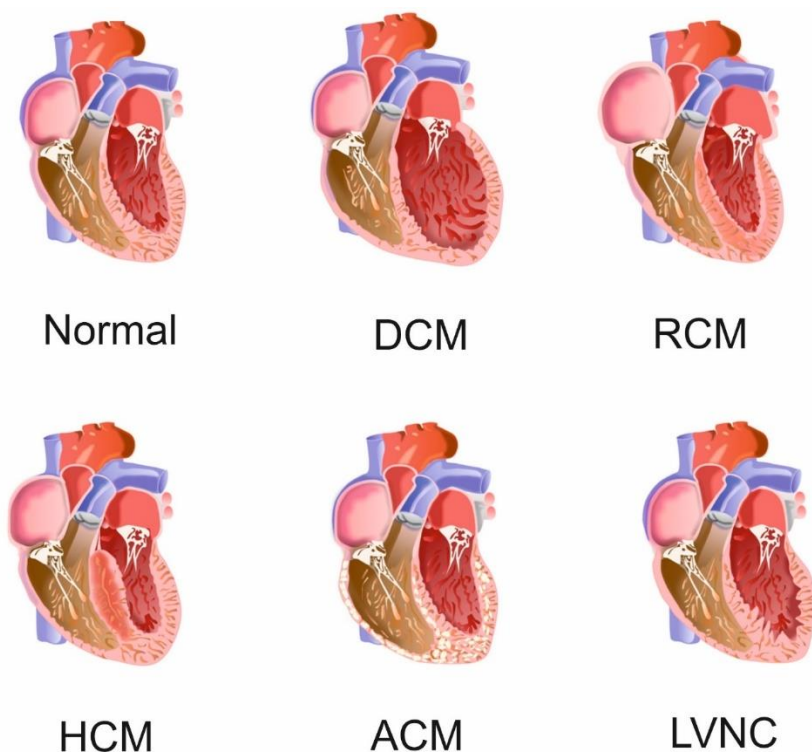
Figure 9. Phenotypes of cardiomyopathies with their characteristic structural abnormalities

DCM presents dilated left ventricle with or without right ventricular involvement. RCM results from decreased ventricular compliance and markedly dilated atria with myocardial stiffness. HCM involves thickened myocardium, which often affects the septum and hypertrophied non-dilated LV. ACM is characterized by fibrofatty infiltration of the right ventricle in almost all cases, with left ventricular involvement in some cases. LVNC presents a sponge-like ventricle and dilation with marked trabeculation. Adapted from Yogasundaram et al.,2021 (31).

4. Arrhythmogenic Cardiomyopathy (ACM)

4.1. General characteristics of ACM

ACM is a heritable cardiac entity mainly characterized by a progressive loss of myocardium and its replacement by fibrofatty tissue that predominantly affects the right ventricle (19,27). However, left ventricular and biventricular phenotypes have also been described (19). The main symptoms are palpitations, syncope, and SCD (27). ACM affects specifically athletes and young people, between the second and fourth decades of life and its prevalence range from around 1 case per 1000 to 5000 persons (27). The main genetic cause is rare deleterious variants in desmosomal genes that are identified in around 50% of all ACM cases and commonly following an autosomal dominant pattern of inheritance (19). It has also been described some cases of autosomal recessive forms, but those are more commonly associated with Naxos disease and Carvajal syndrome, two cardio-cutaneous syndromes that are caused by deleterious rare variants in *JUP* (Junction plakoglobin; codifies for PG) and *DSP* respectively (35). Moreover, it is known that both incomplete penetrance and variable expressivity are frequent.

Athletes are one of the most affected collectives by ACM, it was found that 20% of deaths in young people and athletes were caused by previously undiagnosed ACM (19). Moreover, a study showed

that athletes with ACM were 6 times more susceptible to die on exertion compared to those with other cardiac pathologies (36). It is known that sport triggers the onset of this disease (19,37,38), even though, there are studies that support the hypothesis that extremely elevated training alone may have a role in ACM pathogenesis (39,40). However, it has been shown that gene-negative patients need to train harder to develop ACM and that sports restriction in them contributes to reduce ventricular arrhythmias more often than in gene-positive ACM patients (40–43).

Regarding gender, it has been reported several differences in terms of expressivity, prognosis and manifestations of the disease. There are lots of studies that show that ACM is 1.2 to 3 times more common in men than in women (44–49). However, the North American ACM Registry presents similar numbers of both genders affected equally by ACM (49,50). Although the reasons why men show higher prevalence in ACM versus women is still unclear, it is accepted that men have a worse prognostic. It is known that the incidence of ventricular arrhythmia does not differ by gender in ACM patients (45), but it turns out that men have an increased likelihood to experiment it in a more severe way (49,51), have a greater risk of fast ventricular tachycardia (VT) (50) and also of suffering SCD (47,49,52–57). These disparities between genders could be explained by differences in the amount or intensity of exercise and/or by the effects of sex hormones (19,49).

On the one hand, it has been demonstrated that, in healthy conditions, women have lower RV mass and volume and higher RV ejection than men. In the end, this means that women have better RV function, and it is consistent within all ethnic groups studied (Caucasians, African Americans, Hispanics, and Chinese Americans) (49,58,59). Regarding the role of estrogen in ACM, it has been observed in women that low levels of estradiol are associated with major arrhythmic cardiovascular events and a higher risk of life-threatening arrhythmias (49,60). On the other hand, ACM men patients present higher testosterone levels compared with men controls, but ACM and healthy women do not present any differences in testosterone levels (49,61). Elevated testosterone levels are also associated with a high risk of malignant arrhythmic events in men (49,60,61).

4.2. Diagnosis

ACM diagnosis is based on an International Task Force Criteria (ITFC) proposed in 1994 and updated in 2010 (62,63). These criteria facilitate recognition and interpretation of the ACM common features considering familial and genetic factors, ECG abnormalities and structural/functional ventricular alterations. The 1994 criteria were specific but had low sensitivity for early and familial disease. For that reason, the main aim of the 2010 update was to maintain

the specificity and increase the sensibility of the criteria by incorporating new knowledge and technology (63).

ITFC evaluate the following 6 parameters classifying them into major and minor categories: Global or regional dysfunction and structural alterations (I), Tissue characterization of the wall (II), Repolarization abnormalities (III), Depolarization/conduction abnormalities (IV), Arrhythmias (V) and Family history (VI) (Table 1). To fulfil a definitive diagnosis, the patient has to present 2 major criteria or 1 major and 2 minor criteria or 4 minor criteria from different categories. Those patients that present 1 major and 1 minor or 3 minor criteria from different categories will be classified as borderline and those that present 1 major or 2 minor criteria from different categories will obtain a possible diagnosis (Table 2).

Table 1. Measured major and minor parameters in ITFC to diagnose ACM

PLAX indicates parasternal long-axis view; RVOT, RV outflow tract; BSA, body surface area; PSAX, parasternal short-axis view; aVF, augmented voltage unipolar left foot lead; and aVL, augmented voltage unipolar left arm lead. Adapted from Marcus et al., 2010 (63)

ACM Diagnosis (ITFC)	Major	Minor
Global or regional dysfunction and structural alterations	**By 2D echo:** - Regional RV akinesia, dyskinesia, or aneurysm - and 1 of the following (end diastole): • PLAX RVOT ≥32 mm (corrected for body size [PLAX/BSA] ≥19 mm/m2) • PSAX RVOT ≥36 mm (corrected for body size [PSAX/BSA] ≥21 mm/m2) • or fractional area change ≤33% **By MRI:**	**By 2D echo:** - Regional RV akinesia or dyskinesia - and 1 of the following (end diastole): • PLAX RVOT ≥29 to <32 mm (corrected for body size [PLAX/BSA] ≥16 to <19 mm/m2) • PSAX RVOT ≥32 to <36 mm (corrected for body size [PSAX/BSA] ≥18 to <21 mm/m2) • or fractional area change >33% to ≤40% **By MRI:**

	- Regional RV akinesia or dyskinesia or dyssynchronous RV contraction - and 1 of the following: - Ratio of RV end-diastolic volume to BSA ≥110 mL/m2 (male) or ≥100 mL/m2 (female) - or RV ejection fraction≤40% **By RV angiography:** - Regional RV akinesia, dyskinesia, or aneurysm	- Regional RV akinesia or dyskinesia or dyssynchronous RV contraction - and 1 of the following: - Ratio of RV end-diastolic volume to BSA ≥100 to <110 mL/m2 (male) or ≥90 to <100 mL/m2 (female) - or RV ejection fraction >40% to ≤45%
Tissue characterizatio n of wall	-Residual myocytes <60% by morphometric analysis (or <50% if estimated), with fibrous replacement of the RV free wall myocardium in ≥1 sample, with or without fatty replacement of tissue on endomyocardial biopsy	-Residual myocytes 60% to 75% by morphometric analysis (or 50% to 65% if estimated), with fibrous replacement of the RV free wall myocardium in ≥1 sample, with or without fatty replacement of tissue on endomyocardial biopsy

Repolarization abnormalities	Inverted T waves in right precordial leads (V1, V2, and V3) or beyond in individuals >14 years of age (in the absence of complete right bundle-branch block QRS ≥120 ms)	-Inverted T waves in leads V1 and V2 in individuals >14 years of age (in the absence of complete right bundle-branch block) or in V4, V5, or V6 -Inverted T waves in leads V1, V2, V3, and V4 in individuals >14 years of age in the presence of complete right bundle-branch block
Depolarization /conduction abnormalities	-Epsilon wave (reproducible low-amplitude signals between the end of QRS complex to the onset of the T wave) in the right precordial leads (V1 to V3)	-Late potentials by signal-averaged ECG (SAECG) in ≥1 of 3 parameters in the absence of a QRS duration of ≥110 ms on the standard ECG -Filtered QRS duration (fQRS) ≥114 ms -Duration of terminal QRS <40 mV (low-amplitude signal duration) ≥38 ms -Root-mean-square voltage of terminal 40 ms ≤20 mV -Terminal activation duration of QRS ≥55 ms measured from the nadir of the S wave to the end of the QRS, including R0, in V1, V2, or V3, in the absence of complete right bundle-branch block

Arrhythmias	-Nonsustained or sustained ventricular tachycardia of left bundle-branch morphology with superior axis (negative or indeterminate QRS in leads II, III, and aVF and positive in lead aVL)	-Nonsustained or sustained ventricular tachycardia of RV outflow configuration, left bundle-branch block morphology with inferior axis (positive QRS in leads II, III, and aVF and negative in lead aVL) or of unknown axis - >500 ventricular extrasystoles per 24 hours (Holter)
Family history	-ACM confirmed in a first-degree relative who meets current Task Force criteria -ACM confirmed pathologically at autopsy or surgery in a first-degree relative -Identification of a pathogenic variants categorized as associated or probably associated with ACM in the patient under evaluation	-History of ACM in a first-degree relative in whom it is not possible or practical to determine whether the family member meets current Task Force criteria - Premature sudden death (<35 years of age) due to suspected ACM in a first-degree relative - ACM confirmed pathologically or by current Task Force Criteria in second-degree relative

Table 2. Number of major and minor ITFC required to fulfil definitive, borderline or possible ACM diagnosis

ACM Diagnosis (ITFC)	Major	Minor
Definitive	2	-
	1	2
	-	4
Borderline	1	1
	-	3
Possible	1	-
	-	2

As the ITFC describe, the most common clinical presentation of ACM are ventricular arrhythmias with a left bundle-branch block (LBBB) pattern, right ventricular abnormalities on imaging tests and palpitations or effort-induced syncope with T-wave inversion and epsilon waves in the right precordial leads (V_1 through V_4) on the ECG. Myocardium conduction defects detected as electrocardiographic depolarization abnormalities may also be present (19,27).

Figure 10 shows the typical electrical, functional and structural alterations published in an ACM classical case report (64).
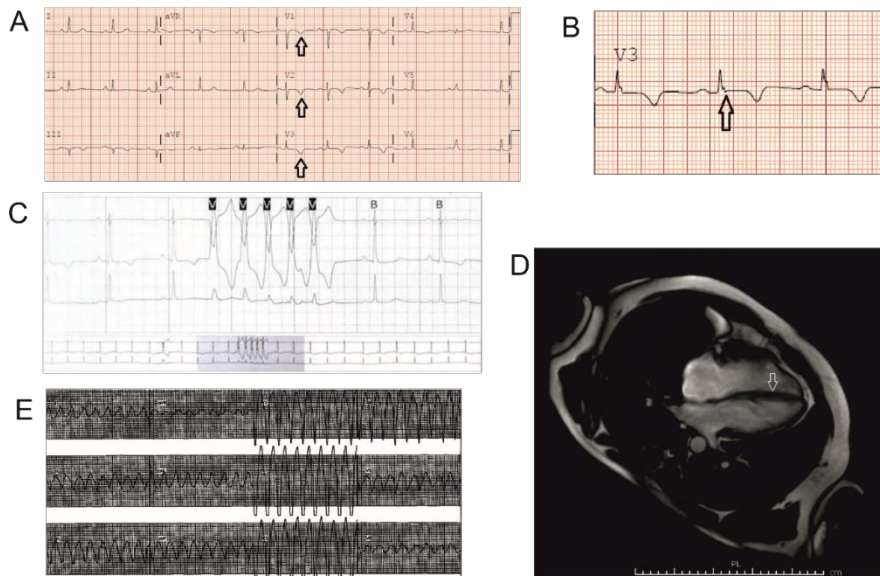
Figure 10. Clinical presentation of a classical ACM case

A) Resting 12-lead ECG showing symmetric T wave inversion in right precordial leads (V1, V2 and V3) (see black arrows). B) Possible epsilon waves in right precordial lead V3 (see black arrow). C) Holter monitor showing non-sustained ventricular tachycardia with left bundle branch block pattern. D) Cardiac MRI showing foci of fat in the right ventricular side of the interventricular septum (see white arrow). E) 12-lead ECG showing inducible ventricular tachycardia with left bundle branch block pattern and superior axis during the electrophysiologic study. Adapted from Latt et al., 2017 (64).

However, some limitations have been identified in ITFC from 2010. For the moment, ITFC only considers gender for cut-off values of the ratio of RV end-diastolic volume to body surface area, but there are evidences that other parameters of ACM could be different depending on gender. It has been demonstrated that, unlike men,

women with normal and abnormal SAECG are equally likely to experiment cardiac events. So, this parameter in current diagnostic criteria is not identifying all women at greater risk (50). Additionally, it seems that the presence of intramyocardial fat by cardiac MRI in men are associated with cardiac events, but this association is not happening in women. On the contrary, adverse cardiac events in women are associated with the presence of intramyocardial fat in RV Outflow Tract (RVOT), but not in men (50). So, maybe it would be necessary to consider gender in more diagnostic parameters to identify all patients at risk and prevent SCD.

Moreover, pediatric patients represent one-sixth of the overall ACM-population, but ITFC was designed in the adult population and it does not consider the age of the patient (65). It has been demonstrated that ACM pediatric patients present some differences in comparison with adult patients. SCD is more often in pediatric age, whereas adult patients are more likely to present VT (66). Furthermore, ACM patients under 18 are much more frequently rare variants carriers than adults.

Finally, another group of patients that are not specifically considered in the current ITFC are those suffering from biventricular or left-predominantly variants. For that reason, it has been proposed "The Padua Criteria" based on 2010 ITFC but incorporating tissue characterization findings by cardiac magnetic resonance for including those patients. Before being used for clinicians, it has to be validated by clinical studies in large cohorts of patients (67–69).

4.3. Treatment

There is no specific treatment to cure ACM, all therapeutic options are focused on reducing the risk of SCD, preventing progression of the disease, improving the quality of life and identifying individuals at-risk in families (19,35,70,71).

- Exercise Restriction

Restrictions of intense sports activity are recommended as a preventive tool for affected patients and also for those who are at risk. However, low-intensity sport could be reasonable depending on the case (35,70,71).

- Beta-blockers

Beta-blockers are recommended for patients with recurrent VT and in patients with supraventricular or atrial arrhythmias (35). Beta-blockers are efficient to prevent arrhythmias, HF and they potentially reduce RV wall stress (71). However, it is not recommended for healthy gene carriers, it has no prophylactic use (35,70,71).

- Antiarrhythmic Therapy

Antiarrhythmic drugs are recommended for suppressing symptoms related to frequent ventricular ectopy or appropriate defibrillator discharges and amiodarone and sotalol are the most commonly

used (35,70,71). Antiarrhythmic agents could be administrated as adjunctive therapy in combination with beta-blockers, catheter ablation or Implanted Cardioverter Defibrillator (ICD). Antiarrhythmic drugs are not recommended for asymptomatic patients.

- Heart Failure Treatment

Standard drug therapy with angiotensin-converting-enzyme inhibitors (ACE-I), angiotensin II receptor blockers (ARB), beta-blockers, and diuretics are recommended for RV or LV failure (35).

- Implanted Cardioverter Defibrillator

Patients that are at high risk for an arrhythmic event rate of >10%/year should receive an ICD. Prophylactic ICD implantation could be considered for those patients at intermediate risk that suffer from syncope, non-sustained VT, moderate or LV dysfunction (35,71). It has been demonstrated that ICD increases patient's survival, a study shows that 24% of ACM patients had an arrhythmic episode that would have been fatal in the absence of an ICD (at an average follow-up of 3.3 years) (70,72). However, ICD has high costs and significant complications during follow-up (70).

- Catheter Ablation

Catheter ablation is addressed to ACM patients with frequent VT episodes and ICD chocks to destroy small areas with abnormal

heartbeat due to fibrofatty replacement. Acute success is achieved in 60-80% of patients, whereas the recurrence rates during long-term follow-up of 3-5 years are as high as 50-70% (71). These VT recurrences are explained by the progressive replacement of cardiomyocytes by fibrofatty tissue that leads to new re-entry circuits. Combined endocardial and epicardial ablation improves long-term VT-free survival of ACM patients (35,70). Catheter ablation could not prevent SCD and it may make a good combination with ICD therapy or other treatments (71).

- Heart Transplant

Transplantation would be indicated as final therapy in cases of severe HF when the patient does not respond to other therapies or with intractable arrhythmias. However, heart transplantation is rarely used in ACM treatment (70,71).

Apart from these treatments, clinical follow-up is important for ACM patients to revaluate the new onset or worsening of symptoms and progression of the disease to reassess the risk of SCD and optimize the treatment (71). For affected patients, this clinical assessment should be performed every 1-2 years on the age, symptoms, and disease severity. Furthermore, healthy gene carriers and family members should also be assessed every 2-3 years because of the age-related penetrance and progressive curse of ACM, especially during adolescence and young adulthood (19,71). Recently, it has been published the updated 2022 ESC Guidelines for the

management of patients with ventricular arrhythmias and the prevention of sudden cardiac death, including all the necessary information and clinical protocols to manage ACM patients (73).

4.4. Genetic causes of ACM and variant classification

In around 50-60% of ACM patients, it is possible to identify the genetic causal variant of the disease (35). However, there are a large number of patients that remain without a genetic cause. Additionally, around 20% of ACM patients present multiple pathogenic variants being compound or digenic heterozygous. Commonly, these cases show a more severe phenotype (35,74).

The majority of the ACM patients present pathogenic rare variants in desmosmal genes, but some genes not directly related to desmosome are also associated with ACM. Based on the Expert Consensus Statements on the state of genetic testing for cardiac diseases, there are 23 genes that are or could be associated with ACM (73) (Table 3). As Table 3 shows, the majority of them are not exclusive for ACM but could be shared with other cardiac diseases.

Table 3. ACM-associated genes

Gene	Phenotype/Syndrome	Protein (Cellular complex)	Frequency	ClinGen classification
PKP2	Classic ARVC. BiVACM and ALVC in a minority of cases.	Plakophilin 2 (desmosome)	20–45%	Definite
DSP	Frequent BiVACM and ALVC. Occasional hair and skin features. Rare homozygous variants—Carvajal Syndrome.	Desmoplakin (desmosome)	2–15%	Definite
DSG2	Frequent BiVACM and ALVC.	Desmoglein 2 (desmosome)	4–15%	Definite
DSC2	ARVC. Less frequent BiVACM and ALVC.	Desmocollin 2 (desmosome)	2–7%	Definite
FLNC	ALVC. Right ventricular involvement is rare	Filamin-C (cytoskeleton)	3%	Definite
JUP	Naxos disease (cardioectodermal)	Plakoglobin (desmosome)	<1% (higher in Naxos, Greece)	Definite
TMEM43	ARVC and BiVACM	Transmembrane protein 43 (nuclear envelope)	<1% (higher in Newfoundland)	Definite
PLN	Frequent ALVC/DCM	Phospholamban (sarcoplasmic reticulum; calcium handling)	1% (10–15% in	Definite

			Netherlands)	
DES	Frequent ALVC. Right ventricular involvement is also possible. Conduction system abnormalities common. Skeletal myopathy possible.	Desmin (cytoskeleton)	1–2%	Moderate
CTNNA3	ARVC/ACM	Catenin alpha-3 (area composita)	<1%	Limited
CDH2	ARVC/ACM	Cadherin-2 (area composita)	<1%	Limited
LMNA	DCM. Prominent conduction system abnormalities and atrial arrhythmias common. Exceptional ARVC/ACM	Lamin A/C (nuclear envelope)	<1%	Limited
SCN5A	DCM. Exceptional ARVC/ACM	Sodium channel protein type 5 subunit alpha (ion channel)	<1%	Limited
TJP1	ARVC/ACM and DCM	Tight junction protein 1 (area composita)	<1%	Limited
ACTC1	HCM. LVNC. DCM	Actin alpha cardiac muscle 1 (sarcomere)	-	Disputed
LDB3	ARVC/ACM	LIM domain-binding protein 3 (sarcomere)	-	Disputed
MYBPC3	HCM. LVNC. DCM	Myosin binding protein C3 (sarcomere)	-	Disputed

MYH7	HCM. DCM. LVNC	Myosin heavy chain 7 (sarcomere)	-	Disputed
MYL2	HCM	Myosin light chain 2 (sarcomere)	-	Disputed
MYL3	HCM	Myosin light chain 3 (sarcomere)	-	Disputed
TGFB3	ARVC/ACM. LDS	Transforming growth factor, beta 3 (signalling pathways)	-	Disputed
TP63	ARVC/ACM	Tumor protein p63 (transcription factors)	-	Disputed
TTN	DCM. ARVC/ACM	Titin (sarcomere related)	-	Disputed

ARVC: arrhythmogenic right ventricular cardiomyopathy, CPVT: catecholaminergic polymorphic ventricular tachycardia; DCM: dilated cardiomyopathy; HCM: hypertrophic cardiomyopathy; LDS: Loeys-Dietz syndrome; LVNC: left ventricular noncompaction cardiomyopathy; MD: muscular dystrophy

4.4.1. Desmosomal genes

- *PKP2*

PKP2 is the most frequent gene carrying deleterious rare variants associated with ACM and leads to the classic RV dominant form (35,74,75). Specifically, PTCs in *PKP2* are the most prevalent genetic alterations in ACM patients (76).

- *DSP*

DSP was firstly associated to ACM in 2002 (77), but before that, it was already described that PTCs in homozygosis in that gene caused Carvajal syndrome, characterized by keratoderma, dry and blister-prone skin, woolly hair and cardiac manifestations (33). Moreover, *DSP* is the second most frequent mutated gene in ACM patients and it is associated with a high risk of ventricular arrhythmias, SCD and a high level of LV involvement. It is known that patients with pathogenic variants in *DSP* could present RV dominant phenotype, biventricular or isolated LV affectation showing high variable phenotypes between cases (35,74). *DSP* pathogenic variants are associated with a more severe phenotype, especially in the presence of a PTC which increases predisposition to HF (35). Moreover, it has been shown that paediatric patients present pathogenic variants more frequently in *DSP* than in others genes (33,66,78). Furthermore, pathogenic variants in *DSP* are also present in 3% of DCM patients, contributing to overlapping between cardiomyopathies (74,79).

- *DSG2*

Pathogenic variants in *DSG2* are frequently found in patients with biventricular involvement and are associated with a higher risk of HF and heart transplantation (35,74,80). Moreover, DSG2 has also been associated with predominant LV involvement (81).

- *DSC2*

DSC2 pathogenic variants basically triggers ARVC, but they can also lead to biventricular forms, especially in homozygous carriers (74,82).

- *JUP*

Homozygous PTCs variants in *JUP* cause Naxos disease which is characterized by keratoderma, woolly hair and cardiac manifestations. Moreover, *JUP* pathogenic variants have also been identified in ACM patients with right or biventricular phenotype affectation and cutaneous manifestations (33,35,83).

4.4.2. Classification of genetic variants

ITFC counts pathogenic variants in associated or probably associated genes with ACM as a major criterion for diagnosis (63). So, detecting a pathogenic variant in the genes listed above is a key factor to identify ACM patients. However, sometimes it is not clear if detected variants are pathogenic or not, there are lots of parameters that could be important for interpreting the variant role

in a specific disease. For that reason, Richards *et al.* presented standards and guidelines of the American College of Medical Genetics and Genomics and the Association for Molecular Pathology -ACMG/AMP- (84). These guidelines recommend to classify variants into 5 categories: pathogenic (P), likely pathogenic (LP), uncertain significance (VUS), likely benign (LB), and benign (B) to facilitate its interpretation.

To perform this classification, they proposed two sets of criteria, one for classification of P or LP variants, and one for classification of B or LB variants. For the pathogenic set, the evidences are divided into very strong (PVS1), strong (PS1-4), moderate (PM1-6) or supporting (PP1-5) while the benign set contains stand-alone (BA1), strong (BS1-4) and supporting (BP1-6) evidences. These sets of criteria and evidences are based on population, computational and predictive, functional, segregation, de novo and allelic data of the variant.

Pathogenic evidences

- **Very Strong**

PVS1: Predicted null variant in a gene where loss of function is a known mechanism of disease

- **Strong**:

PS1: Same amino acid change as an established pathogenic variant regardless of nucleotide change

PS2: *De novo* mutation (both maternity and paternity confirmation) in a patient with the disease and no family history

PS3: Well-established *in vitro* or *in vivo* functional studies show a deleterious effect on the gene or gene product

PS4: Prevalence in affected individuals is statistically increased over controls

- **Moderate**:

PM1: Located in a mutational hot spot and/or well-studied functional domain without benign variation

PM2: Absent or extremely low frequency from controls in Exome Sequencing Project, 1000 Genomes or ExAC

PM3: For recessive disorders, detected in *trans* with a pathogenic variant

PM4: Protein length changes due to in-frame deletions/insertions in a non-repeat region or stop-loss variants

PM5: Novel missense change at an amino acid residue where a different pathogenic missense change has been seen before

PM6: Assumed *de novo* mutation in a patient with the disease and no family history (without maternity and paternity confirmed).

- **Supporting**:

PP1: Co-segregation with disease in multiple affected family members in a gene definitively known to cause the disease

PP2: Missense variant in a gene with low rate of benign missense variants and where missense variants are a common mechanism of disease

PP3: Multiple lines of computational evidence support a deleterious effect on the gene/gene product

PP4: Patient's phenotype or family history is highly specific for a disease with a single genetic aetiology

PP5: Reputable source recently reports variant as pathogenic but evidence is not available to the laboratory to perform an independent evaluation

Benign evidences

- **Stand-alone:**

BA1: Allele frequency is above 5% in Exome Sequencing Project, 1000 Genomes or ExAC

- **Strong:**

BS1: Allele frequency is greater than expected for disorder

BS2: Observed in a healthy adult individual for recessive (homozygous), dominant (heterozygous) or X-linked (hemizygous) disorders with full penetrance expected at an early age

BS3: Well-established *in vitro* or *in vivo* functional studies show no damaging effect on protein function or splicing

BS4: Lack of segregation in affected members of a family

- **Supporting:**

BP1: Missense variant in a gene for which primarily truncating variants are known to cause disease

BP2: Observed in *trans* with a pathogenic variant for a fully penetrant dominant gene/disorder or in *cis* with a pathogenic variant in any inheritance pattern

BP3: In-frame deletions/insertions in a repetitive region without a known function

BP4: Multiple lines of computational evidence suggest no impact on gene/gene product

BP5: Variant found in a case with an alternate molecular basis for disease

BP6: Reputable source recently reports variant as benign but evidence is not available to the laboratory to perform an independent evaluation

BP7: A synonymous (silent) variant for which splicing prediction algorithms predict no impact to the splice consensus sequence nor the creation of a new splice site AND the nucleotide is not highly conserved

These two sets of criteria are combined to classify variants into P, LP, LB or B depending on which and how many premises satisfy

(Table 4). Moreover, those variants that comply with contradictory criteria for benign and pathogenic conditions and are unmet in any of the these 4 categories should be classified as VUS (84).

Table 4. Rules for combining criteria to classify variants

Each category requires a determined number of specific criteria to fulfil its designation. Adapted from Richards et al (84).

	Number of specific criteria required
P	1 very strong *AND* (≥1 strong *OR* ≥2 moderate *OR* 1 moderate *AND* 1 supporting *OR* ≥2 supporting)
	≥2 strong
	1 strong *AND* (≥3 moderate *OR* 2 moderate *AND* ≥2 supporting *OR* 1 moderate *AND* ≥4 supporting)
LP	1 very strong *AND* 1 moderate
	1 strong *AND* 1-2 moderate
	1 strong *AND* ≥ 2 supporting
	≥ 3 moderate
	2 moderate *AND* ≥ 2 supporting
	1 moderate *AND* ≥ 4 supporting
B	1 stand-alone
	≥2 strong
LB	1 strong and 1 supporting
	≥2 supporting

4.5. ACM pathogenesis and molecular mechanisms

4.5.1. Cardiomyocyte loss

Loss of cardiomyocytes is an important feature in the ACM progression. As it is known, the majority of patients present pathogenic variants in desmosomal genes, therefore, the resultant protein could present alterations having a great impact on these cell junctions. When desmosomes are weak, cardiomyocytes present difficulties in resisting mechanical stress caused by heart contraction provoking cell injuries that result in cell death (33). This damage could be aggravated by exercise that increases the mechanical stress in the heart. It is known that in normal conditions, physical activity at the molecular level promotes an up-regulation of *JUP* and associated-gene proteins, as well as GJs proteins to face mechanical stress (38,85–88). Cardiomyocytes with desmosomal pathogenic variants are incapable to respond to the stretch pressure caused by a higher level of physical activity and therefore present altered mechanical properties that lead to myocytes death (38,86,89,90). There is evidence that RV is more susceptible than LV to exercise-induced injury probably due to an increase in pulmonary arterial pressure (41,91).

Another mechanism that contributes to cardiomyocyte loss is apoptosis. This programmed cell death may be triggered by abnormal transduction of mechanical signals. An animal model of

the disease shows aberrant nuclear localization of plakoglobin acting as antagonize of WNT-catenin-β1 that leads cardiomyocytes to apoptosis (33,92). Moreover, the increase of glycogen synthase kinase 3β (GSK-3β) also contributes to apoptosis because it promotes catenin-β1 degradation and therefore a downregulation of WNT pathway (33,93).

Compared with apoptosis, programmed necrosis is less clear as a mechanism of cell death. There is a study of a transgenic mouse model carrying a mutation in *DSG2* that shows that necrosis is the initiating event in myocardial injury and precedes other pathological features. They suggested that mutant *DSG2* affects membrane integrity and mitochondrial permeability with abnormal calcium homeostasis (94). It is true that some samples from ACM patients, mainly those that suffer from myocarditis, show signs of necrosis with inflammatory cells surrounding cardiomyocytes, but it is unknown if it is the cause or the consequence of this mechanical injury (33,95).

4.5.2. Fibrosis

Fibrosis is a common response to cardiomyocyte injury in the heart and, in ACM patients, it is promoted by complex interactions between cytokines, growth factors and hormones (33,96). TGFβ pathway contributes to cardiac fibrosis by phosphorylating and activating the receptor-associated SMAD that triggers expression of

profibrotic genes such as extracellular matrix proteins and inhibitors of matrix metalloproteinases (96–99). There is a study that showed increased TGFβ1 expression and activation of SMAD2 signalling in an ACM mice model with a loss-of-function variant in *JUP* (100). Moreover, the β-adrenergic system could also regulate the extracellular matrix protein turnover. Norepinephrine could trigger the expression of metalloproteinase-2 and decrease the expression of tissue inhibitors of metalloproteinases 1 and 2 (101–103). Furthermore, mechanical stress caused by a high level of physical activity could increase plasmatic levels of TGFβ1 (103–105).

On the other side, the non-canonical TGFβ pathway has also a role in cardiac fibrosis activating mitogen-activated protein kinase (MAPK) signalling and generation of reactive oxygen species (ROS) (106,107). A knockdown of *PKP2* in a cell model presented an upregulation of fibrotic genes via non-canonical TGFβ–MAPK signalling (108). All these data suggest that both canonical and non-canonical TGFβ signalling can have a role in inducing myocardial fibrosis in ACM (33).

Fibrosis is produced by a positive loop that starts in changes in extracellular matrix composition altering tissue properties and increasing its rigidity. Then, tissue stiffness promotes the differentiation of myofibroblasts to produce and release collagen which will continue increasing the stiffness of the tissue (103,109).

4.5.3. Adipogenesis

Adipogenesis is a common feature of ACM that consists of the infiltration of adipocytes, in this case, in heart tissue. The cellular source of these adipocytes and the signals that induce it are still under discussion. Regarding the cellular origin of adipocytes, there are several candidates: cardiomyocytes, differentiated non-myocytes, cardiac progenitor cells and circulating progenitor cells (33). There are numerous studies in mouse models that show that second heart field progenitor cells are involved in the origin of adipocytes (33,110–114). Moreover, it has been shown that fibroadipogenic and mesenchymal progenitors are also contributing to adipocytes source (115–117). Additionally, there is also a study that proves the ability of cardiomyocytes to transdifferentiate into adipocytes in vitro (118). In the same direction, another study in mice showed that adipocytes in the heart present specific marks as descendants of cardiomyocytes (119). All these data contribute to pinning down the origin of adipocytes, but more studies are needed to reach a consensus about the source.

Apart from the origin, molecular signals triggering adipogenesis are also under study to be better understood. Several signalling pathways have been described to be involved in adipogenesis (33). There are evidences that downregulation of WNT pathway contributes to adipogenesis by triggering differentiation of mesenchymal stem cells and preadipocytes into adipocytes (120). In the absence of WNT ligands, GSK-3β phosphorylates catenin-β1,

targeting it to degradation. The interaction between GSK-3β and catenin-β1 is stabilized by axin, which serves as a negative regulator of the canonical WNT pathway (34,121). However, in the presence of WNT ligands, GSK-3β no longer phosphorylates catenin-β1 that accumulates in the cytoplasm and translocate into the nucleus where it co-activates TCF-LEF that will upregulate the expression of adipogenic genes (92,122,123). Suppression of the canonical WNT/catenin-β1 signalling has been implicated in adipogenesis, fibrogenesis, and apoptosis (124–126).

Inhibition of canonical WNT pathway has a critical function in the enhanced adipogenesis in ACM (92,127–129). It has been shown that desmosomal mutations could provoke dislocation of PG from the cell membrane allowing it to play a role in non-structural functions (130–132). PG is a paralogue of catenin-β1, they both present a similar structure and are located at ID where they bind cadherins to the actin cytoskeleton (33). It is known that free PG can compete with catenin-β1 and promote its degradation (133) (Figure 11). Several studies correlate PG nuclear localization with increased adipogenic activity whereas *JUP* KO increases stability and transcriptional activity of catenin-β1 inhibiting adipogenesis (92,127,134). All these data suggest that PG located into the nucleus play an antagonist role in canonical WNT signalling and triggers adipogenesis (33). Moreover, some studies show that inhibition of non-canonical WNT signalling (catenin-β1-independent) in

combination with Rho GTPase can also contribute to adipogenesis in ACM (92,135).

Apart from WNT signalling, it has been described other pathways with great implications in ACM adipogenesis. This is the case of Hippo signalling that regulates organ size and cell proliferation, survival and differentiation (129,136). In normal conditions, Yes associated protein (YAP) and transcriptional co-activator with PDZ-binding motif (TAZ) are activated and translocate into the nucleus where they interact with TEA domain family member (TEAD) transcription factor, leading to stimulation of gene expression that promotes proliferation, differentiation and apoptosis (34,137). However, when Hippo pathway is activated, hippo kinase MST1/2 phosphorylates and activates LATS1/2, which in turn phosphorylates YAP and TAZ promoting their nuclear export and cytoplasmic sequestration resulting in their inactivation of transcriptional activity (137) (Figure 11).

Cell-cell contacts could regulate YAP transcriptional activity due to its interactions with sub-membrane region, where Hippo kinases and YAP localize. NF2 which is also localized there, regulates MST and LATS activity, and in turn, NF2 is regulated by PKCα (137,138). It has been described that ACM causes a remodelling of IDs presenting reduced levels of desmosome proteins (129). This ID remodelling reduces localization of activated PKCα in cell unions provoking a great activation of NF2 and Hippo kinases resulting in increased localization of phosphorylated YAP to cell junctions unsuited to

enter the nucleus resulting in a blocked TEAD expression (137) (Figure 11).

In addition, it has been described a crosstalk between Hippo and WNT pathways. Activation of Hippo triggers phosphorylation of TAZ, promoting its localization to the submembrane region, where it binds and inhibits Dishevelled (Dvl), an essential transducer of WNT signalling (137,139). Moreover, phosphorylated YAP sequestrates catenin-β1 in the cytosol inactivating also WNT pathway. Moreover, in this crosstalk between WNT/ catenin-β1 and Hippo/YAP signalling pathways in ACM, it has been identified a third component that is PG. Chen et al. has described a protein complex formed by YAP, PG and catenin-β1, but it is still unknown its localization in the cell and its significance in ACM (129,137) (Figure 11).
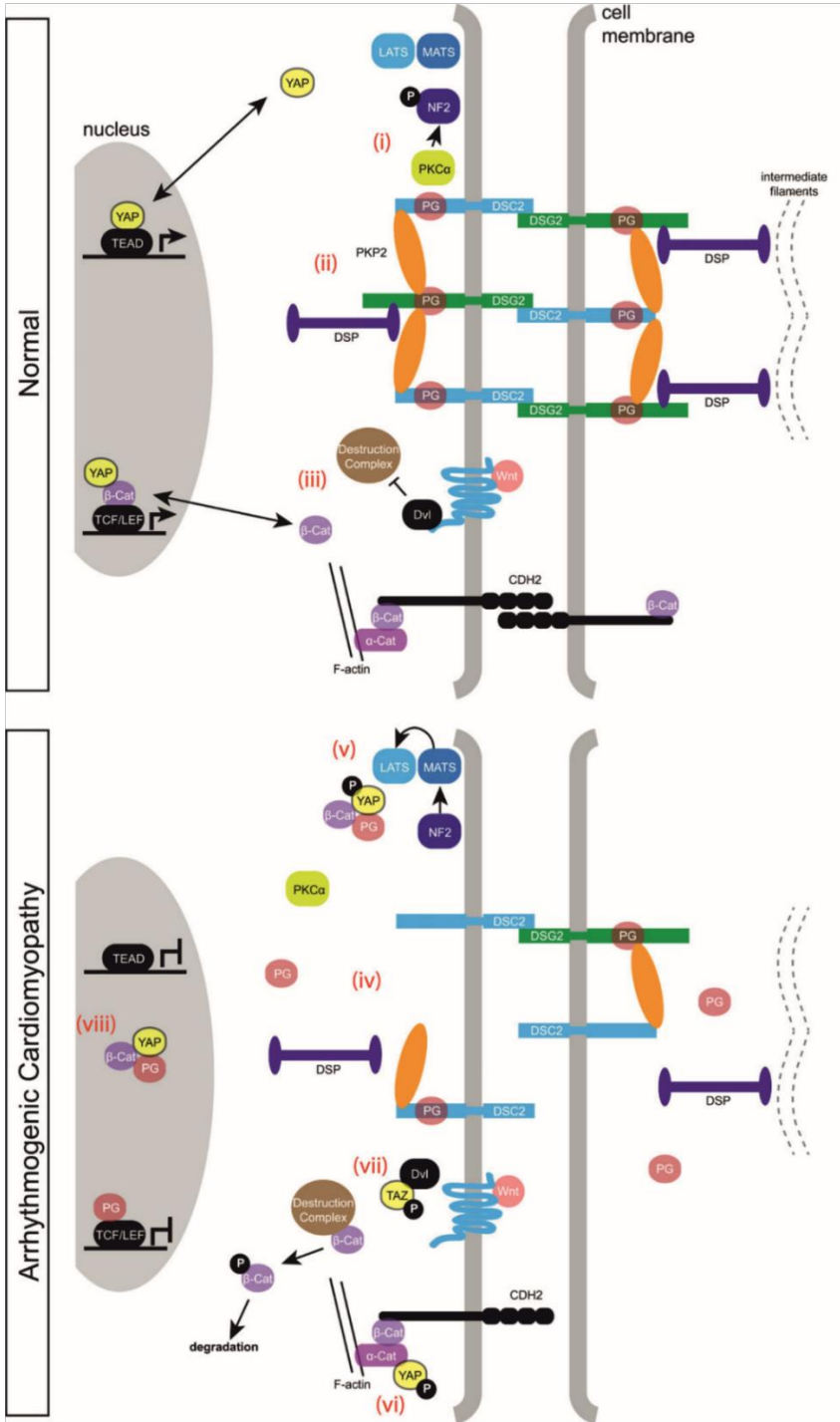
Figure 11. Schematic representation of interaction between Hippo and canonical WNT pathway in ACM

Top panel *shows normal myocardial intercalated disk (ID), containing desmosomes (DSG2/DSC2/PKP2/PG/DSP) and adhesion junctions (CDH2/β-catenin/α-catenin). The intact ID retains PKCα near the membrane, leading to phosphorylation and inactivation of NF2 (i). YAP phosphorylation state is low, and PG is bound to desmosomes and localized at the ID (ii). Wnt/β-catenin signalling can proceed normally (iii).* **Bottom panel** *shows disruption of the ID in AC by a desmosomal mutation (e.g. in PKP2; iv). ID disruption causes both loss of mechanical integrity and aberrant signalling. Loss of PKCα sub-membrane localization activates NF2 and the Hippo kinase cascade (MST and LATS; v). As a result, YAP is phosphorylated and localizes to IDs, perhaps by binding to α-catenin (vi). Phosphorylated TAZ may also bind to Dvl and thereby activate APC to enhance β-catenin degradation (vii). Nuclear PG, perhaps in the form of a complex with β-catenin and YAP, interferes with nuclear β-catenin and possible YAP transcriptional activity (viii). This complex may also have non-transcriptional roles in the cytoplasm or near IDs. Figure and description from Hu and Pu, 2014* (137).

Moreover, some studies suggest that upregulation of proadipogenic transcription factors peroxisome proliferator-activated receptor-ϒ (PPARϒ) and CCAAT enhancer-binding protein-α (C/EBPα) are also implicated in ACM adipogenesis (92,140). To differentiate into mature adipocytes, preadipocytes initially undergo through mitosis regulated by activation of C/EBPβ followed by terminal differentiation regulated through C/EBPα and PPARϒ (141,142). It has been suggested a reciprocal relationship between PPARϒ and

canonical WNT signalling. On the one hand, PPAR$_\gamma$ interacts directly with catenin-β1 promoting its degradation (143) and on the other hand, the canonical WNT pathway can directly antagonize C/EBPα and PPAR$_\gamma$ through activation of TCF/LEF expression (142,144). Several ACM studies have been reported an increased PPAR$_\gamma$ expression and decreased catenin-β1 activity with profound lipogenesis and suppression of canonical WNT signalling in patients or models of the disease (92,145). Moreover, physical activity and androgens have also been associated with an up-regulation of PPAR$_\gamma$ activity (38,146).

4.5.4. Arrhythmogenesis

Arrhythmias in ACM patients are frequent and occurs even before the development of structural abnormalities (147). Not only deleterious rare variants in calcium handling genes or in sodium channels could induce electrical instability, but also those located in desmosmal genes, leading to a remodelling of the IDs resulting in an impairment of the electro-mechanical connections between cells (34). It has been shown that this remodelling could cause a reduction in the protein level and dysfunction of Nav1.5 and Cx43 (85,130,148,149). Moreover, some studies suggest that desmosomal integrity is required for normal localization of Nav 1.5 and Cx43 in IDs since ACM patients and models with desmosomal mutations present mislocalization of these two essential proteins for the proper electrical function (33,150–152). Furthermore,

ankyrin 3 (ankyrin G) which is required for Nav1.5 trafficking, has also been found reduced when *PKP2* is depleted (153). All these alterations, in the end, provoke a reduction in sodium current density which has been found in a *PKP2* knockdown model (85).

Regarding calcium handling, it has been described that deleterious desmosomal variants are associated with aberrant calcium homeostasis (34). Several studies relate it specifically with alterations in *PKP2*, which is the most frequent mutated gene in ACM patients. A deficient *PKP2* cell model showed decreased SERCA expression levels and slower intracellular calcium reduction during relaxation (145). Moreover, it has been suggested that *PKP2* is required for the transcription of genes that control intracellular calcium cycling since a *PKP2* deficient mouse presented reduced expression of several components of calcium cycle. Apart from these expression alterations, this mouse model has also showed disruption of intracellular calcium homeostasis and increased the susceptibility to develop isoproterenol-induced arrhythmias (154). Apart from *PKP2* studies, another publication showed calcium handling disruptions caused by alterations in a different desmosomal gene. A cell model with mutant *DSG2* was found to present abnormal calcium transients with arrhythmogenic early after depolarization events (33,155).

4.5.5. Inflammation

Inflammatory infiltrates are frequently observed in ACM biopsy samples, commonly in fibrotic areas (33). It is known that myocarditis contributes to the onset and progression of ACM and it is mainly caused by cardiotropic viruses infection (156). In some cases, myocarditis and ACM present an overlapping of their clinical features such as desmosome disruption, inflammatory infiltrates and presence of viral genomic material that make it difficult to be distinguished (33,157,158). Some authors suggest that ACM could be a form of myocarditis due to this clinical overlap (33,95). Moreover, it has been published a case report that presents a patient who died of myocarditis but also fit in ACM diagnosis (159).

On the molecular level, it has been shown that truncated PG stimulates the secretion of multiple cytokines and tumour necrosis factor (TNF) apart from inducing cell death (93,160). It seems that desmosomal dysfunction stimulates the production of inflammatory molecules, but it is not clear if myocardial inflammation is a primary cause of ACM or it is just a secondary response to cardiomyocyte death (33).

4.5.6. Other alterations

There are some alterations found enriched in ACM patients or models that have an important role in more than one of the previously explained ACM pathogenic pathways. On one hand, it has

been described some expression patterns of microRNAs (miRNAs) that are associated with ACM pathogenesis. miRNAs are non-coding RNAs that regulate signalling pathways through post-transcriptional effects on gene expression. There are several studies in human samples (161–164) and in cell and animal models (117,165–169) that detect numerous miRNAs differently expressed compared with controls in WNT, Hippo, TFGβ pathways or apoptosis. These molecules present high stability in biological samples and are present in circulation, so they have been proposed as a potentially non-invasive prognostic and diagnostic biomarkers and also as a therapeutic targets for ACM (170).

Additionally, mitochondrial dysfunction is suggested to have an important role in arrhythmogenesis, fibrosis and apoptosis in ACM models (171). In a mouse model without *PKP2* expression, it has been described that altered Cx43 hemichannels provoke an increase of the membrane permeability and cause intracellular Ca^{2+} overload and ISO-induced ventricular arrhythmias (172). Mitochondrial membrane present also Cx43 hemichannels and it could be possible that the same mechanism occurs resulting in an overload of Ca^{2+} in mitochondria leading to electrical disturbances (171). Moreover, one study reported increased ROS in ACM cell model which are produced by mitochondria and are known to cause cardiac fibrotic remodelling and apoptosis (103,145).

As it has been seen, there are several molecular pathways altered in ACM, Figure 12 shows a summary of them.
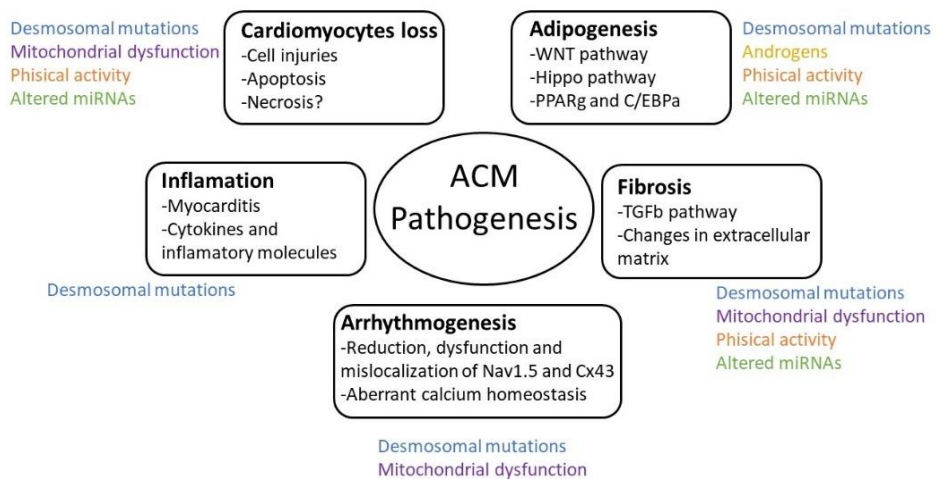
Figure 12. Schematic representation of ACM pathogenesis

Inside the squares, there are the molecular mechanisms that lead to the five most accepted ACM alterations: Cardiomyocyte loss, inflammation, adipogenesis, fibrosis and arrhythmogenesis. Outside the squares, there are the triggering factors of these alterations: Desmosomal mutations, physical activity, sex hormones, miRNAs and mitochondrial dysfunction.

4.6. ACM cellular models

Since the disease was discovered, many *in vitro* models have been used to study ACM pathogenesis, especially cardiomyocytes and cardiac progenitor cells, but also non-cardiac cells. On the one hand, the main advantage to work with cardiomyocytes is that they present intact IDs showing myocardial mechanical strength via desmosomes, electrical coupling via gap junctions and electrical activity via voltage-gated ion channels. On the other hand, the strong point of cardiac progenitor cells is their multipotency and

high adipogenic potential. And finally, non-cardiac cell models used in ACM studies, in general, present a higher maturity state and have a human origin to counteract its non-cardiac identity (173).

In the end, cardiomyocytes seem to be the favourite one for ACM research focused on desmosomes due to its higher developed IDs and desmosomal structures. In fact, the first ACM cell model was HL1 cell line that was obtained with the immortalization of AT-1 mouse atrial cardiomyocytes (173,174). HL1 maintains the differentiated cardiac properties at morphological, biochemical and electrophysiological level (175). Lots of ACM studies have been performed on that cell line regarding lipid accumulation, WNT and Hippo pathway, Cx43 and Nav1.5 channel or validation of mutations (14,150,173,176–189). HL1 cells are easy to cultivate and maintain with no special needs and they can divide during several passages without losing its cardiac properties. However, HL1 has some limitations such as its mouse origin for modelling a human disease or the fact that they come from atria when ACM is mainly a ventricular disease.

Cardiomyocytes from animal models have also been used in ACM research. The two methods mainly used are transfecting the cardiomyocytes of wild type (WT) animals or using cardiomyocytes from animals that already carry an ACM-associated variant. The three animals from which has been studied its cardiomyocytes in primary cultures are rat (182,189–191), mouse (152,192,193) and zebrafish (173,194,195). However, the main limitation of this

approach is the animal origin. Moreover, it implies to work close to an animal facility to be able to obtain fresh cardiomyocytes. Adult cells are more desirable to recapitulate adult onset of the disease, but because of the difficulty to be cultivated due to its incapacity to divide and the low number of survival cells, some studies have also been performed with neonatal cells to guarantee a longer survival in culture.

Cardiomyocytes from human induced pluripotent stem cells (hiPSCs) have also been used as a cell model for ACM (196–198). Their principal advantage is its human origin and the possibility to work with patient's cells with all its genetic background, being a unique tool for personalized-medicine approaches. Its availability is unlimited and they are also suitable for high-throughput screening (173). However, they show a fetal-like phenotype without being able to recapitulate the adult features. As published before, this issue may be partially overcome by stimulating fatty-acid oxidation to induce an adult-like metabolism in ACM-hiPSC cardiomyocytes (145,199). Additionally, it has been reported a high variability among clones obtained from the same donor.

Each of the cell model used for ACM research present different properties and characteristics with strong points and limitations. The focus of the research and also the balance between limitations and advantages are important considerations when selecting a cell model to satisfy the necessities for a specific study.

5. CRISPR/Cas9: Genome editing technique

5.1. CRISPR/Cas system as a defence mechanism

Clustered Regularly Interspaced Short Palindromic Repeats (CRISPR)/CRISPR-associated (Cas) protein system is a bacterial and archaebacterial defence mechanism against phage infection and plasmid transfer in nature (200,201). It is based on the self-nonself discrimination principle in which the system incorporates fragments of foreign DNA into CRISPR cassettes between repeated sequences. This foreign DNA is transcribed and processed to make a guide crRNA (CRISPR RNA) that will be used to specifically target and cleave the genome of the virus or plasmid (202) (Figure 13). This system protects the cells from the entry of foreign mobile genetic elements by generating a memory of past genetic aggressions through capturing and storing its DNA into CRISPR cassettes (203). Cas proteins are the effectors of this prokaryotic immunity system, they are a numerous and diverse group of proteins including DNA polymerases, helicases and nucleases whose origins could be part of an uncharacterized DNA repair system specific to thermophilic organisms (203–205).

CRISPR-Cas systems are divided into two different classes depending on the Cas proteins. Class 1 is characterized by multisubunit effector complexes and it is present in a variety of bacteria and archaea representing around 90% of all identified CRISPR-*Cas* loci. In

contrast, class 2 use a single multidomain effector protein representing the remaining 10% and it is almost exclusively present in bacteria (203,206,207). This simple architecture of class 2 CRISPR/Cas systems has given them the potential to be used as a genome editing technology.
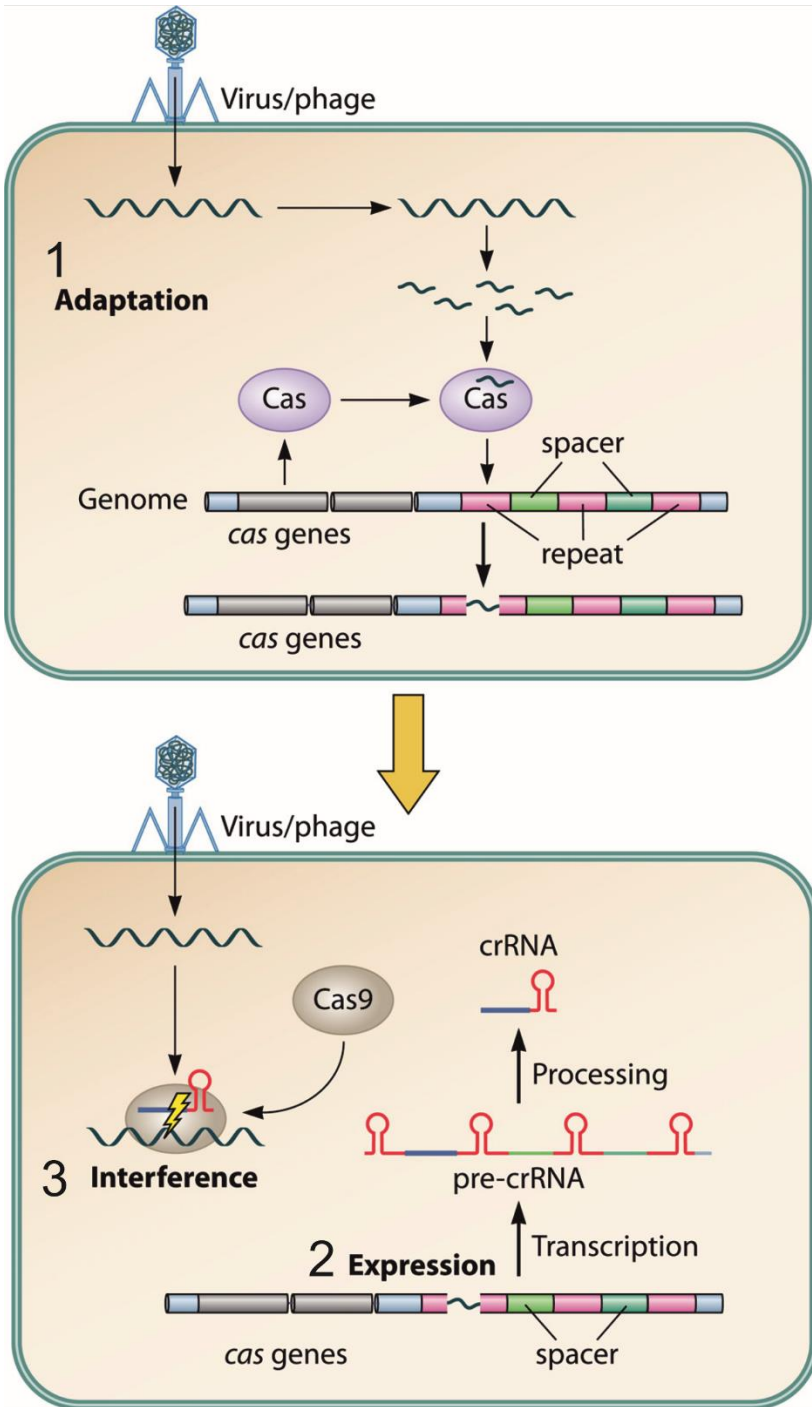
Figure 13. CRISPR-Cas acquired immune system

1) Adaptation: The external DNA is recognized by Cas proteins, fragmented and incorporated into the spacer region of CRISPR, and stored in the genome. 2) Expression: Pre-crRNA is generated by transcription of the CRISPR region and is processed into smaller units of RNA, named crRNA. 3) Interference: By taking advantage of the homology of the spacer sequence present in crRNA, foreign DNA is captured, and a complex with Cas protein having nuclease activity cleaves DNA. Adapted from Ishino et al., 2018 (203).

5.2. CRISPR/Cas9 as a genome editing technique

Class 2 CRISPR/Cas systems are suitable for genome editing being Cas9 the effector protein most studied for that purpose (203). Cas9 is a crRNA-dependent endonuclease that uses a single guide RNA (sgRNA) to form base pairs with DNA target sequences and to introduce a double-strand break (DSB) (208,209). That specific cleavage using a sgRNA only require the presence of a 5'-NGG protospacer adjacent motif (PAM) and it occurs three base pairs (bp) upstream of this PAM sequence (209,210) (Figure 14). After the cleavage, DSBs can be repaired by two different mechanisms, the homology-directed repair (HDR) or the non-homologous end joining (NHEJ). On the one hand, the HDR pathway uses a DNA donor to be recombined at the breaking point resulting in a controlled and accurate repair. HDR can be used to introduce specific genetic variants into a target region of the genome. On the other hand, the NHEJ mechanism is an error-prone system that generates random insertions or deletions and, therefore, it is useful to obtain knockouts (KO) through the generation of frameshift variants (211) (Figure 14).
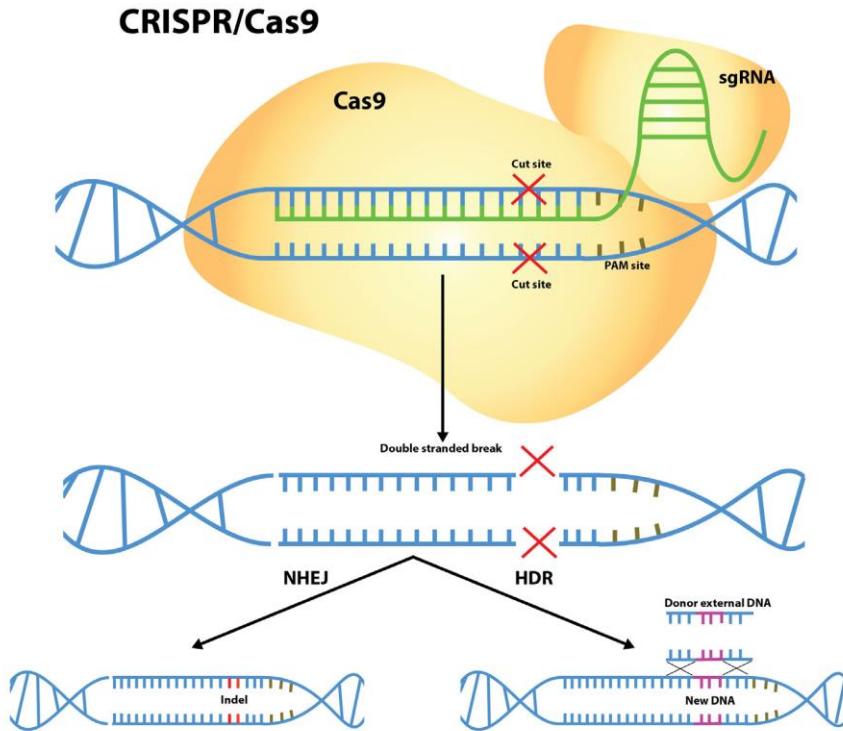
Figure 14. CRISPR/Cas9 system as a genomic editing tool

sgRNA directs Cas9 nuclease to the target DNA that introduces a DBS 3bp upstream the PAM sequence. This DSB could be repaired by NHEJ that can generate indels in the breaking point or by HDR in the presence of a DNA donor incorporating its sequence in the DBS site. Image from Cribbs and Perera, 2017 (212).

Finding this new use of the CRISPR/Cas9 mechanism created a simple two-component system in which changes in the guide sequence of the sgRNA program Cas9 to target any specific DNA sequence of interest and efficiently edit it. However, it has been shown that Cas9 binding can tolerate some mismatches between

sgRNA and the target DNA being able to generate off-target effects in the genome. Nonetheless, it is known that not all the off-targets which Cas9 binds end up cleaved (208,213).

Despite its limitations, nowadays, CRISPR/Cas9 is the most used technique to edit genomes to study genes functions or to generate cell and animal models for a wide range of diseases. Zinc-finger nucleases (ZFNs) and transcription and activator-like effector nuclease (TALEN) are also genome engineering tools that use nucleases to generate genetic modifications. TALEN is easier than ZFNs to produce and validate, but both of these methods are complex and cannot compete with the versatility and simplicity of CRISPR/Cas9 that has revolutionized biomedical science. Not only it is a simple, efficient and useful technique to edit genomes, but also it can be used for many other purposes in biomedical research such as regulation of endogenous gene expression, epigenome editing or live-cell labelling (211).

5.3. Generation of Premature Termination Codons by CRISPR/Cas9

CRISPR/Cas9 is a good technique to generate loss-of function models by introducing a frameshift variant in a genome trough NHEJ that would lead to the appearance of a PTC (214). PTCs could trigger the mRNA degradation or the expression of the truncated protein

depending on whether Nonsense Mediated mRNA Decay (NMD) is activated or not.

NMD is a mechanism in eukaryotes that promotes the mRNA degradation to carry out two functions. On the one hand, it maintains the appropriate level of gene expression depending on the cellular needs by degrading normal mRNAs and, on the other hand, it maintains the quality of gene expression by degrading the aberrant mRNAs such as those that contain PTCs (215). Regarding the second function, cells can discriminate target mRNAs by two different mechanisms: 3'UTR exon junction complex (EJC) dependent or independent NMD (216). These systems are really complex with lots of factors implicated, but to simplify it, the following paragraph contains a summary of the most relevant elements.

On the one hand, the 3'UTR EJC dependent NMD is based on the EJC, a large protein complex located by splicing in around 20-24 nucleotides upstream of most spliced exon-exon junctions. When EJC is positioned downstream a PTC, and PTC is located around 50-55 nucleotides upstream of an exon-exon junction, NMD is strongly activated (216) (Figure 15 B). On the other hand, the 3'UTR EJC independent NMD is activated when the distance between the PTC and the poly A tail is long, being more efficient the closer the PTC is to the 5'cap (216) (Figure 15 C). When these mechanisms target an mRNA to be degraded, the decay factors are recruited and the mRNA is cleaved.
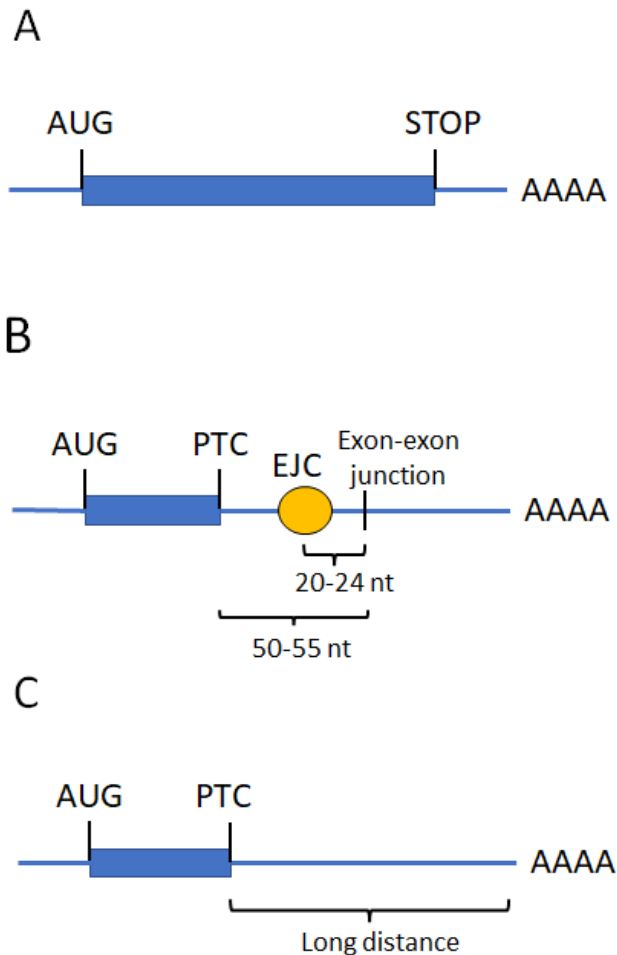
Figure 15. Nonsense Mediated Decay mechanisms to target aberrant mRNAs

A) *No NMD is triggered because there are no signals to trigger it.* **B)** *3'UTR EJC dependent NMD will be activated due to the presence of the EJC and the exon-exon junction downstream the PTC.* **C)** *3'UTR EJC independent NMD will be triggered on that case because of the long distance between the PTC and the poli A tail with no EJC.*

In general, it has been described two exceptions that allow the NMD evasion in the presence of a PTC. On the one hand, PTCs located in the 3' end of the transcript, those positioned in the last exon or in the last 50 nt of the penultimate exon, will not initiate NMD because they will not meet the molecular requirements shown in Figure 15. On the other hand, it has been reported that those PTCs located in the start-proximal codons may trigger a NMD with decreased efficiency, specifically those located in the first 160 codons of the transcript (217). In this case, NMD evasion involve reinitation of translation at a downstream start codon (218).

Moreover, there is a high variability between genes regarding its predisposition to activate or to evade NMD (218). In the case of desmosomal genes, it has been described that PTCs in PKP2 activates NMD and causes the disease by haploinsufficiency (219).

II. RATIONALE AND HYPOTHESIS

ACM is a hereditary rare cardiac entity characterised by the loss of cardiomyocytes and its progressive substitution with fibro-fatty tissue. During the last decade, genetic analysis has been useful to identify rare deleterious variants that can potentially cause the disease, being included as one of the ITFC for ACM diagnosis since 2010 (63).

In terms of genetic predisposition to ACM, the main genetic cause of the disease is rare deleterious variants in desmosomal genes: *PKP2, DSP, DSG2, DSC2* and *JUP*, with high prevalence of variants causing PTCs, especially in the most prevalent gene, *PKP2*. Generally, PTCs are described to trigger NMD causing, therefore, haploinsufficiency which is known to contribute to pathogenesis in ACM.

However, the lack of information on what determines disease progression, incomplete penetrance and the marked variability of phenotype expression is one of the big challenges to be investigated. In this thesis, we used CRISPR edited cell-based model system to describe molecular and cellular alterations triggered by PTCs in desmosomal genes and elucidate potential common alterations shared by these genes. Three different studies conform the bases of the present thesis.

First, we characterized 5' PTC to elucidate the intrinsic variability provided by the genomic context which may lead to either NMD or the reinitiation of translation. Our second study aimed to elucidate common molecular alterations related to expression levels of genes

involved in ACM pathogenesis and also to functional changes in calcium homeostasis among desmosomal genes loss. And finally, in addition to the main experimental approach, we studied how genetic variants identified in ACM patients have been reclassified after 5 years based on new available data.

Taken the above in consideration, we postulated the following **hypotheses** at the beginning of this thesis:

1. CRISPR-edited KO HL1 cell-based models would mimic ACM cellular and molecular phenotype

2. Some desmosomal 5'-PTC might be able to escape from NMD through reinitiation of translation based on their genomic context.

3. Common molecular alterations would be shown among desmosomal PTCs triggering ACM.

4. Gene-specific molecular alterations would be shown among desmosomal PTCs triggering ACM.

5. The interpretation of genetic variants pathogenicity would change in a 5-year time period based on new data generated.

III. OBJECTIVES

Main objective

The main objective of the present thesis is to elucidate and understand the molecular and cellular phenotypic alterations generated by PTCs in desmosomal genes causing ACM.

Specific objectives

1. To generate KO isogenic cell lines for the main desmosomal genes using CRISPR/Cas 9 editing in the HL1 cell model.
2. To evaluate the mechanisms triggered by a PTC in the 5' region of desmosomal genes.
3. To determine common alterations caused by the loss of desmosomal genes in the CRISPR edited KO cell lines.
4. To characterize functionally calcium handling deficits in CRISPR edited KO cell lines
5. To evaluate the impact of new available data on the classification of ACM genetic variants after 5-years

IV. RESULTS

Article 1

"Premature Termination Codon in 5' Region of Desmoplakin and Plakoglobin Genes May Escape Nonsense-Mediated Decay through the Reinitiation of Translation"

Article

Premature Termination Codon in 5′ Region of Desmoplakin and Plakoglobin Genes May Escape Nonsense-Mediated Decay through the Reinitiation of Translation

Marta Vallverdú-Prats [1] , Ramon Brugada [1,2,3,4,*] and Mireia Alcalde [1,2,*]

1 Cardiovascular Genetics Center, IdIBGi, University of Girona, 17190 Girona, Spain; mvallverdu@gencardio.com
2 Centro Investigación Biomédica en Red de Enfermedades Cardiovasculares (CIBERCV), 28029 Madrid, Spain
3 Medical Science Department, School of Medicine, University of Girona, 17071 Girona, Spain
4 Cardiology Service Hospital, University of Girona, 17007 Girona, Spain
* Correspondence: ramon@brugada.org (R.B.); malcalde@gencardio.com (M.A.)

Abstract: Arrhythmogenic cardiomyopathy is a heritable heart disease associated with desmosomal mutations, especially premature termination codon (PTC) variants. It is known that PTC triggers the nonsense-mediated decay (NMD) mechanism. It is also accepted that PTC in the last exon escapes NMD; however, the mechanisms involving NMD escaping in 5′-PTC, such as reinitiation of translation, are less known. The main objective of the present study is to evaluate the likelihood that desmosomal genes carrying 5′-PTC will trigger reinitiation. HL1 cell lines were edited by CRISPR/Cas9 to generate isogenic clones carrying 5′-PTC for each of the five desmosomal genes. The genomic context of the ATG in-frame in the 5′ region of desmosomal genes was evaluated by in silico predictions. The expression levels of the edited genes were assessed by Western blot and real-time PCR. Our results indicate that the 5′-PTC in *PKP2*, *DSG2* and *DSC2* acts as a null allele with no expression, whereas in the *DSP* and *JUP* gene, N-truncated protein is expressed. In concordance with this, the genomic context of the 5′-region of *DSP* and *JUP* presents an ATG in-frame with an optimal context for the reinitiation of translation. Thus, 5′-PTC triggers NMD in the *PKP2*, *DSG2** and *DSC2* genes, whereas it may escape NMD through the reinitiation of the translation in *DSP* and *JUP* genes, with no major effects on ACM-related gene expression.

Keywords: arrhythmogenic cardiomyopathy (ACM); CRISPR; genetics; desmosomal genes; HL1; premature termination codon (PTC); nonsense mediated decay (NMD); alternative translation initiation (ATLI)

1. Introduction

Arrhythmogenic cardiomyopathy (ACM) is a rare disorder characterised by progressive replacement of the myocardium by fibrofatty tissue. This myocyte disorganisation increases the risk of ventricular arrhythmias and sudden cardiac death [1,2]. Tissue substitution occurs predominantly in the right ventricle, but biventricular forms and predominant left ventricular involvement have also been reported [3,4]. The main genetic cause of ACM is mutations in desmosomal genes, representing around 50% of patients [5]. Desmosomes are cell unions that link the extracellular medium to intermediate filaments inside the cells to allow them to resist mechanical forces [6]. In cardiomyocytes, desmosomes are located in intercalated discs (IDs): highly specialised structures that also include adherents and gap junctions. These complexes connect cardiomyocytes electrically and mechanically in a functional syncytium [7]. Genes encoding desmosome proteins are plakophilin2 (*PKP2*), representing 10–45% of ACM cases; desmoplakin (*DSP*), responsible for 10–15% of cases; desmoglein2 (*DSG2*), responsible for 7–10% of cases; and desmocollin2 (*DSC2*) and plakoglobin (*JUP*), responsible for 1–2% of cases [5,8]. It is well known that a loss

of function of desmosomal genes is associated with ACM [9]. In that sense, around 20% of described ACM-related mutations are frameshifts or nonsense mutations that cause premature termination codons (PTCs) in desmosomal genes [10,11].

It is widely accepted that the presence of PTCs in genes causes mRNA degradation via nonsense-mediated decay (NMD): a translation-dependent mRNA surveillance mechanism in eukaryotes that helps to maintain the quality of gene expression [12]. However, there are some cases in which mRNA with PTCs can escape from NMD, such as those located in the last exon [12]. Moreover, it has been described that the reinitiation of translation can occur in front of a PTC close to the start codon [13,14].

Normally, the translation is initiated when ribosome scanning finds the start codon. It is known that there has to be an optimal context around the initial ATG codon, and there are crucial positions with a high level of conservation within the Kozak motif that are essential for the initiation of translation: a purine at position −3 and a G at +4 [15]; in addition, A/C at −2 and no T on position +5 were also shown to be important (where the A of ATG is numbered +1) [14,16]. However, there are alternative ways to initiate translation that start in a non-canonical ATG [14]. This is the case of the reinitiation of translation that occurs when the first ORF is very short, and it starts in an alternative in-frame ATG after that first ORF [14,17]. In this way, translation reinitiation could allow the expression of an N-truncated protein by initiating translation at the in-frame methionines downstream of a PTC [14]. It is well accepted that the reinitiation of translation allows mRNA with PTCs to escape from degradation via NMD [13,18,19]. It has been observed that translation reinitiation is more efficient when the downstream in-frame methionine is located within 50 codons of the PTC when it is located in the first 10% of the coding sequence [13,20]. Moreover, there is evidence that the reinitiation of translation from ATG codons located over 160 codons downstream of the first initiation codon is significant [18]. Furthermore, it is well described that reinitiation is more efficient when the PTC is close to the canonical start codon [13].

Regarding the presence of PTCs in the 5′ region of desmosomal genes, it is uncertain whether those mutations are more susceptible to the activation of NMD or the reinitiation of translation. Moreover, it is not clear whether these five genes react similarly or differently in front of a PTC in the 5′ region. An important question to consider is what role these mechanisms might have in the overall ACM pathophysiology. It is described that the presence of a PTC in PKP2 causes it to lose function; thus, ACM is caused by haploinsufficiency [21]. However, it is unknown whether PTCs in other desmosomal genes have the same effect or not. It is important to describe whether ACM is caused by a null allele due to the mRNA degradation via NMD or by the presence of N-truncated protein caused by the reinitiation of translation in order to better understand the molecular mechanisms of the pathology, and also to classify the pathogenesis of new potential causal variants. There are many decisive factors in classifying rare variants, such as the mutation type, the location of the mutation and the affected gene [22]. Moreover, it is recommended to update the classification of rare variants associated with ACM due to its importance as a diagnostic criterion [23,24]. Understanding which mechanism is triggered by PTCs in the 5′ region of each desmosomal gene could allow a better comprehension of the pathology and more accurate prediction of the pathogenesis of new ACM-associated variants.

For this reason, the present study was aimed at evaluating the likelihood that desmosomal genes carrying PTCs at the 5′ region would trigger the reinitiation mechanism. We hypothesised that downstream reinitiation of translation would be triggered in some cases with optimal genomic context.

2. Results

2.1. PTC Clones and Genotype Distribution

Edited HL1 clones carrying frameshifts leading to a PTC within the 5′ gene sequence (fewer than 160 codons from natural ATG) in five desmosomal genes were selected for the study: *PKP2, DSP, DSG2, DSC2* and *JUP*. A total of 20 clones with at least one allele carrying

PTC were obtained: four homozygous (HM) PKP2-PTC; four HM and two heterozygous (HT) DSP-PTC; four HM DSG2-PTC; two HM DSC2-PTC; and two HM and two HT-like JUP-PTC (Table 1).

Table 1. CRISPR edited desmosomal gene clones.

Desmosomal Gene	Clones		Variants	New Frames	PTC Positions (Codons)
PKP2	27	A1	c.325ins1	−2	93
		A2	c.324del2	−2	93
	31	A1	c.326ins1	−2	93
		A2	c.322del2	−2	93
	32	A1	c.325ins1	−2	93
		A2	c.324del1	−1	115
	35	A1	c.325ins1	−2	93
		A2	c.325del4	−1	115
DSP	28	A1	c.329del2	−2	75
		A2	c.331del5	−2	75
	21	A1	c.332del2	−2	75
		A2	c.332del4	−1	17
	14	A1	c.324del29	−2	75
		A2	NI	-	-
	15	A1	c.326del31	−1	17
		A2	NI	-	-
	17	A1	WT	0	-
		A2	c.324del26	−2	75
	29	A1	WT	0	-
		A2	c.314del32	−2	75
DSG2	1	A1	c.226del4	−1	31
		A2	c.229ins1	−2	38
	6	A1	c.220del 30 + ins7	−2	38
		A2	NI	-	-
	11	A1	c.220del7	−1	31
		A2	c.228del1	−1	31
	14	A1	c.221del10	−1	31
		A2	c.229ins1	−2	38
DSC2	18	A1	c.324del4	−1	20
		A2	NI		
	21	A1	c.325del1	−1	20
		A2	NI		
JUP	1	A1	c.135del13	−1	37
		A2	c.142del4	−1	37
	4	A1	c.142ins1	−2	44
		A2	NI	-	-
	14	A1	c.136del6	0	-
		A2	c.142ins1	−2	44
	18	A1	WT	0	-
		A2	c.135del10	−1	37

Our results indicate that 56.6% (17/30) of edited alleles presented a PTC in frame minus (−)2 and 43.3% (13/30) in frame −1 (Table 1). From all edited alleles, small insertions or deletions of fewer than 20 bp were the main genetic variation introduced in 67.5% of cases (25/37), predominantly deletions (45.94% of total, 17/37). Interestingly, larger

insertions were not detected, while 16.2% (6/37) of PTCs were deletions of 20–50 bp and the remaining 16.2% (6/37) were large deletions (deletions affecting the whole exon, not detected by sequencing exon 1). Thus, deletions were the predominant variant identified, representing 78.3% (29/37) of total variants (Figure 1).
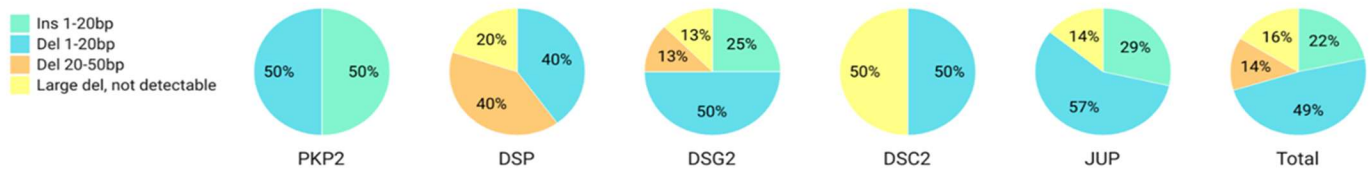
Figure 1. Prevalence of genetic variants introduced after repairing double strand break (DSB) in DNA caused by CRISPR-Cas9. Created with Datawrapper.

2.2. Genomic Context of 5′ Region for Reinitiation

Results from the analysis of the 5′ sequence of the five desmosomal genes predicted that the *DSP* and *JUP* sequences present alternative in-frame ATGs with high optimal sequence context for the reinitiation mechanism within the firsts 160 codons. On the other hand, *PKP2*, *DSG2* and *DSC2* genes present significantly fewer alternative in-frame ATGs, and none of them have high optimal genomic context for reinitiation (Table 2).

Table 2. Sequences of 5′ UTR (lowercase) and the first 160 codons (alternating white and grey; 480 base pairs) of 5 desmosomal mouse genes. Exons are shown in alternating black and blue text. The underlined sequence is the hybridisation region of sgRNA used to edit desmosomal genes in the HL1 cell line by CRISPR/Cas9. ATG codons in-frame are in green, blue or red depending on genomic context for translation reinitiation. ATGs with high optimal context (ANNATGN, GNNATGG) are highlighted in green, moderate context (CNNATGG, UNNATGG, GNNATGH) in blue and weak context (YNNAUGH) in red, where Y = C or U, H = not G (http://wwwmgs.bionet.nsc.ru/AUGWeb/; accessed on 24 September 2021) [25].

PKP2	tctgcggctttgcgggcaggtcctggcagtccctcctggtcactccgccgacgcg **ATG** GCC GTC CCC GGC TCA CTG GCC GAG TGT GGC TAC ATC CGG ACT GTG CTG GGC CAG CAG ATC CTG GGT CAC CTG GAC AGC TCC AGC CTG GCC TTG CCC TCC GAG GCC AGA CTG AGG CTG GCC GGC AGC AGC GGC CGC GGC GAC CCG GCG GCC CGG AGC CAG CGG ATC CAG GAG CAG GTG CAG CAG ACC CTG GCC CGC CGG GGC CGG AGC TCT GCG GTC AGC GGG AAC CTT CAC CGA ACC AGC AGT GTC CCT GAG TAT GTC TAC AAG CTA CAC G TGGTT GAG AAT GAC TTT GTT GGA CGG CAG TCA CCT GTC ACT AGG GAC TAT GAC **ATG** CTT AAG GCT GGA **ATG** ACT GCC ACT TAT GGA AGT CGC TGG GGG AGA GCA GCA GCA CAG TAC AGT TCC CAG AAG TCA GTG GAG GAG AGA TCC TGG AGG CAG CCT CTG AGG AGA CTT GAG ATT TCC CCA GAT AGC AGC CCG GAG AGA GCC CAC
DSP	gaccaggtgtggcctgggcgccgggtgccagcgggggaggagactcgcaccgcctcgaccaacaccaacacccaggcgcgacccagctcctctgagccctcgctgccctc cgagccacagctccactccggttcccgcgcctagccagtcgccgtccccgtctccgccctgctggagcgctgagccctcgccagtcctccgcgttccgcgctcctctcccg gagtccctcgcgtgctccgaggcgacgcctcgcgtatgccgcggcgctgagcggctctcttgagtgaccgcagac **ATG** AGC TGC AAC GGC GGC TCC CAC CCG CGG ATC AAC ACG C TG GGT CGC **ATG** ACC CGC GCG GAG TCC GGC CCG GAC CTG CGC TAC GAG **ATG** ACC TAC AGC GGT GGC GGC GGG GGG GGC GGC GGG GGC GGC GGC GGG GGC ACC AGC AGG ACG TTC TAC TCC CAC TCC CGG CGC TGC ACC GTC AAC GAC CAG AAC TCC GAC GGC TAC TGT CAA ACC GGC ACC **ATG** TCT AGA CAT CAG AAT CAG AAC ACC ATC CAA GAA **ATG** CTG CAA AAT TGC TCA GAC TGT CTG **ATG** CGG GCG GAG CTG ATC GCG CA G CCG GAA CTG AAA TTC GGA GAA GGG **ATG** CAG CTG GCA TGG AAC CGA GAG CTG GAT GAG TAT TTT ACA CAA GCC AAC GAT CAG **ATG** GAA ATC ATA GAC GGC TTG ATC CGA GAG **ATG** AGG CAG **ATG** GGC CAG CCC TGT GAT GCG TAT CAG AAA AGA CTG CTT CAG CTC CAG GAA CAA

Table 2. *Cont.*

DSG2	ctgcctcgtacctcccccgcggagcgaacacattcccctcctccatctaggctgtggcccggcccaaggctacccttctgacccgggcacacctggaaccgcaccccgggtcc cgcagagtcagagaagggcggccccgggagggacctgcccaggaggatccgcagggcgccggcgaggcccggaggcgagggcgcggcggatcgaggcg `ATG` GCG CGG AGC CCG GGT GACCGGTGC GCC CTG CTG CTG CTG GTG CAG CTG CTG GCG GTG GTC TGC TTG GAC TTT GGA AAC GGA CTT CAC TTA GAG GTC TTC AGC CCA AGA AAT GAA GGC AAA CCG TTC CCT AAG CAC ACT CAC TTG GTT CGT CAA AAG AGG GCC TGG ATC ACT GCC CCT GTG GCT CTG CGG GAG GGC GAA GAC CTG TCC AGA AAG AAC CCG ATT GCC AAG ATA CAC TCT GAC CTT GCA GAA GAA AAA GGG ATA AAA ATC ACG TAC AAG TAC ACT GGG AAG GGA ATT ACA GAA CCG CCT TTC GGC ATA TTC GTC TTT GAT AGA AAC ACA GGA GAA CTG AAC ATC ACT AGC ATT CTT GAC CGG GAA GAA ACA CCA TAT TTT CTGCTGACA GGC TAT GCA TTG GAC TCC AGA GGA AAC AAC CTG GAA AAG CCC TTG GAA CTA CGC ATC AAA GTT CTG GAC ATC AAT GAC AAC
DSC2	gggggggtgacaagggacatataggtggcctctgctggtgagaaatacctagtacaggtgaaagggtggcggccagagggagttcccaccggttgaattcttaaagtc atgaagactcaagaaaaataacaaggagtggccgattcgagtcttttggacttgcccagagctccaccctcggacagaggaaaaagcccctggggacccaggcggga gcatcagacaagcgcgagaaaagcgcctgtgtgcgcgctccacctctgcgcagcgggtgcggggcggtgacctgtcccttgagctggcc `ATG` GCG GCT GTG GGA TCT `ATG` CGC TCCGGGAGC CCT GCC TTC GGC CTG GGA CAC CTG TTG ACC CTT GCG ATCCTT GCA CTT GCC TCT GAT GCC TGT AAA GAA GTC GTC CTC CAG GTC CCC TCT GAA CTA CCT GCC GAG AAA TTT GTT GGC AGA G TG AAC CTG `ATG` GAC TGC CTT AAA TCA GCA GAC ATA GTT CAT CTG AGT GAT CCT GAC TTC CAA GTC TTA GAA GAT GGT TCT GTG TAC ACA ACC AGT TCT GTT GTT TTG TCC TCG GGG CAA AGA AGC TTT ACT ATA TGG CTT TTT AGC ACA GAC AGC CAA GAA GAA AGG GAG ATA TCT GTC CAT TTA GAG GGC CCA GTA GAG GTA CTA AAT AAA AGA CCG CAT ACA GAG AAG GTT CTC AGC CGT GCC AAG AGA AGA TGG GCT CCT ATC CCT TGT TCC `ATG` CTA GAG AAT TCA TTG GGT CCC TTC CCA CTT TTC CTT CAA CAG ATC CAG
JUP	gccagagtccggagcagccgccgcccgagtgcgccgagctcagttcgctgcccgcgccggctcctcccggccagacccgaccccgattcggctcagcccggctccac gctcagcagccacc `ATG` GAG GTG `ATG` AAC CT T ATT GAG CAG CCC ATC AAG GTG ACA GAG TGG CAA CAG ACA TAC ACC TAC GAC TCG GGC ATC CAC TCC GGC GTC AAT ACC TGT GTG CCC TCT GTA AGC AGC AAG GGC ATC `ATG` GAT GAG GAT GAT GCC TGC GGC AGA CAG TAC ACA CTC AAG AAG ACT ACC ACC TAT ACA CAA GGG GTG CCA CAG AAC CAA G GT GAC CTG GAA TAC CAG `ATG` TCC ACA ACG GCC AGA GCC AAG CGG GTG CGG GAG GCC `ATG` TGT CCA GGG GTC TCA GGC GAG GAC AGT TCT CTA CTG CTG GCC ACC CAG GTG GAG GGG CAG ACA ACC AAT CTG CAG CGC CTG GCC GAA CCA TCC CAG TTG CTC AAG TCG GCC ATC GTC CAT CTC ATC AAC TAC CAG GAT GAT GCA GAG CTG GCC ACC CGG GCT CTG CCT GAG CTC ACC AAG CTG CTC AAC GAT GAG GAC CCG GTA GTG GTG ACC

Similarly, in silico prediction suggests that *DSP* and *JUP* have in-frame ATGs with high optimal context susceptible to the reinitiation of translation. However, no in-frame ATGs present in *PKP2*, *DSG2*, or *DSC2* genes were predicted to be susceptible to the reinitiation of translation (Table 3).

Table 3. In silico prediction of context for translation reinitation of ATGs within the first 160 codons of 5 desmosomal genes: *PKP2, DSP, DSG2, DSC2* and *JUP*. Prediction takes into account all ATGs, in-frame and not. ORFs that start with ATG in-frame and have high genomic context are highlighted in orange.

	Name	In-Frame	Remark	Context	Mechanism	Position
PKP2	Orf1	Yes	Null, canonical ATG	W	Linear scanning	0
	Orf2	No	AltORF2; predicted translation level: moderate	H	Reinitiation starter	256
DSP	Orf1	Yes	Null, canonical ATG	W	Linear scanning	0
	Orf2	Yes	AltORF2; predicted translation level: weak	W	Leaky scanning	48
	Orf3	Yes	AltORF3; predicted translation level: moderate	M	Leaky scanning	87
	Orf4	Yes	AltORF4; predicted translation level: moderate	H	Reinitiation starter	219
DSG2	Orf1	Yes	Null, canonical ATG	W	Linear scanning	0
	Orf2	No	AltORF2; predicted translation level: moderate	M	Leaky scanning	112
	Orf3	No	AltORF3; predicted translation level: moderate	M	Leaky scanning	403
	Orf4	No	AltORF4; predicted translation level: weak	W	Leaky scanning	472
DSC2	Orf1	Yes	Null, canonical ATG	W	Linear scanning	0
	Orf2	Yes	AltORF2; predicted translation level: weak	W	Leaky scanning	18
	Orf3	No	AltORF3; predicted translation level: weak	W	Leaky scanning	88
	Orf4	Yes	AltORF4; predicted translation level: moderate	M	Leaky scanning	162
	Orf5	No	AltORF5; predicted translation level: moderate	H	Reinitiation starter	226
JUP	Orf1	Yes	Null, canonical ATG	W	Linear scanning	0
	Orf2	Yes	AltORF2; predicted translation level: moderate	M	Leaky scanning	9
	Orf3	Yes	AltORF3; predicted translation level: moderate	H	Reinitiation starter	126

2.3. Expression Levels of PTC Clones and Mechanisms Triggered

Expression levels of genes carrying PTC, either homozygous or heterozygous, were evaluated in all PTC clones. Protein expression levels were undetectable for all PKP2-PTC and DSG2-PTC edited clones (Figure 2A,B). Moreover, *DSC2* mRNA expression levels were null in HM DSC2-PTC clones (Figure 2C).
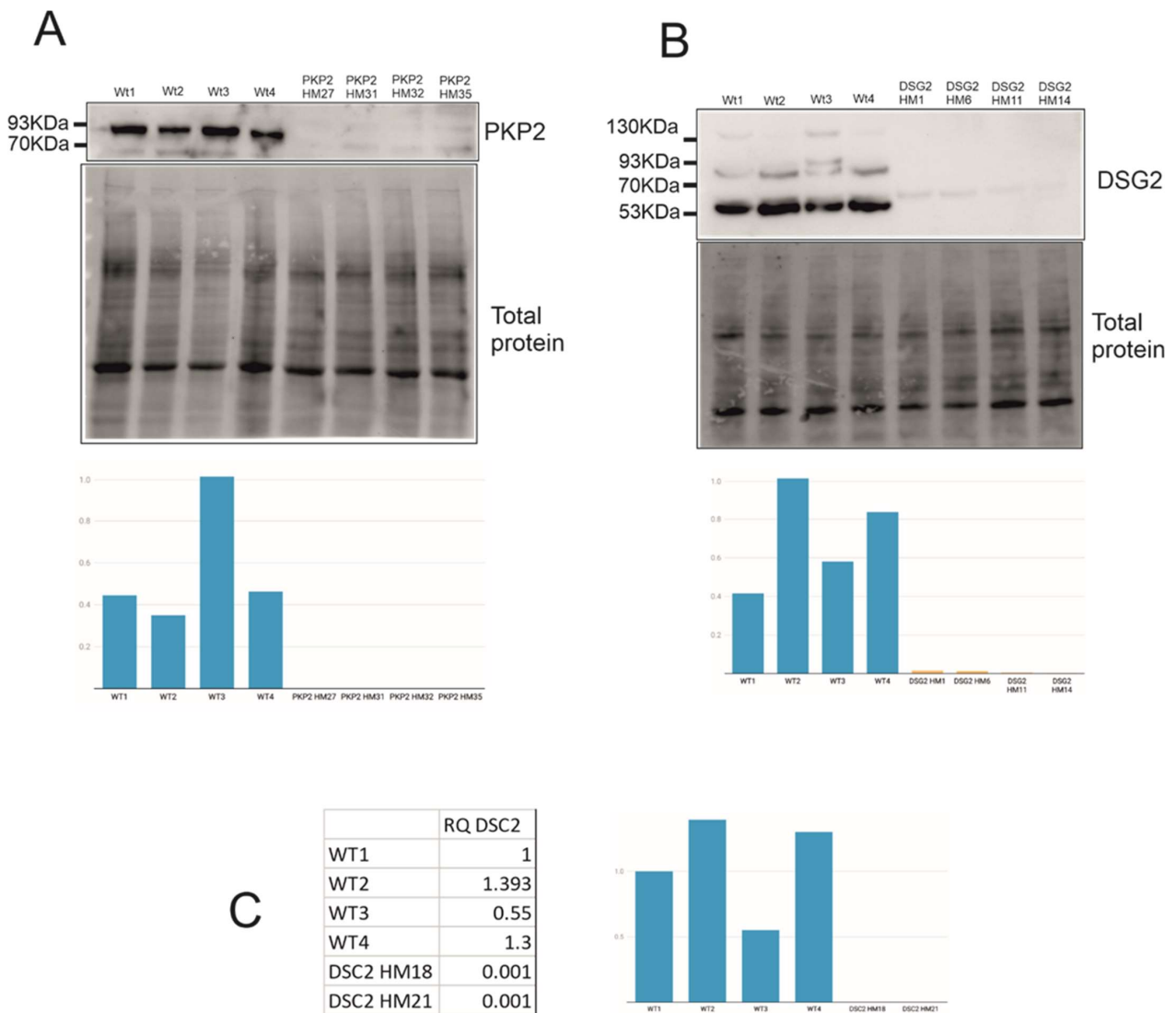
Figure 2. Undetectable levels of edited genes. (**A**) PKP2 protein expression of HM PKP2-PTC clones. (**B**) DSG2 protein expression of HM DSG2-PTC clones. (**C**) *DSC2* mRNA expression of two HM DSC2-PTC clones. Created with Datawrapper.

On the other hand, DSP protein expression was detected in similar levels compared to WT clones in three of the four HM DSP-PTC clones (Figure 3A). The predicted size of WT DSP is 332 KDa (2883aa), whereas the expected size of N-truncated DSP would be around 307 KDa (2664aa), assuming that the translation starts in ATG positioned at c.514 with a high genomic context. Moreover, all HT DSP-PTC clones showed similar levels to WT, suggesting that either the reinitiation mechanism is triggered in the PTC allele or the WT allele can compensate the total expression of DSP.
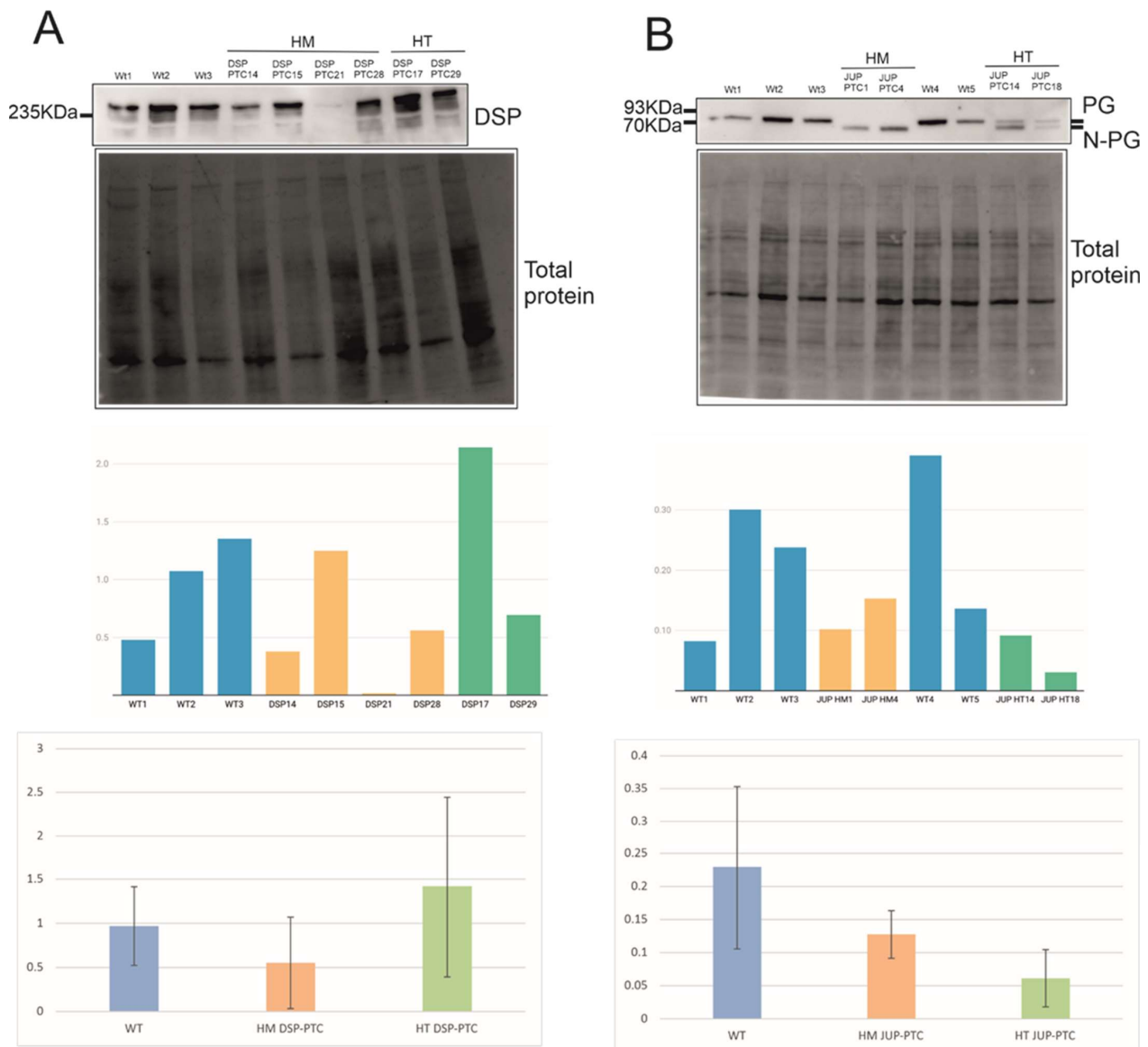
Figure 3. Reinitiation of translation. N-truncated protein expression for (**A**) DSP-PTC and (**B**) JUP-PTC clones.

Finally, PG protein expression in the two HM JUP-PTC clones suggests that the reinitiation mechanism was triggered, translating an N-truncated PG using a downstream alternative in-frame ATG (Figure 3B). N-truncated PG was clearly observed in these clones with a lower weight than PG-WT, compatible with the predicted size of N-truncated PG using a downstream ATG (the predicted size of WT is 81 KDa (745aa) and that of N-truncated PG is around 67 KDa (619aa), assuming that the translation starts in ATG positioned at c.248 with a high genomic context). Interestingly, the two HT JUP-PTC clones showed a double band corresponding to the WT size and the N-truncated PG size, suggesting that the PTC allele would also trigger the reinitiation mechanism in HT genotypes. All PG clones expressed similar levels of the protein compared with WT (Figure 3B).

mRNA expression levels of *PKP2, DSG2, DSP* and *JUP* edited clones are shown in Supplementary Figure S1.

Taking all the data together, the reinitiation mechanism was triggered only in *DSP* and *JUP* genes, which were those predicted to present close downstream in-frame ATGs with optimal sequence context likely to be susceptible to the reinitiation of translation. All

PTC alleles in JUP-PTC clones, in both HM and HT genotypes, produced an N-truncated PG (Figure 3B). However, this mechanism occurred in only 75% of HM in DSP-PTC clones, suggesting that reinitiation is not consistent between individuals, although it is over time. The expression of these PTC alleles does not depend on the distance between PTC and the canonical start in our study. In the *DSP* gene, this distance corresponds to 17 codons in −1 frame, representing 25% (2/8) of the total edited alleles, and 75 codons in −2 frame, representing 75% (6/8) of alleles. In the *JUP* gene, the distance corresponds to 37 codons between PTC and the canonical start in −1 frame, representing 60% (3/5), and 44 codons in −2 frame, representing 40% (2/5) of the total edited alleles (Table 1).

2.4. Effect of N-Truncated DSP and JUP on ACM-Related Gene Expression

Expression levels of genes involved in ACM, such as desmosome, calcium handling and connexome genes, are slightly altered in HM JUP-PTC clones that express the PG N-truncated protein (Figure 4B). Even though these clones showed similar levels of expression of the truncated protein compared with WT, HM JUP-PTC presented significant upregulation in *JUP* and *ANK2* genes (Supplementary Tables S1 and S2).
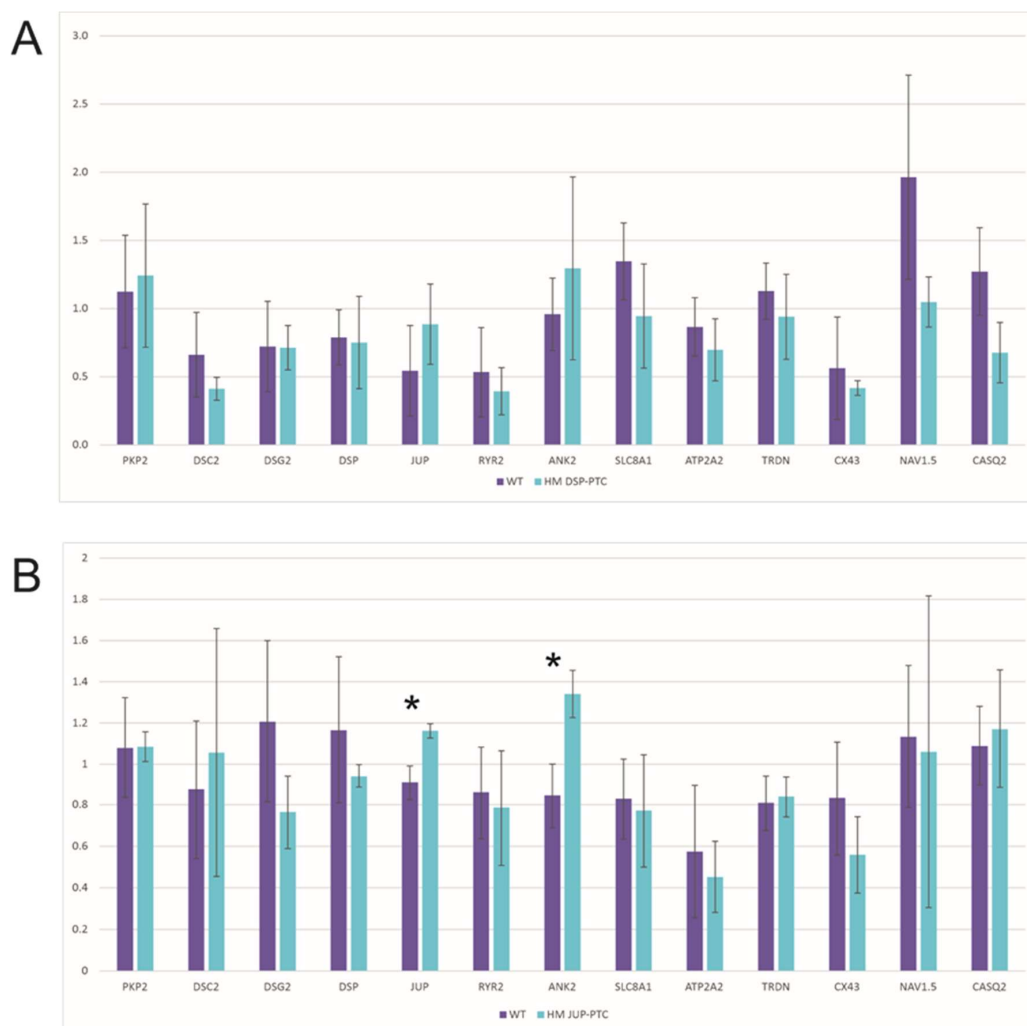
Figure 4. mRNA expression level of desmosomal, calcium handling and connexome genes in (**A**) HM DSP-PTC and (**B**) HM JUP-PTC clones. * Marks those gene expression levels that were significantly different between WT and edited clones.

On the other hand, the three HM DSP-PTC clones that expressed the DSP N-truncated protein did not show any molecular alterations in the studied genes involved in ACM

(Figure 4A, Supplementary Tables S1 and S3). However, only one HM DSP-PTC clone had no detectable levels of DSP protein, suggesting important differential expression at the RNA level compared with WT, but statistical analysis was not possible because only one clone was available. Nevertheless, it is important to note that *DSC2* expression was nearly null in this clone, RQ = 0.001 (Supplementary Table S3).

3. Discussion

In ACM, loss of function due to NMD and triggered by PTC codon variants has been widely supported for all five desmosomal genes [9,21,26–29]. The position of a truncating mutation can govern the resulting phenotype, as mutations in the last exon can evade NMD [12]. In the present study, we investigated the susceptibility to NMD of PTC located at the end 5′ sequence for all five desmosomal genes associated with ACM (*PKP2, DSP, DSG2, DSC2* and *JUP*) and whether they might trigger downstream reinitiation of translation within the optimal genomic context. Concretely, we investigated whether a putative downstream in-frame ATG after a PTC would be susceptible to the reinitiation of translation. Our results show undetectable levels of PKP2, DSG2 protein and *DSC2* mRNA in 100% of clones, suggesting that PTC-mRNA or protein were targeted and degraded by a quality control mechanism when carrying a PTC within the first 160 codons. Interestingly, although *PKP2, DSG2* and *DSC2* genes presented alternative ATG in-frame within the region <160 codons from the natural ATG, none with highly optimal genomic context was found. These results suggest that the optimal genomic context of ATG in-frame may be key for the reinitiation of translation.

On the other hand, both *DSP* and *JUP* presented alternative in-frame ATG close to the initial codon with an optimal context. In the *DSP* sequence, the ATG in-frame with high context accomplished the −3 position of Kozak motif, but not the +4 position. However, it presented C at −2 and no T on position +5, which was also described as being important [14,16]. The *JUP* sequence around the alternative ATG in-frame predicted to present high genomic context accomplished both positions of Kozak motif. Moreover, it presented no T on position +5, and no A/C at −2. In concordance, *DSP* and *JUP* showed expression of N-truncated protein when containing PTC by escaping NMD, probably due to the reinitiation mechanism. Concretely, the *JUP* gene expressed N-truncated PG protein in 100% of cases, and DSP in 75% of homozygous clones, suggesting that other factors might be involved in triggering this mechanism, with consistency over time for each clone. Previous studies showed that the distinguishing feature of most of these mutations evading NMD was proximity to the initiation codon. Evasion of NMD has been proposed to be mediated by the reinitiation of translation [30–32] or by physical proximity to the native ATG initiator codon [33]. However, there is still no knowledge about the possible role of the other allele in the NMD evasion mechanism, i.e., whether carrying other PTCs in trans- or wild-type alleles might have an influence.

Concerning mRNA expression levels of edited clones, results show that *DSP* and *JUP* clones express similar PTC-mRNA levels to WTs clones (Figure S1), in concordance with protein levels (Figure 3). Moreover, *PKP2* clones present a significant downregulation both in PTC-mRNA (Figure S1) and PTC-protein levels (Figure 2), probably due to NMD. On the other hand, two of the four *DSG2* clones present similar PTC-mRNA levels compared with WTs (Figure S1), but no protein expression (Figure 2). This discordance may be explained by the intrinsic dynamic properties of NMD that could be repressed under cellular stress [34]. However, proteolytic machinery could act when NMD misses defective mRNAs [35]. What is important here is that we have proven that *DSG2* edited clones did not experience the reinitiation of translation but NMD or protein degradation was triggered by PTC in the 5′ region. Finally, we were only able to detect PTC-mRNA levels, but no protein levels, in *DSC2* edited clones which were proven to be null (Figure 2), probably also due to NMD.

Regarding the role of DSP N-truncated protein in ACM pathogenesis, our results show that HM DSP-PTC clones had no alterations of the total RNA expression levels in ACM-related genes, suggesting that these PTCs generating N-truncated *DSP* may not be

loss-of-function variants and may not be associated with severe changes in genes involved in the molecular pathomechanism of ACM. First, the *DSP* loss-of-function pathomechanism is supported by several mouse models [36–38], and PTC variants represent a relatively high amount (5–10%) of pathogenic truncating *DSP* mutations associated with the ACM phenotype, preceded only by PTC in the *PKP2* gene. The *PKP2* gene presents PTC variants as the most prevalent type of mutation [39,40]. The results of the present study suggest that the expression of N-truncated protein in *DSP* clones can escape NMD and the molecular alterations associated with ACM. In this sense, some studies have shown that PTC close to the initial codon may be associated with a milder phenotype of diseases due to the reinitiation of translation [13,14,41–44]. To date, there are no studies exploring a similar effect of translation reinitiation in desmosomal genes carrying PTCs at the 5′ region and their association with the ACM phenotype and disease severity. Interestingly, the DSP clone, which did not trigger the reinitiation mechanism and therefore acted as a null clone, showed a different pattern in the gene expression profile in ACM-related genes, such as downregulation of *DSC2*, supporting the idea that N-truncated DSP protein might be associated with milder cellular phenotype or no phenotype at all. However, more studies should be performed to further investigate molecular alterations when DSP is not expressed at the protein level.

On the other hand, PTC in the 5′ region of *JUP* showed reinitiation in 100% of cases synthesising N-truncated instead. These results suggest that the N-ter aminoacids of PG might be important in maintaining the normal RNA levels of *ANK2*, but further studies with larger amounts of clones would be needed to confirm that. It is known that the N-ter of PG protein is a conserved region between human and mouse [45], and it has been described as participating in binding β-catenin and promoting desmoglein-2 association [45–47]. However, it is still unknown whether alterations in PG can affect *ANK2* expression, and more studies should be performed.

Taking all of the above into account, this study suggests that when reinitiation is triggered, the molecular phenotype might be milder than or not associated with the ACM pathomechanism. In this sense, clinical evidence, such as pathogenic variants upstream of the new alternative codon, also points to there being no critical biological relevance of the N-terminal region in relation to the ACM phenotype. The number of PTC mutations described in the first 160 codons of *DSP* and *JUP* genes in the general population and ACM patients supports the supposition that there might not be an association of N-ter loss and ACM phenotype in *DSP* and *JUP*. In the *DSP* gene, only two variants causing PTC have been described in ACM patients [11] and five in the general population [48]. Patients carrying DSP: p.R160X had no cardiac dysfunction at the age of examination (8 months old) [49]. Similarly, in the *JUP* gene, only one variant has been described in ACM patients [11] and three in the general population [48]. *JUP* p.S24X has been identified in a patients with cutaneous disease, but no symptoms of cardiomyopathy in children were reported [50]. In contrast, in the *PKP2* gene, which is the main gene in ACM, according to our results, is not able to trigger reinitiation, showing 17 different 5′-PTC variants in the first 160 codons in ACM patients [11] and only six in the general population [48]. It is accepted that *PKP2* haploinsufficiency causes ACM [21], and this may suggest that PTCs in the first 160 codons of *PKP2* are pathogenic due to the lack of translation reinitiation mechanism.

This raises a concern regarding how to classify 5′-PTC variants in terms of pathogenicity in *DSP* and *JUP* genes. For the interpretation of loss-of-function variants based on ACMG guidelines [22], it is recommended to apply very strong or strong criteria to PTCs in all desmosomal genes [9], regardless of position. Currently, the criterion applied for those PTC variants located in the last exon of the gene is only moderate, taking into account that they are likely to escape NMD decay. Our results suggest not only that last exon PTCs can avoid NMD machinery, but also that end 5′ PTCs in *DSP* and *JUP* genes can synthesise N-truncated proteins with little to no great impact on the expression of ACM-related genes.

Regarding the limitations of the study, one of the most important restrictions is that the number and distribution of genotypes are different for each gene, since it was not possible to predict what would be the final outcome of editing. Second, the distance between the canonical start codon and PTC is not identical among desmosomal genes because of the different nature of each sequence, even though, as is known, the reinitiation of translation is more efficient when this distance is shorter [13]. Third, despite the high similarity between human and mouse desmosomal sequences, the results should be interpreted with caution when applied to human genes, since the two are not identical. Further experimental evidence from human samples would be needed to validate this mechanism in humans. On the other hand, although HM DSC2-PTC showed nearly no mRNA expression of the edited clones suggesting NMD, ideally this also should be checked by immunoblot. Unfortunately, none of the commercial antibodies worked in our cellular model and conditions. Finally, N-truncated DSP was presumably expressed in HM DSP-PTC with around 307 KDa (2664 aa), assuming that the translation starts in ATG positioned at c.514 with high genomic context, only 25 KDa less than full length DSP (7.5% of the total weight), and it was not possible to differentiate N-truncated protein in the electrophoresis gel. Moreover, N-term anti-DSP antibody targeting only full-length DSP and not N-truncated DSP is not available in the market. Finally, further studies to evaluate N-truncated DSP and PG will be needed to understand whether they have full functionality or might be involved in the ACM cellular phenotype and other PTC mutations along the whole sequence of desmosomal genes.

4. Materials and Methods

sgRNA design and cloning into Cas9 px458 vector. The Benchling Web tool (Biology Software, 2018; retrieved from https://benchling.com; accessed on 2 March 2018) was used to design the sgRNAs of the 5 desmosomal genes at the first 160 codons of the sequences for editing by CRISPR/Cas9. sgRNAs with high scores and low off-targets were selected: *PKP2* (GTATGTCTACAAGCTACACG, FW); *DSP* (CCACCCGCGGATCAACACGC, FW); *DSG2* (TGGCGCGGAGCCCGGGTGAC, FW); *DSC2* (GCTGTGGGATCTATGCGCTCC, FW); *JUP* (CCTTGATGGGCTGCTCAATA, RV). px458 vector (plasmid #48138, addgene, Teddington, UK), which encodes Cas9 WT, was digested by BbsI-HF (R3539S, New England BioLabs, Ipswich, MA, USA) at 37 °C overnight and ligated by T4 DNA ligase (M0202L, New England BioLabs, Ipswich, MA, USA) for 1 h at RT with the sgRNA previously annealed (sense and antisense). Annealing of sgRNAs was performed with T4 PNK (M0201S, New England BioLabs, Ipswich, MA, USA) using the following thermocycler program: 30′ at 37 °C, 5′ at 95 °C and 94 to 25 °C going down 1° per 12″. DH5alpha competent cells (18265-017, Invitrogen, Waltham, MA, USA) were transformed with sgRNA-px458 vector during 30′ in ice and 45″ at 42 °C. DNA was extracted using the Plasmid Midi Kit (12143, Qiagen, Hilden, Germany).

HL-1 cell culture and electroporation. HL1 cells were cultured as described previously [51] at 37 °C under 5% CO_2 in fibronectin–gelatin coated slides in supplemented Claycomb medium (51800 C–500 ML, Sigma, St Louis, MO, USA) with 10% fetal bovine serum (10270106, GIBCO, Waltham, MA, USA), 100 U/mL penicillin, 100 µg/mL streptomycin (P4333-100 ML, Sigma, St Louis, MO, USA), 2 mM L-glutamine (35050061, Thermo, Waltham, MA, USA), 10 µM norepinephrine (A9512, Sigma, St Louis, MO, USA) and 0.3 mM ascorbic acid (A7631, Sigma, St Louis, MO, USA). Plasmids were nucleofected into HL-1 in suspension by using the Amaxa Cell Line Nucleofector Kit V (VCA-1003, Lonza, Basel, Switzerland); 10^6 cells per condition were transfected by adding 4 ug of the vector. After that, cells were seeded into 24-well plates, and after 48 h, they were diluted by seeding 10,000 cells in a P100 and 5000 cells into a 6-well plate. When colonies started growing, they were picked and seeded into a 24-well plate. Cells were expanded and frozen in a vial (with claycomb medium and 10% DMSO (D2650-5X5ML, Sigma, St Louis, MO, USA)) and a pellet to extract gDNA.

gDNA extraction and Sanger sequencing. To extract gDNA of the HL1 clones, QuickExtract (QE09050, Lucigen, Middleton, WI, USA) was used. For this process, 20 μL of the reagent was added to each pellet and vortexed for 13 s. Samples were incubated at 65 °C for 6 min, vortexed for 15 s and incubated at 98 °C for 2 min. Primers, PCR conditions and kits used are listed in Supplementary Table S4. After that, ExoZap cleaning (7200100-1000, Ampliqon, Odense, Denmark) and BigDye reaction (4336911, Applied Biosystems, Waltham, MA, USA) were performed. DNA precipitation was done by adding sodium acetate and ethanol 70% and diluted in formamide. Samples were sequenced using a 3500 Genetic Analyzer (Applied Biosystems, Waltham, MA, USA). Sequencing Analysis Software 7 was used to analyse the sequences.

RNA extraction and real-time PCR (rtPCR). Total RNA was purified using the RNeasy Mini Kit (74106, Qiagen, Hilden, Germany) according to the manufacturer's instructions. Prior reverse transcription reaction was performed with an additional step of DNase I treatment and with gDNA Wipeout buffer. Reverse transcription reactions of RNA were done using the QuantiTect Reverse Transcription Kit (205313, Qiagen, Hilden, Germany). For each 20 μL reverse transcription reaction, 1 ug of total RNA was mixed with 4 uL of RT buffer, 1 uL of primer mix, 1 μL of reverse transcriptase in nuclease-free water. cDNA was analysed in real-time PCR reactions using KAPA SYBER FAST Universal Kit (KK4602, KAPA biosystems, St Louis, MO, USA). RPLP0 was used as housekeeping and all data were analysed using the QuantStudio™ Real-Time PCR System and Cloud Software (Thermo Fisher, Waltham, MA, USA). The obtained results were analysed statistically by performing a bilateral Student's *t*-test using SPSS.

Protein extraction and Western blot. Total protein was extracted by lysing the cells with 1% SDS, incubating at 95 °C for 15 min and vortexing for 15 min more. Protein samples were quantified using a Pierce BCA Protein Assay Kit (23225, Thermo Scientific, Waltham, MA, USA) and run in a 10% acrylamide stain-free gel (1610183, Bio-Rad, Hercules, CA, USA) using the BlueStar Prestained Protein Marker Plus (MWPO4, Nippon Genetics, Düren, Germany) for 30 min at 80 V and 1 h at 160 V. Proteins were transferred from gel to PVDF membranes (10600023, GE Healthcare Life Sciences, Boston, MA, USA) for 2 h at 80 V and 4 °C. Stain-free gels were exposed to UV light before protein transfer and then membrane to activate the trihalo compound that reacts with tryptophan residues, allowing rapid fluorescent detection of total protein to normalise the results. Membranes were blocked with PBST + 5% non-fat milk for 1 h at RT and incubated with primary antibody anti-desmoplakin 1/2 (2722-5204, Bio-Rad, Hercules, CA, USA) at 1:500, anti-plakoglobin (13-8500, Invitrogen, Waltham, MA, USA) at 1:1000, anti-plakophilin2 (ab189323, Abcam, Cambridge, UK) at 1:250, anti-desmoglein2 (ab150372, Abcam, Cambridge, UK) at 1:3000 o/n at 4 °C. After several PBS washes, the membranes were incubated with peroxidase-conjugated anti-rabbit antibody (111-035-003, Jackson ImmunoResearch, West Grove, PA, USA) or anti-mouse antibody (115-035-003, Jackson ImmunoResearch, West Grove, PA, USA) and anti-goat (705-035-003, Jackson ImmunoResearch, West Grove, PA, USA) at a 1:10,000 dilution for 1 h at room temperature. Chemiluminescent signal was obtained with clarity substrate (1705061, Bio-Rad, Hercules, CA, USA) and detected using the ChemiDoc MP imaging system. Expression levels were quantified by Image Lab software using total protein of the stain-free gels to normalise [52]. The obtained results were analysed statistically by performing a bilateral Student's *t*-test using SPSS.

Prediction of the score of alternative ATG in the alternative initiation translation. altOR-Fev [25] was used to perform the prediction of translation reinitiation in the 5′ region of the five desmosomal genes. The advanced mode (http://wwwmgs.bionet.nsc.ru/AUGWeb/; accessed on 24 September 2021) was used by pasting the first 160 codons of the coding sequence (without UTRs) and by changing one parameter, the min ORF size. Generally, 30 (codons) is the default value, but in the present study, it was changed by 120 codons because it is the larger distance between the canonical ATG and the PTC of the clones (Table 1); in this way, all alleles were susceptible to the reinitiation of translation. In-frame

ATGs with high, moderate and weak contexts were classified using the criteria from the altORFev tool [25].

5. Conclusions

Our study suggests that the reinitiation of translation may be an important mechanism in evading the NMD machinery in *DSP* and *JUP* genes when carrying PTC variants in the 5′ region due to an optimal genomic context of a non-canonical ATG in-frame. In contrast, PTC variants in the first 160 codons in *PKP2, DSG2* and *DSC2* genes are more likely to trigger the NMD mechanism. Moreover, our data also suggest that molecular alterations associated with the ACM pathomechanism may be milder or non-detectable for N-truncated PG and N-truncated DSP. These data, together with the lower ratio of pathogenic 5′-PTC described in *DSP* and *JUP* versus *PKP2* (which do not show a reinitiation mechanism), also suggest the possibility that the reinitiation mechanism in PG and DSP may also occur in humans, and N-truncated protein synthesis may not be associated with severe ACM disease phenotype. Thus, these findings suggest that PTC variants in 5′ region have different pathogenicity depending on which desmosomal gene is involved. Taking into account that genetics counts as an ACM diagnostic criterion, it would be important to perform more studies in that direction.

Conflicts of Interest: The authors declare no conflict of interest.

References

1. Basso, C.; Corrado, D.; Marcus, F.I.; Nava, A.; Thiene, G. Arrhythmogenic Right Ventricular Cardiomyopathy. *Lancet* **2009**, *373*, 1289–1300. [CrossRef]
2. Karmouch, J.; Protonotarios, A.; Syrris, P. Genetic Basis of Arrhythmogenic Cardiomyopathy. *Mol. Genet.* **2018**, *33*, 6. [CrossRef]
3. Corrado, D.; Basso, C.; Judge, D.P. Arrhythmogenic Cardiomyopathy. *Circ. Res.* **2017**, *121*, 784–802. [CrossRef] [PubMed]
4. Norman, M.; Simpson, M.; Mogensen, J.; Shaw, A.; Hughes, S.; Syrris, P.; Sen-Chowdhry, S.; Rowland, E.; Crosby, A.; McKenna, W.J. Novel Mutation in Desmoplakin Causes Arrhythmogenic Left Ventricular Cardiomyopathy. *Circulation* **2005**, *112*, 636–642. [CrossRef] [PubMed]
5. Basso, C.; Pilichou, K.; Bauce, B.; Corrado, D.; Thiene, G. Diagnostic Criteria, Genetics, and Molecular Basis of Arrhythmogenic Cardiomyopathy. *Heart Fail. Clin.* **2018**, *14*, 201–213. [CrossRef] [PubMed]
6. Najor, N.A. Desmosomes in Human Disease. *Mech. Dis.* **2018**, *13*, 51–70. [CrossRef]
7. Vermij, S.H.; Abriel, H.; van Veen, T.A.B. Refining the Molecular Organization of the Cardiac Intercalated Disc. *Cardiovasc. Res.* **2017**, *113*, 259–275. [CrossRef]
8. Pilichou, K. Arrhythmogenic Cardiomyopathy. *Orphanet J. Rare Dis.* **2016**, *11*, 33. [CrossRef]
9. Carruth, E.D.; Young, W.; Beer, D.; James, C.A.; Calkins, H.; Jing, L.; Raghunath, S.; Hartzel, D.N.; Leader, J.B.; Kirchner, H.L.; et al. Prevalence and Electronic Health Record-Based Phenotype of Loss-of-Function Genetic Variants in Arrhythmogenic Right Ventricular Cardiomyopathy-Associated Genes. *Circ. Genom. Precis. Med.* **2019**, *12*, e002579. [CrossRef]

10. Stenson, P.D.; Mort, M.; Ball, E.V.; Chapman, M.; Evans, K.; Azevedo, L.; Hayden, M.; Heywood, S.; Millar, D.S.; Phillips, A.D.; et al. The Human Gene Mutation Database (HGMD®): Optimizing Its Use in a Clinical Diagnostic or Research Setting. *Hum. Genet.* **2020**, *139*, 1197–1207. [CrossRef]

11. van der Zwaag, P.A.; Jongbloed, J.D.H.; van den Berg, M.P.; van der Smagt, J.J.; Jongbloed, R.; Bikker, H.; Hofstra, R.M.W.; van Tintelen, J.P. A Genetic Variants Database for Arrhythmogenic Right Ventricular Dysplasia/Cardiomyopathy. *Hum. Mutat.* **2009**, *30*, 1278–1283. [CrossRef] [PubMed]

12. Kurosaki, T.; Maquat, L.E. Nonsense-Mediated MRNA Decay in Humans at a Glance. *J. Cell Sci.* **2016**, *129*, 461–467. [CrossRef]

13. Dyle, M.C.; Kolakada, D.; Cortazar, M.A.; Jagannathan, S. How to Get Away with Nonsense: Mechanisms and Consequences of Escape from Nonsense-mediated RNA Decay. *WIREs RNA* **2020**, *11*, e1560. [CrossRef]

14. Van Damme, P.; Gawron, D.; van Criekinge, W.; Menschaert, G. N-Terminal Proteomics and Ribosome Profiling Provide a Comprehensive View of the Alternative Translation Initiation Landscape in Mice and Men. *Mol. Cell. Proteom.* **2014**, *13*, 1245–1261. [CrossRef] [PubMed]

15. Kozak, M. Regulation of Translation via MRNA Structure in Prokaryotes and Eukaryotes. *Gene* **2005**, *361*, 13–37. [CrossRef] [PubMed]

16. Hernández, G.; Osnaya, V.G.; Pérez-Martínez, X. Conservation and Variability of the AUG Initiation Codon Context in Eukaryotes. *Trends Biochem. Sci.* **2019**, *44*, 1009–1021. [CrossRef]

17. Jackson, R.J.; Hellen, C.U.T.; Pestova, T.V. The Mechanism of Eukaryotic Translation Initiation and Principles of Its Regulation. *Nat. Rev. Mol. Cell Biol.* **2010**, *11*, 113–127. [CrossRef]

18. Cohen, S.; Kramarski, L.; Levi, S.; Deshe, N.; Ben David, O.; Arbely, E. Nonsense Mutation-Dependent Reinitiation of Translation in Mammalian Cells. *Nucleic Acids Res.* **2019**, *47*, 6330–6338. [CrossRef]

19. Neu-Yilik, G.; Amthor, B.; Gehring, N.H.; Bahri, S.; Paidassi, H.; Hentze, M.W.; Kulozik, A.E. Mechanism of Escape from Nonsense-Mediated MRNA Decay of Human -Globin Transcripts with Nonsense Mutations in the First Exon. *RNA* **2011**, *17*, 843–854. [CrossRef]

20. Jagannathan, S.; Bradley, R.K. Translational Plasticity Facilitates the Accumulation of Nonsense Genetic Variants in the Human Population. *Genome Res.* **2016**, *26*, 1639–1650. [CrossRef]

21. Rasmussen, T.B.; Nissen, P.H.; Palmfeldt, J.; Gehmlich, K.; Dalager, S.; Jensen, U.B.; Kim, W.Y.; Heickendorff, L.; Mølgaard, H.; Jensen, H.K.; et al. Truncating Plakophilin-2 Mutations in Arrhythmogenic Cardiomyopathy Are Associated with Protein Haploinsufficiency in Both Myocardium and Epidermis. *Circ. Cardiovasc. Genet.* **2014**, *7*, 230–240. [CrossRef]

22. Richards, S.; Aziz, N.; Bale, S.; Bick, D.; Das, S.; Gastier-Foster, J.; Grody, W.W.; Hegde, M.; Lyon, E.; Spector, E.; et al. Standards and Guidelines for the Interpretation of Sequence Variants: A Joint Consensus Recommendation of the American College of Medical Genetics and Genomics and the Association for Molecular Pathology. *Genet. Med.* **2015**, *17*, 405–423. [CrossRef]

23. Marcus, F.I.; McKenna, W.J.; Sherrill, D.; Basso, C.; Bauce, B.; Bluemke, D.A.; Calkins, H.; Corrado, D.; Cox, M.G.P.J.; Daubert, J.P.; et al. Diagnosis of Arrhythmogenic Right Ventricular Cardiomyopathy/Dysplasia: Proposed Modification of the Task Force Criteria. *Eur. Heart J.* **2010**, *31*, 806–814. [CrossRef]

24. Vallverdú-Prats, M.; Alcalde, M.; Sarquella-Brugada, G.; Cesar, S.; Arbelo, E.; Fernandez-Falgueras, A.; Coll, M.; Pérez-Serra, A.; Puigmulé, M.; Iglesias, A.; et al. Rare Variants Associated with Arrhythmogenic Cardiomyopathy: Reclassification Five Years Later. *J. Pers. Med.* **2021**, *11*, 162. [CrossRef]

25. Kochetov, A.V.; Allmer, J.; Klimenko, A.I.; Zuraev, B.S.; Matushkin, Y.G.; Lashin, S.A. AltORFev Facilitates the Prediction of Alternative Open Reading Frames in Eukaryotic MRNAs. *Bioinformatics* **2016**, *3*, 923–925. [CrossRef] [PubMed]

26. Brodehl, A.; Meshkov, A.; Myasnikov, R.; Kiseleva, A.; Kulikova, O.; Klauke, B.; Sotnikova, E.; Stanasiuk, C.; Divashuk, M.; Pohl, G.M.; et al. Hemi- and Homozygous Loss-of-Function Mutations in DSG2 (Desmoglein-2) Cause Recessive Arrhythmogenic Cardiomyopathy with an Early Onset. *Int. J. Mol. Sci.* **2021**, *22*, 3786. [CrossRef] [PubMed]

27. Maruthappu, T.; Posafalvi, A.; Castelletti, S.; Delaney, P.J.; Syrris, P.; O'Toole, E.A.; Green, K.J.; Elliott, P.M.; Lambiase, P.D.; Tinker, A.; et al. Loss-of-function Desmoplakin I and II Mutations Underlie Dominant Arrhythmogenic Cardiomyopathy with a Hair and Skin Phenotype. *Br. J. Dermatol.* **2019**, *180*, 1114–1122. [CrossRef] [PubMed]

28. Pigors, M.; Kiritsi, D.; Krümpelmann, S.; Wagner, N.; He, Y.; Podda, M.; Kohlhase, J.; Hausser, I.; Bruckner-Tuderman, L.; Has, C. Lack of Plakoglobin Leads to Lethal Congenital Epidermolysis Bullosa: A Novel Clinico-Genetic Entity. *Hum. Mol. Genet.* **2011**, *20*, 1811–1819. [CrossRef] [PubMed]

29. Syrris, P.; Ward, D.; Evans, A.; Asimaki, A.; Gandjbakhch, E.; Sen-Chowdhry, S.; McKenna, W.J. Arrhythmogenic Right Ventricular Dysplasia/Cardiomyopathy Associated with Mutations in the Desmosomal Gene Desmocollin-2. *Am. J. Hum. Genet.* **2006**, *79*, 978–984. [CrossRef]

30. Buzina, A.; Shulman, M.J. Infrequent Translation of a Nonsense Codon Is Sufficient to Decrease MRNA Level. *Mol. Biol. Cell* **1999**, *10*, 515–524. [CrossRef] [PubMed]

31. Denecke, J.; Kranz, C.; Kemming, D.; Koch, H.-G.; Marquardt, T. An Activated 5? Cryptic Splice Site in the Human ALG3 Gene Generates a Premature Termination Codon Insensitive to Nonsense-Mediated MRNA Decay in a New Case of Congenital Disorder of Glycosylation Type Id (CDG-Id). *Hum. Mutat.* **2004**, *23*, 477–486. [CrossRef]

32. Perrin-Vidoz, L. The Nonsense-Mediated MRNA Decay Pathway Triggers Degradation of Most BRCA1 MRNAs Bearing Premature Termination Codons. *Hum. Mol. Genet.* **2002**, *11*, 2805–2814. [CrossRef]

33. Inácio, Â.; Silva, A.L.; Pinto, J.; Ji, X.; Morgado, A.; Almeida, F.; Faustino, P.; Lavinha, J.; Liebhaber, S.A.; Romão, L. Nonsense Mutations in Close Proximity to the Initiation Codon Fail to Trigger Full Nonsense-Mediated MRNA Decay. *J. Biol. Chem.* **2004**, *279*, 32170–32180. [CrossRef]

34. Nickless, A.; Bailis, J.M.; You, Z. Control of Gene Expression through the Nonsense-Mediated RNA Decay Pathway. *Cell Biosci.* **2017**, *7*, 26. [CrossRef] [PubMed]

35. Karamyshev, A.L.; Karamysheva, Z.N. Lost in Translation: Ribosome-Associated MRNA and Protein Quality Controls. *Front. Genet.* **2018**, *9*, 431. [CrossRef] [PubMed]

36. Cheedipudi, S.M.; Hu, J.; Fan, S.; Yuan, P.; Karmouch, J.; Czernuszewicz, G.; Robertson, M.J.; Coarfa, C.; Hong, K.; Yao, Y.; et al. Exercise Restores Dysregulated Gene Expression in a Mouse Model of Arrhythmogenic Cardiomyopathy. *Cardiovasc. Res.* **2020**, *116*, 1199–1213. [CrossRef]

37. Garcia-Gras, E. Suppression of Canonical Wnt/ -Catenin Signaling by Nuclear Plakoglobin Recapitulates Phenotype of Arrhythmogenic Right Ventricular Cardiomyopathy. *J. Clin. Investig.* **2006**, *116*, 2012–2021. [CrossRef]

38. Gerull, B.; Brodehl, A. Genetic Animal Models for Arrhythmogenic Cardiomyopathy. *Front. Physiol.* **2020**, *11*, 624. [CrossRef] [PubMed]

39. Gerull, B.; Heuser, A.; Wichter, T.; Paul, M.; Basson, C.T.; McDermott, D.A.; Lerman, B.B.; Markowitz, S.M.; Ellinor, P.T.; MacRae, C.A.; et al. Mutations in the Desmosomal Protein Plakophilin-2 Are Common in Arrhythmogenic Right Ventricular Cardiomyopathy. *Nat. Genet.* **2004**, *36*, 1162–1164. [CrossRef]

40. van Tintelen, J.P.; Entius, M.M.; Bhuiyan, Z.A.; Jongbloed, R.; Wiesfeld, A.C.P.; Wilde, A.A.M.; van der Smagt, J.; Boven, L.G.; Mannens, M.M.A.M.; van Langen, I.M.; et al. Plakophilin-2 Mutations Are the Major Determinant of Familial Arrhythmogenic Right Ventricular Dysplasia/Cardiomyopathy. *Circulation* **2006**, *113*, 1650–1658. [CrossRef] [PubMed]

41. Lopez-Granados, E.; Keenan, J.E.; Kinney, M.C.; Leo, H.; Ma, C.A.; Quinones, R.; Gelfand, E.W.; Jain, A. A Novel Mutation in NFKBIA/IKBA Results in a Degradation- Resistant N-Truncated Protein and Is Associated with Ectodermal Dysplasia With Immunodeficiency. *Hum. Mutat.* **2008**, *29*, 861–868. [CrossRef]

42. McDonald, D.R.; Mooster, J.L.; Reddy, M.; Bawle, E.; Secord, E.; Geha, R.S. Heterozygous N-Terminal Deletion of IκBα Results in Functional Nuclear Factor KB Haploinsufficiency, Ectodermal Dysplasia, and Immune Deficiency. *J. Allergy Clin. Immunol.* **2007**, *120*, 900–907. [CrossRef] [PubMed]

43. Paulsen, M.; Lund, C.; Akram, Z.; Winther, J.R.; Horn, N.; Møller, L.B. Evidence That Translation Reinitiation Leads to a Partially Functional Menkes Protein Containing Two Copper-Binding Sites. *Am. J. Hum. Genet.* **2006**, *79*, 214–229. [CrossRef]

44. Puel, A.; Reichenbach, J.; Bustamante, J.; Ku, C.-L.; Feinberg, J.; Döffinger, R.; Bonnet, M.; Filipe-Santos, O.; de Beaucoudrey, L.; Durandy, A.; et al. The NEMO Mutation Creating the Most-Upstream Premature Stop Codon Is Hypomorphic Because of a Reinitiation of Translation. *Am. J. Hum. Genet.* **2006**, *78*, 691–701. [CrossRef] [PubMed]

45. Witcher, L.L.; Collins, R.; Puttagunta, S.; Mechanic, S.E.; Munson, M.; Gumbiner, B.; Cowin, P. Desmosomal Cadherin Binding Domains of Plakoglobin. *J. Biol. Chem.* **1996**, *271*, 10904–10909. [CrossRef]

46. Hatsell, S.; Medina, L.; Merola, J.; Haltiwanger, R.; Cowin, P. Plakoglobin Is O-Glycosylated Close to the N-Terminal Destruction Box. *J. Biol. Chem.* **2003**, *278*, 37745–37752. [CrossRef]

47. Sacco, P.A.; McGranahan, T.M.; Wheelock, M.J.; Johnson, K.R. Identification of Plakoglobin Domains Required for Association with N-Cadherin and α-Catenin. *J. Biol. Chem.* **1995**, *270*, 20201–20206. [CrossRef]

48. Karczewski, K.J.; Francioli, L.C.; Tiao, G.; Cummings, B.B.; Alföldi, J.; Wang, Q.; Collins, R.L.; Laricchia, K.M.; Ganna, A.; Birnbaum, D.P.; et al. The Mutational Constraint Spectrum Quantified from Variation in 141,456 Humans. *Nature* **2020**, *581*, 434–443. [CrossRef]

49. Bari, O.; Skillman, S.; Lah, M.D.; Haggstrom, A.N. Compound Heterozygous Mutations in Desmoplakin Associated with Skin Fragility, Follicular Hyperkeratosis, Alopecia, and Nail Dystrophy. *Pediatr. Dermatol.* **2018**, *35*, e218–e220. [CrossRef]

50. Cabral, R.M.; Liu, L.; Hogan, C.; Dopping-Hepenstal, P.J.C.; Winik, B.C.; Asial, R.A.; Dobson, R.; Mein, C.A.; Baselaga, P.A.; Mellerio, J.E.; et al. Homozygous Mutations in the 5′ Region of the JUP Gene Result in Cutaneous Disease but Normal Heart Development in Children. *J. Investig. Dermatol.* **2010**, *130*, 1543–1550. [CrossRef] [PubMed]

51. Claycomb, W.C.; Lanson, N.A.; Stallworth, B.S.; Egeland, D.B.; Delcarpio, J.B.; Bahinski, A.; Izzo, N.J. HL-1 Cells: A Cardiac Muscle Cell Line That Contracts and Retains Phenotypic Characteristics of the Adult Cardiomyocyte. *Proc. Natl. Acad. Sci. USA* **1998**, *95*, 2979–2984. [CrossRef] [PubMed]

52. Image Lab. Software. Available online: https://www.bio-rad.com/es-es/product/image-lab-software?ID=KRE6P5E8Z (accessed on 10 August 2021).

Article 2

"Alterations in calcium handling are a common feature in Arrhythmogenic Cardiomyopathy cell models triggered by desmosome genes loss"

Alterations in calcium handling are a common feature in an arrhythmogenic cardiomyopathy cell model triggered by desmosome genes loss

Marta Vallverdú-Prats [1], David Carreras [1], Guillermo J Pérez [1, 2, 3], Oscar Campuzano[1, 2, 3], Ramon Brugada [1, 2, 3, 4], Mireia Alcalde [1] *

[1]Cardiovascular Genetics Center, Biomedical Research Institute of Girona, 17190 Salt, Spain; mvallverdu@gencardio.com, dcarreras@gencardio.com, gperez@gencardio.com, oscar@brugada.org, ramon@brugada.org, malcalde@gencardio.com
[2]Department of Medical Sciences, Universitat de Girona, 17003 Girona, Spain; gperez@gencardio.com, oscar@brugada.org, ramon@brugada.org
[3]Centro de Investigación Biomédica en Red de Enfermedades Cardiovasculares (CIBERCV), 21005 Madrid, Spain; gperez@gencardio.com, oscar@brugada.org, ramon@brugada.org
[4]Hospital Josep Trueta, 17007 Girona, Spain; ramon@brugada.org
***Correspondence: malcalde@gencardio.com, 872 98 70 87

Abstract: Arrhythmogenic cardiomyopathy (ACM) is an inherited cardiac disease characterised by the replacement of cardiomyocytes with fibrofatty tissue. Deleterious variants in desmosomal genes are the main cause of ACM, and lead to common and gene-specific molecular alterations, which are not yet fully understood. This article presents the first systematic in vitro study describing gene and protein expression alterations in desmosomes, electrical conduction related genes, and genes involved in fibrosis and adipogenesis. Moreover, molecular and functional alterations in calcium handling were also characterised. This study was performed with HL1 cells with homozygous knockout of three of the most frequently mutated desmosomal genes in ACM: PKP2 (plakophilin2), DSG2 (desmoglein2) and DSC2 (desmocollin2), all generated by CRISPR/Cas9. Moreover, knockout and N-truncated clones of DSP (desmoplakin) were also included. Our results showed functional alterations in calcium handling in all clones, a slower calcium re-uptake was observed in the absence of PKP2, DSG2, and DSC2, and the DSP knockout clone showed a more rapid re-uptake. We propose that the described functional alterations of the calcium handling genes may be explained by mRNA expression levels of ANK2, CASQ2 (calsequestrin-2), ATP2A2 (ATPase sarcoplasmic/endoplasmic reticulum $Ca2+$ transporter-2), RYR2 (ryanodine receptor-2), and PLN (phospholamban).

Keywords: Arrhythmogenic Cardiomyopathy; calcium handling; CRISPR/Cas9; desmosomes; HL1

Introduction

Arrhythmogenic cardiomyopathy (ACM) is a rare heart disease characterised by progressive loss of cardiomyocytes and its replacement by fibrofatty tissue. It affects predominantly the right ventricle, but biventricular and left-dominant forms have also been reported [1,2]. The principal symptoms are ventricular arrhythmias and sudden cardiac death, which are present in up to 50% of cases [3,4]. ACM affects one in 2000–5000 individuals, and it has been reported that deleterious variants of genes encoding desmosomal proteins are the main cause of ACM [5].

Desmosomes are essential for cardiomyocytes integrity because they provide cells with the ability to resist mechanical forces by joining cells together, connecting extracellular contacts with internal intermediate filaments [6]. These structures are located in intercalated discs and they are composed of plakophilin2 (*PKP2*), desmoplakin (*DSP*), desmoglein2 (*DSG2*), desmocollin2 (*DSC2*), and plakoglobin (*JUP*). Pathogenic variants in any of these genes have been associated with ACM, with *PKP2* the most common mutated gene in ACM patients (10–45%), followed by *DSP* (10–15%), *DSG2* (7–10%), and *DSC2* (2%) [7].

A general molecular feature of the disease is alterations in expression levels of desmosomes or genes related to electrophysiologic functions of the heart. Moreover, it is known that fibrosis and adipogenesis play an important role in ACM, with transforming growth factor beta 1 *(TGFB1)* and peroxisome proliferator activated receptor gamma *(PPARg)*, respectively, the key genes of these pathways [8]. However, part of the pathophysiological mechanism in ACM remains to be clarified.

To date, a great number of animal and cell models with genetic alterations in desmosomal genes have been generated [8–10]. The HL1 cell line is one of the most preferred *in vitro* models due to its capacity to maintain differentiated cardiac properties at morphological, biochemical, and electrophysiological levels after several passages [11]. HL1 was generated from the AT-1 atrial cardiomyocyte tumour lineage and it was the first ACM cell model [10].

Because of all these available models, it has been possible to identify gene-specific molecular alterations in ACM. However, not all desmosomal genes are equally studied.

There are many studies describing molecular and functional consequences of the loss of *PKP2*, both *in vitro* and *in vivo*, but the number of studies is reduced for *DSC2* or *DSG2* in ACM. It is still unknown if the alterations described in *PKP2*, such as disruption in calcium handling [12–15] or downregulation of *Cx43* expression [10,16,17], are shared by all desmosomal genes.

Our study aims to elucidate common molecular alterations triggered by the loss of desmosomal genes to unmask key factors that may be important for ACM development. Specifically, we present the first systematic study characterising molecular alterations using a consistent *in vitro* model to study the main desmosomal genes. Specifically, we studied gene expression of desmosomal, calcium handling, electrical conduction, *TGFB1*, and *PPARg* genes, and functional changes in calcium homeostasis with the loss of *PKP2, DSG2, DSC2*, and *DSP* using CRISPR-edited HL1 cell lines.

Materials and Methods

sgRNA design and cloning into the Cas9 px458 vector. The Benchling web tool (BiologySoftware, 2018; retrieved from https://benchling.com) was used to design the sgRNAs of the four desmosomal genes in the first 160 codons of the sequences for editing by CRISPR/Cas9. sgRNAs with high scores and a low off-target number were selected: PKP2 (5'-GTATGTCTACAAGCTACACG-3', FW); DSP (5'-CCACCCGCGGATCAACACGC-3', FW); DSG2 (5'-TGGCGCGGAGCCCGGGTGAC-3', FW); DSC2 (5'-GCTGTGGGATCTATGCGCTCC-3', FW). The px458 vector (plasmid #48138, Addgene, Teddington, UK), which encodes Cas9 wildtype (WT), was digested by BbsI-HF (R3539S, New England BioLabs, Ipswich, MA, USA) at 37°C overnight and ligated by T4 DNA ligase (M0202L, New England BioLabs, Ipswich, MA, USA) for 1 h at room temperature with the sgRNA previously annealed (sense and antisense). Annealing of sgRNAs was performed with T4 PNK (M0201S, New England BioLabs, Ipswich, MA, USA) using the following thermocycler program: 30 min at 37°C, 5 min at 95°C, and 94 to 25°C, decreasing 1°C per 12 seconds. DH5alpha competent cells (18265-017, Invitrogen, Waltham, MA, USA) were transformed with the sgRNA-px458 vector for 30 min on ice

and 45 seconds at 42°C. DNA was extracted using a Plasmid Midi Kit (12143, Qiagen, Hilden, Germany).

HL-1 cell culture and electroporation. HL1 cells were cultured as described previously [18] at 37°C under 5% CO_2 on fibronectin-gelatin-coated slides in Claycomb medium (51800C, Sigma, St Louis, MO, USA) supplemented with 10% foetal bovine serum (10270106, GIBCO, Waltham, MA, USA), 100 U/mL penicillin, 10 mg/mL streptomycin (P4333-100 ML, Sigma, St Louis, MO, USA), 2 mM L-glutamine (35050061, Thermo, Waltham, MA, USA), 0.1 mM norepinephrine (A9512, Sigma, St Louis, MO, USA), and 0.3 mM ascorbic acid (A7631, Sigma, St Louis, MO, USA). Plasmids were nucleofected into HL-1 cells in suspension by using the Amaxa Cell Line Nucleofector Kit V (VCA-1003, Lonza, Basel, Switzerland); 10^6 cells per condition were transfected by adding 4 ug of the vector. Next, cells were seeded into 24-well plates, and after 48 h, they were diluted by seeding 10,000 cells on a P100 and 5,000 cells on a 6-well plate. When colonies started growing, they were picked and seeded on a 24-well plate. Cells were expanded and frozen in a vial (with Claycomb medium and 10% dimethyl sulfoxide (D2650-5X5ML, Sigma, St Louis, MO, USA)) and a pellet to extract gDNA.

gDNA extraction and Sanger sequencing. To extract gDNA from the HL1 clones, QuickExtract (QE09050, Lucigen, Middleton, WI, USA) was used. For this process, 20 μL of the reagent was added to each pellet and vortexed for 13 s. Samples were incubated at 65°C for 6 min, vortexed for 15 s and incubated at 98°C for 2 min. Primers, PCR conditions, and kits used are listed in Supplementary Table S1. Next, ExoZap cleaning (7200100-1000, Ampliqon, Odense, Denmark) and BigDye reactions (4336911, Applied Biosystems, Waltham, MA, USA) were performed. DNA was precipitated by adding sodium acetate and 70% ethanol diluted in formamide. Samples were sequenced using a 3500 Genetic Analyzer (Applied Biosystems, Waltham, MA, USA). Sequencing Analysis Software 7 was used to analyse the sequences.

RNA extraction and real-time PCR (RT-PCR). Total RNA was purified using the RNeasy Mini Kit (74106, Qiagen, Hilden, Germany) according to the manufacturer's instructions. The prior reverse transcription reaction was performed with an additional step of DNase I treatment and with gDNA Wipeout buffer. Reverse transcription reactions of RNA were performed using the QuantiTect Reverse Transcription Kit (205313, Qiagen, Hilden,

Germany). A final volume of 20 μL of reverse transcription reaction was obtained by mixing 1 μg of total RNA with 4 μL of RT buffer, 1 μL of primer mix, and 1 μL of reverse transcriptase in nuclease-free water. cDNA was analysed with real-time PCR reactions using a KAPA SYBER FAST Universal Kit (KK4602, KAPA Biosystems, St Louis, MO, USA) for desmosomal, calcium handling (except *CACNA1C*), *Cx43*, and *SCN5A* genes. For *CACNA1C*, *TGFB1*, and *PPARg*, TaqMan Fast Advanced Master Mix (4444557, Applied Biosystems, Waltham, MA, USA) was used. *RPLP0* was used as a housekeeping gene for both methods, and all data were analysed using the QuantStudio™ Real-Time PCR System and Cloud Software (ThermoFisher, Waltham, MA, USA). The obtained results were analysed statistically using SPSS by using the Mann–Whitney *U* test for comparisons between two groups and the Kruskal–Wallis H test for comparison between the four groups. In all cases, it was assumed that our data was not normally distributed because there were only four cases per group.

Protein extraction and western blot (WB). Total protein was extracted by lysing the cells with 1% sodium dodecyl sulphate, incubating at 95°C for 15 min and vortexing for 15 min. Protein samples were quantified using a Pierce BCA Protein Assay Kit (23225, Thermo Scientific, Waltham, MA, USA) and separated in a 10% acrylamide stain-free gel (1610183, Bio-Rad, Hercules, CA, USA) using BlueStar Pre-stained Protein Marker Plus (MWPO4, Nippon Genetics, Düren, Germany) for 30 min at 80 V and 1 h at 160 V. Stain-free gels were exposed to UV light before protein transfer to activate the trihalo compound that reacted with tryptophan residues, allowing rapid fluorescent detection of total protein. Proteins were transferred from gels to polyvinylidene fluoride membranes (10600023, GE Healthcare Life Sciences, Boston, MA, USA) for 2 h at 80 V and 4°C. The membrane was also exposed to UV light to obtain a protein charge measurement to normalise the results. Membranes were blocked with phosphate-buffered saline (PBS) with 0.1% Tween and 5% non-fat milk for 1 h at room temperature, and then incubated with the primary antibody anti-desmoplakin 1/2 (2722-5204, Bio-Rad, Hercules, CA, USA) at 1:500, anti-plakoglobin (13-8500, Invitrogen, Waltham, MA, USA) at 1:1000, anti-plakophilin-2 (ab189323, Abcam, Cambridge, UK) at 1:250, anti-desmoglein2 (ab150372, Abcam, Cambridge, UK) at 1:3000, anti-desmocolin-2 (AF7490, Bio-Techne RD systems, Minneapolis, MN, USA) at 1:200, anti-ryanodine receptor-2

(NBP1-19484, Novus Biologicals, Centennial, CO, USA) at 1:1000, anti-connexin-43 (C6219, Sigma, St Louis, MO, USA) at 1:4000, anti-ankiryn-2 (821501, BioLegend, San Diego, CA, USA) at 1:200, and anti-voltage-gated sodium channel 1.5 (23016-1-AP, Proteintech, Minneapolis, MN, USA) at 1:5000 overnight at 4°C. After several PBS washes, the membranes were incubated with peroxidase-conjugated anti-rabbit antibody (111-035-003, Jackson ImmunoResearch, West Grove, PA, USA) or anti-mouse antibody (115-035-003, Jackson ImmunoResearch, West Grove, PA, USA) and anti-goat antibody (705-035-003, Jackson ImmunoResearch, West Grove, PA, USA) at a 1:10,000 dilution for 1 h at room temperature. A chemiluminescent signal was obtained with a substrate (1705061, Bio-Rad, Hercules, CA, USA) and detected using the ChemiDoc MP imaging system. Expression levels were quantified by Image Lab software using the total protein of the stain-free blots to normalise the bands [19]. The obtained results were analysed statistically using SPSS by performing Mann–Whitney U tests only on the blots in which bands were detected in all samples. In all cases, it was assumed that our data was not a normal distribution because there were only four cases per group. The WB bar plots that were generated represented the protein levels of triplicate sample quantification, including data from the blots shown in Fig. 2, 3 and 5 and also for replicates shown in the supplementary material (Fig. S1-S3).

Calcium imaging. HL1 cells (384 cells/mm^2) were seeded on register chambers (BT-CSR1, Cell Microcontrols, Norfolk, VA, USA) 24–48 h prior to the experiments. Cells were loaded with 5 µM of Fluo4-AM (F14201, Invitrogen, Waltham, MA, USA) in the presence of 0.02% Pluronic F-127 (P2443 Sigma-Aldrich, Saint Louis, MO, USA) in NK physiological solution (140 mM NaCl, 3 mM KCl, 10 mM HEPES, 1.2 mM MgCl$_2$, 1.8 mM CaCl$_2$, and 10 mM glucose) for 30 min at room temperature. For the calcium transient measurements, all the solutions were maintained at 35–37°C with a temperature controller (TC^2$_{bip}$, Cell Microcontrols, Norfolk, VA, USA). Calcium transients were induced by a 1-s pulse of 10 mM caffeine applied with a local perfusion pipette (MPRE8, Cell Microcontrols, Norfolk, VA, USA). Calcium transients were recorded at 32 fps using an inverted microscope (Nikon Eclipse Ti, Japan), equipped with an electron multiplying CCD camera (Hamamatsu C900-13, Hamamatsu, Japan) and a fast illumination system (Lambda DG4, Sutter Instrument, Novato, CA, USA). The acquisition was controlled from a personal

computer with MetaFluor Imaging System software (Molecular Devices, Sunnyvale, CA, USA). Peak parameters were measured with Clampfit 10.2 (Molecular Devices, Sunnyvale, CA, USA) and a hierarchical statistical analysis was performed with a Ratonly RStudio script following criteria described previously [20].

Results

Generation and validation of gene-specific knockout clones *PKP2, DSG2* and *DSC2*

The *PKP2*-KO, *DSG2*-KO, and *DSC2*-KO groups comprised four HL1 clones for each edited gene, *PKP2, DSG2*, and *DSC2*, respectively. All of the clones presented frameshifts leading to a premature termination codon (PTC) within the 5' region of the three desmosomal genes studied. None of the edited clones produced detectable levels of the truncated protein (Fig. 1). Genotypes of all 12 edited clones are shown in Supplementary Table S2.
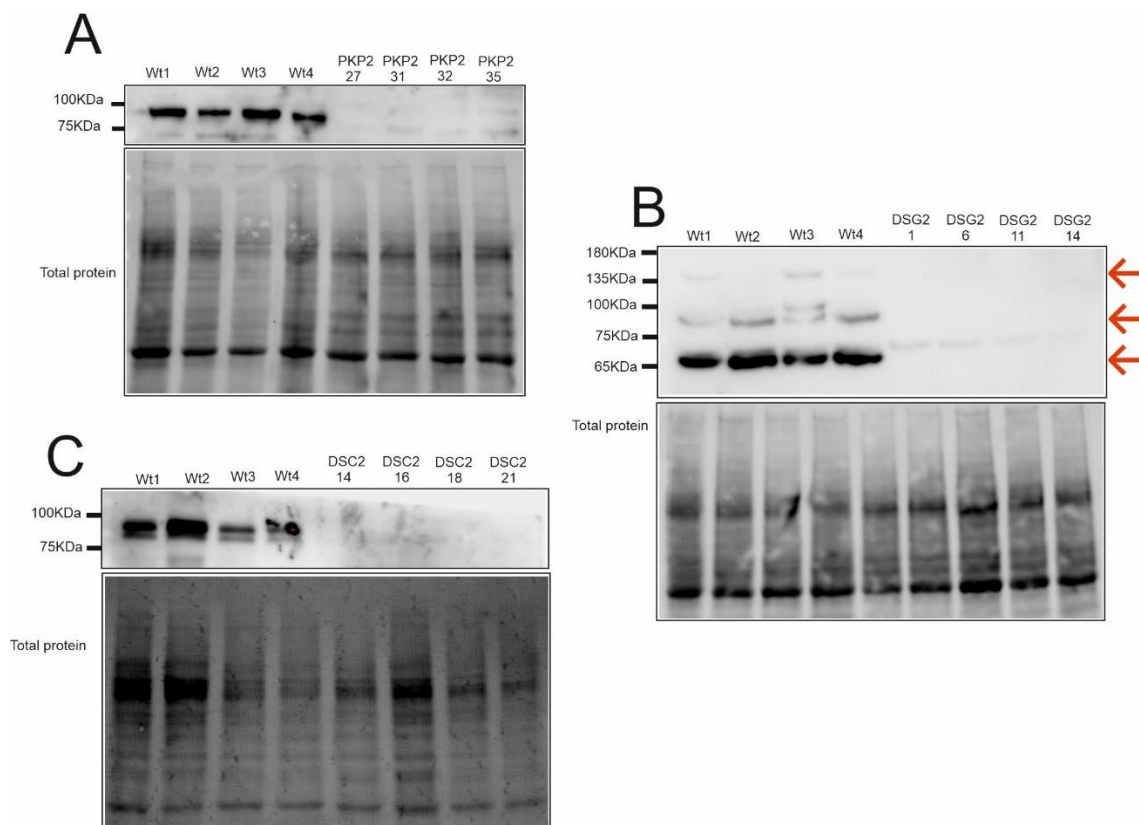
Figure 1. Protein expression levels of the edited gene in each group: PKP2 for *PKP2*-KO **(A)**, DSG2 for *DSG2*-KO **(B)** and DSC2 for *DSC2*-KO **(C)**. The DSG2 antibody recognises three isoforms (canonical 130 kDa, 80 kDa, and 65 kDa) marked with a red arrow.

Alterations in the expression levels of desmosomal genes

The expression levels of mRNA and protein of the five desmosomal genes in the *PKP2*-KO, *DSC2*-KO, and *DSG2*-KO groups were evaluated by RT-PCR and WB. At the mRNA level, all 12 edited clones presented undetectable expression levels of *DSC2* (Fig. 2A), with *DSC2* downregulation the only common feature. Additionally, gene-specific alterations were also found, depending on the knocked out gene, with *DSC2*-KO the only group with no downregulation in the desmosomal genes. The relative quantifications (RQs) of the RT-PCR are shown in Table S3.

Consistently, at the protein level, *DSC2* downregulation was also the only common alteration. However, other alterations were revealed. *PKP2*-KO clones showed undetectable levels of DSC2 and canonical DSG2 (130KDa), and downregulated DSP and PG, with decreased levels of all desmosomal proteins (Fig. 2B). Moreover, *DSG2*-KO clones showed decreased levels of all proteins except for DSP (Fig. 2C). Finally, the only alteration in desmosomal expression found in *DSC2*-KO clones was downregulation of DSP protein (Fig. 2D). Table S4 shows the p-value of the statistical analysis of mRNA and protein expression levels of all edited clones.

Figure 2. Desmosomal expression levels of mRNA **(A)** and protein of the edited clones *PKP2*-KO **(B)**, *DSG2*-KO **(C)**, and *DSC2*-KO **(D)**. *Indicates the gene expression levels that were significantly different between WT and edited clones.
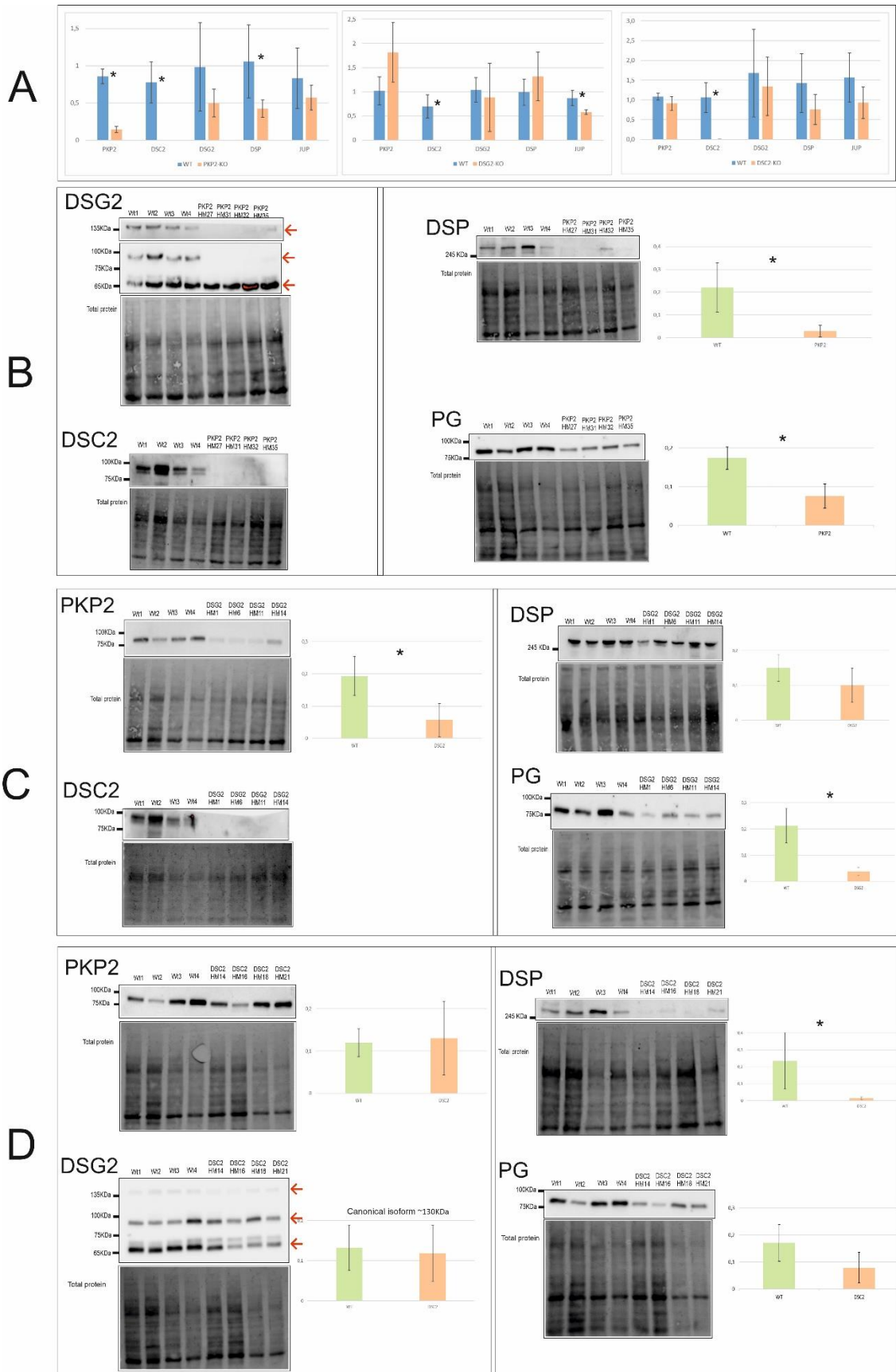
Alterations in the calcium cycle

Expression levels

To detect common alterations regarding calcium handling in the edited clones, both mRNA and protein expression levels of calcium genes known to be decreased in the absence of *PKP2* [12] were studied.

At the mRNA level, all *PKP2, DSG2*, and *DSC2* edited clones shared downregulation of *ANK2, ATP2A2*, and *CASQ2* (Fig. 3A). Gene-specific alterations were also found, with *PKP2*-KO the group with the greatest decrease in the calcium handling genes, showing significant downregulation in all the studied genes except for *PLN*. In contrast, *DSC2*-KO clones, apart from the shared alterations, only showed downregulation of *TRDN,* and was the group with the least molecular alterations. Interestingly, although *PLN* did not show significant differences in any of the desmosomal KO group, it exhibited a tendency of upregulation in all of them. RQs of the RT-PCR results are shown in Table S3.

At the protein level, ANK2 and RYR2 were found to be significantly downregulated in the three groups, which was a common feature among all the clones (Fig. 3B). Replicates of the RYR2 WB are shown in the supplementary material (Fig. S1-S3). Table S4 shows the p-value of the statistical analysis of the mRNA and protein expression levels of all edited clones.
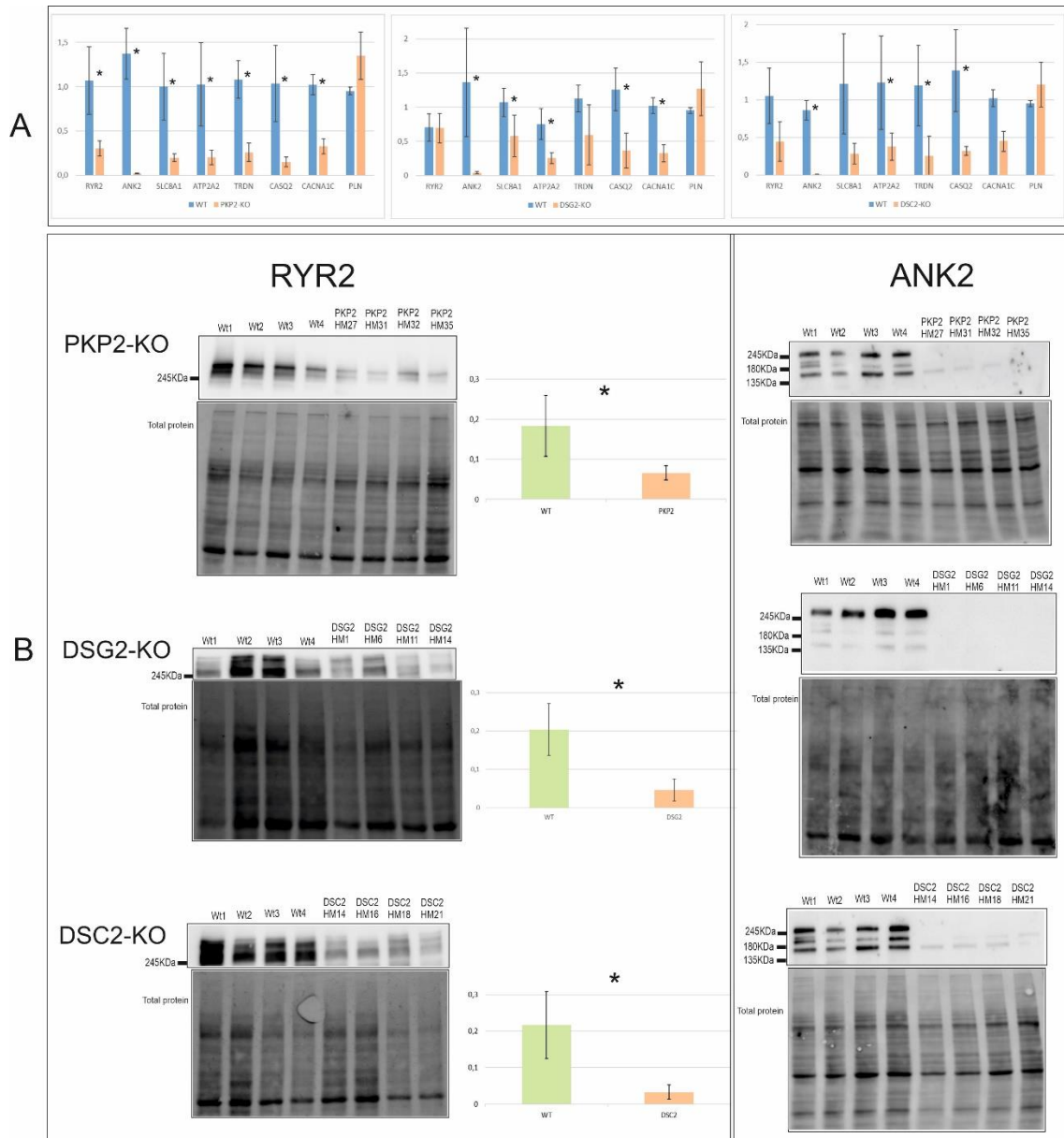
Figure 3. Calcium cycle gene expression at the mRNA **(A)** and protein **(B)** levels. *Indicates the gene expression levels that were significantly different between WT and edited clones.

Calcium imaging

Edited clones were evaluated functionally for calcium handling homeostasis. First, the characteristics of calcium transients elicited by a local pulse of caffeine (10 mM caffeine, 1 s duration) were studied, and second, the rate of the cytosolic calcium rise and the kinetics of the decay were evaluated. To this end, traces of fluorescence of a colorant over time representing cytosolic calcium transients were measured. The number of

traces obtained per cell line are shown in Table S5, and the final plot representing the averaged traces of all KO groups is presented in Fig 4A.

All three KO groups presented similar kinetics but were significantly different compared to WT clones. Additionally, hierarchical statistical analysis was performed on six parameters of the calcium transient: half-width duration, rise time 10–50%, decay time 50–10%, rise time 10–90%, decay time 90–10%, and decay time 90–50% (Fig. 4B, Table S6). Interestingly, all the clones presented a significantly longer half-width duration compared to WT clones, indicating a slower calcium removal. Furthermore, *DSG2*-KO and *DSC2*-KO also presented a significantly longer rise time of 10–90% and decay time of 90–50%, and only *DSG2*-KO showed a significantly longer decay time of 90–10% compared with WT clones. These increased times indicate both slower release and re-uptake in the KO clones *DSG2* and *DSC2*. All values of calcium transients are shown in Table S7.
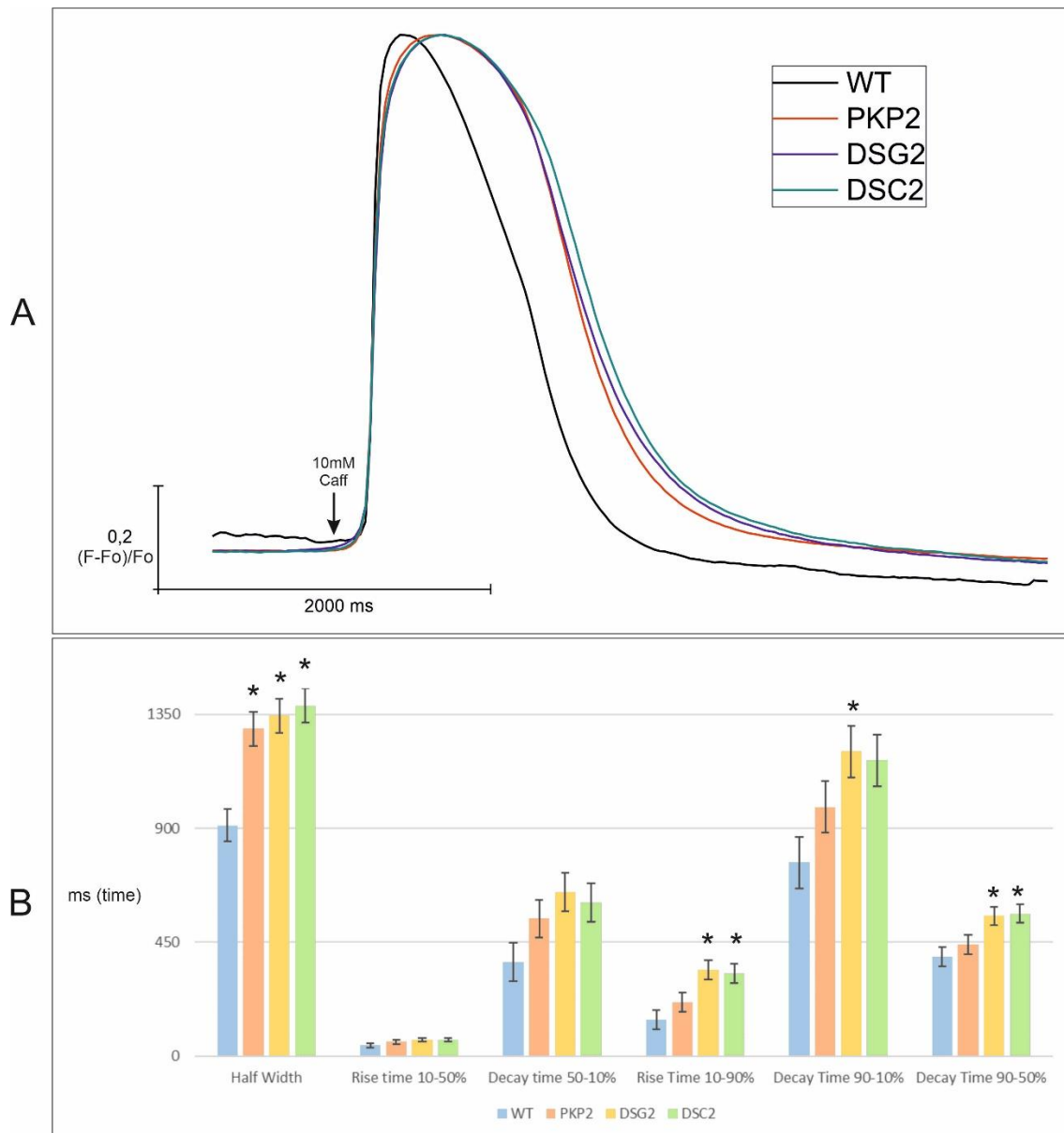
Figure 4. Calcium imaging peaks **(A)** and studied parameters **(B)** of the three KO groups: *PKP2*-KO, *DSG2*-KO, and *DSC2*-KO. The black arrow in section A indicates the pulse of caffeine. *Indicates parameters that were significantly different compared with WT clones.

Alterations in electrical conduction related genes *Cx43* and *Nav1.5*

Connexin-43 *(Cx43)* and cardiac voltage-gated sodium channel (*SCN5A* that encodes Nav1.5) expression levels were evaluated to detect possible shared alterations related to electrical functionality in the edited clones. At the mRNA level, *Cx43* was downregulated in all the clones studied (Fig. 5A), although only *DSG2*-KO showed a significantly lower expression of Cx43 protein (Fig. 5B). Replicates of the CX43 WB are shown in the supplementary material (Fig. S1-S3). *SCN5A* showed downregulation only

in the *PKP2*-KO clones at the mRNA level (Fig. 5A). However, all edited clones showed undetectable levels of Nav1.5 protein. RQs of the RT-PCR are shown in Table S3. Table S4 shows the p-value of the statistical analysis of the mRNA and protein expression levels of all edited clones.
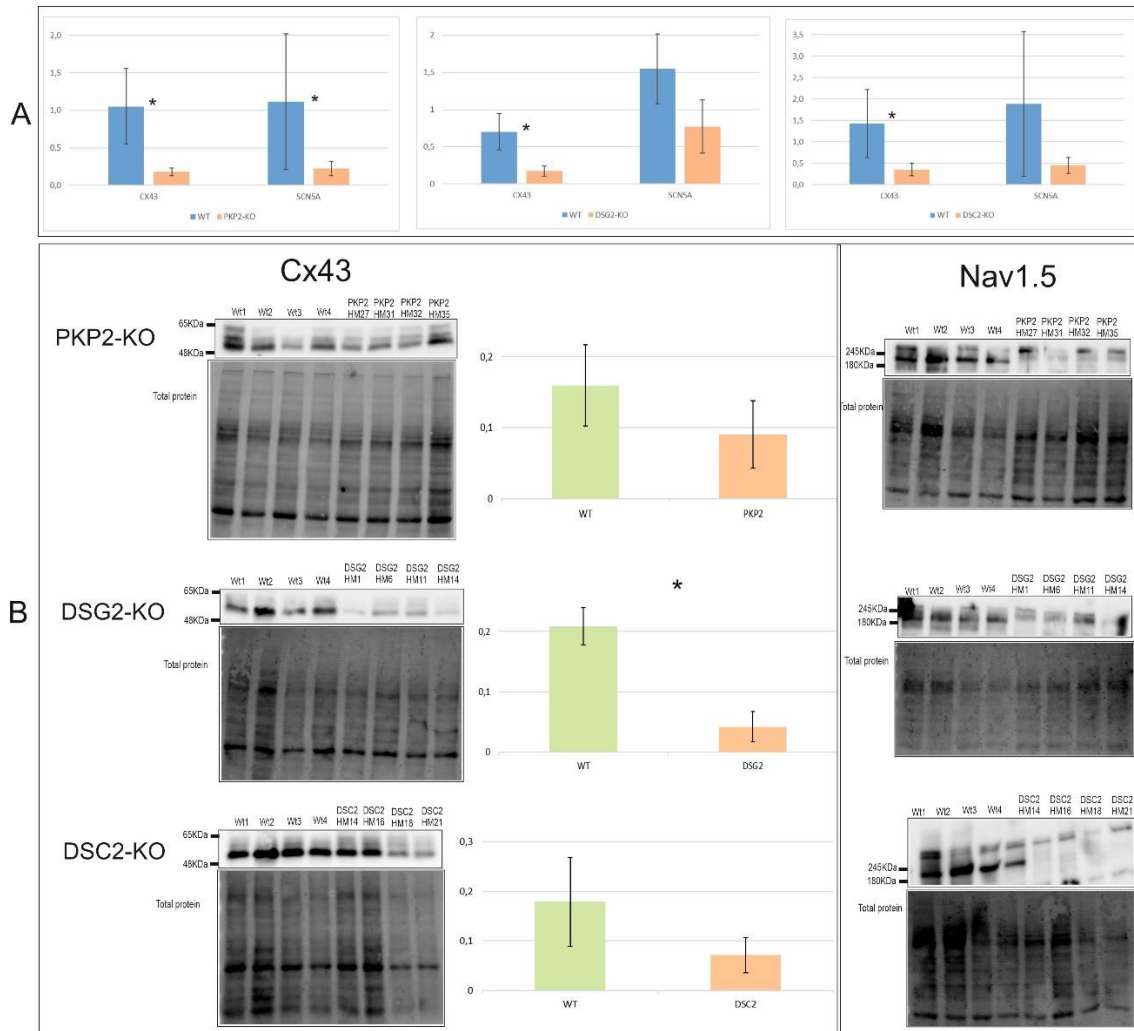

Figure 5. Cx43 and SCN5A expression at the mRNA **(A)** and protein **(B)** levels of the three KO groups *PKP2*-KO, *DSG2*-KO, and *DSC2*-KO. *Indicates parameters that were significantly different compared with WT clones.

Fibrosis and adipogenesis: alterations in *TGFB1* and *PPARg* genes

The expression levels of *TGFB1* and *PPARg* genes, as key factors of fibrosis and adipogenesis, were evaluated by RT-PCR. The results revealed that *TGFB1* was significantly downregulated in *DSG2*-KO and *DSC2*-KO groups while *PKP2*-KO showed only a tendency in the same direction (Fig. 6). Table S8 shows the p-value of the statistical analysis, and RQs of the RT-PCR are shown in Table S9. Additionally, higher

levels of *PPARg* were detected in *PKP2*-KO, *DSG2*-KO, and *DSC2*-KO groups (Table S10). RQs could not be calculated for *PPARg* as no expression was detected in any of the four WT clones (cycle threshold (CT) >35 cycles, CTs mean= 36.18), while edited clones showed CT <35 cycles (*PKP2*-KO CT mean = 32.5, *DSG2*-KO CT mean = 31.06, and *DSC2*-KO CT mean = 33.65).
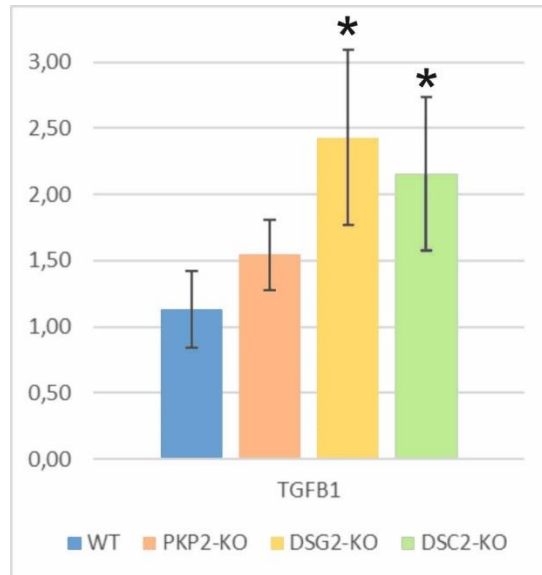
Figure 6. mRNA expression levels of several genes involved in ACM molecular pathways in the edited clones. *Indicates gene expression levels that were significantly different compared with WT clones.

Molecular and functional evaluation of N-truncated *DSP* and *DSP*-KO

The *DSP*-KO edited clones, in contrast to the *PKP2*-KO, *DSC2*-KO, and *DSG2*-KO clones, triggered re-initiation of translation and were able to synthesise N-DSP [21]. Molecular and functional characterisation of N-DSP and *DSP*-KO in this group were performed qualitatively as statistical analyses were not possible because one *DSP*-KO clone did not trigger re-initiation of translation, while the remaining clones synthesised N-DSP [21].

Expression levels

mRNA levels of N-DSP and *DSP*-KO clones were analysed by RT-PCR for *CACNA1C* and *PLN*, which were not included in our previous study [21], and suggested *PLN*

downregulation in *DSP*-KO (Fig. 7A), in contrast to the higher *PLN* levels observed in *PKP2*-KO, *DSG2*-KO, and *DSC2*-KO clones (Fig. 3A). RQs are shown in Table S11.

WB was performed for N-*DSP* and *DSP*-KO clones to analyse DSC2, ANK2, and Nav1.5 protein levels, which were undetectable for the *PKP2*-KO, *DSG2*-KO, and *DSC2*-KO clones and thus a possible common feature of desmosomal genes loss. From these proteins, *DSP*-KO clones had undetectable DSC2 levels while N-*DSP* showed normal DSC2 expression (Fig. 7B). However, loss of ANK2 and Nav1.5 was not observed for *DSP*-KO or N-*DSP* clones (Fig. 7B). Finally, DSG2 protein levels were also studied, but none of the clones showed any change in the levels of total DSG2 (Fig. 7B).
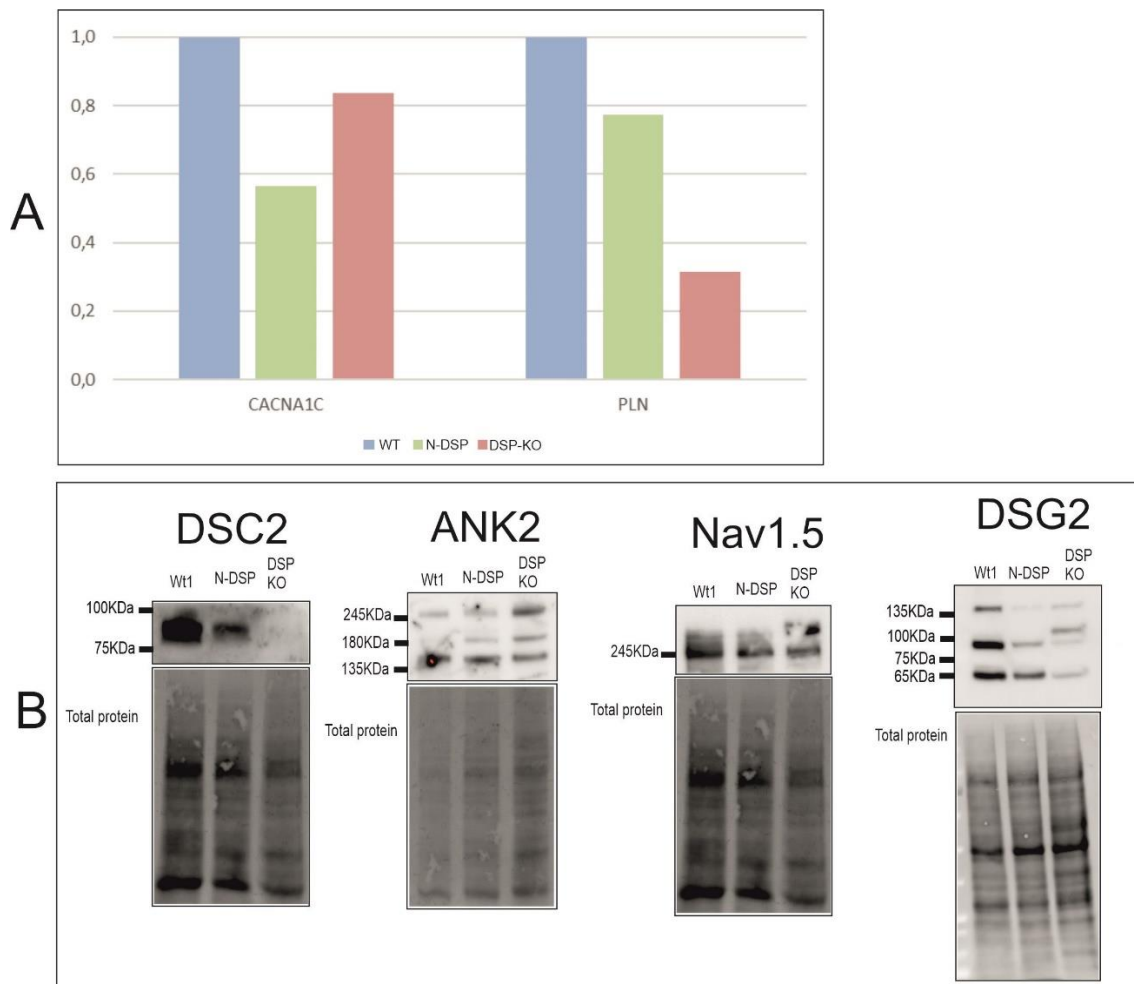
Figure 7. mRNA expression levels of *CACNA1C* and *PLN* **(A)** and protein levels of DSC2, ANK2, Nav1.5, and DSG2 **(B)** in DSP clones.

Calcium imaging

Finally, a 10-mM caffeine peak was performed on N-*DSP* and *DSP*-KO clones to describe their calcium handling homeostasis at a functional level. The number of traces per clone are shown in Table S5 and the peak is shown in Fig. 8A. Both clones, N-*DSP* and *DSP*-KO, presented different kinetics compared with the other three groups evaluated (*PKP2-KO*, *DSG2*-KO, and *DSC2*-KO) (Fig. 4A). The N-*DSP* peak was similar compared with the WT clones, showing an analogous amplitude. However, *DSP*-KO presented slightly different kinetics compared to both WT and N-*DSP* clones with a shorter amplitude, indicating a quicker calcium removal. Results for the six kinetic parameters are represented in Fig. 8B and Table S12. All clones had similar values for all parameters with a high standard deviation. However, the half-width may have been shorter in *DSP*-KO compared with WT and N-*DSP* clones (Fig. 8B, Table S12). Hierarchical statistical analysis was not performed due to the limited number of clones.
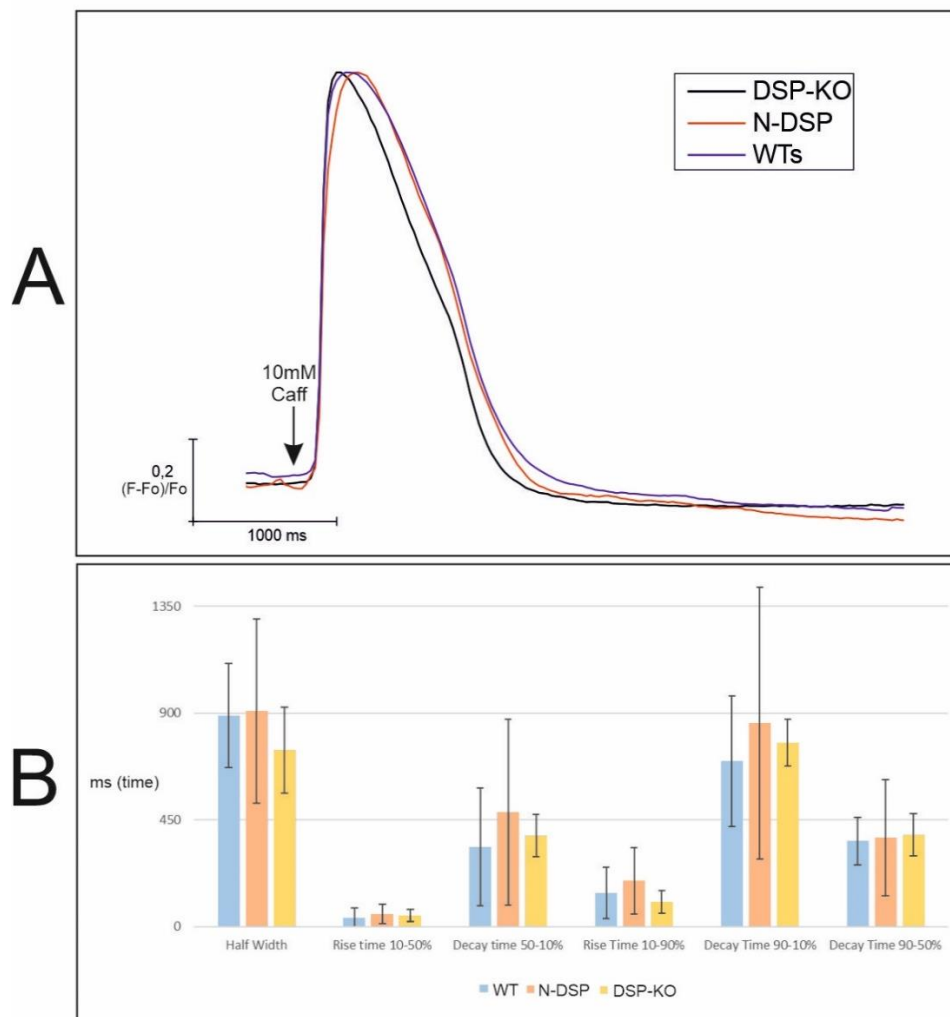
Figure 8. Calcium imaging peaks **(A)** and studied parameters **(B)** of the DSP clones. The black arrow in section A indicates the pulse of caffeine

Discussion

ACM is an inherited cardiomyopathy mainly caused by rare pathogenic variants in genes encoding desmosomal proteins. Although there are several studies describing molecular alterations found in ACM cell and animal models, most of them are only focused on *PKP2*, the main gene currently associated with ACM. Few studies including all desmosomal genes using the same technical approach have been published so far. For this reason, the present study aimed to elucidate ACM common alterations shared by the loss of desmosomal genes. Here, we presented the first systematic *in vitro* study using CRISPR-edited HL1 cells to characterise gene expression profiles and functional alterations following the loss of *PKP2, DSG2, DSC2*, and *DSP*.

DSC2 downregulation

This study revealed a dramatic downregulation of *DSC2* as a common feature of the ACM cellular models, shared by all desmosomal KOs studied. These results suggested that *DSC2* downregulation may be a common molecular feature of the ACM cellular phenotype. In this sense, previous studies in explanted hearts of ACM indicated the same findings, showing a general decrease of either *DSC2* mRNA levels [22] or DSC2 protein levels [23]. However, the molecular mechanisms leading to this common *DSC2* downregulation remain unknown and further studies will be needed.

Interestingly, some previous studies using ACM heart samples found divergent results in desmosomal protein expression. One study described downregulation of all desmosomal genes [24] while another only found differences in some of them [22], and a third did not find significant differences at all [23]. These discrepancies might be explained by the different causal genes of the ACM samples. Our systematic study showed downregulation of *DSC2* was a common feature caused by the absence of *PKP2, DSG2, DSC2*, or *DSP*, but it is still unclear if this alteration was also shared by different variants other than those with PTCs or by other ACM-associated genes. Moreover, here, no other

common alterations in desmosomal expression genes have been described, suggesting that the downregulation of the other desmosomal genes found in the present study might be gene-specific.

Cx43 and Nav1.5 downregulation

To date, alterations in Cx43 and Nav1.5 levels or sodium currents have been widely associated with *PKP2* [10,16,17,25–27] or *DSP* [28–31] decreases or silencing, while they are quite unknown for *DSG2* and *DSC2*. It has been reported that a null allele in *DSG2* caused regional differences regarding Cx43 expression, but no significant differences in the total Cx43 protein content [32]. Moreover, another publication indicated that a null mutation in *DSC2* was associated with gap junction remodelling and decreased Cx43 in the intercalated discs [33]. However, only one patient was involved in that study, and possible alterations in Nav1.5 levels remain unknown for *DSC2* and *DSG2* mutations. Our study showed a significant downregulation of Cx43 at the transcriptional level among all *PKP2*-KO, *DSG2*-KO, and *DSC2*-KO clones. This downregulation was also validated at the protein level in *DSG2*-KO clones, while no significant differences were found for *PKP2*-KO and *DSC2*-KO clones, although our results suggested a tendency to downregulation of protein levels.

Nav1.5 protein was not detected in any of the *PKP2*-KO, *DSG2*-KO, or *DSC2*-KO groups, indicating that, as previously reported for *PKP2* loss [27,25], the absence of *DSG2* or *DSC2* may also produce alterations in the sodium current. Additionally, unlike the other groups, the *DSP*-KO clones presented detectable levels of Nav1.5. However, our results did not determine if the total levels of Nav1.5 were significantly different from WT, as described earlier [31], because of the very limited number of DSP-KO clones.

TGFB1 and PPARg upregulation

Our results showed an increase in *TGFB1* and *PPARg* shared by the *PKP2*-KO, *DSG2*-KO, and *DSC2*-KO clones. Specifically, the results demonstrated that *TGFB1* was significantly increased in *DSG2*-KO and *DSC2*-KO clones, suggesting that the loss of *DSG2* and *DSC2*

could activate fibrosis. It was previously reported that the loss of *PKP2* increased the expression of *TGFB1* [34]. Interestingly, *Dubash et al.* demonstrated that it was the loss of *DSP* expression in a *PKP2* knockdown that provoked the increased expression of *TGFB1,* since the rescue of *DSP* expression restored normal levels of *TGFB1* in that model [34]. Our results of the *DSC2*-KO clones showed that increased levels of *TGFB1* and a reduction of *DSP* levels were in concordance with the proposed mechanism in this previous publication. However, our results of the *DSG2*-KO clones also showed increased levels of *TGFB1* but unaltered levels of *DSP*, suggesting that the *TGFB1* upregulation may also occur through a *DSP*-loss-independent manner. More studies would be needed to elucidate the underlying mechanisms in these clones.

An increase in *PPARg* expression was also shared by the *PKP2*-KO, *DSG2*-KO, and *DSC2*-KO groups. These results point in the same direction as previously published studies. It has been reported that the right ventricles from ACM patients expressed higher levels of *PPARg*, independently of the mutated gene [35]. Furthermore, cell models with alterations in *PKP2* or *DSC2* also showed increased levels of *PPARg* [24,36,37]. Thus, our results support the idea that increased *PPARg* is a common molecular feature in the ACM cellular phenotype, and it is triggered by either a *PKP2, DSG2*, or *DSC2* loss, potentially leading to an adipogenic process.

Downregulation in calcium handling gene expression

In the last few years, a small number of studies have been published describing calcium handling gene alterations associated with a desmosomal protein loss [12,14,15,38]. Three of them were focused on the loss of *PKP2*, which is the most studied gene in this field. In fact, it is well described that transcription of genes involved in the calcium cycle requires *PKP2* [12]. The present study characterised, for the first time, the permanent loss of different desmosomal proteins using CRISPR editing in the same *in vitro* model, thus avoiding differences between the selected models.

The main shared feature among *PKP2*-KO, *DSG2*-KO, and *DSC2*-KO clones was the dramatic downregulation of RYR2 and ANK2 proteins. Our results supported previous studies showing a significant decrease in *RYR2* and *ANK2* in a *PKP2*-KO mouse model

[12,15], and also revealed these downregulations to be a common feature between *PKP2* loss and cadherin (*DSG2* and *DSC2)* loss.

Finally, the *DSP*-KO clones exhibited detectable levels of ANK2 protein while the *PKP2*-KO, *DSG2*-KO, and *DSC2*-KO groups did not. Moreover, the shared tendency for the upregulation of *PLN* among the *PKP2*-KO, *DSG2*-KO, and *DSC2*-KO groups was remarkable, even more so given that *DSP*-KO showed the opposite tendency. These data together suggest that *DSP* loss might have different impacts on calcium handling gene expression.

Calcium imaging

Slower re-uptake of calcium with PKP2, DSG2, or DSC2 loss

Several studies have been published describing calcium cycling alterations using different *in vivo* and *in vitro* experimental approaches [12,14,38]. Our study explored these functional alterations triggered by desmosomal protein loss using, for the first time, the same *in vitro* system for all the main genes. Our results with *PKP2*-KO, *DSG2*-KO, and *DSC2*-KO clones showed similar calcium transient kinetics with a slower re-uptake of calcium with a significantly longer duration, while the DSP-KO clones presented completely different kinetics with a shorter amplitude. Our results are in concordance with previously published studies showing that the loss of *PKP2* caused a delayed amplitude of the peak in a mouse model [12]. However, regarding the loss of *DSG2*, it was previously shown to produce a shorter amplitude of the peak in heterozygous cardiomyocytes derived from iPSC cells [38]. These discordant results may be explained by the heterozygosity of the previously reported model and the different methodology used to measure calcium transients.

Taking together the massive dysregulation on calcium handling gene expression and subsequently altered calcium transient kinetics, we hypothesised putative molecular mechanisms underlying these results. *PKP2*-KO, *DSC2*-KO, and *DSG2*-KO clones presented shared downregulated levels of *ATP2A2, CASQ2, RYR2*, and *ANK2. ATP2A2* encodes SERCA2 and a decrease of this protein could be responsible for the delay in re-uptake of calcium to the sarcoplasmic reticulum. *CASQ2* encodes calsequestrin-2 that is

located inside the sarcoplasmic reticulum and acts as a calcium buffer, regulating the calcium release by RYR2 [39]. Thus, downregulation of *CASQ2* and *RYR2* might be the mechanism underlying the dysregulation of calcium release, shown as a significantly increased rise time in *DSG*2-KO and *DSC2*-KO clones. Interestingly, although *CASQ2* and *RYR2* were also downregulated in *PKP2*-KO, the rise time was not significantly increased in this group. For this reason, the *PKP2* loss might trigger other additional mechanisms associated with these functional alterations. In this sense, it was previously published that the loss of *PKP2* triggered the phosphorylation of the RYR2 T2809 residue that led to an increased sarcoplasmic reticulum calcium load and higher diastolic calcium concentration due to a function gain of RYR2 [14]. This gain of function of RYR2 could compensate for the decreased levels of RYR2 protein in *PKP2*-KO clones, and this may explain the unaltered rise time. Therefore, our results are compatible with this previous idea that *PKP2* loss may trigger specific mechanisms related to RYR2 phosphorylation that was not found in the other desmosomal gene clones.

ANK2 was commonly downregulated in *PKP2*-KO, *DSC2*-KO, and *DSG2*-KO clones. This protein plays an essential role in the localisation and membrane stabilisation of NCX1 (encoded by *SLC8A1*) and SERCA2 [39].Therefore, we hypothesise that decreased *ANK2* might be involved in the delayed re-uptake of calcium because NCX1 and SERCA2 may be less efficient in returning calcium to the extracellular medium and to the sarcoplasmic reticulum, respectively. In agreement with this hypothesis, *DSP*-KO clones, which showed detectable levels of ANK2 protein, presented a slightly shorter amplitude in the calcium peak. Therefore, ANK2 could be causing these differences in peak amplitude in the studied clones. In fact, previous studies showed that heterozygous *ANK2*-KO mice presented more frequent Ca^{2+} sparks and waves compared with WT mice [40,41]. Ca^{2+} waves are caused by a higher Ca^{2+} content in the sarcoplasmic reticulum [42], indicating that the absence of *ANK2* causes a dysregulation of calcium homeostasis.

Additionally, *PLN* is an inhibitor of the activity of *ATP2A2*, decreasing SERCA affinity for calcium in its unphosphorylated state [43]. An increased expression of *PLN* may reduce ATP2A2 activity, producing a delay in the re-uptake of calcium into the sarcoplasmic reticulum, and thus causing the delayed amplitude of the peak in *PKP2*-KO, *DSG2*-KO, and *DSC2*-KO clones. However, in the *DSP*-KO clones, downregulated levels of *PLN* may

trigger higher activity of *ATP2A2*, leading to a more rapid re-uptake of calcium to the sarcoplasmic reticulum. Therefore, changes in *PLN* mRNA expression levels could explain the functional alterations in all clones*.

Finally, our study also demonstrated that N-*DSP* proteins were produced by re-initiation of translation triggered by a 5'-PTC, with no major alterations in the expression profile [21], and were also revealed to be fully functional in terms of calcium handling.

Limitations

This study was designed using sgRNA targeting the first exon of each desmosomal gene to generate KO clones; however, most of the *DSP*-KO clones triggered re-initiation of translation, synthesising N-DSP. Thus, there was a very reduced number of *DSP*-KO clones, which made it not possible to perform statistical analyses on the experimental data produced for those clones. For this reason, *DSP*-KO results, unlike other groups, were described qualitatively in this study.

Conclusions

This study presented the first systematic *in vitro* study using CRISPR-edited HL1 cells to define common molecular and functional effects of *PKP2, DSG2, DSC2*, and *DSP* loss using the same experimental approach.

Our study revealed that *DSC2* downregulation was the only common alteration in desmosomal expression genes shared by the absence of *PKP2, DSG2, DSC2*, or *DSP*. Interestingly, *PKP2* loss triggered major alterations in desmosomal and calcium handling gene expression. Regarding electrical conduction alterations, *PKP2, DSG2*, and *DSC2*-KO caused downregulation of Nav1.5 but this was not shared by *DSP*-KO. Moreover, upregulation of *TFGB1* and *PPARg* was also found to be a common molecular feature for *PKP2, DSG2*, and *DSC2* loss, although no data was available for the loss of *DSP*.

Finally, our results showed massive dysregulation in calcium handling genes shared by *PKP2, DSC2*, or *DSG2* loss associated with a slower calcium re-uptake that might be

related to the *ANK2*, *CASQ2, ATP2A2*, and *RYR2* decrease or *PLN* increase. In contrast, *DSP*-KO clones produced a shorter amplitude of the calcium peak, which might be associated with the downregulation of *PLN*, which was only shown in *DSP*-KO clones. More studies would be needed to corroborate these associations. Moreover, the present study demonstrated that N-DSP proteins are fully functional in terms of calcium cycling.

Author contributions

Marta Vallverdú-Prats: Conceptualisation, Methodology, Validation, Formal Analysis, Investigation, Data Curation, Writing-Original Draft, Visualisation; **David Carreras**: Methodology, Validation, Investigation, Writing-Review and editing; **Guillermo J Pérez**: Validation, Writing-Review and Editing, Supervision; **Oscar Campuzano**: Conceptualisation, Validation, Writing-Review and Editing; **Ramon Brugada**: Resources, Writing-Review and Editing, Supervision, Project Administration, Funding Acquisition; **Mireia Alcalde**: Conceptualisation, Validation, Investigation, Data Curation, Writing-Original Draft, Visualisation, Supervision, Project Administration.
All authors have read and agreed to the published version of the manuscript.

Conflict of Interests

The authors declare no conflict of interest.

Funding

Aknowledgments:

References:

1. Corrado D, Basso C, Judge DP. Arrhythmogenic Cardiomyopathy. Published online 2017:19.

2. He J, Xu J, Li G, et al. Arrhythmogenic Left Ventricular Cardiomyopathy: A Clinical and CMR Study. *Sci Rep*. 2020;10(1):533. doi:10.1038/s41598-019-57203-2

3. Dalal D, James C, Tichnell C, Calkins H. Arrhythmogenic right ventricular dysplasia: A United States experience. *Heart Rhythm*. 2005;2(5):S115. doi:10.1016/j.hrthm.2005.02.357

4. Hoorntje ET, te Rijdt WP, James CA, et al. Arrhythmogenic cardiomyopathy: pathology, genetics, and concepts in pathogenesis. *Cardiovasc Res*. 2017;113(12):1521-1531. doi:10.1093/cvr/cvx150

5. Mattesi G, Zorzi A, Corrado D, Cipriani A. Natural History of Arrhythmogenic Cardiomyopathy. *J Clin Med*. 2020;9(3):878. doi:10.3390/jcm9030878

6. Najor NA. Desmosomes in Human Disease. *Annu Rev Pathol Mech Dis*. 2018;13(1):51-70. doi:10.1146/annurev-pathol-020117-044030

7. Domenico Corrado, Peter J. van Tintelen, William J. McKenna, et al. Arrhythmogenic right ventricular cardiomyopathy: evaluation of the current diagnostic criteria and differential diagnosis. *Eur Heart J*. 2020;41:1414-1427. doi:10.1093/eurheartj/ehz669

8. Austin KM, Trembley MA, Chandler SF, et al. Molecular mechanisms of arrhythmogenic cardiomyopathy. *Nat Rev Cardiol*. 2019;16(9):519-537. doi:10.1038/s41569-019-0200-7

9. Gerull B, Brodehl A. Genetic Animal Models for Arrhythmogenic Cardiomyopathy. *Front Physiol*. 2020;11:624. doi:10.3389/fphys.2020.00624

10. Sommariva E, Stadiotti I, Perrucci GL, Tondo C, Pompilio G. Cell models of arrhythmogenic cardiomyopathy: advances and opportunities. *Dis Model Mech*. 2017;10(7):823-835. doi:10.1242/dmm.029363

11. Claycomb WC, Lanson NA, Stallworth BS, et al. HL-1 cells: A cardiac muscle cell line that contracts and retains phenotypic characteristics of the adult cardiomyocyte. *Proc Natl Acad Sci*. 1998;95(6):2979-2984. doi:10.1073/pnas.95.6.2979

12. Cerrone M, Montnach J, Lin X, et al. Plakophilin-2 is required for transcription of genes that control calcium cycling and cardiac rhythm. *Nat Commun*. 2017;8(1):106. doi:10.1038/s41467-017-00127-0

13. Lyon A, van Opbergen CJM, Delmar M, Heijman J, van Veen TAB. In silico Identification of Disrupted Myocardial Calcium Homeostasis as Proarrhythmic Trigger in Arrhythmogenic Cardiomyopathy. *Front Physiol*. 2021;12:732573. doi:10.3389/fphys.2021.732573

14. Kim JC, Pérez-Hernández M, Alvarado FJ, et al. Disruption of Ca $^{2+}_i$ Homeostasis and Connexin 43 Hemichannel Function in the Right Ventricle Precedes Overt Arrhythmogenic Cardiomyopathy in Plakophilin-2–Deficient Mice. *Circulation*. 2019;140(12):1015-1030. doi:10.1161/CIRCULATIONAHA.119.039710

15. van Opbergen CJM, Noorman M, Pfenniger A, et al. Plakophilin-2 Haploinsufficiency Causes Calcium Handling Deficits and Modulates the Cardiac Response Towards Stress. *Int J Mol Sci*. 2019;20(17):4076. doi:10.3390/ijms20174076

16. Oxford EM, Musa H, Maass K, Coombs W, Taffet SM, Delmar M. Connexin43 Remodeling Caused by Inhibition of Plakophilin-2 Expression in Cardiac Cells. *Circ Res*. 2007;101(7):703-711. doi:10.1161/CIRCRESAHA.107.154252

17. Fidler LM, Wilson GJ, Liu F, et al. Abnormal connexin43 in arrhythmogenic right ventricular cardiomyopathy caused by plakophilin-2 mutations. *J Cell Mol Med*. 2009;13(10):4219-4228. doi:10.1111/j.1582-4934.2008.00438.x

18. Claycomb WC, Lanson NA, Stallworth BS, et al. HL-1 cells: A cardiac muscle cell line that contracts and retains phenotypic characteristics of the adult cardiomyocyte. *Proc Natl Acad Sci*. 1998;95(6):2979-2984. doi:10.1073/pnas.95.6.2979

19. *Image Lab Software*. BIO-RAD https://www.bio-rad.com/es-es/product/image-lab-software?ID=KRE6P5E8Z

20. Sikkel MB, Francis DP, Howard J, et al. Hierarchical statistical techniques are necessary to draw reliable conclusions from analysis of isolated cardiomyocyte studies. *Cardiovasc Res*. 2017;113(14):1743-1752. doi:10.1093/cvr/cvx151

21. Vallverdú-Prats M, Brugada R, Alcalde M. Premature Termination Codon in 5' Region of Desmoplakin and Plakoglobin Genes May Escape Nonsense-Mediated Decay through the Reinitiation of Translation. *Int J Mol Sci*. 2022;23(2):656. doi:10.3390/ijms23020656

22. Vite A, Gandjbakhch E, Prost C, et al. Desmosomal Cadherins Are Decreased in Explanted Arrhythmogenic Right Ventricular Dysplasia/Cardiomyopathy Patient Hearts. Mohanraj R, ed. *PLoS ONE*. 2013;8(9):e75082. doi:10.1371/journal.pone.0075082

23. Akdis D, Medeiros-Domingo A, Gaertner-Rommel A, et al. Myocardial expression profiles of candidate molecules in patients with arrhythmogenic right ventricular cardiomyopathy/dysplasia compared to those with dilated cardiomyopathy and healthy controls. *Heart Rhythm*. 2016;13(3):731-741. doi:10.1016/j.hrthm.2015.11.010

24. Chen SN, Gurha P, Lombardi R, Ruggiero A, Willerson JT, Marian AJ. The Hippo Pathway Is Activated and Is a Causal Mechanism for Adipogenesis in Arrhythmogenic Cardiomyopathy. *Circ Res*. 2014;114(3):454-468. doi:10.1161/CIRCRESAHA.114.302810

25. Cerrone M, Lin X, Zhang M, et al. Missense Mutations in Plakophilin-2 Cause Sodium Current Deficit and Associate With a Brugada Syndrome Phenotype. *Circulation*. 2014;129(10):1092-1103. doi:10.1161/CIRCULATIONAHA.113.003077

26. Khudiakov A, Zaytseva A, Perepelina K, et al. Sodium current abnormalities and deregulation of Wnt/β-catenin signaling in iPSC-derived cardiomyocytes generated from patient with arrhythmogenic cardiomyopathy harboring compound genetic variants in plakophilin 2 gene. *Biochim Biophys Acta BBA - Mol Basis Dis*. 2020;1866(11):165915. doi:10.1016/j.bbadis.2020.165915

27. Sato PY, Musa H, Coombs W, et al. Loss of Plakophilin-2 Expression Leads to Decreased Sodium Current and Slower Conduction Velocity in Cultured Cardiac Myocytes. :4.

28. Zhang Q, Deng C, Rao F, et al. Silencing of desmoplakin decreases connexin43/Nav1.5 expression and sodium current in HL-1 cardiomyocytes. *Mol Med Rep*. 2013;8(3):780-786. doi:10.3892/mmr.2013.1594

29. Kam CY, Dubash AD, Magistrati E, et al. Desmoplakin maintains gap junctions by inhibiting Ras/MAPK and lysosomal degradation of connexin-43. *J Cell Biol*. 2018;217(9):3219-3235. doi:10.1083/jcb.201710161

30. Patel DM, Dubash AD, Kreitzer G, Green KJ. Disease mutations in desmoplakin inhibit Cx43 membrane targeting mediated by desmoplakin–EB1 interactions. *J Cell Biol*. 2014;206(6):779-797. doi:10.1083/jcb.201312110

31. Gomes J, Finlay M, Ahmed AK, et al. Electrophysiological abnormalities precede overt structural changes in arrhythmogenic right ventricular cardiomyopathy due to mutations in desmoplakin-A combined murine and human study. *Eur Heart J*. 2012;33(15):1942-1953. doi:10.1093/eurheartj/ehr472

32. Gehmlich K, Syrris P, Reimann M, et al. Molecular changes in the heart of a severe case of arrhythmogenic right ventricular cardiomyopathy caused by a desmoglein-2 null allele. *Cardiovasc Pathol*. 2012;21(4):275-282. doi:10.1016/j.carpath.2011.09.005

33. Gehmlich K, Syrris P, Peskett E, et al. Mechanistic insights into arrhythmogenic right ventricular cardiomyopathy caused by desmocollin-2 mutations. *Cardiovasc Res*. 2011;90(1):77-87. doi:10.1093/cvr/cvq353

34. Dubash AD, Kam CY, Aguado BA, et al. Plakophilin-2 loss promotes TGF-β1/p38 MAPK-dependent fibrotic gene expression in cardiomyocytes. *J Cell Biol*. 2016;212(4):425-438. doi:10.1083/jcb.201507018

35. Djouadi F, Lecarpentier Y, Hebert JL, Charron P, Bastin J, Coirault C. A potential link between peroxisome proliferator-activated receptor signalling and the pathogenesis of arrhythmogenic right ventricular cardiomyopathy. *Cardiovasc Res*. 2009;84(1):83-90. doi:10.1093/cvr/cvp183

36. Caspi O, Huber I, Gepstein A, et al. Modeling of Arrhythmogenic Right Ventricular Cardiomyopathy With Human Induced Pluripotent Stem Cells. *Circ Cardiovasc Genet*. 2013;6(6):557-568. doi:10.1161/CIRCGENETICS.113.000188

37. Reisqs J, Moreau A, Charrabi A, et al. The PPARγ pathway determines electrophysiological remodelling and arrhythmia risks in DSC2 arrhythmogenic cardiomyopathy. *Clin Transl Med*. 2022;12(3). doi:10.1002/ctm2.748

38. Hawthorne RN, Blazeski A, Lowenthal J, et al. Altered Electrical, Biomolecular, and Immunologic Phenotypes in a Novel Patient-Derived Stem Cell Model of Desmoglein-2 Mutant ARVC. *J Clin Med*. 2021;10(14):3061. doi:10.3390/jcm10143061

39. The UniProt Consortium, Bateman A, Martin MJ, et al. UniProt: the universal protein knowledgebase in 2021. *Nucleic Acids Res*. 2021;49(D1):D480-D489. doi:10.1093/nar/gkaa1100

40. Camors E, Mohler PJ, Bers DM, Despa S. Ankyrin-B reduction enhances Ca spark-mediated SR Ca release promoting cardiac myocyte arrhythmic activity. *J Mol Cell Cardiol*. 2012;52(6):1240-1248. doi:10.1016/j.yjmcc.2012.02.010

41. Skogestad J, Aronsen JM, Tovsrud N, et al. Coupling of the Na+/K+-ATPase to Ankyrin B controls Na+/Ca2+ exchanger activity in cardiomyocytes. *Cardiovasc Res*. 2020;116(1):78-90. doi:10.1093/cvr/cvz087

42. Eisner D. Calcium in the heart: from physiology to disease: Calcium in the heart: from physiology to disease. *Exp Physiol*. 2014;99(10):1273-1282. doi:10.1113/expphysiol.2013.077305

43. Eisner DA, Caldwell JL, Kistamás K, Trafford AW. Calcium and Excitation-Contraction Coupling in the Heart. *Circ Res*. 2017;121(2):181-195. doi:10.1161/CIRCRESAHA.117.310230

Article 3

"Rare Variants Associated with Arrhythmogenic

Cardiomyopathy: Reclassification Five Years Later"

Article

Rare Variants Associated with Arrhythmogenic Cardiomyopathy: Reclassification Five Years Later

Marta Vallverdú-Prats [1,†], Mireia Alcalde [1,2,†], Georgia Sarquella-Brugada [3,4], Sergi Cesar [4], Elena Arbelo [2,5], Anna Fernandez-Falgueras [1,6], Mónica Coll [1,2], Alexandra Pérez-Serra [1,2], Marta Puigmulé [1,2], Anna Iglesias [1,2], Victoria Fiol [4], Carles Ferrer-Costa [1], Bernat del Olmo [1,2], Ferran Picó [1], Laura Lopez [1], Paloma Jordà [2,5], Ana García-Álvarez [2,5], Coloma Tirón de Llano [6], Rocío Toro [7], Simone Grassi [8], Antonio Oliva [8], Josep Brugada [2,5], Ramon Brugada [1,2,3,6,*] and Oscar Campuzano [1,2,3,*]

1   Cardiovascular Genetics Center, University of Girona—IdIBGi, 17190 Girona, Spain; mvallverdu@gencardio.com (M.V.-P.); malcalde@gencardio.com (M.A.); afernandez@gencardio.com (A.F.-F.); mcoll@gencardio.com (M.C.); aperez@idibgi.org (A.P.-S.); mpuigmule@gencardio.com (M.P.); annai@brugada.org (A.I.); cferrer@gencardio.com (C.F.-C.); bdelolmo@gencardio.com (B.d.O.); ferran.pico@gencardio.com (F.P.); llopez@gencardio.com (L.L.)
2   Centro Investigación Biomédica en Red de Enfermedades Cardiovasculares (CIBERCV), 28029 Madrid, Spain; EARBELO@clinic.cat (E.A.); paloma.jorda.b@gmail.com (P.J.); ANAGARCI@clinic.cat (A.G.-Á.); jbrugada@clinic.cat (J.B.)
3   Medical Science Department, School of Medicine, University of Girona, 17071 Girona, Spain; georgia@brugada.org
4   Arrhythmias Unit, Hospital Sant Joan de Déu, University of Barcelona, 08950 Barcelona, Spain; sergi.cesar@gmail.com (S.C.); jvfiolramis@gmail.com (V.F.)
5   Arrhythmias Unit, Hospital Clinic de Barcelona, University of Barcelona, 08036 Barcelona, Spain
6   Cardiology Service, Hospital Dr. Josep Trueta, University of Girona, 17007 Girona, Spain; colomatiron@gmail.com
7   Medicine Department, School of Medicine, 11003 Cadiz, Spain; rociotorogreen@gmail.com
8   Institute of Public Health, Section Legal Medicine, Catholic University, 00153 Rome, Italy; simone.grassi@unicatt.it (S.G.); antonio.oliva@unicatt.it (A.O.)
*   Correspondence: rbrugada@idibgi.org (R.B.); oscar@brugada.org (O.C.)
†   Both authors equally contributed as first author.

Abstract: Genetic interpretation of rare variants associated with arrhythmogenic cardiomyopathy (ACM) is essential due to their diagnostic implications. New data may relabel previous variant classifications, but how often reanalysis is necessary remains undefined. Five years ago, 39 rare ACM-related variants were identified in patients with features of cardiomyopathy. These variants were classified following the American College of Medical Genetics and Genomics' guidelines. In the present study, we reevaluated these rare variants including novel available data. All cases carried one rare variant classified as being of ambiguous significance (82.05%) or likely pathogenic (17.95%) in 2016. In our comprehensive reanalysis, the classification of 30.77% of these variants changed, mainly due to updated global frequencies. As in 2016, nowadays most variants were classified as having an uncertain role (64.1%), but the proportion of variants with an uncertain role was significantly decreased (17.95%). The percentage of rare variants classified as potentially deleterious increased from 17.95% to 23.07%. Moreover, 83.33% of reclassified variants gained certainty. We propose that periodic genetic reanalysis of all rare variants associated with arrhythmogenic cardiomyopathy should be undertaken at least once every five years. Defining the roles of rare variants may help clinicians obtain a definite diagnosis.

Keywords: sudden cardiac death; arrhythmogenic cardiomyopathy; genetics; rare variants; reclassification

1. Introduction

Arrhythmogenic cardiomyopathy (ACM) is a rare disorder characterized by progressive replacement of the myocardium by fibrofatty tissue, and this myocyte disorganization

increases the risk for ventricular arrhythmias and sudden cardiac death [1,2]. Tissue substitution occurs predominantly in the right ventricle, but biventricular forms have also been reported [3]. Moreover, isolated forms affecting only the left ventricle have also been published [4]. Diagnosis of ACM does not rely on a single gold standard test but is achieved using a scoring system proposed in 1994 by Task Force Criteria (TFC), encompassing familial and genetic factors, electrocardiogram (ECG) abnormalities, and structural/functional ventricular alterations [5,6]. In 2010, a revision of the TFC was proposed to incorporate new knowledge and technology to improve diagnostic sensitivity while maintaining diagnostic specificity [7]. This is important because correct diagnosis prevents over- or under-treatment and reduces the morbidity and mortality of ACM patients [8]. Also, there is evidence that differences in the propensity for life-threatening arrhythmias, left ventricular dysfunction, and heart failure can be explained by gene-specific alterations [9].

A definite genetic variant classified as pathogenic represents a major criterion for ACM diagnosis in the TFC [10]. Currently, comprehensive genetic analysis allows identification of a genetic cause in up to 60% of ACM cases [11]. Although there are several genes reported to be associated with ACM, most ACM patients carry pathogenic alterations in genes encoding desmosomal proteins, with *PKP2* being the main gene currently associated with ACM [12]. However, genetic diagnosis is challenging in ACM families because the clinical role of rare variants located in known genes is not always clear due to a lack of conclusive data as well as overlap of causal genes with other inherited cardiomyopathies [10,12,13]. This ambiguity impedes inclusion of genetic results in a definite diagnosis of ACM. The American College of Medical Genetics and Genomics (ACMG) standards and guidelines have structured standard terminology for classifying sequence variants using available evidence weighted according to a system developed through expert opinion, work-group consensus, and community input [14]. Accurate genetic interpretation following ACMG recommendations facilitates clinical translation of rare genetic variants and more individualized clinical management of patients [15].

Continuous improvement in the genetic data concerning rare variants may modify previous classifications and thus alter patient diagnosis and treatment, prenatal diagnosis or pre-implantation genetic diagnosis [16], and screening of at-risk family members [13,16]. To date, few studies have focused on proper genetic reinterpretation of available data before clinical translation [17,18]. These limited studies have focused on inherited arrhythmogenic diseases but have not addressed how often reanalysis is necessary in ACM-related genes. Our study aims to clarify this crucial point, facilitating accurate genetic classification, clinical diagnosis, and the adoption of personalized measures in families afflicted by ACM.

2. Materials and Methods

2.1. Cohort

We reanalysed and reinterpreted 39 rare variants identified in 2016 from 39 patients that presented features of ACM (definite, borderline or possible diagnosis following TFC). These rare variants were originally classified as pathogenic (P), likely pathogenic (LP), or variants of unknown significance (VUS) following ACMG recommendations [14]. Variants classified as likely benign (LB) and/or benign (B) in 2016 were not reanalysed because their global frequencies in 2016 were >1%, and they were already reported to be definitively non-causative in ACM. Genetic analysis was approved by the ethics committee of Hospital Josep Trueta (Girona, Spain) following the World Medical Association Declaration of Helsinki. Clinical and genetic data concerning all patients were kept anonymous. Written informed consent was obtained from all patients included in the study before genetic analysis.

2.2. Genetic Analysis

Genomic DNA was extracted from whole blood, and its concentration and purity were determined. Comprehensive genetic analysis was performed, including all genes associated with ACM in 2016 and all isoforms described in Ensembl 75 (www.ensembl.org/) linked to RefSeq code (www.ncbi.nlm.nih.gov/refseq/) or CCDS (www.ncbi.nlm.nih.gov/

CCDS/). Sequence data coordinates were based on the UCSC human genome version hg19 (NCBI GRCh37 build). Secondary, bioinformatic analysis included adaptor and low-quality base-trimming of the FASTQ files. Variant calling from the cleaned BAM files was performed with SAMtools v.1.2 and an ad hoc developed script. The final annotation steps provided information included in public databases. Non-common (minor allele frequency [MAF] <1%) genetic variants were confirmed by Sanger sequencing. Exons and exon–intron boundaries of each gene were amplified in both directions with posterior analysis, comparing obtained results with the reference sequence from hg19.

Identified rare variants were compared with with HapMap (www.hapmap.ncbi.nlm.nih.gov/), the 1000 Genomes Project (www.1000genomes.org/), the Exome Variant Server (EVS) (www.evs.gs.washington.edu/EVS/) in 2016, and the Genome Aggregation Database (gnomAD) (www.gnomad.broadinstitute.org/) in 2021. All rare variants were described following HGVS (www.hgvs.org/) and consulted in ClinGen (www.clinicalgenome.org/), VarSome (www.varsome.com/), the SCD-associated Variants Annotation Database (SVAD) (www.svad.mbc.nctu.edu.tw/), CardioClassifier (www.cardioclassifier.org/), InterVar (www.wintervar.wglab.org/), CardioVAI (www.cardiovai.engenome.com/ and CardioBoost (www.cardiodb.org/cardioboost/).

2.3. Data

An exhaustive review of the literature concerning each variant was performed through January 2021. Data was collected from HGMD (www.hgmd.org), ClinVar (www.ncbi.nlm.nih.gov/clinvar/intro/), the National Center for Biotechnology Information SNP database (www.ncbi.nlm.nih.gov/SNP), Index Copernicus (www.en.indexcopernicus.com), Google Scholar (www.scholar.google.es), Springer Link (www.link.springer.com), Science Direct (www.sciencedirect.com), Excerpta Medica Database (www.elsevier.com/solutions/embase-biomedical-research), and IEEE Xplore Digital Library (www.ieeexplore.ieee.org/Xplore/home.jsp).

2.4. Classification

In 2016, rare variants were classified following the same ACMG standards currently in use [14]. In 2021, variants were classified following the updated ACMG standards [19,20]. The PM2 item in the ACMG classification was calculated based on [21] to find the threshold of the rare variant frequency.

The classification "high degree of pathogenicity" should only be used for rare variants in genes in which loss of function is a well-established disease mechanism [22]. Genetic data were independently evaluated and classified by six experts (three cardiologists and three clinical geneticists). All investigators discussed and agreed on final classification of all variants to avoid bias.

3. Results

We reinterpreted 39 rare variants in ACM related genes identified in 39 non-related Caucasian patients with features of ACM in 2016 (9 definite and 30 possible diagnosis in 2016. These rare variants were mainly located in desmosomal genes (35/39 = 89.75%): 11 in *PKP2*, 15 in *DSP*, six in *DSG2*, two in *DSC2* and one in *JUP*. There were also four rare variants in non-desmosomal genes (4/39 = 10.25%): three in *TMEM43* and one in *DES* (Figure 1A). Most rare variants were missense (27, 69.23%), and there were also seven indels (17.94%), three intronic variants (7.69%), and two nonsense variants (5.13%) (Figure 1B).

After a comprehensive analysis, 12 of the 39 rare variants (30.77%) were reclassified (Table 1). Most of the rare variants were classified as variants of unknown significance (VUS) in 2016 (32 rare variants, 82.05%) and in the current reclassification the number has been significantly reduced (25 rare variants, 64.10%). Thus, the number of variants classified as VUS was reduced by 17.95% in our reassessment.

Of the nine reclassified VUS variants, two were now classified as benign, three as likely benign (LB) and four as likely pathogenic (LP). In 2016 we identified seven likely

pathogenic (LP) variants (17.94%), but only four remained LP five years after. Two of the 2016 LP variants changed to VUS and one to P (Figure 2).
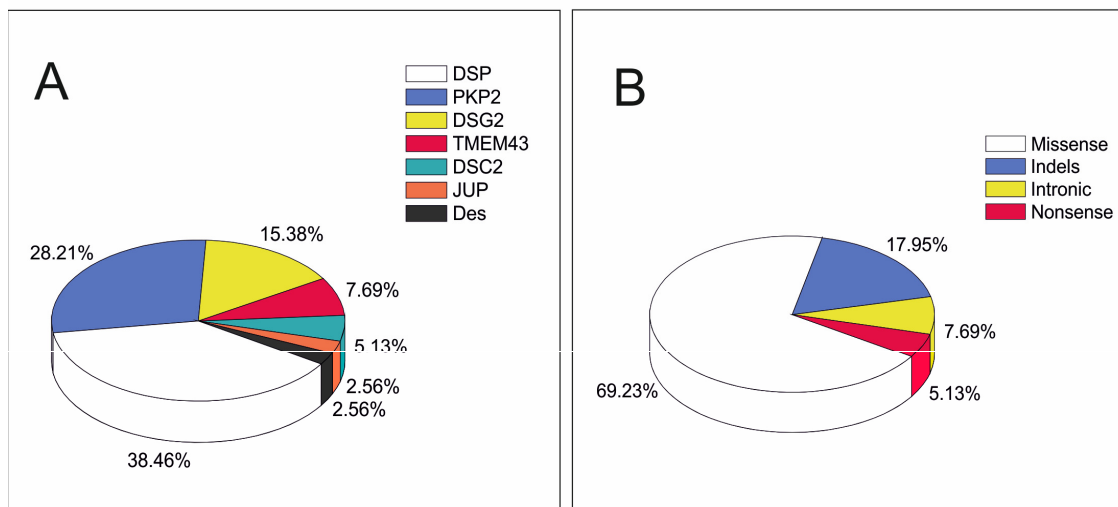
Figure 1. Rare variant distribution in genes and mutation types. (**A**) Localization of the 39 evaluated variants in arrhythmogenic cardiomyopathy (ACM)-causal genes. (**B**) Distribution of mutation types of the 39 evaluated variants.

Importantly, 10 out of 12 (83.33%) reclassified variants gained certainty upon reclassification. Among likely pathogenic mutations, 37.5% (3/8) qualified as predicted null variants in a gene where loss of function is a known mechanism of disease (very strong criteria-PVS1). Only one missense variant (variant 4 DSG2;c.146G>A) was classified as P due to the sum of different criteria and with several strong supporting clinical reports available (very strong criteria-PP5) (Table 2). On the other hand, all LB and B variants (in desmosomal genes) were frequent enough to qualify as strong criteria in the population data (BA1/BS1) (Table 2). In 2016, the ExAC database showed a total of 31 rare variants without frequency data in the global population (79.48%). Updated global frequencies in the gnomAD database showed that the absolute number of rare variants found in the general population increased in comparison to 2016, and only 18 rare variants still remain unidentified in the general population (46.15%).
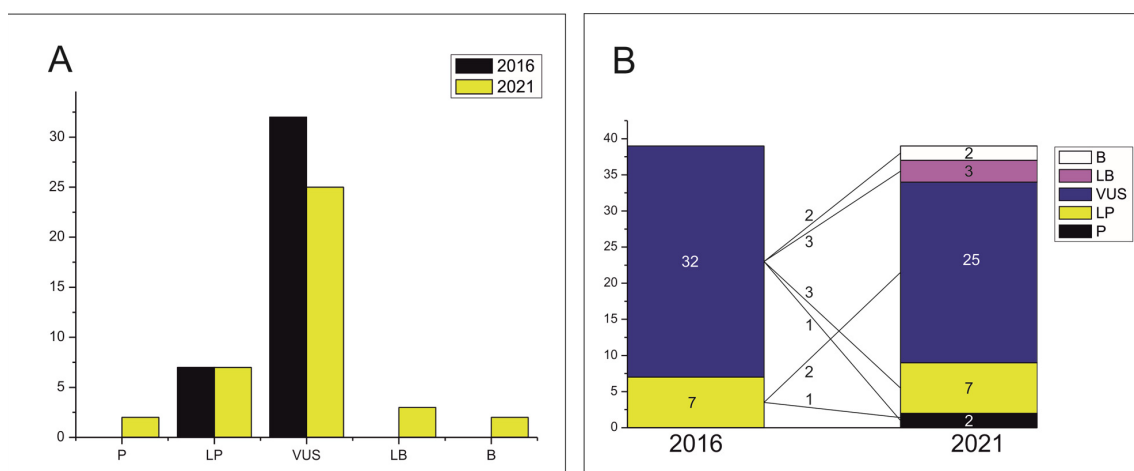
Figure 2. Distribution of the 39 revaluated variants into five groups of variant significance *. (**A**) Comparison of the number of variants in each group of significance. (**B**) Comparison of the number of variants between 2016 and 2021 classifications. * Five groups of variant significance: P = pathogenic; LP = likely pathogenic; VUS =variant of uncertain significance; LB = likely benign, and B = benign.

Table 1. Rare variants found in ACM patients (grey indicates variants that have been reclassified).

Proband	Diagnosis 2016	Gene	Nucleotide	Protein	dbSNP	ExAC (2016)	GnomAD (2021)	2016 Classification	2021 Classification
1	Possible	*DES*	c.158T>C	p.(Val53Ala)	NI	NI	NI	VUS	VUS
2	Possible	*DSC2*	c.430A>G	p.(Met144Val)	NI	NI	NI	VUS	VUS
3	Definite	*DSC2*	c.2587G>A	p.(Gly863Arg)	rs147109895	6/1,3001 (0.04%)	69/25,1128 (0.02%)	VUS	VUS
4	Definite	*DSG2*	c.146G>A	p.(Arg49His)	rs121913006	NI	1/24,9482 (0.0004%)	LP	P
5	Possible	*DSG2*	c.484delG	p.(Asp162Metfs*10)	rs1158782181	NI	NI	LP	LP
6	Definite	*DSG2*	c.1003A>G	p.(Thr335Ala)	rs191564916	5/1,1919 (0.04%)	130/24,9422 (0.05%)	VUS	LB
7	Possible	*DSG2*	c.1885C>T	p.(Pro629S)	rs200804638	NI	6/24,9336 (0.002%)	VUS	VUS
8	Possible	*DSG2*	c.2825C>T	p.(Thr942Ile)	rs771429752	NI	1/24,8492 (0.0004%)	VUS	VUS
9	Possible	*DSG2*	c.3266G>A	p.(Gly1089Asp)	rs200264407	9/1,2173 (0.07%)	28/24,9268 (0.01%)	VUS	LB
10	Possible	*DSP*	c.130C>T	p.(Arg44Trp)	rs1255744065	NI	2/17,7516 (0.001%)	VUS	VUS
11	Possible	*DSP*	c.559G>T	p.(Val187Phe)	NI	NI	NI	VUS	VUS
12	Possible	*DSP*	c.1063C>T	p.(Gln355*)	rs1561686893	NI	NI	LP	LP
13	Definite	*DSP*	c.1267-2A>G	NI	rs1554106830	NI	NI	LP	LP
14	Possible	*DSP*	c.1297C>T	p.(Arg433Cys)	rs767032884	NI	2/25,1302 (0.0007%)	VUS	VUS
15	Possible	*DSP*	c.1639delC	p.(Leu547Trpfs*8)	NI	NI	NI	LP	LP
16	Possible	*DSP*	c.1696G>A	p.(Ala566Thr)	rs148147581	5/1,3001 (0.03%)	50/25,1036 (0.01%)	LP	VUS
17	Possible	*DSP*	c.2515C>T	p.(His839Tyr)	rs1561693806	NI	1/25,1454 (0.0003%)	VUS	VUS
18	Possible	*DSP*	c.2723G>A	p.(Arg908His)	rs142494121	14/1,2992 (0.1%)	289/25,1322 (0.1%)	VUS	B
19	Possible	*DSP*	c.2723G>T	p.(Arg908Leu)	rs142494121	NI	4/25,1322 (0.001%)	VUS	VUS
20	Possible	*DSP*	c.2867A>G	p.(Asn956Ser)	rs1373071129	NI	1/24,8880 (0.0004%)	VUS	VUS
21	Possible	*DSP*	c.3398A>G	p.(Asp1133Gly)	NI	NI	NI	VUS	VUS
22	Possible	*DSP*	c.3550_3551delCGinsAC	p.(Arg1184Thr)	NI	NI	NI	VUS	VUS
23	Possible	*DSP*	c.3643_3644delAAinsTG	p.(Asn1215Cys)	NI	NI	NI	VUS	VUS
24	Possible	*DSP*	c.8498C>G	p.(Ser2833Cys)	rs767961179	NI	3/24,6912 (0.001%)	VUS	VUS
25	Definite	*JUP*	c.1235C>T	p.(Thr412Met)	rs782551865	NI	2/25,1412 (0.0007%)	VUS	VUS
26	Possible	*PKP2*	c.122C>G	p.(Ala41Gly)	rs1220759009	NI	1/3,1346 (0.003%)	VUS	VUS
27	Definite	*PKP2*	c.259G>C	p.(Val87Leu)	rs750028032	NI	3/25,1410 (0.001%)	VUS	VUS
28	Possible	*PKP2*	c.505A>G	p.(Ser169Gly)	rs139139859	21/1,2979 (0.1%)	294/25,1282 (0.1%)	VUS	B

Table 1. *Cont.*

Proband	Diagnosis 2016	Gene	Nucleotide	Protein	dbSNP	ExAC (2016)	GnomAD (2021)	2016 Classification	2021 Classification
29	Possible	*PKP2*	c.635G>T	p.(Arg212Leu)	NI	NI	NI	VUS	VUS
30	Possible	*PKP2*	c.1034+2dupT	NI	NI	NI	NI	VUS	LP
31	Possible	*PKP2*	c.1093A>G	p.(Met365Val)	rs143900944	2/1,3004 (0.01%)	67/25,1320 (0.02%)	VUS	LB
32	Definite	*PKP2*	c.1489C>T	p.(Arg497*)	rs151212477	NI	2/21,7850 (0.0009%)	VUS	LP
33	Definite	*PKP2*	c.1643delG	p.(Gly548Valfs*15)	rs794729137	NI	NI	VUS	LP
34	Definite	*PKP2*	c.2104_2111dupTCCTTAGC	p.(Ala705Profs*2)	NI	NI	NI	VUS	LP
35	Possible	*PKP2*	c.2245_2246delGCinsAT	p.(Ala749Ile)	rs1565574704	NI	NI	VUS	VUS
36	Possible	*PKP2*	c.2633C>T	p.(Ser878Phe)	rs1216433436	NI	1/25,1470 (0.0003%)	LP	VUS
37	Possible	*TMEM43*	c.780+3A>G	NI	NI	NI	NI	VUS	VUS
38	Possible	*TMEM43*	c.1026C>G	p.(Asp342Glu)	NI	1/1,3005 (0.007%)	NI	VUS	VUS
39	Possible	*TMEM43*	c.1145T>C	p.(Leu382Pro)	NI	NI	NI	VUS	VUS

NI: allele not identified; VUS, variant of unknown significance; P, pathogenic; LP, likely pathogenic; LB, likely benign; B, benign.

Table 2. Most relevant indicators in the reanalyses.

				Indicators for Gene			Indicators for Variant				
		Nucleotide	*Protein*	*2021 Class*	P Gene (%) [1]	P Variant Rate [2]	Loss of Function [3]	Population Data (MAF)	Allelic Data [4]	Hot Spot [5]	Computational and Predictive Data [6]	Clinically Reported P before [7]
1	Des	c.158T>C	p.(Val53Ala)	VUS	N/A	N/A	-	NI	NI	Yes	6/13	No
2	DSC2	c.430A>G	p.(Met144Val)	VUS	B.T	B.T	-	NI	NI	Yes	1/13	No
3	DSG2	c.2587G>A	p.(Gly863Arg)	VUS	B.T	B.T	-	0.02%	69/25,1128	No	10/13	No
4	DSG2	c.146G>A	p.(Arg49His)	P	B.T	B.T	-	0.0004%	1/24,9482	Yes	13/13	>10 and no conflict
5	DSG2	c.484delG	p.(Asp162Metfs*10)	LP	N/A	N/A	Yes	NI	NI	N/A	N/A	No
6	DSG2	c.1003A>G	p.(Thr335Ala)	LB	B.T	B.T	-	0.05%	130/2,4942	Yes	4/13	Unclear
7	DSG2	c.1885C>T	p.(Pro629S)	VUS	B.T	B.T	-	0.002%	6/24,9336	No	8/13	No
8	DSG2	c.2825C>T	p.(Thr942Ile)	VUS	B.T	B.T	-	0.0004%	1/24,8492	N/A	5/13	No
9	DSG2	c.3266G>A	p.(Gly1089Asp)	LB	B.T	B.T	-	0.01%	28/24,9268	No	0/13	No
10	DSP	c.130C>T	p.(Arg44Trp)	VUS	B.T	B.T	-	0.001%	2/17,7516	Yes	6/13	No
11	DSP	c.559G>T	p.(Val187Phe)	VUS	B.T	B.T	-	NI	NI	Yes	4/13	No
12	DSP	c.1063C>T	p.(Gln355*)	LP	N/A	N/A	Yes	NI	NI	N/A	N/A	No
13	DSP	c.1267-2A>G	NI	LP	N/A	N/A	Yes	NI	NI	N/A	Moderate	No
14	DSP	c.1297C>T	p.(Arg433Cys)	VUS	B.T	B.T	-	0.0007%	2/25,1302	Yes	10/13	No
15	DSP	c.1639delC	p.(Leu547Trpfs*8)	LP	N/A	N/A	Yes	NI	NI	N/A	N/A	No

Table 2. Cont.

		Nucleotide	Protein	2021 Class	Indicators for Gene					Indicators for Variant		
					P Gene (%)[1]	P Variant Rate[2]	Loss of Function[3]	Population Data (MAF)	Allelic Data[4]	Hot Spot[5]	Computational and Predictive Data[6]	Clinically Reported P before[7]
16	DSP	c.1696G>A	p.(Ala566Thr)	VUS	B.T	B.T	-	0.01%	50/25,1036	Yes	0/13	No
17	DSP	c.2515C>T	p.(His839Tyr)	VUS	B.T	B.T	-	0.0003%	1/25,1454	Yes	4/13	No
18	DSP	c.2723G>A	p.(Arg908His)	B	B.T	B.T	-	0.10%	289/25,1322	Yes	8/13	No
19	DSP	c.2723G>T	p.(Arg908Leu)	VUS	B.T	B.T	-	0.001%	4/25,1322	Yes	7/13	No
20	DSP	c.2867A>G	p.(Asn956Ser)	VUS	B.T	B.T	-	0.0004%	1/24,8880	Yes	3/13	No
21	DSP	c.3398A>G	p.(Asp1133Gly)	VUS	B.T	B.T	-	NI	NI	No	6/13	No
22	DSP	c.3550_3551delCGinsAC	p.(Arg1184Thr)	VUS	B.T	B.T	-	NI	NI	No	N/A	No
23	DSP	c.3643_3644delAAinsTG	p.(Asn1215Cys)	VUS	B.T	B.T	-	NI	NI	No	N/A	No
24	DSP	c.8498C>G	p.(Ser2833Cys)	VUS	B.T	B.T	-	0.001%	3/24,6912	Yes	8/13	No
25	JUP	c.1235C>T	p.(Thr412Met)	VUS	B.T	B.T	-	0.0007%	2/25,1412	No	8/13	No
26	PKP2	c.122C>G	p.(Ala41Gly)	VUS	A.T	A.T	-	0.003%	1/3,1346	No	5/13	No
27	PKP2	c.259G>C	p.(Val87Leu)	VUS	A.T	A.T	-	0.001%	3/25,1410	No	9/13	No
28	PKP2	c.505A>G	p.(Ser169Gly)	B	A.T	A.T	-	0.10%	294/25,1282	No	12/13	No
29	PKP2	c.635G>T	p.(Arg212Leu)	VUS	A.T	A.T	-	NI	NI	No	5/13	No
30	PKP2	c.1034+2dupT	NI	LP	N/A	N/A	Yes	NI	NI	N/A	N/A	No
31	PKP2	c.1093A>G	p.(Met365Val)	LB	A.T	A.T	-	0.02%	67/25,1320	No	2/13	No
32	PKP2	c.1489C>T	p.(Arg497*)	LP	A.T	A.T	Yes	0.0009%	2/21,7850	N/A	N/A	1
33	PKP2	c.1643delG	p.(Gly548Valfs*15)	LP	N/A	N/A	Yes	NI	NI	N/A	Very Strong	>17 and no conflict
34	PKP2	c.2104_2111dupTCCTTAGG	p.(Ala705Profs*2)	LP	N/A	N/A	Yes	NI	NI	N/A	N/A	No
35	PKP2	c.2245_2246delGCinsAT	p.(Ala749Ile)	VUS	A.T	A.T	-	NI	NI	No	N/A	No
36	PKP2	c.2633C>T	p.(Ser878Phe)	VUS	A.T	A.T	-	0.00030%	1/25,1470	No	11/13	No
37	TMEM43	c.780+3A>G	NI	VUS	N/A	N/A	No	NI	NI	No	N/A	No
38	TMEM43	c.1026C>G	p.(Asp342Glu)	VUS	B.T	B.T	-	NI	NI	No	2/13	No
39	TMEM43	c.1145T>C	p.(Leu382Pro)	VUS	B.T	B.T	-	NI	NI	No	4/13	No

Criteria and threshold based on Varsome. In grey meets criteria for pathogenicity. [1] Pathogenic non-VUS missense variants in gene (%). [2] Missense variant in a gene with a low rate of benign missense variation and in which missense variants are a common mechanism of disease. [3] Loss of function is a well-established disease mechanism (premature termination codon (PTC) only). [4] Allele count for dominant gene threshold. [5] Located in a mutational hot spot and/or critical and well-established functional domain. [6] Computational evidence (conservation, evolutionary, splicing impact, etc.) using 13 in silico predictors for missense variants. AutoPVS1 used for intronic variants. [7] Reputable source recently reported variant as pathogenic in probands with consistent phenotypes (P). B.T, below threshold; A.T, above threshold; NI, allele not identified; N/A, data not available or variant does not meet criteria to apply indicator; MAF, minor allele frequency; VUS, variant of unknown significance; P, pathogenic; LP, likely pathogenic; LB, likely benign.

4. Discussion

In our study, 39 rare variants in ACM-related genes were identified in 39 non-related Caucasian patients with features of ACM five years ago. Using currently available data, we updated the 2016 classifications of 30.77% of the rare variants. Importantly, 83.33% of these relabelled rare variants gained certainty in their significance. Our results support periodic evaluation of rare variants associated with ACM at least once every five years as this may directly impact final diagnosis as described in a previous study [18]. They also have found that a significant number of variants have changed their classification after the revaluation, so it is important to perform that kind of reassessments in possible or definitive ACM patients. Moreover, they also have focused on the impact that genetic testing has in the ACM diagnosis taking into account the 2010 TFC. However, there are some important differences between the two studies. Their initial classification was not performed systematically following the 2015 ACMG criteria in all patients, only some of them: 53.2% were performed before the 2015 ACMG criteria, whereas 43.8% were performed thereafter. In their study, criteria were significantly less likely to be reclassified in the latter group with 35.1% of variant reclassification. Here, we classified all variants taking into account the 2015 ACMG criteria at the beginning and after 5 years in the same way, with very similar results (30.77 % of change). We propose a limit of time of 5 years to perform the reclassification due to the results that we obtained; after 5 years, a significant number of variants have changed its classification.

VUS variants represented 82.05% of variants in ACM carriers in the original classification in 2016 but only 64.1% of variants in the present study. Moreover, other studies in different cardiomyopathies have similarly concluded that uncertainty is reduced after variant reclassification [23,24]. In the present study, 83.33% of reclassified variants gained certainty, only two of them (DSP c.1696G>A; PKP2 c.2633C>T) have lost certainty changing from LP to VUS. It is important to say that in those two cases, the new data released did not bring uncertainty. A better-performed variant classification may have a major impact in clarifying the origin of ACM in patients as well as in relatives who have borderline phenotypic manifestations. Our genetic results did not impact in clinical diagnosis due to no borderline cases existing in our cohort, either in 2016 or today. It is important to remark that VUS results have been associated with increased patient anxiety, incorrect recall of results, reduced uptake of family screening, and lower rates of sharing information with family [8]. VUS are a remarkable topic also from a forensic point of view, since when they represent the only finding in a negative autopsy case, it is impossible to determine the cause of the death [25]. The fact that VUS represent the majority of the variants found at the genetic testing in cases of sudden cardiac death, is one of the reasons why some authors do not support the mandatory use of post-mortem genetic testing in SCD cases with ambiguous or no macroscopic/microscopic anomalies. However, as shown by this paper, when more information useful to define the significance of the variants is obtained, a noteworthy share of VUS is reinterpreted as P, proving the importance of collecting and sharing data both in clinical and in forensic contexts [26–28]. In detail, in our study, four VUS variants changed to LP or P; three of these variants were *PKP2* premature termination codon (PTC), with new global genetic studies identifying no alleles or alleles with an extremely low frequency. Haploinsufficiency in *PKP2* is well established to be disease-causing in ACM [29], so novel rare variants, especially PTC, should be considered as having a potential deleterious role in ACM. Moreover, the other VUS variant that changed into LP (c.1034+2dupT) is an intronic duplication also in *PKP2*.

On the other hand, three other VUS variants in 2016 changed to LB in our reanalysis. In all these cases, massive genotyping data released in the past five years played a key role in reclassification. Therefore, the absolute number of alleles is currently higher than expected for a rare genetic disease such as ACM. Importantly, updated global frequencies allow us to identify data in 53.85% of ACM carriers compared to only 20% of ACM variants identified five years ago. In a recent study, a common reason for genetic reclassification of variants in ACM was a high minor allele frequency in the general population [18].

In addition to updated global frequencies, it is also important to take into account specific scientific findings regarding rare variants to improve knowledge and clarify their role in ACM pathophysiology. In this sense, all rare variants with novel available in vitro and/or family co-segregation data have been reclassified into a higher degree of certainty. In our view, complete family segregation is the most important data to clarify the role of a rare variant, especially if a recessive pattern of inheritance is suspected, as observed in *DSG2*_p.(Thr335Ala) [30]. High variant frequencies in ACM patients (classified as LB in heterozygosis) cannot exclude a pathogenic role if a recessive pattern is suspected, reinforcing the need for cautious personalized interpretation before clinical translation. Several studies demonstrate pathogenesis of recessive mutations in *DSC2* that cause ACM [31–33].

Moreover, we should be especially careful in interpreting variants, taking into account suspected disease, affected genes, and previous classification. The *PKP2*_ p.(Met365Val) variant was previously described as potentially disease-causing in Brugada syndrome (BrS) [34]. Although in vitro studies show its effect on the nav1.5 current in a cellular model, its role in ACM is still unclear with no clinical data. Moreover, ECG abnormalities observed in the early stages of ACM may be similar to those in BrS [35,36]. However, the current global frequency of the *PKP2*_ p.(Met365Val) variant has increased during these five years, suggesting a non-deleterious role. Thus, new in vitro studies are also important for reclassifying rare variants into a group with higher certainty. In our study, *DSG2*_ p.(Arg49His) has been reclassified as definitively P based on co-segregation [37] and an in vitro study [38] published in the last 5 years.

Finally, a report has been published recently concerning the role of VUS in inherited arrhythmias and cardiomyopathies [8]. The VUS classification does not provide enough information to make an accurate interpretation, so it is acceptable to consider the variant as "non-actionable" [16,39]. All data conclude that interpretation of a variant classified as a VUS is complex and, sometimes, this result causes a mistaken reduction in familial screenings [40]. It is important to avoid that possibility, so the final objective will be to reduce VUS results as much as possible, although performing segregation studies, when possible, is highly recommended even in VUS variants when there are no more plausible genetic variants to be causal. For this reason, it is appropriate to revaluate variant significance from time to time, at least once every 5 years for ACM-related genes.

5. Conclusions

Identifying a definite pathogenic variant is a key point in the diagnosis of ACM. Therefore, accurate interpretation of variants identified in patients should be mandatory. An exhaustive and updated genetic clarification of rare variants associated with ACM is warranted because it has practical consequences for patients and their relatives. Most rare variants remain of ambiguous significance due to lack of functional data, conclusive family segregation, and updated global frequency. It is important to highlight this data because VUS is an uninformative genetic result in translation into clinical practice, and genetic and clinical professionals cannot make informed clinical decisions based on such a classification. We recommend reanalysing rare variants associated with ACM at least once every five years. When significant changes in classification occur, cardiologists should promptly inform interested patients and, if necessary, modify their therapeutic approach.

6. Limitations

A different interpretation of genetic data for some rare variants included in our study may induce controversy regarding their role, especially for variants classified as VUS. To minimize controversy, all authors came to a consensus regarding the final classification decision. Importantly, reclassifications in our study should be corroborated in additional larger cohorts of ACM families. Finally, we have not assessed the time or economic cost of reinterpretation.

References

1. Karmouch, J.; Protonotarios, A.; Syrris, P. Genetic basis of arrhythmogenic cardiomyopathy. *Curr. Opin. Cardiol.* **2018**, *33*, 276–281. [CrossRef] [PubMed]
2. Basso, C.; Corrado, D.; Marcus, F.I.; Nava, A.; Thiene, G. Arrhythmogenic right ventricular cardiomyopathy. *Lancet* **2009**, *373*, 1289–1300. [CrossRef]
3. Corrado, D.; Basso, C.; Judge, D.P. Arrhythmogenic Cardiomyopathy. *Circ. Res.* **2017**, *121*, 784–802. [CrossRef] [PubMed]
4. He, J.; Xu, J.; Li, G.; Zhou, D.; Li, S.; Zhuang, B.; Chen, X.; Duan, X.; Li, L.; Fan, X.; et al. Arrhythmogenic Left Ventricular Cardiomyopathy: A Clinical and CMR Study. *Sci. Rep.* **2020**, *10*, 533. [CrossRef]
5. Corrado, D.; Link, M.S.; Calkins, H. Arrhythmogenic Right Ventricular Cardiomyopathy. *N. Engl. J. Med.* **2017**, *376*, 1489–1490. [CrossRef]
6. McKenna, W.J.; Thiene, G.; Nava, A.; Fontaliran, F.; Blomstrom-Lundqvist, C.; Fontaine, G.; Camerini, F. Diagnosis of arrhythmogenic right ventricular dysplasia/cardiomyopathy. Task Force of the Working Group Myocardial and Pericardial Disease of the European Society of Cardiology and of the Scientific Council on Cardiomyopathies of the International Society and Federation of Cardiology. *Br. Heart J.* **1994**, *71*, 215–218. [PubMed]
7. Marcus, F.I.; McKenna, W.J.; Sherrill, D.; Basso, C.; Bauce, B.; Bluemke, D.A.; Calkins, H.; Corrado, D.; Cox, M.G.; Daubert, J.P.; et al. Diagnosis of arrhythmogenic right ventricular cardiomyopathy/dysplasia: Proposed modification of the Task Force Criteria. *Eur. Heart J.* **2010**, *31*, 806–814. [CrossRef] [PubMed]
8. Muller, R.D.; McDonald, T.; Pope, K.; Cragun, D. Evaluation of Clinical Practices Related to Variants of Uncertain Significance Results in Inherited Cardiac Arrhythmia and Inherited Cardiomyopathy Genes. *Circ. Genom. Precis. Med.* **2020**, *13*, e002789. [CrossRef] [PubMed]
9. Bhonsale, A.; Groeneweg, J.A.; James, C.A.; Dooijes, D.; Tichnell, C.; Jongbloed, J.D.; Murray, B.; te Riele, A.S.; van den Berg, M.P.; Bikker, H.; et al. Impact of genotype on clinical course in arrhythmogenic right ventricular dysplasia/cardiomyopathy-associated mutation carriers. *Eur. Heart J.* **2015**, *36*, 847–855. [CrossRef]
10. Musunuru, K.; Hershberger, R.E.; Day, S.M.; Klinedinst, N.J.; Landstrom, A.P.; Parikh, V.N.; Prakash, S.; Semsarian, C.; Sturm, A.C.; American Heart Association Council on Genomic and Precision Medicine; et al. Genetic Testing for Inherited Cardiovascular Diseases: A Scientific Statement From the American Heart Association. *Circ. Genom. Precis. Med.* **2020**, *13*, e000067. [CrossRef] [PubMed]
11. Groeneweg, J.A.; Bhonsale, A.; James, C.A.; te Riele, A.S.; Dooijes, D.; Tichnell, C.; Murray, B.; Wiesfeld, A.C.; Sawant, A.C.; Kassamali, B.; et al. Clinical Presentation, Long-Term Follow-Up, and Outcomes of 1001 Arrhythmogenic Right Ventricular Dysplasia/Cardiomyopathy Patients and Family Members. *Circ. Cardiovasc. Genet.* **2015**, *8*, 437–446. [CrossRef] [PubMed]
12. Austin, K.M.; Trembley, M.A.; Chandler, S.F.; Sanders, S.P.; Saffitz, J.E.; Abrams, D.J.; Pu, W.T. Molecular mechanisms of arrhythmogenic cardiomyopathy. *Nat. Rev. Cardiol.* **2019**, *16*, 519–537. [CrossRef] [PubMed]
13. Hershberger, R.E.; Givertz, M.M.; Ho, C.Y.; Judge, D.P.; Kantor, P.F.; McBride, K.L.; Morales, A.; Taylor, M.R.G.; Vatta, M.; Ware, S.M.; et al. Genetic evaluation of cardiomyopathy: A clinical practice resource of the American College of Medical Genetics and Genomics (ACMG). *Genet. Med.* **2018**, *20*, 899–909. [CrossRef]

14. Richards, S.; Aziz, N.; Bale, S.; Bick, D.; Das, S.; Gastier-Foster, J.; Grody, W.W.; Hegde, M.; Lyon, E.; Spector, E.; et al. Standards and guidelines for the interpretation of sequence variants: A joint consensus recommendation of the American College of Medical Genetics and Genomics and the Association for Molecular Pathology. *Genet. Med. Off. J. Am. Coll. Med. Genet.* **2015**, *17*, 405–424. [CrossRef] [PubMed]

15. Campuzano, O.; Sarquella-Brugada, G.; Fernandez-Falgueras, A.; Coll, M.; Iglesias, A.; Ferrer-Costa, C.; Cesar, S.; Arbelo, E.; Garcia-Alvarez, A.; Jorda, P.; et al. Reanalysis and reclassification of rare genetic variants associated with inherited arrhythmogenic syndromes. *EBioMedicine* **2020**, *54*, 102732. [CrossRef] [PubMed]

16. Towbin, J.A.; McKenna, W.J.; Abrams, D.J.; Ackerman, M.J.; Calkins, H.; Darrieux, F.C.C.; Daubert, J.P.; de Chillou, C.; DePasquale, E.C.; Desai, M.Y.; et al. 2019 HRS expert consensus statement on evaluation, risk stratification, and management of arrhythmogenic cardiomyopathy: Executive summary. *Heart Rhythm* **2019**, *16*, e373–e407. [CrossRef] [PubMed]

17. Bennett, J.S.; Bernhardt, M.; McBride, K.L.; Reshmi, S.C.; Zmuda, E.; Kertesz, N.J.; Garg, V.; Fitzgerald-Butt, S.; Kamp, A.N. Reclassification of Variants of Uncertain Significance in Children with Inherited Arrhythmia Syndromes is Predicted by Clinical Factors. *Pediatric Cardiol.* **2019**, *40*, 1679–1687. [CrossRef] [PubMed]

18. Costa, S.; Medeiros-Domingo, A.; Gasperetti, A.; Akdis, D.; Berger, W.; James, C.A.; Ruschitzka, F.; Brunckhorst, C.B.; Duru, F.; Saguner, A.M. Impact of Genetic Variant Reassessment on the Diagnosis of Arrhythmogenic Right Ventricular Cardiomyopathy Based on the 2010 Task Force Criteria. *Circulation. Genomic and precision medicine* **2021**, *14*, e003047. [CrossRef]

19. Harrison, S.M.; Biesecker, L.G.; Rehm, H.L. Overview of Specifications to the ACMG/AMP Variant Interpretation Guidelines. *Curr. Protoc. Hum. Genet.* **2019**, *103*, e93. [CrossRef] [PubMed]

20. Whiffin, N.; Minikel, E.; Walsh, R.; O'Donnell-Luria, A.H.; Karczewski, K.; Ing, A.Y.; Barton, P.J.R.; Funke, B.; Cook, S.A.; MacArthur, D.; et al. Using high-resolution variant frequencies to empower clinical genome interpretation. *Genet. Med. Off. J. Am. Coll. Med. Genet.* **2017**, *19*, 1151–1158. [CrossRef] [PubMed]

21. Walsh, R.; Thomson, K.L.; Ware, J.S.; Funke, B.H.; Woodley, J.; McGuire, K.J.; Mazzarotto, F.; Blair, E.; Seller, A.; Taylor, J.C.; et al. Reassessment of Mendelian gene pathogenicity using 7,855 cardiomyopathy cases and 60,706 reference samples. *Genet. Med. Off. J. Am. Coll. Med. Genet.* **2017**, *19*, 192–203. [CrossRef] [PubMed]

22. Abou Tayoun, A.N.; Pesaran, T.; DiStefano, M.T.; Oza, A.; Rehm, H.L.; Biesecker, L.G.; Harrison, S.M. ClinGen Sequence Variant Interpretation Working Group. Recommendations for interpreting the loss of function PVS1 ACMG/AMP variant criterion. *Hum. Mutat.* **2018**, *39*, 1517–1524. [CrossRef]

23. Quiat, D.; Witkowski, L.; Zouk, H.; Daly, K.P.; Roberts, A.E. Retrospective Analysis of Clinical Genetic Testing in Pediatric Primary Dilated Cardiomyopathy: Testing Outcomes and the Effects of Variant Reclassification. *J. Am. Heart Assoc.* **2020**, *9*, e016195. [CrossRef] [PubMed]

24. Das, K.J.; Ingles, J.; Bagnall, R.D.; Semsarian, C. Determining pathogenicity of genetic variants in hypertrophic cardiomyopathy: Importance of periodic reassessment. *Genet. Med.* **2014**, *16*, 286–293. [CrossRef]

25. Grassi, S.; Campuzano, O.; Coll, M.; Brion, M.; Arena, V.; Iglesias, A.; Carracedo, A.; Brugada, R.; Oliva, A. Genetic variants of uncertain significance: How to match scientific rigour and standard of proof in sudden cardiac death? *Legal Med.* **2020**, *45*, 101712. [CrossRef] [PubMed]

26. Coll, M.; Allegue, C.; Partemi, S.; Mates, J.; Del Olmo, B.; Campuzano, O.; Pascali, V.; Iglesias, A.; Striano, P.; Oliva, A.; et al. Genetic investigation of sudden unexpected death in epilepsy cohort by panel target resequencing. *Int. J. Legal Med.* **2016**, *130*, 331–339. [CrossRef] [PubMed]

27. Partemi, S.; Vidal, M.C.; Striano, P.; Campuzano, O.; Allegue, C.; Pezzella, M.; Elia, M.; Parisi, P.; Belcastro, V.; Casellato, S.; et al. Genetic and forensic implications in epilepsy and cardiac arrhythmias: A case series. *Int. J. Legal Med.* **2015**, *129*, 495–504. [CrossRef] [PubMed]

28. Campuzano, O.; Alcalde, M.; Iglesias, A.; Barahona-Dussault, C.; Sarquella-Brugada, G.; Benito, B.; Arzamendi, D.; Flores, J.; Leung, T.K.; Talajic, M.; et al. Arrhythmogenic right ventricular cardiomyopathy: Severe structural alterations are associated with inflammation. *J. Clin. Pathol.* **2012**, *65*, 1077–1083. [CrossRef] [PubMed]

29. Rasmussen, T.B.; Nissen, P.H.; Palmfeldt, J.; Gehmlich, K.; Dalager, S.; Jensen, U.B.; Kim, W.Y.; Heickendorff, L.; Molgaard, H.; Jensen, H.K.; et al. Truncating plakophilin-2 mutations in arrhythmogenic cardiomyopathy are associated with protein haploinsufficiency in both myocardium and epidermis. *Circ. Cardiovasc. Genet.* **2014**, *7*, 230–240. [CrossRef]

30. Qadri, S.; Anttonen, O.; Viikila, J.; Seppala, E.H.; Myllykangas, S.; Alastalo, T.P.; Holmstrom, M.; Helio, T.; Koskenvuo, J.W. Case reports of two pedigrees with recessive arrhythmogenic right ventricular cardiomyopathy associated with homozygous Thr335Ala variant in DSG2. *BMC Med. Genet.* **2017**, *18*, 86. [CrossRef]

31. Gerull, B.; Kirchner, F.; Chong, J.X.; Tagoe, J.; Chandrasekharan, K.; Strohm, O.; Waggoner, D.; Ober, C.; Duff, H.J. Homozygous founder mutation in desmocollin-2 (DSC2) causes arrhythmogenic cardiomyopathy in the Hutterite population. *Circ. Cardiovasc. Genet.* **2013**, *6*, 327–336. [CrossRef]

32. Lorenzon, A.; Pilichou, K.; Rigato, I.; Vazza, G.; De Bortoli, M.; Calore, M.; Occhi, G.; Carturan, E.; Lazzarini, E.; Cason, M.; et al. Homozygous Desmocollin-2 Mutations and Arrhythmogenic Cardiomyopathy. *Am. J. Cardiol.* **2015**, *116*, 1245–1251. [CrossRef] [PubMed]

33. Brodehl, A.; Weiss, J.; Debus, J.D.; Stanasiuk, C.; Klauke, B.; Deutsch, M.A.; Fox, H.; Bax, J.; Ebbinghaus, H.; Gartner, A.; et al. A homozygous DSC2 deletion associated with arrhythmogenic cardiomyopathy is caused by uniparental isodisomy. *J. Mol. Cell Cardiol.* **2020**, *141*, 17–29. [CrossRef] [PubMed]

34. Cerrone, M.; Lin, X.; Zhang, M.; Agullo-Pascual, E.; Pfenniger, A.; Chkourko Gusky, H.; Novelli, V.; Kim, C.; Tirasawadichai, T.; Judge, D.P.; et al. Missense mutations in plakophilin-2 cause sodium current deficit and associate with a Brugada syndrome phenotype. *Circulation* **2014**, *129*, 1092–1103. [CrossRef] [PubMed]

35. Peters, S. Arrhythmogenic cardiomyopathy and provocable Brugada ECG in a patient caused by missense mutation in plakophilin-2. *Int. J. Cardiol.* **2014**, *173*, 317–318. [CrossRef]

36. Moncayo-Arlandi, J.; Brugada, R. Unmasking the molecular link between arrhythmogenic cardiomyopathy and Brugada syndrome. *Nat. Rev. Cardiol.* **2017**, *14*, 744–756. [CrossRef]

37. Chen, X.; Peng, H.; Zheng, C.; Zhang, H.; Yan, C.; Ma, H.; Dai, X.; Li, X. Two pedigrees with arrhythmogenic right ventricular cardiomyopathy linked with R49H and F531C mutation in DSG2. *Hum. Genome Var.* **2019**, *6*, 38. [CrossRef]

38. Vite, A.; Gandjbakhch, E.; Hery, T.; Fressart, V.; Gary, F.; Simon, F.; Varnous, S.; Hidden Lucet, F.; Charron, P.; Villard, E. Desmoglein-2 mutations in propeptide cleavage-site causes arrhythmogenic right ventricular cardiomyopathy/dysplasia by impairing extracellular 1-dependent desmosomal interactions upon cellular stress. *Europace* **2020**, *22*, 320–329. [CrossRef] [PubMed]

39. Arscott, P.; Caleshu, C.; Kotzer, K.; Kreykes, S.; Kruisselbrink, T.; Orland, K.; Rigelsky, C.; Smith, E.; Spoonamore, K.; Larsen Haidle, J.; et al. A Case for Inclusion of Genetic Counselors in Cardiac Care. *Cardiol. Rev.* **2016**, *24*, 49–55. [CrossRef] [PubMed]

40. Ingles, J.; Semsarian, C. The value of cardiac genetic testing. *Trends Cardiovasc. Med.* **2014**, *24*, 217–224. [CrossRef]

V. DISCUSSION

ACM is mainly caused by rare deleterious variants located in desmosomal genes that trigger structural alterations in the heart being the loss of cardiomyocytes and its progressive substitution with fibro-fatty tissue the principal features of the disease. The identification of the causal variant is crucial for the diagnosis, being PTCs the most frequent deleterious alteration type among patients, especially in the *PKP2* gene. Although a significant number of studies have been focused in ACM in the recent years, there are still uncertainties regarding its progression, incomplete penetrance, variable expressivity or molecular mechanisms underlying ACM pathogenesis. Specifically, our main aim was to study the molecular and cellular phenotypic differences in ACM generated by PTCs in desmosomal genes.

Generated results from this thesis project have been presented into three independent publications: the first two papers were based on studying CRISPR-edited cellular models and the latter was focused on genetic analysis of ACM patients.

In the first one, entitled "*Premature Termination Codon in 5' Region of Desmoplakin and Plakoglobin Genes May Escape Nonsense-Mediated Decay through the Reinitiation of Translation*" we have described that reinitiation of translation is triggered in *DSP* and *JUP* but not in *PKP2, DSG2* or *DSC2* when a PTC is located in the 5' region. In the second one, entitled "*Alterations in calcium handling are a common feature in Arrhythmogenic Cardiomyopathy cell models triggered by desmosome genes loss*" our results showed common molecular and functional alterations shared by the absence of

desmosomal genes. Concretely, our results described a massive dysregulation in calcium handling genes shared by *PKP2, DSC2* and *DSG2* loss associated with a slower calcium uptake. However, *DSP-*KO presented shorter amplitude of the calcium peak.

Finally, the third article presented here, entitled "*Rare Variants Associated with Arrhythmogenic Cardiomyopathy: Reclassification Five Years Later*" showed that a significant number of genetic variants, previously identified in ACM patients, changed their classification after being reanalyzed (5 years later) towards a higher level of certainty, mainly because of the new data generated.

These 3 articles and their more relevant results are discussed together in the following sections. The first five correspond to the discussion of each hypothesis and the last one, the sixth, discusses global considerations of our research and future perspectives.

1. CRISPR-edited KO HL1 as an ACM cellular model

1.1. Generation of the HL1 CRISPR-edited cell lines

As explained in the introduction of the present thesis, HL1 is an immortalized cell line that comes from mouse atrial cardiomyocytes (175). It was the first ACM cell model and currently, it is still considered a good cell line to study ACM and inherited cardiac diseases because it maintains the ability to contract and the cardiac differentiated morphological, biochemical and electrophysiological properties after several passages (173,175).

We initiated the experimental part of the present thesis by editing HL1 cell line using CRISPR/Cas9 to introduce a PTC in the 5' region for all 5 desmosomal genes. Although there were several ACM studies using HL1 lines with transitory inhibition of desmosomal protein expression (150,176,177,179), there were no studies with a permanent absence of them in that cellular model. To our knowledge, only 3 studies of cardiac diseases have been performed on an HL1 cell line using CRISPR technology, and none of them were focused on ACM (220–222). We thought that performing such editions and studying the resulting clones could generate important and novel data to better understand the disease.

As it has been described, HL1 cell line has to be maintained in a high confluence to preserve cardiac properties (175). During the CRISPR

edition process, it was necessary to dilute the cells after the transfection to make them grow separately for obtaining isogenic clones. This low confluency was the main limitation point for the survival of the isolated cells, cellular death was high, but after several rounds of edition we were able to generate around 2-4 isogenic homozygous clones per gene (presented in article 1 and 2). Those articles are the firsts studies using a genome edited HL1 cell line with permanent PTCs in desmosomal genes to investigate ACM-related alterations.

1.2. Evaluation of the HL1 CRISPR-edited cell lines in mimicking the ACM molecular alterations

Once the KOs were obtained and after checking the absence of its protein expression, we wanted to evaluate if our generated cell models were reproducing the known ACM molecular alterations, such as alterations of gene expression levels in desmosomal, connexome, calcium handling or fibrotic and adipogenic genes (33). In some cases, it was complicated to compare our results with the already published data to discuss the reproducibility of our cell model because of the high variability of the different studies in terms of methodology, models or mutation type. In fact, this was the main purpose of article 2, to perform a systematical study with the same cell model following the same methodology and performing the same experiments to be able to compare alterations caused by the loss of different desmosomal genes.

Desmosomal expression levels

HL1 edited lines showed a general downregulation of *DSC2* as exhibited two different cohorts of ACM patients (223,224). However, some of the expression levels of the other desmosomal genes did not match with previous studies. For example, a study based in iPSC-derived cardiomyocyte model carrying heterozygous truncated *PKP2* (199) showed normal levels of *DSP* and *JUP* while our homozygous *PKP2*-KOs exhibits normal *JUP*, but decreased *DSP* levels. Moreover, another study with a cohort of 4 ACM patients with unknown genetic background concluded that all 5 desmosomal genes were decreased in all patients (129). We think that these discrepancies may be explained by the different experimental approach, methodology, homozygous or heterozygous conditions or mutation type of the samples.

Calcium handling

Moreover, in concordance to a previous publication describing calcium handling alterations in the absence of *PKP2* (154), *PKP2*-KOs showed a general downregulation of genes involved in calcium cycle at RNA level and a delayed calcium uptake. In that sense, it seems that our cell model is reproducing calcium alterations triggered by the loss of *PKP2* and for that reason, the obtained results in *DSG2*, *DSC2* and *DSP*-KO generated in the present investigation seems to be reliable.

Cx43 and Nav1.5 expression levels

Apart from our article 2, there is only available data regarding alterations in Cx43 and Nav1.5 for mutations in *PKP2* and *DSP,* but not for *DSG2* nor *DSC2*. In that sense, it is accepted that mutations in *PKP2* or *DSP* cause decreased levels of Cx43 and Nav1.5 (14,150,173,179,190,225). Our HL1 *PKP2*-KO showed non-detectable levels of Nav1.5 protein and decreased levels of *CX43* RNA but not at protein level probably because of the lowest sensitivity of WB. In the case of *DSP*-KO, we could detect Nav1.5 protein, but because it was not possible to perform statistical analysis, we could not determine if it presented significant differences. Observing that *PKP2*-KOs reproduced the alterations in Cx43 and Nav1.5 expression levels, the obtained results in *DSG2* and *DSC2*-KOs seems to be strong.

Fibrosis and adipogenesis

Finally, we evaluated the expression levels of *TGFB1* and *PPARg* as known factors for fibrosis and adipogenesis, respectively (33). Our *PKP2*-KOs reproduced alterations previous described on *TGFB1* (108), although they were not significant. Moreover, we found a tendency of decreased levels of *PPARg* when *PKP2, DSG2* and *DSC2* were lost as have shown different models and patients' cohorts (129,199,226,227).

Taking all the above into account, our cell model reproduced the main ACM alterations, as descried in article 2. We obtained similar results compared with what is known about calcium handling alterations at molecular and functional level and expression levels of CX43, sodium channel, desmosomal genes and genes involved in fibrosis and adipogenesis. After analyzing the known ACM alterations in our cell lines, the following sections discuss the new data generated in the presented articles.

2. Desmosomal 5'-PTCs and reinitiation of translation

It is well accepted that PTC triggers the mRNA degradation via NMD as a qualitative control of the gene expression (215). But if the PTC is located in the 3' end of the transcript or in the start-proximal codons, the transcript could evade the NMD (217). This evasion in front of a PTC located in the 5' region is possible thanks to reinitiation of translation mechanism, that it depends on the genomic context of each gene. It is crucial the presence of an alternative ATG in-frame and with an optimal genomic context downstream the PTC when it is located in the firsts 160 codons of the transcript (217,228,229).

In article 1, it was analyzed the genomic sequence of the first 160 codons of the 5 desmosomal genes. It was found out that only *DSP* and *JUP* had an alternative ATG in-frame with optimal genomic context needed for the reinitation of translation. Even the in-silico predictors used conclude that this mechanism may occur in *DSP* and *JUP* genes but not in *PKP2, DSG2* and *DSC2*.

Beside the predictions and the genomic sequence analyses, our experimental results showed that KOs for *PKP2, DSG2* and *DSC2* genes had no protein expression when carrying a 5'-PTC. Oppositely, homozygous *JUP* clone synthetized a N-truncated PG with no difference in the total protein expression levels compared to WTs. JUP heterozygous clones expressed both N-truncated and WT

isoforms. In the case of *DSP*, homozygous clones presumably synthetized an N-truncated protein through reinitation of translation, but it was not possible to differentiate it from the full-length form by WB. The N-truncated DSP lost only a 7.5% of its weight while N-truncated PG lost a 17.2% of it, being not possible to appreciate this small difference in weight in the electrophoresis gel.

Moreover, it is also important to say that in the case of *JUP*, all edited clones showed an N-truncated PG indicating that the reinitation of translation is occurring in the 100% of the *JUP* clones. However, one of the homozygous *DSP* clones had undetectable levels of DSP protein showing that in this case, 75% of the homozygous clones triggered the reinitation of translation while 25% of them undergo to NMD. Which other factors are involved to determine if NMD or reinitation of translation is triggered by 5'-PTC of *DSP* are still unknown, but we observed NMD or reinitiation of translation consistently over time for each clone.

3. Common molecular alterations triggered by PTCs in an ACM cellular model

In the literature, there are many studies contributing to the ACM knowledge and describing the pathophysiology and the alterations at molecular and functional level triggered by the loss of desmosomal genes (33). In article 2, we aimed to describe the common alterations triggered by the loss of *PKP2, DSG2, DSC2* and *DSP* by performing a systematical study using CRISPR-edited HL1 cell lines. Our results support the previous known ACM alterations as analyzed in section 1 of the discussion, but also describe novel alterations.

Desmosomal expression levels

The only alteration commonly found in the absence of *PKP2, DSG2, DSC2* and *DSP* was the downregulation of DSC2, at both RNA and protein level, supporting the idea that this downregulation may be present independently of the causal gene as showed previous cohort studies (223,224).

Cx43 and Nav1.5 expression levels

Nav1.5 was find decreased at protein level in the absence of *PKP2, DSG2* and *DSC2,* but it was not possible to determine if our *DSP*-KO clone presented decreased levels of Nav1.5. For the moment, this

alteration was only previously described to be caused by *PKP2* and *DSP* loss (230,152,14), suggesting that the absence of the cadherins may also have an impact in sodium current. For future studies, it would be interesting to analyze the sodium current of the *DSG2* and *DSC2*-KOs to corroborate if the loss of cadherins is also causing functional alterations.

Fibrosis and adipogenesis

Moreover, we studied the expression levels of two of the main genes related to fibrosis and adipogenesis, *TGFB1* and *PPARg* respectively, two molecular mechanisms associated to ACM pathogenesis (33). Our results showed an upregulation of *TGFB1* and *PPARg* in the loss of *PKP2, DSG2* and *DSC2* supporting the idea that these alterations may be caused independently of the causal gene. Previous studies have also related the increase of *PPARg* to ACM phenotype (129,199,226,227) while the increase of *TGFB1* for the moment was associated with the loss of *PKP2* (108) and *TMEM43* (231), but not with *DSG2* or *DSC2*.

Calcium handling

Finally, our most relevant results from article 2 were the alterations found in calcium handling because it is quite unknown field for desmosomal genes, with the exception of *PKP2* (154,172,232,233). In this study, ANK2 protein was detected in *DSP*-KO clone, but not in

PKP2, DSG2 or *DSC2*-KOs and it was described a tendency to upregulation of *PLN* in those three groups, but not in *DSP*-KO, indicating that the loss of *DSP* may not be involved in the same pathways than the other 3 desmosomal genes. Moreover, *ATP2A2, CASQ2* and *RYR2* were commonly found decreased in the absence of *PKP2, DSG2* and *DSC2.*

In addition to the molecular alterations in calcium cycle, we also studied functional changes in relation to the calcium release and the calcium uptake of the SR by performing the 10mM caffeine peak in all the edited clones. Our results showed that *PKP2, DSG2* and *DSC2*-KOs experimented a delayed uptake of calcium while *DSP*-KO presented a shorter amplitude of the peak indicating a quickest uptake. For the moment, it was only described that the loss of *PKP2* caused a delayed amplitude of the peak in a mouse model (154), so these are novel results for the loss of *DSG2, DSC2* and *DSP*.

4. Gene-specific alterations triggered by PTCs in an ACM cellular model

As discussed in the previous section, some common alterations caused by the loss of desmosomal genes have been elucidated studying the HL1 edited clones. In addition to these alterations, some gene-specific differences between the studied genes have also been found indicating that although their absence cause shared ACM alterations, each gene has also particular characteristics triggering ACM cellular phenotype that have been elucidated in the presented articles 1 and 2.

4.1. Pathogenesis of PTCs located in the 5' region in *DSP* and *JUP*

One of the most relevant results that we obtained in article 1 is that a PTC in the 5'region in *DSP* and *JUP* evades the NMD and an N-truncated protein is expressed through reinitiation of translation. Thus, it may indicate that this variant in these genes may not be as pathogenic as it is located in *PKP2, DSG2* or *DSC2* genes.

In this sense, our results show that the expression of the DSP or PG N-truncated protein have non-significant impact on the pathogenesis of the ACM based on RNA expression levels of genes involved in the disease (article 1) and that N-truncated DSP have no alterations in calcium handling at molecular nor functional level

(article 2). However, the loss of *PKP2, DSG2* or *DSC2* has great impact on calcium handling, as it has been shown in article 2 results.

Moreover, related to clinical phenotype, it is important to say that there have only been described 2 nonsense variants in *DSP* and 1 in *JUP* 5' regions in ACM patients while in general populations the numbers are 5 and 3, respectively (234,235). Oppositely, only 6 *PKP2* variants located in the first 160 codons were found in general population while 17 were identified in ACM patients (234,235). So, around 75% (17/23) of variants located in the 5' region of *PKP2* are associated to ACM while when located in *DSP* or *JUP* only 25% (2/7 or 1/4) are associated to the disease. Furthermore, these described variants in *DSP* or *JUP* in ACM patients have not been associated with cardiac alterations nor symptoms (236,237).

All these data support the idea that the expression of DSP or PG N-truncated protein may not participate in the ACM pathogenesis, or at least with no important effect.

4.2. *DSP* loss and calcium handling

The most noticeable gene-specific characteristic found in article 2 was the role of the *DSP* loss in calcium handling alterations. Although the absence of all studied desmosomal genes caused alterations at molecular and at functional level of calcium cycle, DSP-KO clone was totally different compared with *PKP2, DSG2* or *DSC2* clones. It has been elucidated that DSP loss triggers a quicker calcium uptake with shorter amplitude of the peak while the

absence of *PKP2, DSG2* or *DSC2* causes higher amplitude of Ca^{2+} peak. Altered expression levels of the calcium handling genes supported these functional differences. Specifically, ANK2 protein and *PLN* RNA levels, which have been found oppositely expressed between *DSP*-KO and the other clones.

These gene-specific alterations observed in *DSP*-KO clone could explain some differences in ACM phenotype. It is known that HF is more frequent in those ACM patients that carry pathogenic variants in *DSG2* or *DSP* (35), but it is still uncertain if specific alterations in calcium handling could contribute to this propensity to HF. It is known that depending on the Ca^{2+} content, different clinical alterations can be manifested (5). A high Ca^{2+} content in the SR could contribute to propagate wave of Ca^{2+} induced - Ca^{2+} release increasing the propensity to arrhythmias while a low Ca^{2+} content is associated with HF (5). Our experimental approach was not able to determine the Ca^{2+} content of each cell line, but for future experiments it would be interesting to measure it to see if there is any association between arrhythmias or HF with the loss of a determinate desmosomal protein via calcium handling.

Interestingly, it has been described a distinct form of ACM, the DSP cardiomyopathy, that is characterized by episodic myocardial injury, left ventricular fibrosis that precedes systolic dysfunction, and a high incidence of ventricular arrhythmias (238,239). Molecular and functional differences of our *DSP*-KO clone compared with the other edited clones could contribute to the evidences that molecular

mechanisms of pathogenic variants in *DSP* causing ACM may be partially different.

5. Reanalysis of ACM genetic variants in a 5-year period

In the third article, the most important finding is that analyzing new data generated of ACM genetic variants could contribute to its reclassification into a more certain group. It has been shown that around 30% of the studied variants were classified after 5 years considering global frequencies in general population, family co-segregation and *in-vitro* studies, computational and predictive data and the intrinsic characteristics of the variant and the gene. It is remarkable that 83% of the reclassified variants gained certainty in their significance, reducing in a 18% the VUS group. To gain certainty and reduce VUS is important for the patient management and for its well-being because VUS results are associated with increased patient anxiety, incorrect recall of results, reduced uptake of family screening, and lower rates of sharing information with family (240). The main reason of this gain of certainty has been the updated global frequencies, but in vitro and/or family co-segregation have also been crucial considering that all variants provided with these studies were classified into a higher degree of certainty.

In that sense, our results presented in article 1 and 2 are a good example to see how data generated in *in-vitro* studies could contribute to rate more precisely variants' pathogenesis. ACMG/AMP guidelines for classification of genetic variants (241) recommends to apply very strong or strong criteria to PTCs in all desmosomal genes (242), with an exception for those PTCs in the

last exon due to its tendency in escaping NMD. But non-exclusion is applied for those PTCs specifically located in 5' region in *DSP* or *JUP* genes. After seeing the results presented in article 1 and 2 regarding N-truncated proteins, we recommend that it may be considered the tendency of *DSP* or *JUP* genes to activate the reinitiation of translation when classifying the pathogenesis of a PTC in their 5' region.

It is important to remain that changes in the classification of ACM genetic variants have a direct impact on diagnosis (243). Our results in article 3 showed no changes on clinical diagnosis of the patients, none of them had a borderline diagnosis. However, this may be of great relevance on those cases because an adjustment in variant classification may had big impact on the major or minor criteria for ITFC and could change the diagnosis, hopefully in the main cases, gaining certainty and better personal attention regarding the necessities of each patient.

6. Global considerations and necessities for future studies in ACM

The present thesis contributed to the knowledge of the activation of reinitiation of translation by a PTC in 5' region of desmosomal genes, the characterization of the common alterations in ACM cellular phenotype by the loss of desmosomal genes and the impact of new data of ACM genetic variants in its reclassification. After discussing the results of the 3 presented articles, we realized that although a lot of work has been done in the understanding of the ACM pathophysiology, there are still uncounted uncertainties and unknown mechanisms underlying the disease.

One thing that it is important to remember is that, for the moment, there is no treatment to cure ACM. Considering that it is a disease characterized by phenotypic variability, incomplete penetrance, with several genes associated that cause different alterations and with a high percentage of patients with still no identified genetic cause, it is difficult to say what is more important to elucidate first. Provably, several of these uncertainties could be explained by the differences between causal genes.

In that sense, we think that our edited cell lines are a powerful tool to continue investigating ACM focusing on the gene-specific alterations. Studying deeply the role of each causal gene could be the key to relate them to specific molecular alteration that, at the same time, could explain a part of the ACM clinical features. In that way, when detecting the causal gene in the future, and its molecular

alteration associated, it would be possible to foresee the most provable ACM clinical phenotype such as HF or arrythmias. If it would be possible to determinate these connections between causal gene, molecular alteration and clinical phenotype, it would be easy to perform a risk stratification and an accurate follow-up of the patients, and also to find therapeutic targets to go forward into a personalized treatment for ACM.

VI. CONCLUSIONS

1. Using CRISPR/Cas9 to introduce a PTC in the 5' region of desmosomal genes in HL1 cell model has been a feasible methodology to study the impact of the loss of desmosomal genes in relation to ACM cellular phenotype.

2. HL1 CRISPR-edited lines reproduced the described ACM molecular alterations regarding calcium handling, desmosomes, connexome and ACM molecular pathways expression.

3. A PTC in 5' region in *DSP* or *JUP* genes are prone to trigger reinitation of translation while in *PKP2, DSG2* or *DSC2* activates NMD.

4. A nonsense variant in 5' region of *DSP* or *JUP* may have mild or no effect on ACM cellular pathogenesis due to the presence of an N-truncated protein because of the reinitation of translation.

5. Downregulation of DSC2 protein expression has been detected as a common alteration in KOs of *PKP2, DSG2, DSC2* and *DSP*, being a possible common feature in ACM.

6. A general downregulation of expression of genes involved in calcium cycle have been found in KOs of *PKP2, DSG2* and *DSC2*.

7. Calcium handling alterations were identified in all the generated KOs. On the one hand, the loss of *PKP2, DSG2* or *DSC2* provokes a delayed uptake of calcium and in the other hand; the loss of *DSP* triggers a quicker uptake of it. The source of this alteration may be the expression levels of *ANK2, CASQ2, ATP2A2*, *RYR2* or *PLN.*

8. Updated global frequencies and family co-segregation studies of ACM genetic variants allowed to reclassificate a significant number of them into a more certain group while performing *in vitro* studies is a guarantee to increase the certainty of its pathogenic role.

VII. REFERENCES

1. Van Wynsberghe, Noback, Carola. Human Anatomy and Physiology. 3th ed.

2. Lumen learning [Internet]. Available from: https://courses.lumenlearning.com/

3. Guyton, Hall. Textbook of Medical Phisyology. 12th ed.

4. Eisner DA, Caldwell JL, Kistamás K, Trafford AW. Calcium and Excitation-Contraction Coupling in the Heart. Circ Res. 2017 Jul 7;121(2):181–95.

5. Eisner D. Calcium in the heart: from physiology to disease: Calcium in the heart: from physiology to disease. Exp Physiol. 2014 Oct 1;99(10):1273–82.

6. Vermij SH, Abriel H, van Veen TAB. Refining the molecular organization of the cardiac intercalated disc. Cardiovasc Res. 2017 Jan 8;cvw259.

7. Kobirumaki-Shimozawa F, Nakanishi T, Shimozawa T, Terui T, Oyama K, Li J, et al. Real-Time In Vivo Imaging of Mouse Left Ventricle Reveals Fluctuating Movements of the Intercalated Discs. Nanomaterials. 2020 Mar 16;10(3):532.

8. Rhett JM, Gourdie RG. The perinexus: A new feature of Cx43 gap junction organization. Heart Rhythm. 2012 Apr;9(4):619–23.

9. Cirillo N. Desmosome assembly, homeostasis, and desmosomal disease. Cell Health Cytoskelet. 2016 Feb;9.

10. Chen X, Bonné S, Hatzfeld M, van Roy F, Green KJ. Protein Binding and Functional Characterization of Plakophilin 2. J Biol Chem. 2002 Mar;277(12):10512–22.

11. Bolling MC, Veenstra MJ, Jonkman MF, Diercks GFH, Curry CJ, Fisher J, et al. Lethal acantholytic epidermolysis bullosa due to a novel homozygous deletion in *DSP* : expanding the phenotype and implications for desmoplakin function in skin and heart: LAEB due to novel homozygous *DSP* mutation. Br J Dermatol. 2010 Jun;162(6):1388–94.

12. Nekrasova O, Green KJ. Desmosome assembly and dynamics. Trends Cell Biol. 2013 Nov;23(11):537–46.

13. Chen J, Nekrasova OE, Patel DM, Klessner JL, Godsel LM, Koetsier JL, et al. The C-terminal unique region of desmoglein 2 inhibits its internalization via tail–tail interactions. J Cell Biol. 2012 Nov 12;199(4):699–711.

14. Cerrone M, Lin X, Zhang M, Agullo-Pascual E, Pfenniger A, Chkourko Gusky H, et al. Missense Mutations in Plakophilin-2 Cause Sodium Current Deficit and Associate With a Brugada Syndrome Phenotype. Circulation. 2014 Mar 11;129(10):1092–103.

15. Wilson AJ, Schoenauer R, Ehler E, Agarkova I, Bennett PM. Cardiomyocyte growth and sarcomerogenesis at the intercalated disc. Cell Mol Life Sci. 2014 Jan;71(1):165–81.

16. Bagnall RD, Singer ES, Tfelt-Hansen J. Sudden Cardiac Death in the Young. Heart Lung Circ. 2020 Apr;29(4):498–504.

17. Isbister J, Semsarian C. Sudden cardiac death: an update. Intern Med J. 2019 Jul;49(7):826–33.

18. Morin DP, Homoud MK, Estes NAM. Prediction and Prevention of Sudden Cardiac Death. Card Electrophysiol Clin. 2017 Dec;9(4):631–8.

19. Corrado D, Link MS, Calkins H. Arrhythmogenic Right Ventricular Cardiomyopathy. Jarcho JA, editor. N Engl J Med. 2017 Jan 5;376(1):61–72.

20. Gräni C, Benz DC, Gupta S, Windecker S, Kwong RY. Sudden Cardiac Death in Ischemic Heart Disease. JACC Cardiovasc Imaging. 2020 Oct;13(10):2223–38.

21. Osman J, Tan SC, Lee PY, Low TY, Jamal R. Sudden Cardiac Death (SCD) – risk stratification and prediction with molecular biomarkers. J Biomed Sci. 2019 Dec;26(1):39.

22. Jazayeri MA, Emert MP. Sudden Cardiac Death. Med Clin North Am. 2019 Sep;103(5):913–30.

23. Gillum RF. Sudden cardiac death in Hispanic Americans and African Americans. Am J Public Health. 1997 Sep;87(9):1461–6.

24. Ciarambino T, Menna G, Sansone G, Giordano M. Cardiomyopathies: An Overview. Int J Mol Sci. 2021 Jul 19;22(14):7722.

25. Lombardi R, Chen SN. Editorial of Special Issue "Genetics and Molecular Pathogenesis of Non-Ischemic Cardiomyopathies." Int J Mol Sci. 2020 Dec 10;21(24):9398.

26. Maron BJ, Towbin JA, Thiene G, Antzelevitch C, Corrado D, Arnett D, et al. Contemporary Definitions and Classification of the Cardiomyopathies: An American Heart Association Scientific Statement From the Council on Clinical Cardiology, Heart Failure and Transplantation Committee; Quality of Care and Outcomes Research and Functional Genomics and Translational Biology Interdisciplinary Working Groups; and Council on Epidemiology and Prevention. Circulation. 2006 Apr 11;113(14):1807–16.

27. Brieler J, Breeden MA, Tucker J, University SL, Louis S. Cardiomyopathy: An Overview. 2017;96(10):8.

28. Cimiotti D, Budde H, Hassoun R, Jaquet K. Genetic Restrictive Cardiomyopathy: Causes and Consequences—An Integrative Approach. Int J Mol Sci. 2021 Jan 8;22(2):558.

29. Muchtar E, Blauwet LA, Gertz MA. Restrictive Cardiomyopathy: Genetics, Pathogenesis, Clinical Manifestations, Diagnosis, and Therapy. Circ Res. 2017 Sep 15;121(7):819–37.

30. Ciarambino T, Menna G, Sansone G, Giordano M. Cardiomyopathies: An Overview. Int J Mol Sci. 2021 Jul 19;22(14):7722.

31. Yogasundaram H, Alhumaid W, Dzwiniel T, Christian S, Oudit GY. Cardiomyopathies and Genetic Testing in Heart Failure: Role in Defining Phenotype-Targeted Approaches and Management. Can J Cardiol. 2021 Apr;37(4):547–59.

32. McKenna WJ, Judge DP. Epidemiology of the inherited cardiomyopathies. Nat Rev Cardiol. 2021 Jan;18(1):22–36.

33. Austin KM, Trembley MA, Chandler SF, Sanders SP, Saffitz JE, Abrams DJ, et al. Molecular mechanisms of arrhythmogenic cardiomyopathy. Nat Rev Cardiol. 2019 Sep;16(9):519–37.

34. Gao S, Puthenvedu D, Lombardi R, Chen SN. Established and Emerging Mechanisms in the Pathogenesis of Arrhythmogenic Cardiomyopathy: A Multifaceted Disease. Int J Mol Sci. 2020 Aug 31;21(17):6320.

35. Bennett RG, Haqqani HM, Berruezo A, Della Bella P, Marchlinski FE, Hsu CJ, et al. Arrhythmogenic Cardiomyopathy in 2018–2019: ARVC/ALVC or Both? Heart Lung Circ. 2019 Jan;28(1):164–77.

36. Finocchiaro G, Papadakis M, Robertus JL, Dhutia H, Steriotis AK, Tome M, et al. Etiology of Sudden Death in Sports. J Am Coll Cardiol. 2016 May;67(18):2108–15.

37. Zorzi A, Cipriani A, Mattesi G, Vio R, Bettella N, Corrado D. Arrhythmogenic Cardiomyopathy and Sports Activity. J Cardiovasc Transl Res. 2020 Jun;13(3):274–83.

38. Gasperetti A, James CA, Cerrone M, Delmar M, Calkins H, Duru F. Arrhythmias right ventricular cardiomyopathy and sports activity: from molecular pathways in diseased hearts to new insights into the athletic heart mimicry. 2020;17.

39. Sawant AC, Bhonsale A, te Riele ASJM, Tichnell C, Murray B, Russell SD, et al. Exercise has a Disproportionate Role in the Pathogenesis of Arrhythmogenic Right Ventricular Dysplasia/Cardiomyopathy in Patients Without Desmosomal Mutations. J Am Heart Assoc [Internet]. 2014 Dec 17 [cited 2021 Dec 20];3(6). Available from: https://www.ahajournals.org/doi/10.1161/JAHA.114.001471

40. Zorio E. Facts and Gaps in Exercise Influence on Arrhythmogenic Cardiomyopathy: New Insights From a Meta-Analysis Approach. Front Cardiovasc Med. 2021;8:13.

41. Sawant AC, Bhonsale A, te Riele ASJM, Tichnell C, Murray B, Russell SD, et al. Exercise has a Disproportionate Role in the Pathogenesis of Arrhythmogenic Right Ventricular Dysplasia/Cardiomyopathy in Patients Without Desmosomal Mutations. J Am Heart Assoc [Internet]. 2014 Dec 17 [cited 2021 Dec 20];3(6). Available from: https://www.ahajournals.org/doi/10.1161/JAHA.114.001471

42. Saberniak J, Hasselberg NE, Borgquist R, Platonov PG, Sarvari SI, Smith HJ, et al. Vigorous physical activity impairs myocardial function in patients with arrhythmogenic right ventricular cardiomyopathy and in mutation positive family members. 2014;8.

43. Salas AR, Cordero AB, Navarro-Arce I, Navarro MJ, Pinilla JMG, Bueno FC, et al. Impact of dynamic physical exercise on high risk definite arrhythmogenic RV cardiomyopathy. :21.

44. Corrado D, Basso C, Thiene G, McKenna WJ, Davies MJ, Fontaliran F, et al. Spectrum of Clinicopathologic Manifestations of Arrhythmogenic Right Ventricular Cardiomyopathy/Dysplasia: A Multicenter Study. J Am Coll Cardiol. 1997 Nov;30(6):1512–20.

45. Bauce B, Frigo G, Marcus FI, Basso C, Rampazzo A, Maddalena F, et al. Comparison of Clinical Features of Arrhythmogenic Right Ventricular Cardiomyopathy in Men Versus Women. Am J Cardiol. 2008 Nov;102(9):1252–7.

46. Arrhythmogenic Right Ventricular Dysplasia/Cardiomyopathy. :11.

47. Bhonsale A, Groeneweg JA, James CA, Dooijes D, Tichnell C, Jongbloed JDH, et al. Impact of genotype on clinical course in arrhythmogenic right ventricular dysplasia/cardiomyopathy-associated mutation carriers. Eur Heart J. 2015 Apr 7;36(14):847–55.

48. Groeneweg JA, Bhonsale A, James CA, te Riele AS, Dooijes D, Tichnell C, et al. Clinical Presentation, Long-Term Follow-Up, and Outcomes of 1001 Arrhythmogenic Right Ventricular Dysplasia/Cardiomyopathy Patients and Family Members. Circ Cardiovasc Genet. 2015 Jun;8(3):437–46.

49. Keen J, Prisco SZ, Prins KW. Sex Differences in Right Ventricular Dysfunction: Insights From the Bench to Bedside. Front Physiol. 2021 Jan 18;11:623129.

50. Choudhary N, Tompkins C, Polonsky B, Mcnitt S, Calkins H, Mark Estes NA, et al. Clinical Presentation and Outcomes by Sex in Arrhythmogenic Right Ventricular Cardiomyopathy: Findings from the North American ARVC Registry: Clinical Presentation and Outcomes. J Cardiovasc Electrophysiol. 2016 May;27(5):555–62.

51. Rigato I, Bauce B, Rampazzo A, Zorzi A, Pilichou K, Mazzotti E, et al. Compound and Digenic Heterozygosity Predicts Lifetime Arrhythmic Outcome and Sudden Cardiac Death in Desmosomal Gene–Related Arrhythmogenic Right Ventricular Cardiomyopathy. Circ Cardiovasc Genet. 2013 Dec;6(6):533–42.

52. Hodgkinson KA, Parfrey PS, Bassett AS, Kupprion C, Drenckhahn J, Norman MW, et al. The impact of implantable cardioverter-defibrillator therapy on survival in autosomal-dominant arrhythmogenic right ventricular cardiomyopathy (ARVD5). J Am Coll Cardiol. 2005 Feb;45(3):400–8.

53. Kimura Y, Noda T, Otsuka Y, Wada M, Nakajima I, Ishibashi K, et al. Potentially Lethal Ventricular Arrhythmias and Heart Failure in Arrhythmogenic Right Ventricular Cardiomyopathy. JACC Clin Electrophysiol. 2016 Oct;2(5):546–55.

54. Lin CY, Chung FP, Lin YJ, Chang SL, Lo LW, Hu YF, et al. Gender differences in patients with arrhythmogenic right ventricular dysplasia/cardiomyopathy: Clinical manifestations, electrophysiological properties, substrate characteristics, and prognosis of radiofrequency catheter ablation. Int J Cardiol. 2017 Jan;227:930–7.

55. Bosman LP, Sammani A, James CA, Cadrin-Tourigny J, Calkins H, van Tintelen JP, et al. Predicting arrhythmic risk in arrhythmogenic right ventricular cardiomyopathy: A systematic review and meta-analysis. Heart Rhythm. 2018 Jul;15(7):1097–107.

56. Maupain C, Badenco N, Pousset F, Waintraub X, Duthoit G, Chastre T, et al. Risk Stratification in Arrhythmogenic Right Ventricular Cardiomyopathy/Dysplasia Without an Implantable Cardioverter-Defibrillator. JACC Clin Electrophysiol. 2018 Jun;4(6):757–68.

57. Dominguez F, Zorio E, Jimenez-Jaimez J, Salguero-Bodes R, Zwart R, Gonzalez-Lopez E, et al. Clinical characteristics and determinants of the phenotype in TMEM43 arrhythmogenic right ventricular cardiomyopathy type 5. Heart Rhythm. 2020 Jun;17(6):945–54.

58. Tandri H, Daya SK, Nasir K, Bomma C, Lima JAC, Calkins H, et al. Normal Reference Values for the Adult Right Ventricle by Magnetic Resonance Imaging. Am J Cardiol. 2006 Dec;98(12):1660–4.

59. Kawut SM, Lima JAC, Barr RG, Chahal H, Jain A, Tandri H, et al. Sex and Race Differences in Right Ventricular Structure and Function: The Multi-Ethnic Study of Atherosclerosis–Right Ventricle Study. Circulation. 2011 Jun 7;123(22):2542–51.

60. Akdis D, Saguner AM, Shah K, Wei C, Medeiros-Domingo A, von Eckardstein A, et al. Sex hormones affect outcome in arrhythmogenic right ventricular cardiomyopathy/dysplasia: from a stem cell derived cardiomyocyte-based model to clinical biomarkers of disease outcome. Eur Heart J. 2017 May 14;38(19):1498–508.

61. Ren J, Chen L, Zhang N, Chen X, Zhao Q, Chen K, et al. Plasma testosterone and arrhythmic events in male patients with arrhythmogenic right ventricular cardiomyopathy. ESC Heart Fail. 2020 Aug;7(4):1547–59.

62. McKenna WJ, Thiene G, Nava A, Fontaliran F, Blomstrom-Lundqvist C, Fontaine G. Diagnosis of arrhythmogenic right ventricular dysplasia/cardiomyopathy. :4.

63. Marcus FI, McKenna WJ, Sherrill D, Basso C, Bauce B, Bluemke DA, et al. Diagnosis of arrhythmogenic right ventricular cardiomyopathy/dysplasia: Proposed Modification of the Task Force Criteria. Eur Heart J. 2010 Apr 1;31(7):806–14.

64. Latt H, Tun Aung T, Roongsritong C, Smith D. A classic case of arrhythmogenic right ventricular cardiomyopathy (ARVC) and literature review. J Community Hosp Intern Med Perspect. 2017 Apr 3;7(2):115–21.

65. Domenico Corrado, Peter J. van Tintelen, William J. McKenna, Richard N.W. Hauer, Aris Anastastakis, Angeliki Asimaki, et al. Arrhythmogenic right ventricular cardiomyopathy: evaluation of the current diagnostic criteria and differential diagnosis. Eur Heart J. 2020;41:1414–27.

66. Te Riele ASJM, James CA, Sawant AC, Bhonsale A, Groeneweg JA, Mast TP, et al. Arrhythmogenic Right Ventricular Dysplasia/Cardiomyopathy in the Pediatric Population. JACC Clin Electrophysiol. 2015 Dec;1(6):551–60.

67. Patel V, Asatryan B, Siripanthong B, Munroe PB, Tiku-Owens A, Lopes LR, et al. State of the Art Review on Genetics and Precision Medicine in Arrhythmogenic Cardiomyopathy. Int J Mol Sci. 2020;47.

68. Corrado D, Perazzolo Marra M, Zorzi A, Beffagna G, Cipriani A, Lazzari MD, et al. Diagnosis of arrhythmogenic cardiomyopathy: The Padua criteria. Int J Cardiol. 2020 Nov;319:106–14.

69. Corrado D, Zorzi A, Cipriani A, Bauce B, Bariani R, Beffagna G, et al. Evolving Diagnostic Criteria for Arrhythmogenic Cardiomyopathy. J Am Heart Assoc. 2021 Sep 21;10(18):e021987.

70. Elias Neto J, Tonet J, Frank R, Fontaine G. Arrythmogenic Right Ventricular Cardiomiopathy/Dysplasia (ARVC/D) - What We Have Learned after 40 Years of the Diagnosis of This Clinical Entity. Arq Bras Cardiol [Internet]. 2018 [cited 2021 Nov 16]; Available from: https://www.scielo.br/scielo.php?script=sci_arttext&pid=S0066-782X2019000100091

71. Corrado D, Wichter T, Link MS, Hauer R, Marchlinski F, Anastasakis A, et al. Treatment of arrhythmogenic right ventricular cardiomyopathy/dysplasia: an international task force consensus statement. Eur Heart J. 2015 Jul 27;ehv162.

72. Corrado D, Leoni L, Link MS, Bella PD, Gaita F, Curnis A, et al. Implantable Cardioverter-Defibrillator Therapy for Prevention of Sudden Death in Patients With Arrhythmogenic Right Ventricular Cardiomyopathy/Dysplasia. Circulation. 2003 Dec 23;108(25):3084–91.

73. 2022 ESC Guidelines for the management of patients with ventricular arrhythmias and the prevention of sudden cardiac death. :130.

74. Gandjbakhch E, Redheuil A, Pousset F, Charron P, Frank R. Clinical Diagnosis, Imaging, and Genetics of Arrhythmogenic Right Ventricular Cardiomyopathy/Dysplasia. J Am Coll Cardiol. 2018 Aug;72(7):784–804.

75. Gerull B, Heuser A, Wichter T, Paul M, Basson CT, McDermott DA, et al. Mutations in the desmosomal protein plakophilin-2 are common in arrhythmogenic right ventricular cardiomyopathy. Nat Genet. 2004 Nov 1;36(11):1162–4.

76. James CA, Syrris P, van Tintelen JP, Calkins H. The role of genetics in cardiovascular disease: arrhythmogenic cardiomyopathy. :10.

77. Rampazzo A, Nava A, Malacrida S, Beffagna G, Bauce B, Rossi V, et al. Mutation in Human Desmoplakin Domain Binding to Plakoglobin Causes a Dominant Form of Arrhythmogenic Right Ventricular Cardiomyopathy. Am J Hum Genet. 2002 Nov;71(5):1200–6.

78. Bauce B, Rampazzo A, Basso C, Mazzotti E, Rigato I, Steriotis A, et al. Clinical phenotype and diagnosis of arrhythmogenic right ventricular cardiomyopathy in pediatric patients carrying desmosomal gene mutations. Heart Rhythm. 2011 Nov;8(11):1686–95.

79. Elliott P, O'Mahony C, Syrris P, Evans A, Rivera Sorensen C, Sheppard MN, et al. Prevalence of Desmosomal Protein Gene Mutations in Patients With Dilated Cardiomyopathy. Circ Cardiovasc Genet. 2010 Aug;3(4):314–22.

80. Pilichou K, Nava A, Basso C, Beffagna G, Bauce B, Lorenzon A, et al. Mutations in Desmoglein-2 Gene Are Associated With Arrhythmogenic Right Ventricular Cardiomyopathy. Circulation. 2006 Mar 7;113(9):1171–9.

81. Casella M, Gasperetti A, Sicuso R, Conte E, Catto V, Sommariva E, et al. Characteristics of Patients With Arrhythmogenic Left Ventricular Cardiomyopathy: Combining Genetic and Histopathologic Findings. Circ Arrhythm Electrophysiol [Internet]. 2020 Dec [cited 2021 Dec 3];13(12). Available from: https://www.ahajournals.org/doi/10.1161/CIRCEP.120.009005

82. Syrris P, Ward D, Evans A, Asimaki A, Gandjbakhch E, Sen-Chowdhry S, et al. Arrhythmogenic Right Ventricular Dysplasia/Cardiomyopathy Associated with Mutations in the Desmosomal Gene Desmocollin-2. Am J Hum Genet. 2006 Nov;79(5):978–84.

83. McKoy G, Protonotarios N, Crosby A, Tsatsopoulou A, Anastasakis A, Coonar A, et al. Identification of a deletion in plakoglobin in arrhythmogenic right ventricular cardiomyopathy with palmoplantar keratoderma and woolly hair (Naxos disease). The Lancet. 2000 Jun;355(9221):2119–24.

84. Richards S, Aziz N, Bale S, Bick D, Das S, Gastier-Foster J, et al. Standards and guidelines for the interpretation of sequence variants: a joint consensus recommendation of the American College of Medical Genetics and Genomics and the Association for Molecular Pathology. Genet Med. 2015 May;17(5):405–24.

85. Sato PY, Musa H, Coombs W, Guerrero-Serna G, Patiño GA, Taffet SM, et al. Loss of Plakophilin-2 Expression Leads to Decreased Sodium

Current and Slower Conduction Velocity in Cultured Cardiac Myocytes. Circ Res. 2009 Sep 11;105(6):523–6.

86. Kirchhof P, Fabritz L, Zwiener M, Witt H, Schäfers M, Zellerhoff S, et al. Age- and Training-Dependent Development of Arrhythmogenic Right Ventricular Cardiomyopathy in Heterozygous Plakoglobin-Deficient Mice. Circulation. 2006 Oct 24;114(17):1799–806.

87. Yin T, Getsios S, Caldelari R, Godsel LM, Kowalczyk AP, Müller EJ, et al. Mechanisms of Plakoglobin-dependent Adhesion. J Biol Chem. 2005 Dec;280(48):40355–63.

88. Yamada K, Green KG, Samarel AM, Saffitz JE. Distinct Pathways Regulate Expression of Cardiac Electrical and Mechanical Junction Proteins in Response to Stretch. Circ Res. 2005 Aug 19;97(4):346–53.

89. Hariharan V, Asimaki A, Michaelson JE, Plovie E, MacRae CA, Saffitz JE, et al. Arrhythmogenic right ventricular cardiomyopathy mutations alter shear response without changes in cell–cell adhesion. Cardiovasc Res. 2014 Nov 1;104(2):280–9.

90. Heidbüchel H. High prevalence of right ventricular involvementin endurance athletes with ventricular arrhythmias Role of an electrophysiologic study in risk stratification. Eur Heart J. 2003 Aug;24(16):1473–80.

91. Heidbuchel H, Prior DL, La Gerche A. Ventricular arrhythmias associated with long-term endurance sports: what is the evidence? Br J Sports Med. 2012 Nov;46(Suppl 1):i44–50.

92. Garcia-Gras E. Suppression of canonical Wnt/ -catenin signaling by nuclear plakoglobin recapitulates phenotype of arrhythmogenic right ventricular cardiomyopathy. J Clin Invest. 2006 Jul 3;116(7):2012–21.

93. Asimaki A, Kapoor S, Plovie E, Karin Arndt A, Adams E, Liu Z, et al. Identification of a New Modulator of the Intercalated Disc in a Zebrafish Model of Arrhythmogenic Cardiomyopathy. Sci Transl Med [Internet]. 2014 Jun 11 [cited 2021 Dec 21];6(240). Available from: https://www.science.org/doi/10.1126/scitranslmed.3008008

94. Pilichou K, Remme CA, Basso C, Campian ME, Rizzo S, Barnett P, et al. Myocyte necrosis underlies progressive myocardial dystrophy in

mouse dsg2-related arrhythmogenic right ventricular cardiomyopathy. J Exp Med. 2009 Aug 3;206(8):1787–802.

95. Basso C, Corrado D, Valente M, Angelini A, Nava A, Thiene G. Arrhythmogenic right ventricular cardiomyopathy: Dysplasia, dystrophy or myocarditis? J Am Coll Cardiol. 1996 Feb;27(2):394.

96. Leask A. Getting to the Heart of the Matter. New Insights Into Cardiac Fibrosis. Circulation Research. 2015;8.

97. Leask A. TGFβ, cardiac fibroblasts, and the fibrotic response. Cardiovasc Res. 2007 May 1;74(2):207–12.

98. Dobaczewski M, Bujak M, Li N, Gonzalez-Quesada C, Mendoza LH, Wang XF, et al. Smad3 Signaling Critically Regulates Fibroblast Phenotype and Function in Healing Myocardial Infarction. Circ Res. 2010 Aug 6;107(3):418–28.

99. Khalil H, Kanisicak O, Prasad V, Correll RN, Fu X, Schips T, et al. Fibroblast-specific TGF-β–Smad2/3 signaling underlies cardiac fibrosis. J Clin Invest. 2017 Sep 11;127(10):3770–83.

100. Li D, Liu Y, Maruyama M, Zhu W, Chen H, Zhang W, et al. Restrictive loss of plakoglobin in cardiomyocytes leads to arrhythmogenic cardiomyopathy. Hum Mol Genet. 2011 Dec 1;20(23):4582–96.

101. Briest W, Holzl A, Raßler B, Deten A, Leicht M, Baba HA, et al. Cardiac remodeling after long term norepinephrine treatment in rats. Cardiovasc Res. 2001;9.

102. Meier H, Bullinger J, Deten A, Marx G, Rabald S, Zimmer HG, et al. Tissue Inhibitor of Matrix Metalloproteinase-1 in Norepinephrine-Induced Remodeling of the Mouse Heart. Cell Physiol Biochem. 2007;20(6):825–36.

103. Maione AS, Pilato CA, Casella M, Gasperetti A, Stadiotti I, Pompilio G, et al. Fibrosis in Arrhythmogenic Cardiomyopathy: The Phantom Thread in the Fibro-Adipose Tissue. Front Physiol. 2020 Apr 3;11:279.

104. Heinemeier K, Langberg H, Kjaer M. Exercise-induced changes in circulating levels of transforming growth factor-β-1 in humans: methodological considerations. Eur J Appl Physiol. 2003 Sep;90(1–2):171–7.

105. Czarkowska-Paczek B, Bartlomiejczyk I, Przybylski J. THE SERUM LEVELS OF GROWTH FACTORS: PDGF, TGF-BETA AND VEGF ARE INCREASED AFTER STRENUOUS PHYSICAL EXERCISE. :9.

106. Yu L. TGF-b receptor-activated p38 MAP kinase mediates Smad-independent TGF-b responses. :11.

107. Jain M, Rivera S, Monclus EA, Synenki L, Zirk A, Eisenbart J, et al. Mitochondrial Reactive Oxygen Species Regulate Transforming Growth Factor-β Signaling. J Biol Chem. 2013 Jan;288(2):770–7.

108. Dubash AD, Kam CY, Aguado BA, Patel DM, Delmar M, Shea LD, et al. Plakophilin-2 loss promotes TGF-β1/p38 MAPK-dependent fibrotic gene expression in cardiomyocytes. J Cell Biol. 2016 Feb 15;212(4):425–38.

109. Hinz B. Tissue stiffness, latent TGF-β1 Activation, and mechanical signal transduction: Implications for the pathogenesis and treatment of fibrosis. Curr Rheumatol Rep. 2009 Apr;11(2):120–6.

110. Moses KA, DeMayo F, Braun RM, Reecy JL, Schwartz RJ. Embryonic expression of anNkx2-5/Cre gene usingROSA26 reporter mice. genesis. 2001 Dec;31(4):176–80.

111. Zhou B, Gise A von, Ma Q, Rivera-Feliciano J, Pu WT. Nkx2-5- and Isl1-expressing cardiac progenitors contribute to proepicardium. Biochem Biophys Res Commun. 2008 Oct;375(3):450–3.

112. Verzi MP, McCulley DJ, De Val S, Dodou E, Black BL. The right ventricle, outflow tract, and ventricular septum comprise a restricted expression domain within the secondary/anterior heart field. Dev Biol. 2005 Nov;287(1):134–45.

113. Agah R, Frenkel PA, French BA, Michael LH, Overbeek PA, Schneider MD. Gene recombination in postmitotic cells. Targeted expression of Cre recombinase provokes cardiac-restricted, site-specific rearrangement in adult ventricular muscle in vivo. J Clin Invest. 1997 Jul 1;100(1):169–79.

114. Lombardi R, Dong J, Rodriguez G, Bell A, Leung TK, Schwartz RJ, et al. Genetic Fate Mapping Identifies Second Heart Field Progenitor Cells As a Source of Adipocytes in Arrhythmogenic Right Ventricular Cardiomyopathy. Circ Res. 2009 May 8;104(9):1076–84.

115. Lombardi R, Chen SN, Ruggiero A, Gurha P, Czernuszewicz GZ, Willerson JT, et al. Cardiac Fibro-Adipocyte Progenitors Express Desmosome Proteins and Preferentially Differentiate to Adipocytes Upon Deletion of the Desmoplakin Gene. Circ Res. 2016 Jun 24;119(1):41–54.

116. Chong JJH, Chandrakanthan V, Xaymardan M, Asli NS, Li J, Ahmed I, et al. Adult Cardiac-Resident MSC-like Stem Cells with a Proepicardial Origin. Cell Stem Cell. 2011 Dec;9(6):527–40.

117. Sommariva E, Brambilla S, Carbucicchio C, Gambini E, Meraviglia V, Dello Russo A, et al. Cardiac mesenchymal stromal cells are a source of adipocytes in arrhythmogenic cardiomyopathy. Eur Heart J. 2016 Jun 14;37(23):1835–46.

118. Dorn T, Kornherr J, Parrotta EI, Zawada D, Ayetey H, Santamaria G, et al. Interplay of cell–cell contacts and RhoA/ MRTF -A signaling regulates cardiomyocyte identity. EMBO J [Internet]. 2018 Jun 15 [cited 2022 Jan 4];37(12). Available from: https://onlinelibrary.wiley.com/doi/10.15252/embj.201798133

119. Lyon RC, Mezzano V, Wright AT, Pfeiffer E, Chuang J, Banares K, et al. Connexin defects underlie arrhythmogenic right ventricular cardiomyopathy in a novel mouse model. Hum Mol Genet. 2014 Mar 1;23(5):1134–50.

120. Laudes M. Role of WNT pathway in the determination of human mesenchymal stem cells into preadipocytes. J Mol Endocrinol. 2011 Jan 19;JME-10-0169.

121. Willert K, Shibamoto S, Nusse R. Wnt-induced dephosphorylation of Axin releases ꞵ-catenin from the Axin complex. :6.

122. Hoorntje ET, te Rijdt WP, James CA, Pilichou K, Basso C, Judge DP, et al. Arrhythmogenic cardiomyopathy: pathology, genetics, and concepts in pathogenesis. Cardiovasc Res. 2017 Oct 1;113(12):1521–31.

123. Niehrs C. The complex world of WNT receptor signalling. Nat Rev Mol Cell Biol. 2012 Dec;13(12):767–79.

124. Chen S, Guttridge DC, You Z, Zhang Z, Fribley A, Mayo MW, et al. Wnt-1 Signaling Inhibits Apoptosis by Activating. J Cell Biol. 2001;152:10.

125. Ross SE, Hemati N, Longo KA, Bennett CN, Lucas PC, Erickson RL, et al. Inhibition of Adipogenesis by Wnt Signaling. Science. 2000 Aug 11;289(5481):950–3.

126. Longo KA, Kennell JA, Ochocinska MJ, Ross SE, Wright WS, MacDougald OA. Wnt Signaling Protects 3T3-L1 Preadipocytes from Apoptosis through Induction of Insulin-like Growth Factors. J Biol Chem. 2002 Oct;277(41):38239–44.

127. Lombardi R, da Graca Cabreira-Hansen M, Bell A, Fromm RR, Willerson JT, Marian AJ. Nuclear Plakoglobin Is Essential for Differentiation of Cardiac Progenitor Cells to Adipocytes in Arrhythmogenic Right Ventricular Cardiomyopathy. Circ Res. 2011 Dec 9;109(12):1342–53.

128. Lombardi R, Marian AJ. Arrhythmogenic right ventricular cardiomyopathy is a disease of cardiac stem cells. Curr Opin Cardiol. 2010 May;25(3):222–8.

129. Chen SN, Gurha P, Lombardi R, Ruggiero A, Willerson JT, Marian AJ. The Hippo Pathway Is Activated and Is a Causal Mechanism for Adipogenesis in Arrhythmogenic Cardiomyopathy. Circ Res. 2014 Jan 31;114(3):454–68.

130. Noorman M, Hakim S, Kessler E, Groeneweg JA, Cox MGPJ, Asimaki A, et al. Remodeling of the cardiac sodium channel, connexin43, and plakoglobin at the intercalated disk in patients with arrhythmogenic cardiomyopathy. Heart Rhythm. 2013 Mar;10(3):412–9.

131. Quarta G, Syrris P, Ashworth M, Jenkins S, Zuborne Alapi K, Morgan J, et al. Mutations in the Lamin A/C gene mimic arrhythmogenic right ventricular cardiomyopathy. Eur Heart J. 2012 May;33(9):1128–36.

132. Asimaki A, Tandri H, Huang H, Halushka MK, Gautam S, Basso C, et al. A New Diagnostic Test for Arrhythmogenic Right Ventricular Cardiomyopathy. N Engl J Med. 2009 Mar 12;360(11):1075–84.

133.   Salomon D, Sacco PA, Roy SG, Simcha I, Johnson KR, Wheelock MJ, et al. Regulation of ▯-Catenin Levels and Localization by Overexpression of Plakoglobin and Inhibition of the Ubiquitin-Proteasome System. J Cell Biol. 1997;139:11.

134.   Li J, Swope D, Raess N, Cheng L, Muller EJ, Radice GL. Cardiac Tissue-Restricted Deletion of Plakoglobin Results in Progressive Cardiomyopathy and Activation of β-Catenin Signaling. Mol Cell Biol. 2011 Mar 15;31(6):1134–44.

135.   Ellawindy A, Satoh K, Sunamura S, Kikuchi N, Suzuki K, Minami T, et al. Rho-Kinase Inhibition During Early Cardiac Development Causes Arrhythmogenic Right Ventricular Cardiomyopathy in Mice. Arterioscler Thromb Vasc Biol. 2015 Oct;35(10):2172–84.

136.   Yu FX, Zhao B, Guan KL. Hippo Pathway in Organ Size Control, Tissue Homeostasis, and Cancer. Cell. 2015 Nov;163(4):811–28.

137.   Hu Y, Pu WT. Hippo Activation in Arrhythmogenic Cardiomyopathy. Circ Res. 2014 Jan 31;114(3):402–5.

138.   Zhang N, Bai H, David KK, Dong J, Zheng Y, Cai J, et al. The Merlin/NF2 Tumor Suppressor Functions through the YAP Oncoprotein to Regulate Tissue Homeostasis in Mammals. Dev Cell. 2010 Jul;19(1):27–38.

139.   Kim W, Khan SK, Gvozdenovic-Jeremic J, Kim Y, Dahlman J, Kim H, et al. Hippo signaling interactions with Wnt/β-catenin and Notch signaling repress liver tumorigenesis. J Clin Invest. 2016 Nov 21;127(1):137–52.

140.   Lefterova MI, Haakonsson AK, Lazar MA, Mandrup S. PPARγ and the global map of adipogenesis and beyond. Trends Endocrinol Metab. 2014 Jun;25(6):293–302.

141.   Tang QQ, Zhang JW, Daniel Lane M. Sequential gene promoter interactions of C/EBPβ, C/EBPα, and PPARγ during adipogenesis. Biochem Biophys Res Commun. 2004 Jun;319(1):235–9.

142.   Davis JE, Hastings D. Transcriptional Regulation of TCF/LEF and PPAR γ by Daidzein and Genistein in 3T3-L1 Preadipocytes. J Med Food. 2018 Aug;21(8):761–8.

143.   Liu J, Wang H, Zuo Y, Farmer SR. Functional Interaction between Peroxisome Proliferator-Activated Receptor γ and β-Catenin. Mol Cell Biol. 2006 Aug;26(15):5827–37.

144.   Katoh M, Katoh M. WNT Signaling Pathway and Stem Cell Signaling Network: Fig. 1. Clin Cancer Res. 2007 Jul 15;13(14):4042–5.

145.   Kim C, Wong J, Wen J, Wang S, Wang C, Spiering S, et al. Studying arrhythmogenic right ventricular dysplasia with patient-specific iPSCs. Nature. 2013 Feb 7;494(7435):105–10.

146.   Thomas AW, Davies NA, Moir H, Watkeys L, Ruffino JS, Isa SA, et al. Exercise-associated generation of PPARγ ligands activates PPARγ signaling events and upregulates genes related to lipid metabolism. J Appl Physiol. 2012 Mar 1;112(5):806–15.

147.   Akdis D, Department of Cardiology, University Heart Center, Zurich, Switzerland, Brunckhorst C, Department of Cardiology, University Heart Center, Zurich, Switzerland, Duru F, Department of Cardiology, University Heart Center, Zurich, Switzerland, et al. Arrhythmogenic Cardiomyopathy: Electrical and Structural Phenotypes. Arrhythmia Electrophysiol Rev. 2016;5(2):90.

148.   Kaplan SR, Gard JJ, Protonotarios N, Tsatsopoulou A, Spiliopoulou C, Anastasakis A, et al. Remodeling of myocyte gap junctions in arrhythmogenic right ventricular cardiomyopathy due to a deletion in plakoglobin (Naxos disease). Heart Rhythm. 2004 May;1(1):3–11.

149.   Rizzo S, Lodder EM, Verkerk AO, Wolswinkel R, Beekman L, Pilichou K, et al. Intercalated disc abnormalities, reduced Na+ current density, and conduction slowing in desmoglein-2 mutant mice prior to cardiomyopathic changes. Cardiovasc Res. 2012 Sep 1;95(4):409–18.

150.   Fidler LM, Wilson GJ, Liu F, Cui X, Scherer SW, Taylor GP, et al. Abnormal connexin43 in arrhythmogenic right ventricular cardiomyopathy caused by plakophilin-2 mutations. J Cell Mol Med. 2009 Oct;13(10):4219–28.

151.   Oxford EM, Musa H, Maass K, Coombs W, Taffet SM, Delmar M. Connexin43 Remodeling Caused by Inhibition of Plakophilin-2 Expression in Cardiac Cells. Circ Res. 2007 Sep 28;101(7):703–11.

152. Gomes J, Finlay M, Ahmed AK, Ciaccio EJ, Asimaki A, Saffitz JE, et al. Electrophysiological abnormalities precede overt structural changes in arrhythmogenic right ventricular cardiomyopathy due to mutations in desmoplakin-A combined murine and human study. Eur Heart J. 2012 Aug;33(15):1942–53.

153. Sato PY, Coombs W, Lin X, Nekrasova O, Green KJ, Isom LL, et al. Interactions Between Ankyrin-G, Plakophilin-2, and Connexin43 at the Cardiac Intercalated Disc. Circ Res. 2011 Jul 8;109(2):193–201.

154. Cerrone M, Montnach J, Lin X, Zhao YT, Zhang M, Agullo-Pascual E, et al. Plakophilin-2 is required for transcription of genes that control calcium cycling and cardiac rhythm. Nat Commun. 2017 Dec;8(1):106.

155. El-Battrawy I, Zhao Z, Lan H, Cyganek L, Tombers C, Li X, et al. Electrical dysfunctions in human-induced pluripotent stem cell-derived cardiomyocytes from a patient with an arrhythmogenic right ventricular cardiomyopathy. EP Eur. 2018 Jun 1;20(FI1):f46–56.

156. Calabrese F, Basso C, Carturan E, Valente M, Thiene G. Arrhythmogenic right ventricular cardiomyopathy/dysplasia: is there a role for viruses? Cardiovasc Pathol. 2006 Jan;15(1):11–7.

157. Campuzano O, Alcalde M, Iglesias A, Barahona-Dussault C, Sarquella-Brugada G, Benito B, et al. Arrhythmogenic right ventricular cardiomyopathy: severe structural alterations are associated with inflammation. J Clin Pathol. 2012 Dec;65(12):1077–83.

158. Belkaya S, Kontorovich AR, Byun M, Mulero-Navarro S, Bajolle F, Cobat A, et al. Autosomal Recessive Cardiomyopathy Presenting as Acute Myocarditis. J Am Coll Cardiol. 2017 Apr;69(13):1653–65.

159. Tanawuttiwat T, Sager SJ, Hare JM, Myerburg RJ. Myocarditis and ARVC/D: Variants or mimics? Heart Rhythm. 2013 Oct;10(10):1544–8.

160. Asimaki A, Kléber AG, MacRae CA, Saffitz JE. Arrhythmogenic cardiomyopathy — New insights into disease mechanisms and drug discovery. Prog Pediatr Cardiol. 2014 Dec;37(1–2):3–7.

161. Zhang H, Liu S, Dong T, Yang J, Xie Y, Wu Y, et al. Profiling of differentially expressed microRNAs in arrhythmogenic right ventricular cardiomyopathy. Sci Rep. 2016 Sep;6(1):28101.

162.   Sommariva E, D'Alessandra Y, Farina FM, Casella M, Cattaneo F, Catto V, et al. MiR-320a as a Potential Novel Circulating Biomarker of Arrhythmogenic CardioMyopathy. Sci Rep. 2017 Dec;7(1):4802.

163.   Yamada S, Hsiao YW, Chang SL, Lin YJ, Lo LW, Chung FP, et al. Circulating microRNAs in arrhythmogenic right ventricular cardiomyopathy with ventricular arrhythmia. EP Eur. 2018 Jun 1;20(FI1):f37–45.

164.   Bueno Marinas M, Celeghin R, Cason M, Bariani R, Frigo AC, Jager J, et al. A microRNA Expression Profile as Non-Invasive Biomarker in a Large Arrhythmogenic Cardiomyopathy Cohort. Int J Mol Sci. 2020 Feb 24;21(4):1536.

165.   Gurha P, Chen X, Lombardi R, Willerson JT, Marian AJ. Knockdown of Plakophilin 2 Downregulates miR-184 Through CpG Hypermethylation and Suppression of the E2F1 Pathway and Leads to Enhanced Adipogenesis In Vitro. Circ Res. 2016 Sep 2;119(6):731–50.

166.   Mazurek SR, Calway T, Harmon C, Farrell P, Kim GH. MicroRNA-130a Regulation of Desmocollin 2 in a Novel Model of Arrhythmogenic Cardiomyopathy. MicroRNA [Internet]. 2017 Aug 16 [cited 2022 Jan 8];6(2). Available from: http://www.eurekaselect.com/147210/article

167.   Calore M, Lorenzon A, Vitiello L, Poloni G, Khan MAF, Beffagna G, et al. A novel murine model for arrhythmogenic cardiomyopathy points to a pathogenic role of Wnt signalling and miRNA dysregulation. Cardiovasc Res. 2019 Apr 1;115(4):739–51.

168.   Rainer J, Meraviglia V, Blankenburg H, Piubelli C, Pramstaller PP, Paolin A, et al. The arrhythmogenic cardiomyopathy-specific coding and non-coding transcriptome in human cardiac stromal cells. BMC Genomics. 2018 Dec;19(1):491.

169.   Puzzi L, Borin D, Gurha P, Lombardi R, Martinelli V, Weiss M, et al. Knock Down of Plakophillin 2 Dysregulates Adhesion Pathway through Upregulation of miR200b and Alters the Mechanical Properties in Cardiac Cells. Cells. 2019 Dec 14;8(12):1639.

170.   Bueno Marinas M, Celeghin R, Cason M, Thiene G, Basso C, Pilichou K. The Role of MicroRNAs in Arrhythmogenic Cardiomyopathy: Biomarkers or Innocent Bystanders of Disease Progression? Int J Mol Sci. 2020 Sep 3;21(17):6434.

171.   van Opbergen CJM, den Braven L, Delmar M, van Veen TAB. Mitochondrial Dysfunction as Substrate for Arrhythmogenic Cardiomyopathy: A Search for New Disease Mechanisms. Front Physiol. 2019 Dec 10;10:1496.

172.   Kim JC, Pérez-Hernández M, Alvarado FJ, Maurya SR, Montnach J, Yin Y, et al. Disruption of Ca $^{2+}$ ᵢ Homeostasis and Connexin 43 Hemichannel Function in the Right Ventricle Precedes Overt Arrhythmogenic Cardiomyopathy in Plakophilin-2–Deficient Mice. Circulation. 2019 Sep 17;140(12):1015–30.

173.   Sommariva E, Stadiotti I, Perrucci GL, Tondo C, Pompilio G. Cell models of arrhythmogenic cardiomyopathy: advances and opportunities. Dis Model Mech. 2017 Jul 1;10(7):823–35.

174.   Field LJ. Atrial Natriuretic Factor-SV40 T Antigen Transgenes Produce Tumors and Cardiac Arrhythmias in Mice. Science. 1988 Feb 26;239(4843):1029–33.

175.   Claycomb WC, Lanson NA, Stallworth BS, Egeland DB, Delcarpio JB, Bahinski A, et al. HL-1 cells: A cardiac muscle cell line that contracts and retains phenotypic characteristics of the adult cardiomyocyte. Proc Natl Acad Sci. 1998 Mar 17;95(6):2979–84.

176.   Garcia-Gras E. Suppression of canonical Wnt/ -catenin signaling by nuclear plakoglobin recapitulates phenotype of arrhythmogenic right ventricular cardiomyopathy. J Clin Invest. 2006 Jul 3;116(7):2012–21.

177.   Chen SN, Gurha P, Lombardi R, Ruggiero A, Willerson JT, Marian AJ. The Hippo Pathway Is Activated and Is a Causal Mechanism for Adipogenesis in Arrhythmogenic Cardiomyopathy. Circ Res. 2014 Jan 31;114(3):454–68.

178.   Wang L, Liu S, Zhang H, Hu S, Wei Y. RhoA activity increased in myocardium of arrhythmogenic cardiomyopathy patients and affected connexin 43 protein expression in HL-1 cells. :8.

179.   Zhang Q, Deng C, Rao F, Modi RM, Zhu J, Liu X, et al. Silencing of desmoplakin decreases connexin43/Nav1.5 expression and sodium current in HL-1 cardiomyocytes. Mol Med Rep. 2013 Sep;8(3):780–6.

180.   Siragam V, Cui X, Masse S, Ackerley C, Aafaqi S, Strandberg L, et al. TMEM43 Mutation p.S358L Alters Intercalated Disc Protein

Expression and Reduces Conduction Velocity in Arrhythmogenic Right Ventricular Cardiomyopathy. Ai X, editor. PLoS ONE. 2014 Oct 24;9(10):e109128.

181. George CH, Higgs GV, Lai FA. Ryanodine Receptor Mutations Associated With Stress-Induced Ventricular Tachycardia Mediate Increased Calcium Release in Stimulated Cardiomyocytes. Circ Res. 2003 Sep 19;93(6):531–40.

182. Beffagna G, De Bortoli M, Nava A, Salamon M, Lorenzon A, Zaccolo M, et al. Missense mutations in Desmocollin-2 N-terminus, associated with arrhythmogenic right ventricular cardiomyopathy, affect intracellular localization of desmocollin-2 in vitro. BMC Med Genet. 2007 Dec;8(1):65.

183. De Bortoli M, Beffagna G, Bauce B, Lorenzon A, Smaniotto G, Rigato I, et al. The p.A897KfsX4 frameshift variation in desmocollin-2 is not a causative mutation in arrhythmogenic right ventricular cardiomyopathy. Eur J Hum Genet. 2010 Jul;18(7):776–82.

184. Gehmlich K, Syrris P, Peskett E, Evans A, Ehler E, Asimaki A, et al. Mechanistic insights into arrhythmogenic right ventricular cardiomyopathy caused by desmocollin-2 mutations. Cardiovasc Res. 2011 Apr 1;90(1):77–87.

185. Kirchner F, Schuetz A, Boldt LH, Martens K, Dittmar G, Haverkamp W, et al. Molecular Insights into Arrhythmogenic Right Ventricular Cardiomyopathy Caused by Plakophilin-2 Missense Mutations. Circ Cardiovasc Genet. 2012 Aug;5(4):400–11.

186. Schlipp A, Schinner C, Spindler V, Vielmuth F, Gehmlich K, Syrris P, et al. Desmoglein-2 interaction is crucial for cardiomyocyte cohesion and function. Cardiovasc Res. 2014 Nov 1;104(2):245–57.

187. Forleo C, Carmosino M, Resta N, Rampazzo A, Valecce R, Sorrentino S, et al. Clinical and Functional Characterization of a Novel Mutation in Lamin A/C Gene in a Multigenerational Family with Arrhythmogenic Cardiac Laminopathy. Kimura A, editor. PLOS ONE. 2015 Apr 2;10(4):e0121723.

188. Notari M, Hu Y, Sutendra G, Dedeić Z, Lu M, Dupays L, et al. iASPP, a previously unidentified regulator of desmosomes, prevents arrhythmogenic right ventricular cardiomyopathy (ARVC)-induced

sudden death. Proc Natl Acad Sci [Internet]. 2015 Mar 3 [cited 2022 Jul 14];112(9). Available from: https://pnas.org/doi/full/10.1073/pnas.1408111112

189.   van Hengel J, Calore M, Bauce B, Dazzo E, Mazzotti E, De Bortoli M, et al. Mutations in the area composita protein αT-catenin are associated with arrhythmogenic right ventricular cardiomyopathy. Eur Heart J. 2013 Jan 14;34(3):201–10.

190.   Oxford EM, Musa H, Maass K, Coombs W, Taffet SM, Delmar M. Connexin43 Remodeling Caused by Inhibition of Plakophilin-2 Expression in Cardiac Cells. Circ Res. 2007 Sep 28;101(7):703–11.

191.   Sato PY, Musa H, Coombs W, Guerrero-Serna G, Patiño GA, Taffet SM, et al. Loss of Plakophilin-2 Expression Leads to Decreased Sodium Current and Slower Conduction Velocity in Cultured Cardiac Myocytes. Circ Res. 2009 Sep 11;105(6):523–6.

192.   Swope D, Cheng L, Gao E, Li J, Radice GL. Loss of Cadherin-Binding Proteins β-Catenin and Plakoglobin in the Heart Leads to Gap Junction Remodeling and Arrhythmogenesis. Mol Cell Biol. 2012 Mar 15;32(6):1056–67.

193.   Cerrone M, Noorman M, Lin X, Chkourko H, Liang FX, van der Nagel R, et al. Sodium current deficit and arrhythmogenesis in a murine model of plakophilin-2 haploinsufficiency. Cardiovasc Res. 2012 Sep 1;95(4):460–8.

194.   Asimaki A, Kapoor S, Plovie E, Karin Arndt A, Adams E, Liu Z, et al. Identification of a New Modulator of the Intercalated Disc in a Zebrafish Model of Arrhythmogenic Cardiomyopathy. Sci Transl Med [Internet]. 2014 Jun 11 [cited 2021 Dec 21];6(240). Available from: https://www.science.org/doi/10.1126/scitranslmed.3008008

195.   MacRae CA. Cardiac arrhythmia: *in vivo* screening in the zebrafish to overcome complexity in drug discovery. Expert Opin Drug Discov. 2010 Jul;5(7):619–32.

196.   Hawthorne RN, Blazeski A, Lowenthal J, Kannan S, Teuben R, DiSilvestre D, et al. Altered Electrical, Biomolecular, and Immunologic Phenotypes in a Novel Patient-Derived Stem Cell Model of Desmoglein-2 Mutant ARVC. J Clin Med. 2021 Jul 10;10(14):3061.

197. Ma D, Wei H, Lu J, Ho S, Zhang G, Sun X, et al. Generation of patient-specific induced pluripotent stem cell-derived cardiomyocytes as a cellular model of arrhythmogenic right ventricular cardiomyopathy. Eur Heart J. 2013 Apr 14;34(15):1122–33.

198. El-Battrawy I, Zhao Z, Lan H, Cyganek L, Tombers C, Li X, et al. Electrical dysfunctions in human-induced pluripotent stem cell-derived cardiomyocytes from a patient with an arrhythmogenic right ventricular cardiomyopathy. EP Eur. 2018 Jun 1;20(FI1):f46–56.

199. Caspi O, Huber I, Gepstein A, Arbel G, Maizels L, Boulos M, et al. Modeling of Arrhythmogenic Right Ventricular Cardiomyopathy With Human Induced Pluripotent Stem Cells. Circ Cardiovasc Genet. 2013 Dec;6(6):557–68.

200. Zhang C, Quan R, Wang J. Development and application of CRISPR/Cas9 technologies in genomic editing. Hum Mol Genet. 2018 Aug 1;27(R2):R79–88.

201. Jiang F, Doudna JA. CRISPR–Cas9 Structures and Mechanisms. Annu Rev Biophys. 2017 May 22;46(1):505–29.

202. Makarova KS, Koonin EV. Annotation and Classification of CRISPR-Cas Systems. In: Lundgren M, Charpentier E, Fineran PC, editors. CRISPR [Internet]. New York, NY: Springer New York; 2015 [cited 2021 Nov 18]. p. 47–75. (Methods in Molecular Biology; vol. 1311). Available from: http://link.springer.com/10.1007/978-1-4939-2687-9_4

203. Ishino Y, Krupovic M, Forterre P. History of CRISPR-Cas from Encounter with a Mysterious Repeated Sequence to Genome Editing Technology. Margolin W, editor. J Bacteriol [Internet]. 2018 Apr [cited 2021 Nov 18];200(7). Available from: https://journals.asm.org/doi/10.1128/JB.00580-17

204. Makarova KS, Grishin NV, Shabalina SA, Wolf YI, Koonin EV. A putative RNA-interference-based immune system in prokaryotes: computational analysis of the predicted enzymatic machinery, functional analogies with eukaryotic RNAi, and hypothetical mechanisms of action. Biol Direct. 2006 Dec;1(1):7.

205.   Jansen Ruud, Embden JanDA van, Gaastra Wim, Schouls LeoM. Identification of genes that are associated with DNA repeats in prokaryotes. Mol Microbiol. 2002 Mar;43(6):1565–75.

206.   Burstein D, Harrington LB, Strutt SC, Probst AJ, Anantharaman K, Thomas BC, et al. New CRISPR–Cas systems from uncultivated microbes. Nature. 2017 Feb 9;542(7640):237–41.

207.   Shmakov S, Smargon A, Scott D, Cox D, Pyzocha N, Yan W, et al. Diversity and evolution of class 2 CRISPR–Cas systems. Nat Rev Microbiol. 2017 Mar;15(3):169–82.

208.   Doudna JA, Charpentier E. The new frontier of genome engineering with CRISPR-Cas9. Science. 2014 Nov 28;346(6213):1258096.

209.   Bothmer A, Phadke T, Barrera LA, Margulies CM, Lee CS, Buquicchio F, et al. Characterization of the interplay between DNA repair and CRISPR/Cas9-induced DNA lesions at an endogenous locus. Nat Commun. 2017 Apr;8(1):13905.

210.   Jinek M, Chylinski K, Fonfara I, Hauer M, Doudna JA, Charpentier E. A Programmable Dual-RNA–Guided DNA Endonuclease in Adaptive Bacterial Immunity. Science. 2012 Aug 17;337(6096):816–21.

211.   Torres-Ruiz R, Rodriguez-Perales S. CRISPR-Cas9 technology: applications and human disease modelling. Brief Funct Genomics. 2017 Jan;16(1):4–12.

212.   Cribbs AP, Perera SMW. Science and Bioethics of CRISPR-Cas9 Gene Editing: An Analysis Towards Separating Facts and Fiction. :11.

213.   Hryhorowicz M, Lipiński D, Zeyland J, Słomski R. CRISPR/Cas9 Immune System as a Tool for Genome Engineering. Arch Immunol Ther Exp (Warsz). 2017 Jun;65(3):233–40.

214.   Lindeboom RGH, Vermeulen M, Lehner B, Supek F. The impact of nonsense-mediated mRNA decay on genetic disease, gene editing and cancer immunotherapy. Nat Genet. 2019 Nov;51(11):1645–51.

215.   Kurosaki T, Maquat LE. Nonsense-mediated mRNA decay in humans at a glance. J Cell Sci. 2016 Feb 1;129(3):461–7.

216.   Kurosaki T, Popp MW, Maquat LE. Quality and quantity control of gene expression by nonsense-mediated mRNA decay. Nat Rev Mol Cell Biol. 2019 Jul;20(7):406–20.

217.   Cohen S, Kramarski L, Levi S, Deshe N, Ben David O, Arbely E. Nonsense mutation-dependent reinitiation of translation in mammalian cells. Nucleic Acids Res. 2019 Jul 9;47(12):6330–8.

218.   Supek F. To NMD or Not To NMD: Nonsense-Mediated mRNA Decay in Cancer and Other Genetic Diseases. Trends Genet. :12.

219.   Rasmussen TB, Nissen PH, Palmfeldt J, Gehmlich K, Dalager S, Jensen UB, et al. Truncating Plakophilin-2 Mutations in Arrhythmogenic Cardiomyopathy Are Associated With Protein Haploinsufficiency in Both Myocardium and Epidermis. Circ Cardiovasc Genet. 2014 Jun;7(3):230–40.

220.   Kunkel GH, Chaturvedi P, Thelian N, Nair R, Tyagi SC. Mechanisms of TFAM-mediated cardiomyocyte protection. Can J Physiol Pharmacol. 2018 Feb;96(2):173–81.

221.   Srivastava U, Aromolaran AS, Fabris F, Lazaro D, Kassotis J, Qu Y, et al. Novel function of α 1D L-type calcium channel in the atria. Biochem Biophys Res Commun. 2017 Jan;482(4):771–6.

222.   Heliste J, Chheda H, Paatero I, Salminen TA, Akimov Y, Paavola J, et al. Genetic and functional implications of an exonic TRIM55 variant in heart failure. J Mol Cell Cardiol. 2020 Jan;138:222–33.

223.   Vite A, Gandjbakhch E, Prost C, Fressart V, Fouret P, Neyroud N, et al. Desmosomal Cadherins Are Decreased in Explanted Arrhythmogenic Right Ventricular Dysplasia/Cardiomyopathy Patient Hearts. Mohanraj R, editor. PLoS ONE. 2013 Sep 23;8(9):e75082.

224.   Akdis D, Medeiros-Domingo A, Gaertner-Rommel A, Kast JI, Enseleit F, Bode P, et al. Myocardial expression profiles of candidate molecules in patients with arrhythmogenic right ventricular cardiomyopathy/dysplasia compared to those with dilated cardiomyopathy and healthy controls. Heart Rhythm. 2016 Mar;13(3):731–41.

225.   Khudiakov A, Zaytseva A, Perepelina K, Smolina N, Pervunina T, Vasichkina E, et al. Sodium current abnormalities and deregulation of

Wnt/β-catenin signaling in iPSC-derived cardiomyocytes generated from patient with arrhythmogenic cardiomyopathy harboring compound genetic variants in plakophilin 2 gene. Biochim Biophys Acta BBA - Mol Basis Dis. 2020 Nov;1866(11):165915.

226. Djouadi F, Lecarpentier Y, Hebert JL, Charron P, Bastin J, Coirault C. A potential link between peroxisome proliferator-activated receptor signalling and the pathogenesis of arrhythmogenic right ventricular cardiomyopathy. Cardiovasc Res. 2009 Oct 1;84(1):83–90.

227. Reisqs J, Moreau A, Charrabi A, Sleiman Y, Meli AC, Millat G, et al. The PPARγ pathway determines electrophysiological remodelling and arrhythmia risks in DSC2 arrhythmogenic cardiomyopathy. Clin Transl Med [Internet]. 2022 Mar [cited 2022 Jun 10];12(3). Available from: https://onlinelibrary.wiley.com/doi/10.1002/ctm2.748

228. Dyle MC, Kolakada D, Cortazar MA, Jagannathan S. How to get away with nonsense: Mechanisms and consequences of escape from nonsense-mediated RNA decay. WIREs RNA [Internet]. 2020 Jan [cited 2021 Apr 20];11(1). Available from: https://onlinelibrary.wiley.com/doi/abs/10.1002/wrna.1560

229. Van Damme P, Gawron D, Van Criekinge W, Menschaert G. N-terminal Proteomics and Ribosome Profiling Provide a Comprehensive View of the Alternative Translation Initiation Landscape in Mice and Men. Mol Cell Proteomics. 2014 May;13(5):1245–61.

230. Sato PY, Musa H, Coombs W, Guerrero-Serna G, Patino GA, Taffet SM, et al. Loss of Plakophilin-2 Expression Leads to Decreased Sodium Current and Slower Conduction Velocity in Cultured Cardiac Myocytes. :4.

231. Rouhi L, Cheedipudi SM, Chen SN, Fan S, Lombardi R, Chen X, et al. Haploinsufficiency of *Tmem43* in cardiac myocytes activates the DNA damage response pathway leading to a late-onset senescence-associated pro-fibrotic cardiomyopathy. Cardiovasc Res. 2021 Sep 28;117(11):2377–94.

232. Lyon A, van Opbergen CJM, Delmar M, Heijman J, van Veen TAB. In silico Identification of Disrupted Myocardial Calcium Homeostasis as Proarrhythmic Trigger in Arrhythmogenic Cardiomyopathy. Front Physiol. 2021 Sep 24;12:732573.

233. van Opbergen CJM, Noorman M, Pfenniger A, Copier JS, Vermij SH, Li Z, et al. Plakophilin-2 Haploinsufficiency Causes Calcium Handling Deficits and Modulates the Cardiac Response Towards Stress. Int J Mol Sci. 2019 Aug 21;20(17):4076.

234. van der Zwaag PA, Jongbloed JDH, van den Berg MP, van der Smagt JJ, Jongbloed R, Bikker H, et al. A genetic variants database for arrhythmogenic right ventricular dysplasia/cardiomyopathy. Hum Mutat. 2009 Sep;30(9):1278–83.

235. Genome Aggregation Database Consortium, Karczewski KJ, Francioli LC, Tiao G, Cummings BB, Alföldi J, et al. The mutational constraint spectrum quantified from variation in 141,456 humans. Nature. 2020 May 28;581(7809):434–43.

236. Bari O, Skillman S, Lah MD, Haggstrom AN. Compound heterozygous mutations in desmoplakin associated with skin fragility, follicular hyperkeratosis, alopecia, and nail dystrophy. Pediatr Dermatol. 2018 Jul;35(4):e218–20.

237. Cabral RM, Liu L, Hogan C, Dopping-Hepenstal PJC, Winik BC, Asial RA, et al. Homozygous Mutations in the 5' Region of the JUP Gene Result in Cutaneous Disease but Normal Heart Development in Children. J Invest Dermatol. 2010 Jun;130(6):1543–50.

238. Smith ED, Lakdawala NK, Papoutsidakis N, Aubert G, Mazzanti A, McCanta AC, et al. Desmoplakin Cardiomyopathy, a Fibrotic and Inflammatory Form of Cardiomyopathy Distinct From Typical Dilated or Arrhythmogenic Right Ventricular Cardiomyopathy. Circulation. 2020 Jun 9;141(23):1872–84.

239. Yuan ZY, Cheng LT, Wang ZF, Wu YQ. Desmoplakin and clinical manifestations of desmoplakin cardiomyopathy. Chin Med J (Engl). 2021 Aug 5;134(15):1771–9.

240. Muller RD, McDonald T, Pope K, Cragun D. Evaluation of Clinical Practices Related to Variants of Uncertain Significance Results in Inherited Cardiac Arrhythmia and Inherited Cardiomyopathy Genes. Circ Genomic Precis Med. 2020 Aug;13(4).

241. Richards S, Aziz N, Bale S, Bick D, Das S, Gastier-Foster J, et al. Standards and guidelines for the interpretation of sequence variants: a joint consensus recommendation of the American College of

Medical Genetics and Genomics and the Association for Molecular Pathology. Genet Med. 2015 May;17(5):405–23.

242.   Carruth ED, Young W, Beer D, James CA, Calkins H, Jing L, et al. Prevalence and Electronic Health Record-Based Phenotype of Loss-of-Function Genetic Variants in Arrhythmogenic Right Ventricular Cardiomyopathy-Associated Genes. Circ Genomic Precis Med [Internet]. 2019 Nov [cited 2021 May 11];12(11). Available from: https://www.ahajournals.org/doi/10.1161/CIRCGEN.119.002579

243.   Sarah Costa, Argelia Medeiros-Domingo, Alessio Gasperetti, Deniz Akdis, Wolfgang Berger, Cynthia A. James, et al. Impact of Genetic Variant Reassessment on the Diagnosis of Arrhythmogenic Right Ventricular Cardiomyopathy Based on the 2010 Task Force Criteria. Circ Genomic Precis Med. 2020;34.